European Commission

technical steel research

Steel structures

Design tools for the behaviour of multi-storey steel-framed buildings exposed to natural fires

L. Twilt, C. Both, A. J. Breunese
TNO Building and Construction Research
Van Mourik Broekmanweg 6, Postbus 49, 2600 AA Delft, Netherlands

D. O'Callaghan, M. O'Connor
Corus UK
Swinden Technology Centre, Moorgate, Rotherham S60 3AR, United Kingdom

M. Rotter, A. Usmani
University of Edinburgh
University of Edinburgh, Old College, South Bridge, Edinburgh EH8 9YL, United Kingdom

L. G. Cajot
ProfilArbed
66, rue de Luxembourg, L-4421 Esch-sur-Alzette

B. Zhao
CTICM
Domaine de Saint-Paul, 102, route de Limoux, F-78470 Saint-Rémy-lès-Chevreuse

G. M. Newman
The Steel Construction Institute
Silwood Park, Ascot SL5 7QN, Berkshire, United Kingdom

Contract No 7210-PR/112
1 July 1998 to 30 June 2002

Final report

Directorate-General for Research

2004 EUR 20953 EN

Europe Direct is a service to help you find answers to your questions about the European Union

Freephone number:
00 800 6 7 8 9 10 11

A great deal of additional information on the European Union is available on the Internet. It can be accessed through the Europa server (http://europa.eu.int).

Cataloguing data can be found at the end of this publication.

Luxembourg: Office for Official Publications of the European Communities, 2004

ISBN 92-894-0749-2

Printed in Luxembourg

PRINTED ON WHITE CHLORINE-FREE PAPER

Abstract

The Cardington pilot project (CARD(1)) has shown that, under circumstances, it is not necessary to apply passive fire protection on composite steel framed buildings exposed to natural fires. In the scope of the present project (CARD(2)), the conditions under which the floor beams can remain unprotected, are reviewed more precisely. For this end, numerical design tools - suitable for the structural fire safety design of buildings of the type investigated in the CARD(1) project - have been selected/further developed. These tools have been used to undertake a parametric study into the effect of the factors influencing the structural behaviour under natural fire exposure. The outcomes have been generalised were possible. Also, a design procedure has been developed, with a view to systematically identify the options for leaving the steel beams unprotected and to identify necessary (additional) fire safety measures, if any.

More in particular, the research has resulted in the following:

- Three operational FEM computer codes are available for the structural response of 3D composite steel framed buildings exposed to natural fire conditions; these codes have been validated for their intended use and also the mutual consistency between the models has been demonstrated.
- The above FEM computer codes form, in combination with computer codes for fire models and for thermal response models developed in the scope of previous ECSC projects, a set of operational design tools for the prediction of the structural behaviour of composite steel framed buildings exposed to natural fire conditions.
- A set of parameters, affecting the possible use of unprotected steel beams in composite steel framed buildings has been identified and their effect is demonstrated in quantitative terms.
- From the above analysis, it follows that the most important parameters are the fire load density and the so-called opening factor (representing the ventilation conditions). Other investigated parameters are:
  - Mechanical loading.
  - Amount of reinforcement.
  - Choice of structural grid system.
  - Type of concrete (normal weight vs. light weight).

  The effect of the latter parameters appears often to be rather limited.
- A design procedure has been developed with a view to assess possible use of unprotected steel beams in composite steel framed buildings.
- Key design parameter in the above design procedure is the fire load density. The other parameters mentioned above are mainly used for fine-tuning, if necessary.
- The design procedure includes the possibility to specify additional (active) fire safety measures, where appropriate; the latter option is mainly based on earlier ECSC work, carried out in the scope of the Natural Fire Safety Concept project.

A Design Guide, meant for architects, designer and (structural) fire safety engineers, has separately been published, with emphasis on the practical aspects of research carried out.

Part 1: Design tools for the behaviour of multi-storey steel framed buildings exposed to natural fire conditions (CARD2)

Table of contents

Annexes

1. Introduction

1.1 Aim

Traditionally, the fire resistance of load-bearing structures is assessed by considering the behaviour of single structural components, rather than the whole structure. Also, strongly schematised, standard fire conditions are taken into account. This approach is quite conservative for modern steel framed structures, as experience in real fires shows (Broadgate, London [1]). Recent large scale fire tests confirm this (Cardington LBTF Demonstration Project [2], ECCS; BRP, Australia [3]).

More in particular, the Cardington LBTF Demonstration project has shown that, under well monitored, fully developed fire conditions, the floors and steel beams of composite steel framed buildings may remain unprotected, without failure of the building structure. However, with a view to use these results for practical design purposes, the conditions under which such conclusions hold, need to be specified more precisely. This is the challenge of the underlying research project, which - because of the close relationship with the Cardington LBT Demonstration Project - will be referred to as the "Cardington (2) project", shortened to: CARD(2).

One of the main objectives of the CARD(2) project is, therefore, to provide operational design guidance with regard to the structural behaviour of multi-storey composite steel framed buildings under natural fire conditions. This guidance is to be obtained by means of a series of computer simulations of the thermal and mechanical response of multi-storey steel framed, composite metal deck buildings, in which parameters such as fire load density, location & size of the fire compartments, the mechanical loading etc., are systemically varied (termed a parametric study).

Tools for the above simulations are computer models by which the (natural) fire exposure and the thermal and mechanical response of the structure are predicted.

For the parametric study, a great deal of calculation is required. Therefore the models must be capable of carrying out their calculations in reasonable (i.e. limited) time. Also it is important that simulation of the same case, using different models, must lead to similar results. Meeting the above two conditions is no problem for the fire and thermal response models, since sufficient experience has been obtained in earlier ECSC projects. This has not however proven to be the case for the structural response models. Consequently, much attention has been paid to the development and verification of structural response models, necessary for performing the parametric study.

This Final Report is meant as a scientific & technical declaration of the work carried out in the scope of the CARD(2) project. As such, the report emphases on a systematic description of the efforts to develop and verify the above mechanical response models. The set up of the parametric study will be discussed in detail and a systematic overview of the calculation results will be presented. The design recommendations following from the CARD(2) project will be presented in a summary way only. For details refer to a Design Guide, which provides more general information and is addressed to end users, such as architects, designers and structural fire safety engineers. This Design Guide has been issued as a separate delivery of the project.

1.2 Set up

To date, advanced numerical models are available, validated against full-scale fire tests. Ideally, a parameter study with these models should be carried out with a view to investigate the influence of all relevant parameters. It appears however, that this is not feasible, because of the large amount of computer time involved. Therefore, a methodology is put forward in which - based on the advanced rigorous numerical models - more simple models are developed, which can readily be used as design tools. Also, a number of design scenarios have been identified, representative for modern steel framed buildings. Based on these design scenarios, a parameter study is performed, using the streamlined numerical models, with a view to deduce practical design guidance. See Fig. 1.

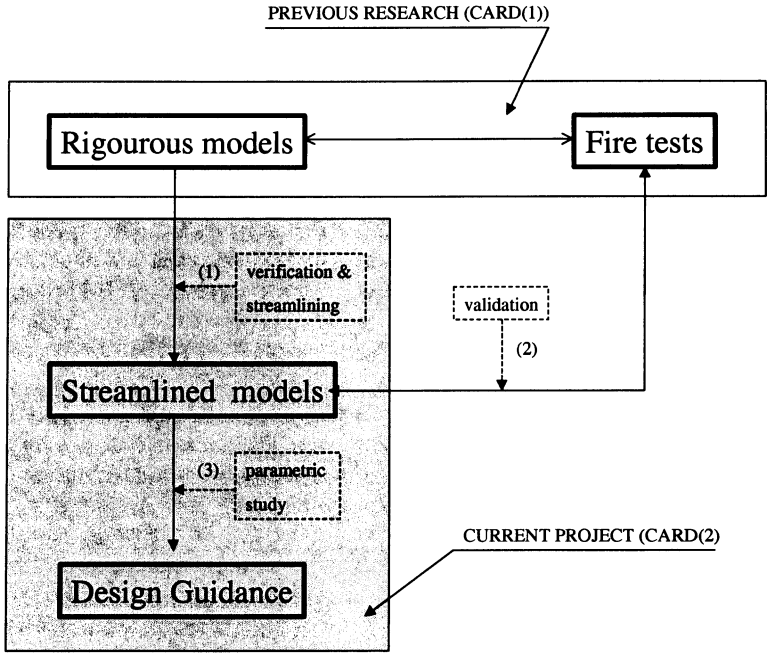

Fig. 1.1: Set up of the CARD(2) project

The following steps are considered:

(1) Evaluation of the available rigorous numerical models and the identification of design scenarios.

(2) Stream lining of the available rigorous models and their validation; also their suitability for the envisaged parametric study should be verified.

(3) Identification of design scenarios and the performance a parametric study with the stream lined models.

(4) Analysis of the outcomes of the parametric study, in view of current fire safety engineering practice.

Main deliveries of the study are this Final Report and a Design Guide, in which the practical outcomes of the project are presented for architects, designers and structural fire safety engineers.

1.3 Management review

The following organisations have participated in the project:

- Corus (former British Steel, UK)
- CTICM (France)
- ProfilArbed (Luxembourg)
- TNO (convenor, The Netherlands)

The University of Edinburgh (Edinburgh) and the Steel Construction Institute (London), acted as sub contractors on behalf of Corus.

As a platform for decision making and to monitor the progress, a Steering Committee has been established, in which all partners and sub-contractors are represented. The membership was as follows:

- L-G. Cajot ProfilArbed
- M. O'Connor Corus
- L. Twilt (chairman), C. Both, A. Breunesse TNO
- A. Usmani, M. Rotter UoE
- B. Zhao, J. Kruppa CTICM

In addition, the following 2 Working Groups have been set up for detail discussion on work level:

- WG (1) Modellers Group: TNO, Corus, CTICM, UoE
- WG (2) Parametric Study Group: TNO, SCI, ProfArbed, UoE

The Steering Committee has met 13 times. For an overview of dates and meeting places, refer to Table 1. The Working Groups normally met in conjunction to a meeting of the Steering Committee.

Table 1.1: Meetings Steering Committee

meeting no.	date(s)	place	country
1	March 11, 1999	Rijswijk	NL
2	September 2, 1999	Paris	F
3	March 2, 2000	London	UK
4	May 16, 2000	Paris	F
5	September 22, 2000	Luxembourg	L
6	March 2, 2001	London	UK
7	May 18, 2001	London	UK
8	August 20, 2001	Rijswijk	NL
9	February 8, 2002	Paris	F
10	April 16, 2002	London	UK
11	June 6, 2002	Rijswijk	NL
12	September 3, 2002	Paris	F
13	November 28, 2002	London	UK

The project duration was originally scheduled for three years, starting on 30-06-1998. However, by the beginning of 2001 it became clear that the work could not be completed in the anticipated time frame. Main reason were the complications experienced when verifying (the suitability) of the streamlined versions of the rigorous models for mechanical response. See also the discussion in chapter 3. Therefore, a request has been put forward to the European Commission, DG RTD.G3, with a view to obtain an elongation of the project duration by on year, i.e. till 30-06-2002. This request was granted.

During the project, semi annual reports have been produced, describing the progress & perspectives with regard to the preceding 6 months. For an overview, refer to Table 2.

Table 1.2: Semi annual reports

no.	period	reference	date
1	01-07-1998 / 31-12-1998	TNO report 1999-CVB-R1009	22-04-1999
2	01-01-1999 / 30-06-1999	TNO report 1999-CVB-R2113	11-01-1999
3	01-07-1999 / 31-12-1999	TNO report 2000-CVB-R00684	26-04-2000
4	01-01-2000 / 30-06-2000	TNO report 2000-CVB-R01733	26-09-2000
5	01-07-2000 / 31-12-2000	TNO report 2001-CVB-R03028	30-03-2001
6	01-01-2001 / 30-06-2001	TNO report 2001-CVB-R04167	24-09-2001
7	01-07-2001 / 31-12-2001	TNO report 2002-CVB-R05261	30-09-2002
8	01-01-2002 / 30-06-2002	TNO report 2002-CVB-R06144	30-09-2002

This Final Report was written by L. Twilt, and supervised by an Editing Committee with the following membership:

- L-G. Cajot ProfilArbed
- G. Newman SCI
- M. O'Connor Corus
- L. Twilt (chairman) TNO
- A. Usmani University of Edinburgh
- B. Zhao CTICM

2. Models needed

2.1 Overview

For a complete analysis of the structural behaviour of composite steel framed building under natural fire conditions, the following computer models are needed:

- a fire model, by which the temperature development in the fire compartment is predicted as function of the various parameters involved (dimension & lay out of the fire compartment, fire load density, ventilation conditions etc.);
- a thermal response model, by which the temperature distribution & development in the various structural elements (beams, columns, slabs) is predicted, given the thermal loading;
- a mechanical response model, by which the structural performance (deflections, deformations, moment distribution etc.) is predicted, given the thermal response.

As far as the fire and thermal response models are concerned, use is made of computer codes, developed in the scope of earlier ECSC projects: OZONE, for the fire models (ref. project 7210-SA/125, 126 ...) and CEFICOSS[1], for the thermal response (ref. project 7210-SA/502). Hence, in this Final Report, these models will only be discussed in a summary way.

For mechanical response models, use is made of advanced computer codes, developed elsewhere. Three such codes have been selected:

- DIANA, in use at TNO (NL);
- ANSYS, in use at CTICM (F);
- ABAQUS, in use at CORUS (UK).

The development of structural response models has turned out to be much more complex than was originally envisaged, mainly because the adopted international standard advanced programs have only recently been used in fire applications involving real, three dimensional buildings. One consequence of this has been that the structural models needed significant "streamlining" in order to obtain results in reasonable calculation times without compromising their predictive capability. Another concern was to check the trustworthiness of the final versions of the three above mentioned mechanical response models by verifying that the three models produce the same predictions when applied to a tightly defined problem. This implies the need to specify very carefully a calibration case as well as the working procedures. See chapter 3.

2.2 Fire model

The computer code OZone V2 has been developed to help engineers in designing structural elements submitted to compartment fires [4]. The code is based on several recent developments regarding compartment fire modelling on one hand and regarding the effect of localised fires on structures on the other hand. It includes a single compartment fire model that combines a two-zone model and a one-zone model.

OZone is composed of a main model, which includes:

- A two-zone model (compartment and partitions).
- A one-zone model (compartment and partitions).
- A model to switch from the two-zone to the one-zone model.

Some sub-models are connected to the main model. Submodels enable the evaluation of:

- The heat and mass transfer between the inside of the compartment and the ambient external environment through vertical, horizontal and forced vents (vent model).
- The heat and mass produced by the fire (combustion model).
- The mass transfer from the lower to the upper layer by the fire plume (air entrainment model).

Fig. 2.1 shows a schematic view of the two-zone model and its sub-models for heat and mass transfer.

---

[1] In a later stage of the project, CEFICOS is replaced by SAFIR, which can be considered as a "successor" of CEFICOS; both codes are developed at the University of Liege.

In the two-zone model, the compartment is divided in an upper and a lower layer. In each layers the gas properties (temperature, density...) are assumed to be uniform. The pressure is assumed to be constant throughout the whole compartment volume (except when evaluated mass exchange through vents).
The layers are separated by an adiabatic horizontal plane (at height Z_s). An air entrainment model only connects them. An air entrainment model is an empirical model, which enables the estimation of the rate of mass entrained from the lower to the upper layer by buoyancy in the fire plume. The plume volume is not considered (no mass or heat balance is calculated on it). It is thus included in the lower layer volume.

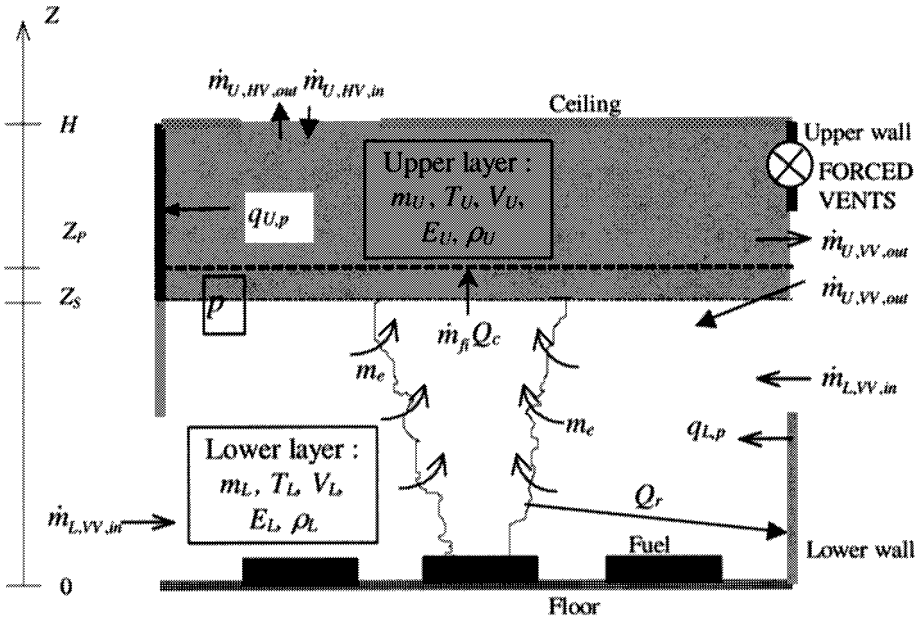

Fig. 2.1: Schematic view of two-zone model and associated submodels

The upper zone is supposed to be opaque and upper layer partitions (wall and ceiling) are connected to it by radiative and convective heat transfers. The lower layer is clear and convective heat transfer connects lower layer partitions to it. Vertical partitions are thus divided in 2 parts, one in the lower layer and one in the upper layer. The height of the two parts is equal to the relative zone height. These heights are varying with time.
The fire is defined by its rate of mass loss, its rate of heat release (*RHR*) and its area. Q_c is the convective part of the *RHR* and Q_r is the radiative part of the *RHR*. Q_c is often in the range of 0.6 to 0.8 *RHR* and has been fixed in the code to 0.7 *RHR*. The radiative part is thus fixed to 0.3 *RHR*. In this model Q_c is transmitted to the upper layer and Q_r to the lower layer partitions (through a source term in the lower layer partition formulation). In the lower layer, the heat is thus transferred by radiation from the fire to the lower layer partitions and then transferred by convection from the partitions to the lower layer and by conduction within the partitions.
Heat and mass transfer through horizontal, vertical and forced vents are exchanged with the layer at the same height, with some exceptions (vertical vent and forced vent close to the zone interface) where the incoming air is always added to the lower layer.
Some switch criteria are defined so that they represent a limit beyond which one-zone model assumptions becomes closer to the physics of the fire situation than the two-zone model ones. If during a two-zone model simulation, a switch criterion is met (time t_s), the two-zone model is left and replaced by a one-zone model. The switch is made so that the total energy and mass present in the 2ZM system at time of switch are fully conserved in the 1ZM system, Fig. 2.2.
Fig. 2.3 shows a schematic view of the one-zone model and its sub models for heat and mass transfer. In the one-zone model, a single zone represents the compartment. In this zone the temperature and density are assumed to be uniform. The pressure is assumed to be constant on the whole compartment volume (except while evaluating mass exchange through vents). The zone is supposed to be opaque and radiative and convective heat transfers connect partitions to it.

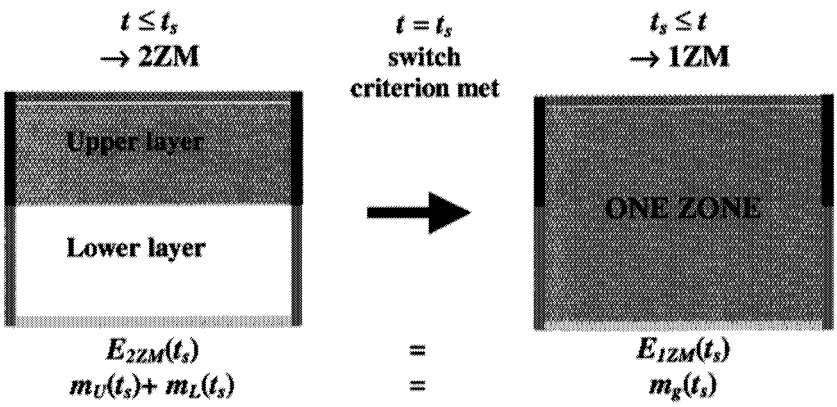

Fig. 2.2: Transition from 2ZM to 1ZM

The fire is defined by its rate of mass loss, its rate of heat release and its area. All mass and energy coming from the fire are added to the single zone.
Heat and mass transfer through horizontal, vertical and forced vents are exchanged with the single zone.

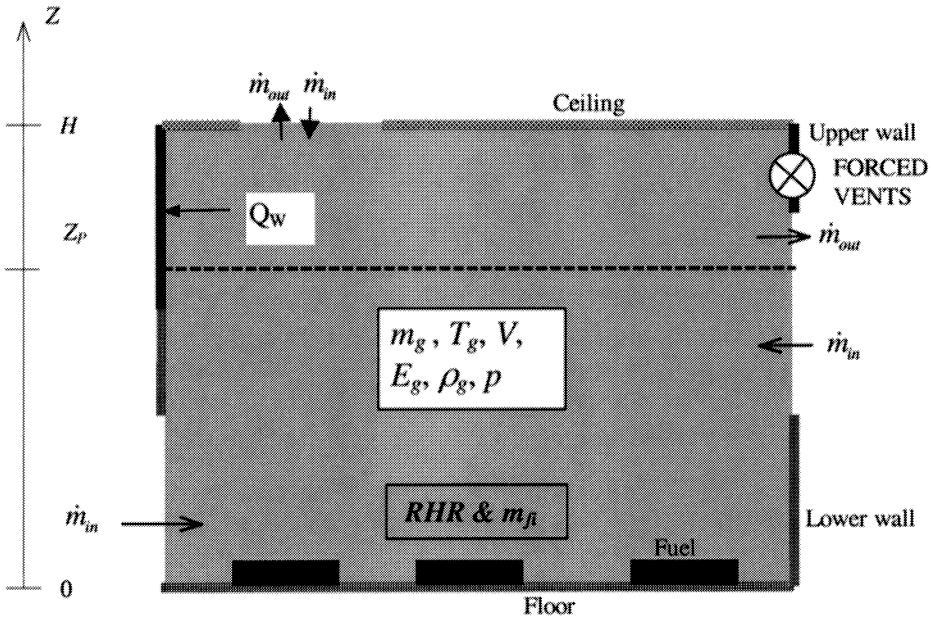

Fig. 2.3: Schematic view of one-zone model and associated sub-models

In 2ZM as well as in 1ZM, the fire is defined by a heat release rate, rate of mass loss and fire area curves function of time. These three curves have to be defined by the user. The input curves correspond to fuel controlled fire, i.e. to the fire, which would occur without any influence of the compartment. These curves are automatically modified if the ventilation is limited (combustion models) or if gas temperature is sufficiently high to ignite the fuel (flash-over).

2.3 Thermal response model

Two models have been used: CEFICOSS and SAFIR[2].

The main part of the results has been provided by SAFIR due to the fact that the complex cross section, including trapezoidal steel sheet, is more adapted to the Finite Element Method (used in SAFIR) than to the Finite Difference Method (used in CEFICOSS)

- *CEFICOSS [5]*

CEFICOSS stands for Computer Engineering of the FIre resistance of Composite and Steel Structures. This two-dimensional numerical program performs a step-by-step simulation of the behaviour of columns, beams or plane frames submitted to the fire.

The thermal part of the program calculates the temperature distribution in the cross-sections of the structure for different instants. As rectangular meshes discretise the sections, it is possible to analyse various shapes of pure steel, reinforced concrete or composite steel-concrete sections. The transient conductive equations are solved by an explicit finite difference scheme, the time step of which being automatically calculated in order to ensure convergence with the shortest computing time. As thermal conductivity and specific heat of the building materials are temperature dependent, this time step varies during the calculation.

The boundary conditions are convection and radiation or symmetry. The temperature of the gases with various possibilities represents the outside world: ambient temperature, ISO curve or any other curve natural including a cooling down phase. Evaporation and transportation of the moisture in wet materials is considered.

- *SAFIR [6]*

SAFIR is a special purpose computer program for the analysis of structures under ambient and elevated temperature conditions. The program, which is based on the Finite Element Method, can be used to study the behaviour of one, two and three-dimensional structures.

The thermal analysis is usually performed while the structure is exposed to fire. For a complex structure, the sub-structuring technique is used, where the total structure is divided into several substructures and a temperature calculation is performed successively for each of the substructures. This kind of situation does arise in a structure where the members are made of different section types, or made of sections submitted to different fire exposures. The thermal analysis is made using 2-D SOLID elements, to be used later on cross sections of BEAM elements or on the thickness of SHELL elements.

a) **Temperatures in beams**
   The temperature is non-uniform in the sections of the beam, but there is no heat transfer along the axis of the beams.

b) **Temperatures in shells**
   The temperature is non-uniform over the thickness of the shell, but there is no heat transfer in the plane of the shell. The temperature analysis is performed on a section having the thickness of the shell and an arbitrary width, 1cm for example.

In this research, CEFICOSS and SAFIR have not been used for structural analysis. Only the thermal module has been activated and has provided 2D-temperature field in the cross section of the structural elements.

[2] See also the note on page 11

2.4 Mechanical response models

- *DIANA*

DIANA is a general-purpose three-dimensional finite element programme, suitable for the simulation of the thermal and structural response of structures including physical and geometrical non linear behaviour, dynamic effects and time and temperature dependent problems [7].

Default models are available for concrete and steel among other materials such as non linear elasticity models, plasticity models according to various yield contours like Tresca, von Mises and Drucker Prager, all facilitating hardening/softening, and concrete crack models based on discrete cracks, smeared cracks, total strain concept or the Rankine plasticity concept, all of which can be combined with various softening branches. All these models can be temperature dependent and also thermal expansion and transient creep can be included. Furthermore, maturing and aging phenomena such as shrinkage and creep can be included. For steel-concrete interfaces, special models are available, including bond-slip, gap analyses, contact analyses, dry friction and non linear springs.

Actually, steel has been modelled with a von Mises yield contour including hardening according to Eurocode 4. Concrete has been modelled with a Drucker-Prager yield contour for compression including hardening. After evaluation of the effect of the inclusion of cracking, it appeared that the effect on the response was minimal while the effect on the numerical stability was detrimental. Therefore, in the end, no additional cracking criterion was applied.
Various types of elements are available in DIANA, such as springs, trusses, beams, plates, shells, plane stress elements, plane strain elements and solids. In modelling the Cardington building, steel members such as beams and columns and ribs of steel-concrete composite slabs are being modelled with numerically integrated curved beam elements. These beam elements can be subdivided into zones to describe the actual cross sectional shape. Over each zone a time dependent temperature and temperature gradient can be prescribed. The slabs have been modelled with numerically integrated curved shell elements, also provided with temperatures and temperature gradients. In both beam and shell elements, embedded reinforcement was placed were appropriate.
If two structural elements are connected to the same node, all degrees of freedom, i.e. the displacements and rotations, are compatible. If appropriate, the joints between structural elements have been modelled as hinges or with different nodes that were tied only for the required degrees of freedom. Alternatively, spring elements or interface elements could have been used.

The simulations have been carried out in an incremental-iterative way. First the mechanical load has been applied. Hereafter, time has been increased incrementally. In each time step, the temperatures increase according to the results of the thermal response analyses. The temperature increase results in thermal expansion and degradation of the mechanical properties. Within each time or load step, the equilibrium has been searched in an iterative way using a secant stiffness approach. Within each iteration, the strain decomposition in each element is also carried out in a iterative way.

- *ANSYS*

ABAQUS ANSYS is a general finite element computer code capable of dealing with multi-physical problems such as heat transfer, structural mechanics, fluid mechanics, electro-magnetic, explicit dynamics etc. [8].

In the parametric analysis of this project, three types of elements are used:

- BEAM24 : 3D beam element with both material and geometric non-linear capabilities;
- SHELL91: multi-layer shell element with both material and geometric non-linear capabilities;
- PIPE16: pipe beam element with linear and elastic capabilities.

The element BEAM24 is used to model the steel beams, columns and ribs of composite slabs as well as steel sheet. The element SHELL91 is used for modelling the solid part of composite slabs with the reinforcement represented by one of five layers. The element PIPE16 is adopted to model the connection between steel beams and composite slabs. It is nearly an infinite rigid element in order to represent a full connection between beams and slab (see Fig. 2.4).

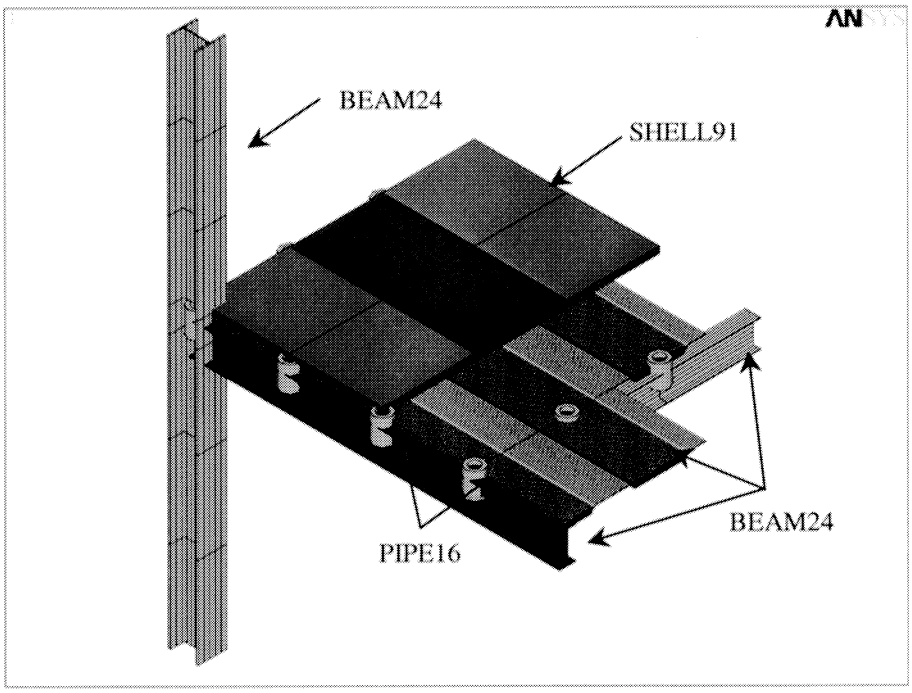

Fig. 2.4: ANSYS modelling of composite floor system

The section mesh technique used in ANSYS for beam elements is very similar to that of DIANA.

Concerning the material laws, they are fully temperature dependent. A multi-linear stress-strain relationship with Von Mises yield surface and isotropic hardening flow rule is adopted for steel. As far as concrete is concerned, it is represented with bi-linear stress-strain relationships using Drucker yield surface with a non-associated flow rule.

In ANSYS modelling, steel members and composite slab of the same floor are considered to locate at different levels corresponding to their real physical positions. The simple joints between steel members (beam-column, beam to beam, etc) are modelled using coupled DOF technique.

The numerical simulation is fully based on incremental static analysis with full New Raphson method combined with scaled displacement vector technique (line search option).

- ***ABAQUS***

ABAQUS/Standard is a general-purpose finite element program designed specifically for advanced analysis applications. A wide variety of problems can be addressed with the available modelling tools. ABAQUS/Standard is designed to run effectively on computers ranging from notebooks and desktop systems through workstations and high-end multi-processor servers, running various Windows, UNIX, or LINUX operating systems [9].

ABAQUS/Standard provides a variety of time- and frequency-domain analysis procedures. These procedures are divided into two classes: "general analyses," in which the response may be linear or nonlinear, and "linear perturbation analyses," in which linear response is computed about a general, possibly nonlinear, base state. A single simulation can include multiple analysis types.

Material models are provided for metals, hydrostatic fluids, rubber, plastics, composites, resilient and crushable foams, concrete, sand, clay, and jointed rock. The material response for each of these models may be highly nonlinear and temperature dependent. General elastic, elastic-plastic, and elasto-viscoplastic behaviors are provided. Both isotropic and an isotropic behavior can be modeled. User-defined materials can also be created with a subroutine interface.

Structures and continua can be modeled. One-, two-, and three-dimensional continuum elements are provided, as well as shells, membranes, beams, and trusses. The beam and shell elements are based on

modern discrete Kirchhoff or shear flexible theories and are very cost-effective. Shell elements are provided for heat transfer and stress analysis, which makes it straightforward to analyze shell structures subjected to thermal loads. Several other specialized elements are available to accurately model different types of components. ABAQUS/Standard is a modular code: any combination of elements, each with any appropriate material model, can be used in the same analysis.

All elements in ABAQUS/Standard (except for some special-purpose elements) are formulated to provide accurate modeling for arbitrary magnitudes of displacements, rotations, and strains.

Boundary conditions can include prescribed kinematic conditions (single- and multipoint constraints) and prescribed foundation conditions. Loading conditions can include point loads, distributed loads, and thermal loading. A special tool for prescribing forces on assemblies allows direct specification of bolt or other fastener loads. Follower force effects such as pressure, centrifugal, and Coriolis forces are included where appropriate. Loads and boundary conditions for pore fluid pressure, electric potential, and other scalar fields are also available. Initial conditions for temperature, velocity, stress, and numerous other fields can be specified.

ABAQUS/Standard has general capabilities for modeling interactions between bodies, including surface-to-surface contact, with or without friction. Fully coupled thermal-stress interfaces are provided, where heat and traction may both be transmitted and where the thermal resistance of the interface may depend on the pressure between contacting surfaces or the mechanical separation of the surfaces. Surface-based interactions are available to couple structural and acoustic medium models for dynamic and vibration analysis. Coupled pore fluid flow-stress and coupled thermal electrical interactions are also available.

3. Evaluation of the mechanical response models

3.1 Overview

For reasons explained in section 2.1, the evaluation of the models needed in the scope of the underlying research will be limited to the mechanical response models, i.e. DIANA, ABAQUS and ANSYS The discussion is focused on the following issues:

- Validation of the original versions of the mechanical response models;
- "Streamlining" of the original versions, in order to make them suitable for parametric study purposes;
- Check on consistency of the streamlined versions.

3.2 Validation of the original mechanical response models

Validation of the original mechanical response model is necessary, since these models have been developed for normal conditions of use (i.e. room temperature conditions). With none of the used models extensive experience is available to predict the mechanical response of 3D structural systems under fire conditions. The following validation cases have been chosen:

- Validation case I: 2 D composite slab (unrestrained)
- Validation case II: 2D steel frames
- Validation case III: 3D composite frame (restrained)

In the subsequent discussion, each of the above validation cases will briefly be discussed. In the cases I and II, the discussion is limited to the validation the DIANA and ABAQUS codes. In the last and most relevant validation case (i.e. 3D composite restrained frame), also the calculation results obtained by ANSYS have been taken into account[3]

Ad. Validation case I: 2D composite slab (unrestrained)

Considered was a fire test on a continuous span slab, consisting of two end-spans, with a draped reinforcement mesh, carried out at TNO [10]. The static system and loading conditions are depicted in Fig. 3.1. To optimise the fire behaviour with one reinforcement mesh, the mesh was draped, as shown. In the left span (I), the mesh was fastened to the upper flanges of the steel decking. In the right span (II), the concrete cover, measured from the unexposed side at midspan was 55 mm. For other details refer to [10]. The thermal response was simulated with DIANA on the basis of average measured steel decking temperatures and average measured temperatures at the unexposed side. Actual average mechanical material properties measured under ambient conditions were used. With respect to the mechanical material properties at elevated temperatures, the relations as put forward in Eurocode 3 [11] and 4 [12] were adopted.

[3] Reason is that in the first phase of the project significant problems have been encountered when applying ANSYS for elevated temperature conditions. See e.g. Annex 2 of the 2nd semi annual report. After solving these problems (see next section) it has – for practical reasons – been decided not to carry out the ANSYS validation analysis for cases I and II, but to concentrate on validation case III.

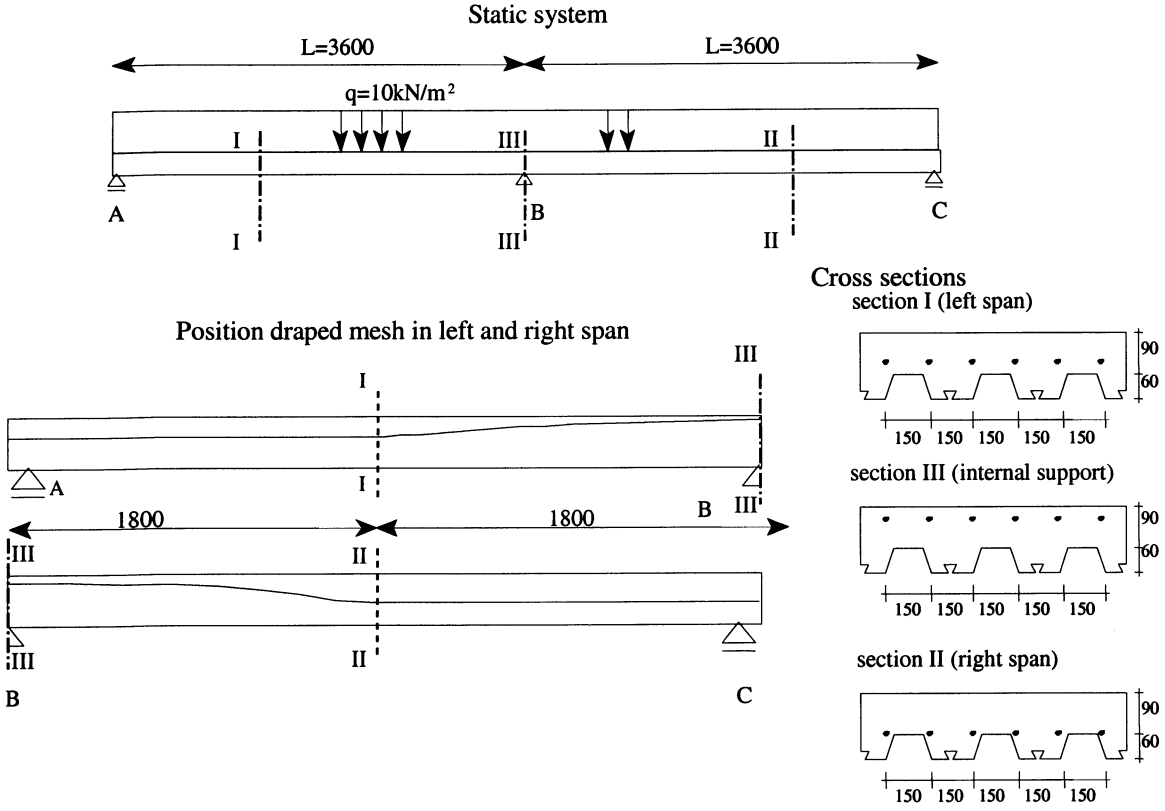

Fig. 3.1: Validation case I: unrestrained composite slab; static system

Numerical results in terms of measured end-support forces and mid span deflections obtained with a DIANA numerical model comprising of CL18B beam elements are compared to experimental results in figs. 3.2 and 3.3. From the comparison it can be seen that the numerical model satisfactorily predicts the flexural behaviour. Moreover, the-run-a-way conditions (where relevant, see left span) are in reasonable agreement with experimental findings.

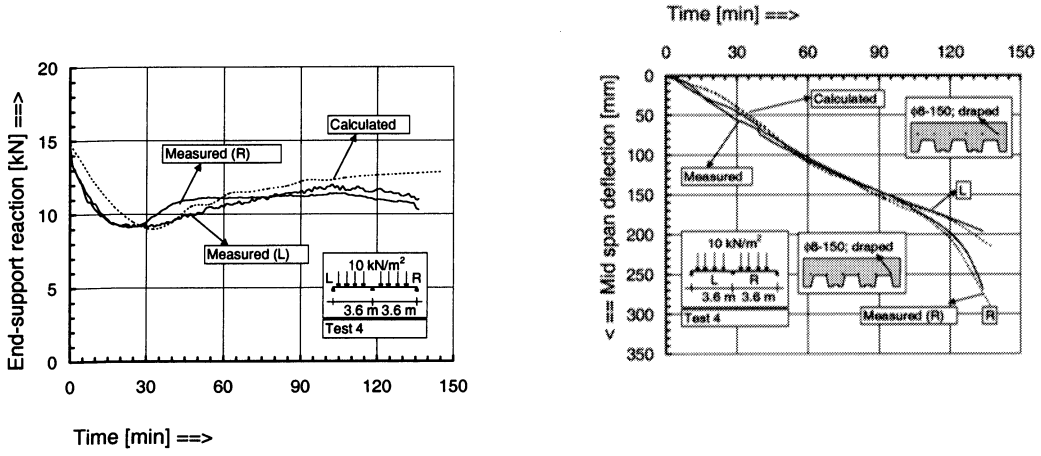

(a) measured vs. calculated reaction forces

(b) measured vs. calculated deflections

Fig. 3.2: Validation unrestrained composite slab (DIANA)

Starting point of the ABAQUS analysis was the thermal response, calculated by DIANA (see above). In the ABAQUS analysis, the slab was modelled using three nodded beam elements with the lower ribbed section simplified to a rectangular section. Beam elements were also used to model the steel profile ribbed deck with its cross section representing ribbed profile using co-ordinates of each corner of the rib section detail. The deck was tied to the concrete slab using constrained conditions. The rebars, which –as mentioned before - were draped to different depths on either side of the mid support, were modelled using the rebar facility in ABAQUS. Non-linear spring elements were included at locations of max bending and hogging. The load was applied at eight evenly spaced points as described in the test details [10]. Temperature loading was applied at 15 minute intervals based on thermocouple readings from the test and applied to the five through thickness integration levels in the slab using an average from both the upper and lower ribs.

For some results, refer to Figs. 3.3[a,b]. The results showed good agreement between the calculated maximum deflections and end support reaction forces to the test results, thus verifying the capability of ABAQUS to model unrestrained conditions.

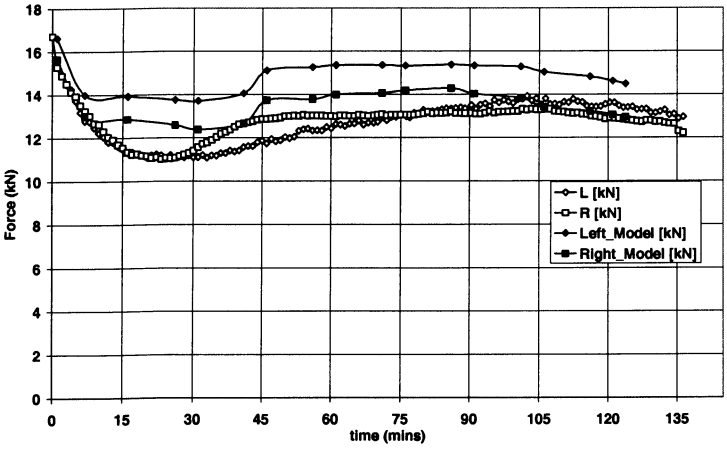

(a) measured vs. calculated reaction forces

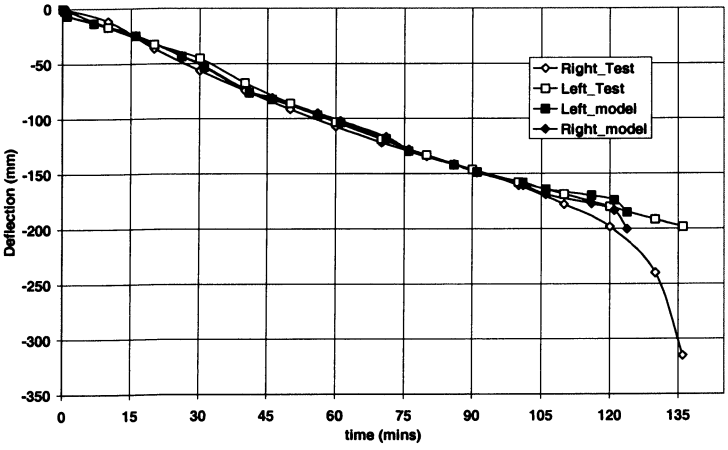

(b) measured vs. calculated deflections

Fig. 3.3: Validation unrestrained composite slab (ABAQUS)

ad. Validation case II: 2D steel frames

General

In the validation analysis of 2D steel frames three different situations have been considered:

- Case II[a]: 1 bay – 2 stories.
- Case II[b]: 2 bays – 1 storey (sway).
- Case II[c]: 2 bays – 1 storey (braced).

All tests have been carried out by CTICM in the seventies. Experimental results are only available in terms of temperature distribution in the steel elements and displacements of the beams. The steel temperatures measured during the tests haven been taken as input for the calculation of the mechanical response. Measured displacements of the beams have been compared with calculated displacements. For the mechanical properties of steel at elevated temperatures Eurocode values have been taken [11]. Alternatively, also the mechanical properties proposed by Anderberg, have been used [13]. See Annex A.

Case II[a]: 1 bay – 2 stories

The test results analysed in this paragraph refer to a test on a sway frame with one bay and two stories [14]. The dimensions of this frame as well as the loading condition are given in Fig. 3.4[a]. During the test, the frame is exposed to fire at the first level only (Fig. 3.4[b]); the second level is located outside the fire furnace. All steel elements are unprotected.

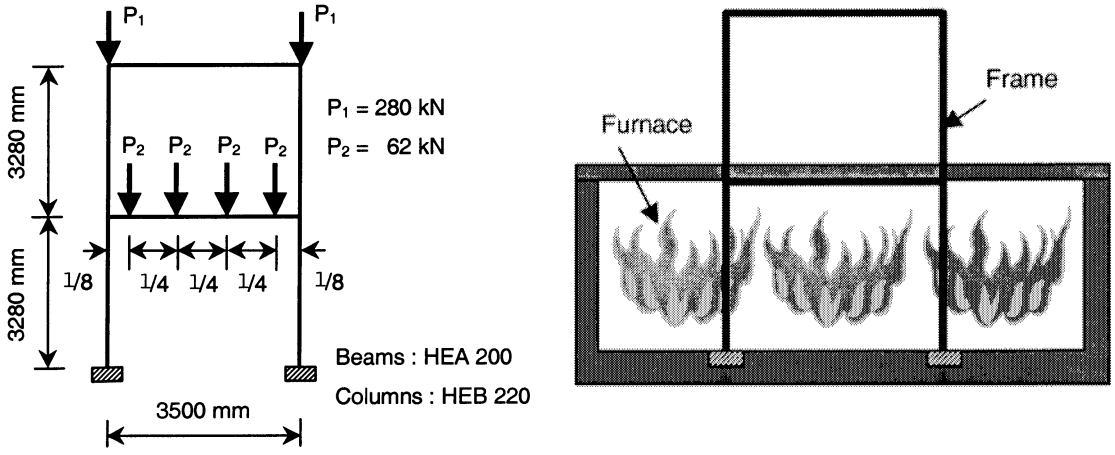

(a) static system

(b) heating conditions

Fig. 3.4: Validation case II: 2D steel frames; 1 bay – 2 stories

Temperature-deflection plots for various points on the frame are given in Figs. 3.5 (ABAQUS) and 3.6 (DIANA) together with measures values. Note that the displacements at the mid span measuring points (i.e. D2, D4) are fairly well described by both models. This holds in particularly for the run-a-way conditions. For the measuring points D1, D2 (i.e. on the spot of the columns), the agreement between test and calculation results (see Fig. 3.5, ANSYS only) is less satisfactory. However, the displacements at these points are relatively small and their relevancy is therefore doubtful. In all cases the calculation results on the basis of the EC material properties give more conservative results than those applying those using the proposal by Anderberg. Qualitatively, this can be explained by comparing the respective sets of stress strain diagrams. See Annex A.

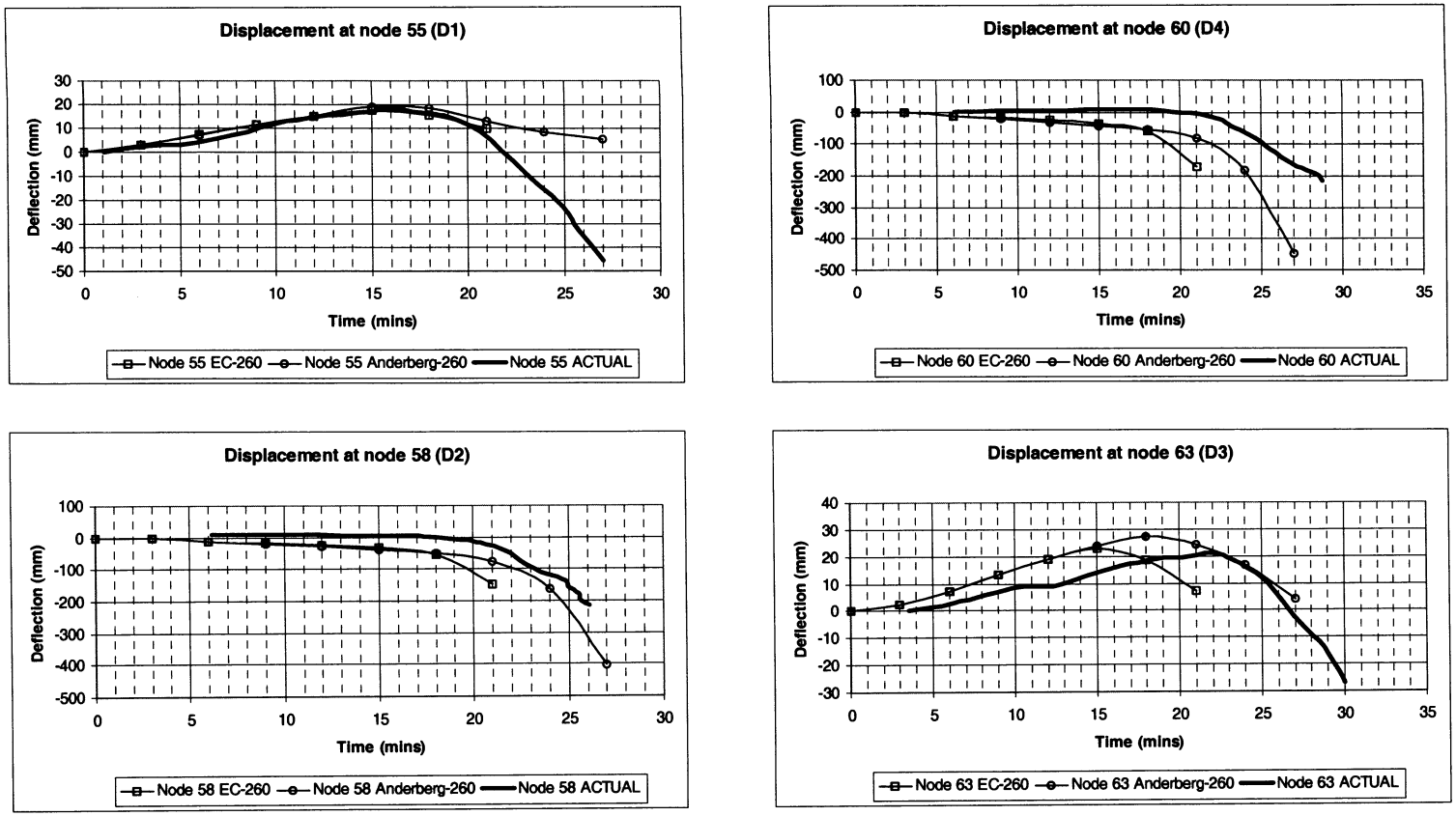

Fig. 3.5: Validation case II[a]: 2D steel frame: 1 bay – 2 stories; time displacement curves (ABAQUS).

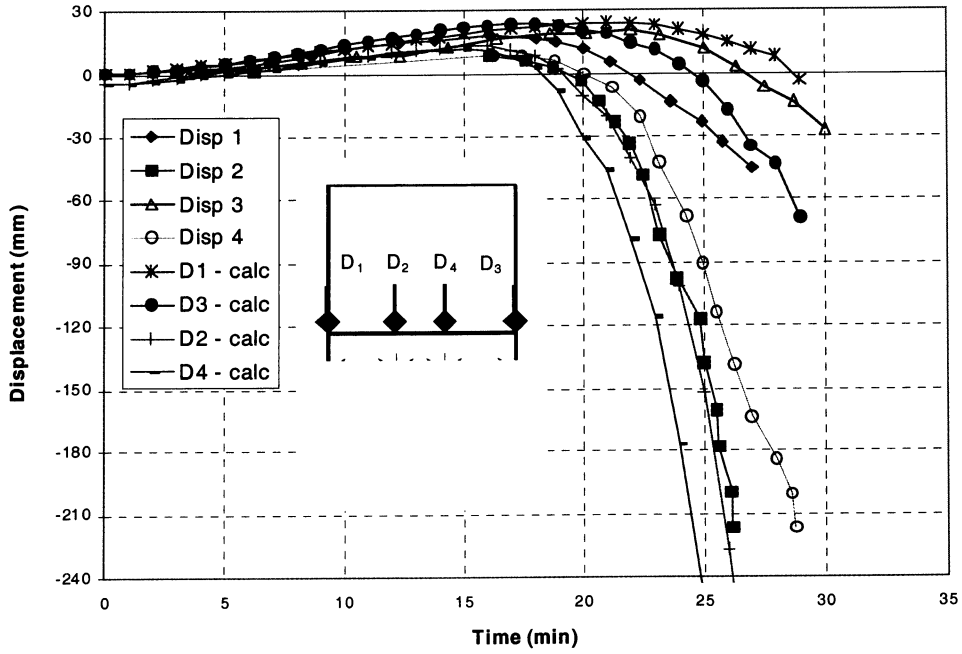

Fig. 3.6: Validation case II[a]: 2D steel frame: 1 bay – 2 stories; time displacement curves (DIANA)

Case II[b]: 2 bays – 1 storey (sway)

The test under consideration refers to a two-bay-one storey sway frame [14]. The dimensions of the frame as well as the mechanical loading conditions are given in Fig. 3.7[a]. During the test, all the steel elements of the frame are exposed to fire. The columns are exposed to fire from four sides; the beams from three sides only, by keeping their upper face unexposed. See also Fig. 3.7[b].

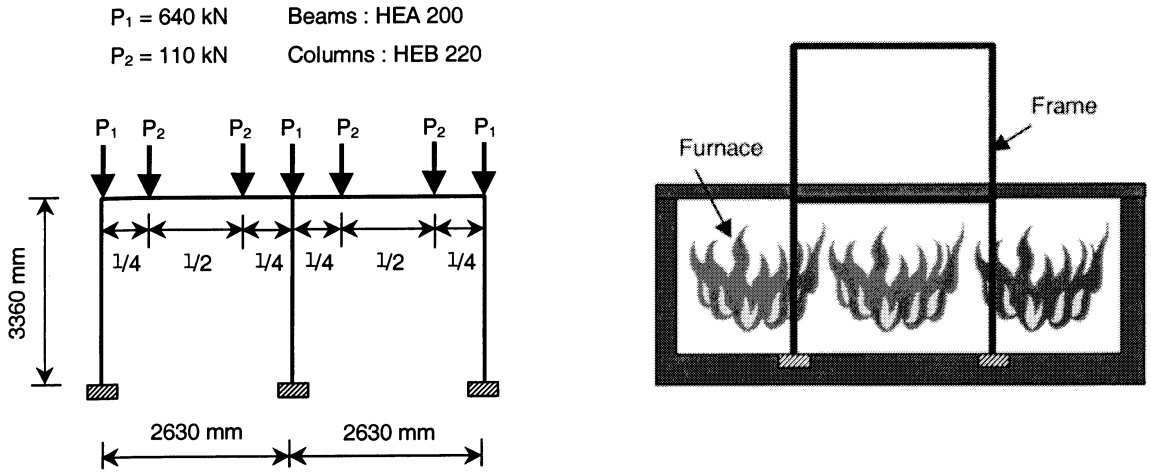

(a) static system

(b) heating conditions

Fig. 3.7: Validation case II[b]: 2D steel frame: 2 bays – 1 storey (unrestrained)

Temperature-deflection plots for various points on the frame are given in Fig. 3.8 (ABAQUS) and 3.9 (DIANA), together with measured values. Note that the measured deformation mode is asymmetric: only for the left hand bay, run-a-way conditions are approached during the test. These do, during the test, not occur in the right hand side bay. In the calculations, the run-a-way conditions of the left bay are reasonably well described by both ANSYS and DIANA. For the right hand bay, the computer models do not predict run-a-way conditions either[4]. As for case II[a], the EC-material properties of steel give rise to more conservative calculation results than those base on the proposal by Anderberg.

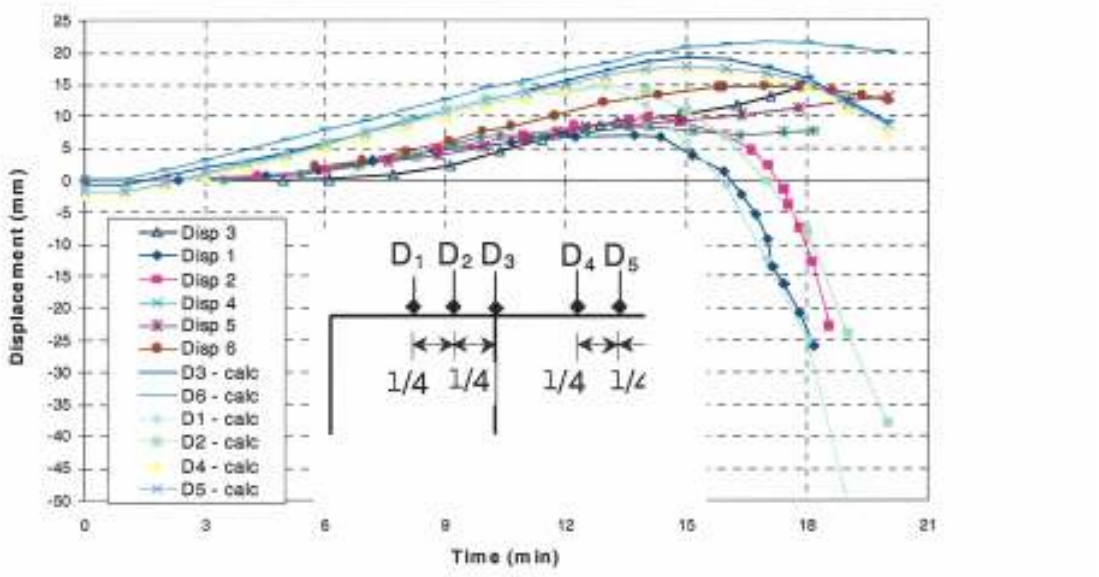

Fig. 3.9: Validation case II[b]: 2D steel frame: 2 bays – 1 storey (unrestrained); time-displacement curves (DIANA)

Case II[c]: 2 bays – 1 storey (braced)

The test under consideration refers to is a two-bay-one storey braced [14]. The dimensions of the frame as well as the mechanical loading conditions are given in Fig. 3.10[a]. During the test, all the steel elements of the frame are exposed to fire. The columns are exposed to fire from four sides; the beams from three sides only, by keeping their upper face unexposed (as in validation case II[b]). See also Fig. 3.10[b].

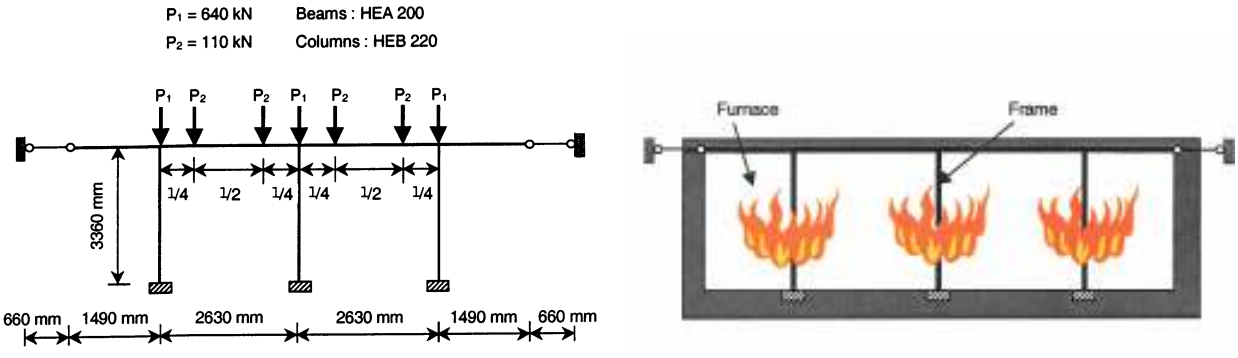

(a) Static system (b) Heating conditions

Fig. 3.10: Validation case II[b]: 2D steel frame: 2 bays – 1 storey (restrained)

[4] Note in this respect the difference in scale of the vertical axis for displacement curves for the left hand and for the right hand bay.

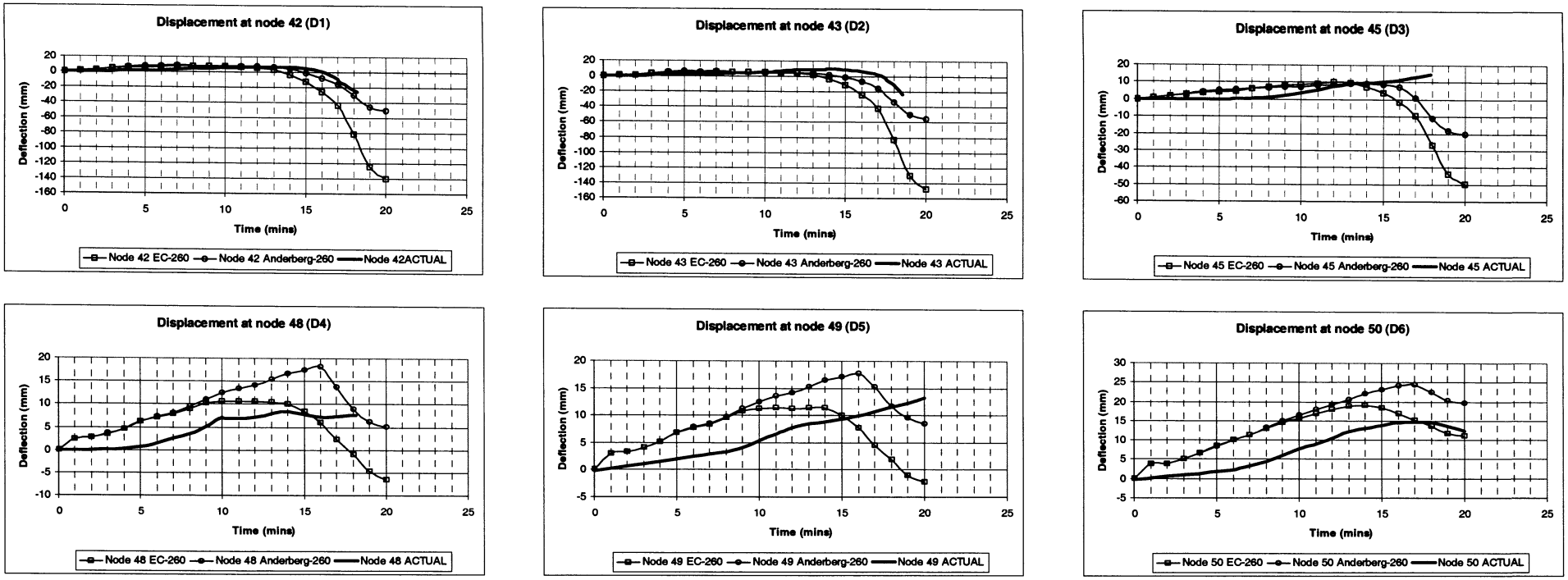

Fig. 3.8: Validation case II[b]: 2D steel frame: 2 bays – 1 storey (unrestrained); time-displacement curves (ABAQUS)

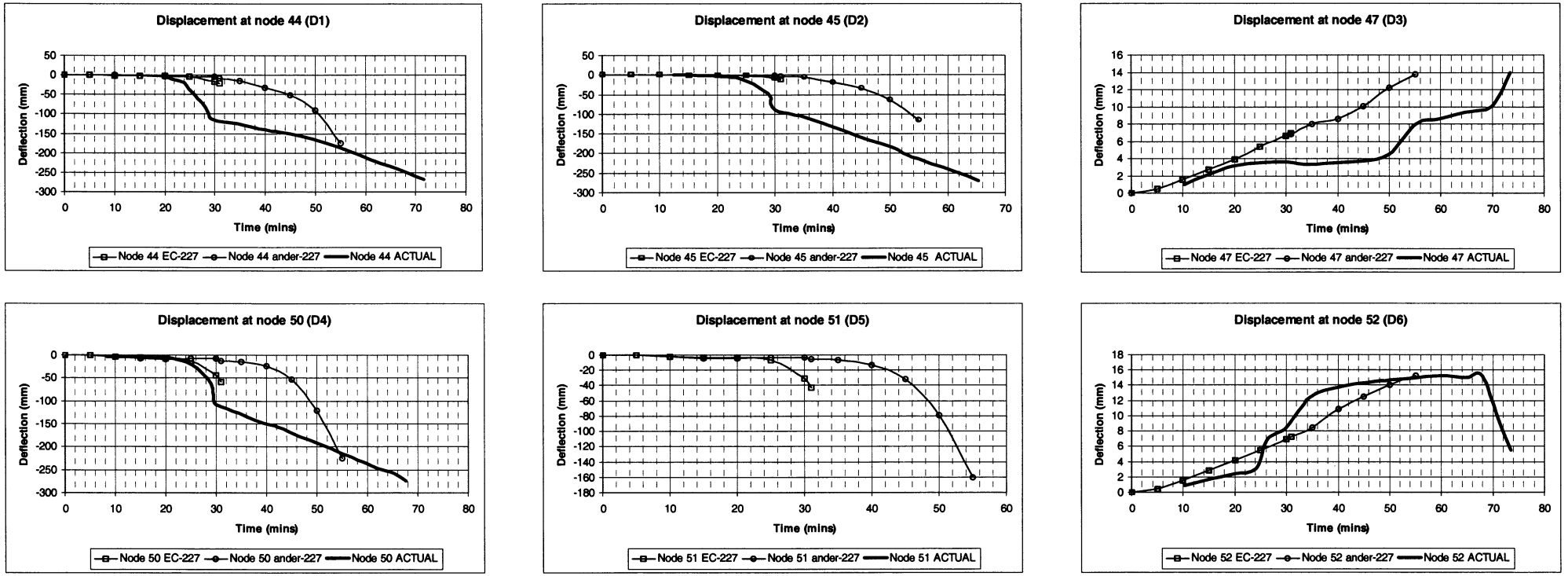

Fig. 3.11: Validation case III^c: 2D steel frame: 2 bays – 1 storey (unrestrained); time-displacement curves (ABAQUS)

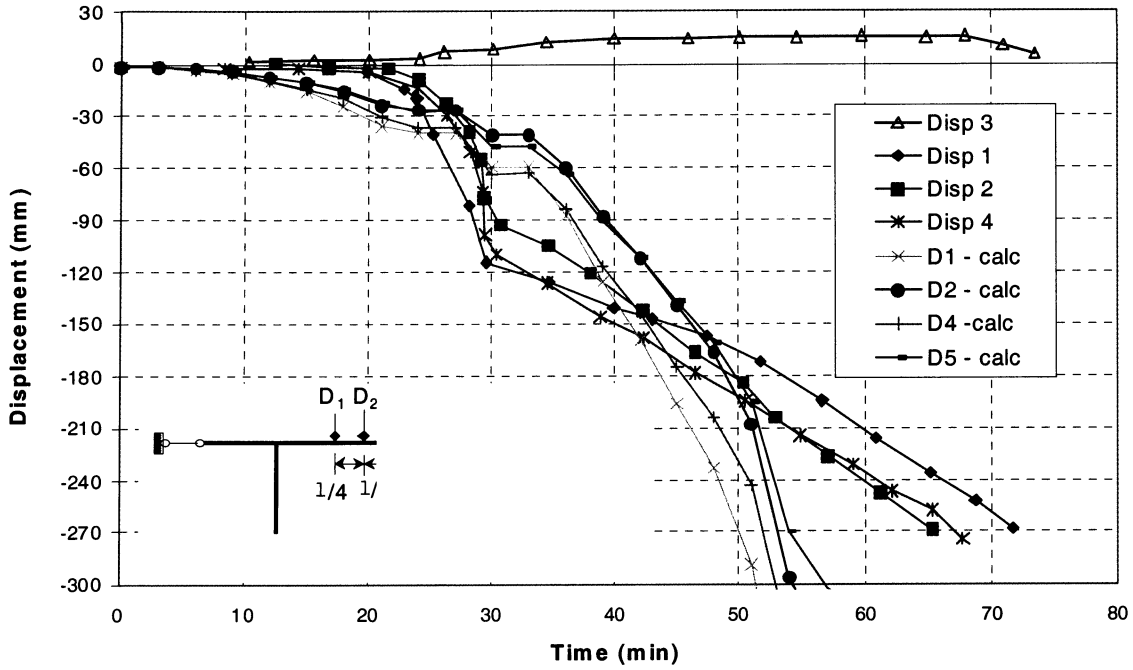

Fig. 3.12: Validation case III^c: 2D steel frame: 2 bays – 1 storey (unrestrained); time displacement curves (DIANA)

Temperature-deflection plots for various points on the frame using both material models are given in Figs. 3.11 (ABAQUS) and 3.12 (DIANA), together with the measured values. Note that the deformation mode is more or less symmetric, which is not amazing in view of the restraint end conditions. No run-a-way conditions occur, suggesting that equilibrium towards the end of the test is maintained by membrane action. The displacements calculated by means of DIANA are in reasonable agreement with the test results (see Fig. 3.12). For the ABAQUS calculations, this agreement is less satisfactory. Note in respect that for the EC-based material values, after about 30 minutes lead to numerical instability. No conclusions on the use of the EC-material model can be drawn for the remaining part of testing period.

Conclusions for validation cases II

Although there is no exact match between the displacements measured the in steel frame tests described above and the values calculated by means of DIANA and ABAQUS, the computer models reasonably well describe the test results, both in terms of displacements and in terms of general mechanical performance. This is an indication that DIANA and ABAQUS give rise to consistent results. Compared to the material model proposed by Anderberg, the EC3 model for mechanical steel properties at elevated temperatures leads to conservative (but not unrealistic) results. Hence, it was decided to solely use the EC3 model for further calculations in the scope of this project.

ad. Validation case III: 3D composite frame (restrained)

The corner test, carried out in the scope of the Cardington test programme, is chosen as the last reference case [2]. In the following discussion, details of the test and the essentials of the modelling used to simulate the structural behaviour in fire are presented. Also, the results obtained are briefly reviewed, with emphasis on the comparison between calculation results obtained by the various mechanical response models.

The objective of the corner test was to evaluate the behaviour of a complete composite floor system and, in particular, the importance of membrane action in the concrete slab. A compartment with a floor area of approximately 80 m^2 was built on the first floor in one corner of the structure. To ensure that the gable end walls and wind posts did not provide a load bearing function, all the restraints and ties were removed. Fig. 3.13 shows the location of the test.

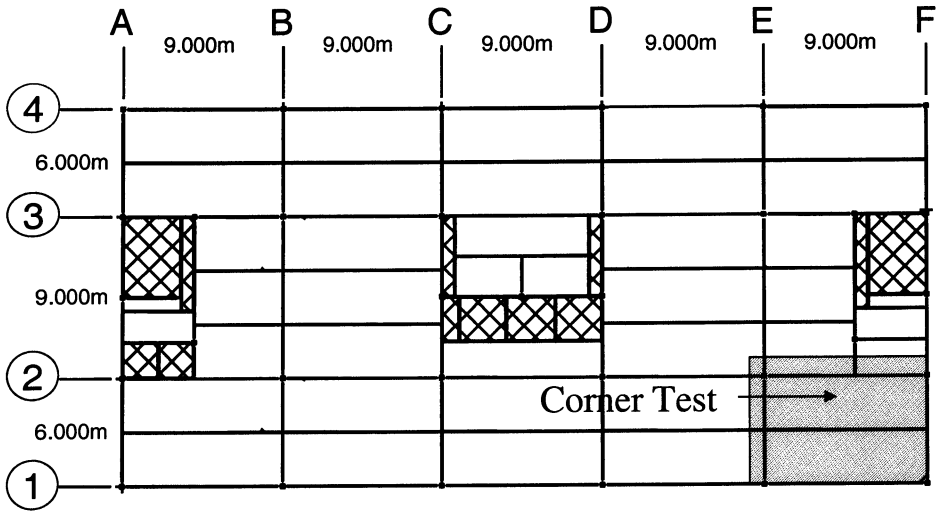

Fig. 3.13: Validation case IV: location of corner test in the CARDINGTON test frame

All the columns were protected to their full height including the main beam to column connections, using 25 mm ceramic fibre blanket. The edge beams were also protected in the same manner. However, all the internal beams (primary and secondary) remained totally exposed including the beam-to-beam fin plate connections.

During the fire, the unprotected 356 mm deep primary beam attained a maximum temperature of 864 °C in the lower flange, with the unprotected secondary beams achieving up to 1021°C in a similar location in the profile. Deflections at mid-span of the unprotected primary and secondary beams varied from 164 mm (356 mm beam, 6 m span) equivalent to span/37, up to 428 mm (305 mm beam, 9 m span) equivalent to span/21.

A model of the Cardington test floor was developed (Fig. 3.14 – the deformed shape is shown here) to simulate the test conditions. Half the floor is modelled, as obtaining the correct degree of restraint to thermal expansion is critical in simulating the response of the structure under fire. Beam elements are used to model the beams and columns in the structure. These beam elements are placed at the centreline of the real beams. All beams are assumed to be rotationally unrestrained about the major and minor axis at their support points with primary beams or columns. All beams are torsionally restrained at these support points. The concrete slab is represented using shell elements for the top 70 mm of the slab with beam elements in the main slab spanning direction to simulate the effect of the trapezoidal down stand at the bottom of the slab. The shell elements representing the slab are located at the centreline of the top 70 mm of concrete and are constrained to act with the steel beam elements using rigid beam constraint equations. This simulates a fully composite beam.

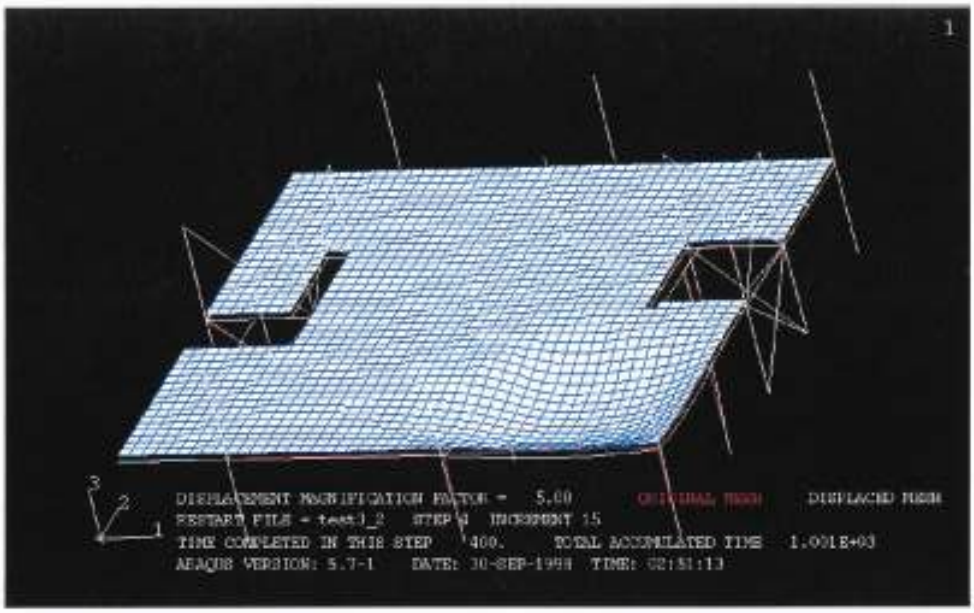

Fig. 3.14: Validation case IV: Half floor model of the CARDINGTON test frame

The constitutive models used for all (beam and shell) elements are based on temperature-dependent non-linear properties according to the respective Eurocodes [11], [12]. For the base case calculation, the actual values of the material parameters for steel and concrete are taken as per the design of the Cardington building.

One (typical) floor of the Cardington building has been modelled as well as the columns connecting this floor level to the levels above and below. The boundary conditions, that are considered suitable to model the structural behaviour of a compartment on this floor under fire loading, consist of:

- Column ends at the floor level below the heated floor: fully fixed.
- Column ends at the floor level above the heated floor: fully fixed, except for vertical displacement.
- Stiff cores modelled as supports at locations A2, A3, C2, C3, D2, D3, F2, F3: fully fixed.

Note that the stiff cores are not modelled in detail, but are modelled by means of appropriate boundary conditions.

With regard to the mechanical loading, a distributed load of 7.5 kN/m^2 is taken on the heated floor; on the columns connecting to the floor above, the weight of the above floors is applied.

The thermal response is taken directly from the temperature calculations carried with OZONE. In the input deck, temperatures in the elements are defined in increments of 15 minutes. For the temperature development in the protected beams and columns conventional values are assumed on the basis of a fixed fraction of the temperatures (and gradients) of (similar) unprotected beams, as follows:

- Internal protected beams: 0.6.
- Edge beams: 0.8.
- Columns: 0.4 (no gradient assumed).

A DIANA finite element model supplied by TNO was calibrated using ABAQUS and ANSYS. Calibration of the results from those three finite element packages was carried out to ensure that the modelling assumptions made by each code did not affect the structural behaviour.

The results, in terms of deflections in the heated compartment, are shown in Figures 3.15^{a-c}.

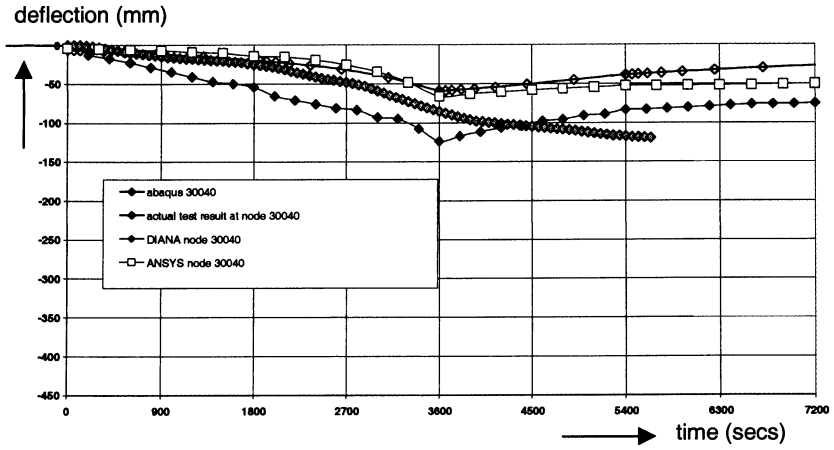

a) basis: node 30040

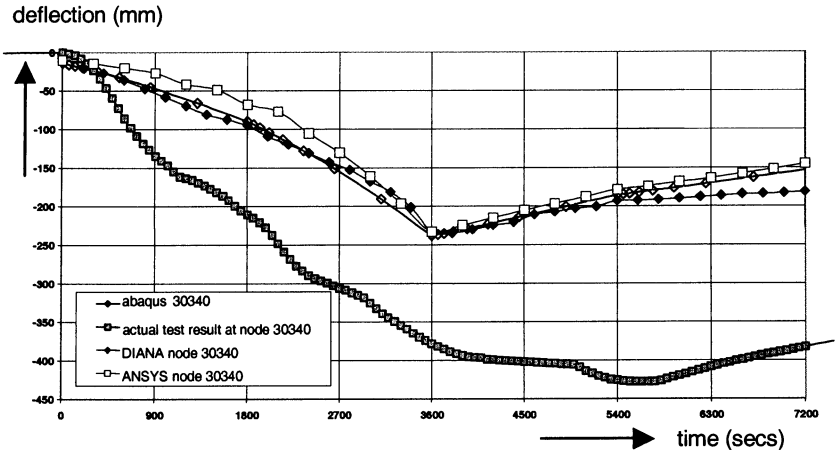

b) basis: node 30340

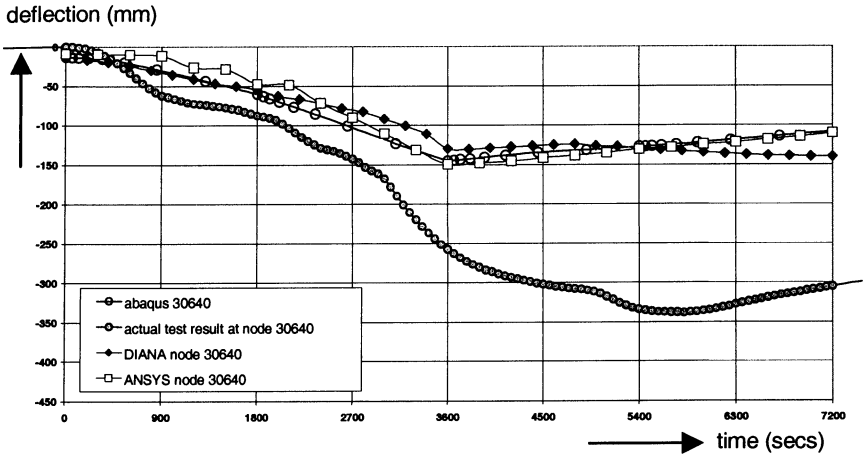

c) basis: node 30640

Fig. 3.15: Validation case IV: 3D composite frame; time displacement curves (DIANA, ABAQUS, ANSYS)

Examination of these deflections shows the close agreement of the results obtained with the various finite element packages. Note that discrepancy between the computer predictions on one hand and the measured displacements on the other hand, is significant. This is because in the computer analysis the thermal response of the structure is not taken from the test results, but from (schematised) OZONE calculation results. An attempt to use the actual (measured) temperature response in the calculations failed for reasons of numerical instability as a result of the irregular behaviour of the temperature development.

In view of the specific aim of the present exercise (i.e. to investigate the ability of the available mechanical response models to describe the behaviour of 3D composite frames) and taking due account of the results of calibration cases I and II, it is concluded that DIANA, ABAQUS and ANSYS are successfully validated. However, in their original versions, streamlining is necessary is necessary to reduce the necessary calculation time. Also the consistency of the streamlined models has to be investigated in detail. These aspects will be reviewed in the next paragraphs.

3.3 Streamlining of the original models

In order to reduce the necessary calculation time of the mechanical response models – without violating their predictive capabilities - it is necessary to "streamline" the models. This streamlining has focussed on two issues:

a. Optimisation of the number of elements.
b. Choice of adequate crack model for the concrete.

Ad. a: optimisation of the number of element

A prerequisite of the three available mechanical response FEM models (DIANA, ABAQUS and ANSYS) is that a linear temperature gradient over the element has to be assumed. Thus, the temperature distribution over an element is identified by a mean value and by a gradient in two directions. A linear temperature distribution over the steel concrete slab and (other) linear temperature distributions over the primary and secondary steel beams, would give rise to a significant simplification. However, no representative temperature distributions could be identified, by which the actual behaviour of a slab could be approximated.

For this reason it has been decided to increase the number of elements in the concrete slab, with a linear temperature distribution in each of them, in order to be able to simulate a more realistically temperature in the concrete slab. The assumptions & procedures necessary in this respect are described hereafter.

For an illustration of temperature distribution over the cross section of a concrete slab exposed to natural fire conditions from below, refer to Fig. 3.16. This temperature distribution has been calculated by means of SAFIR, using a dense element net.

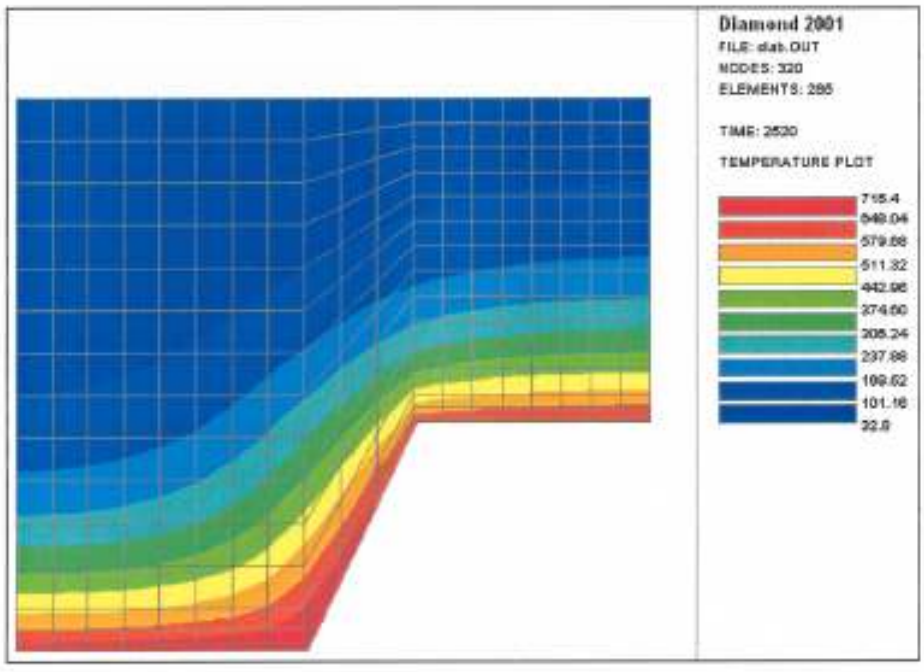

Fig. 3.16: Typical temperature distribution over the cross section of composite steel concrete slab

To simulate the 'real' temperature distribution of Fig. 3.16 by linear gradients, the cross section of the floor has been divided into 'big' elements for which the corresponding mean temperature and gradient have been provided. The procedure is as follows:

The element mesh shown in Fig. 3.17 has been taken as starting point. Mean values and gradients of the temperature have been provided for each of the 9 'big' elements representing the cross section. Fig. 3.18 defines the values for a typical beam element.

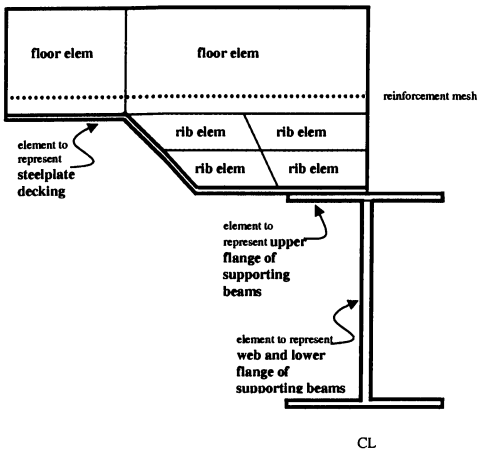

Fig. 3.17: The element mesh chosen in the linearisation procedure

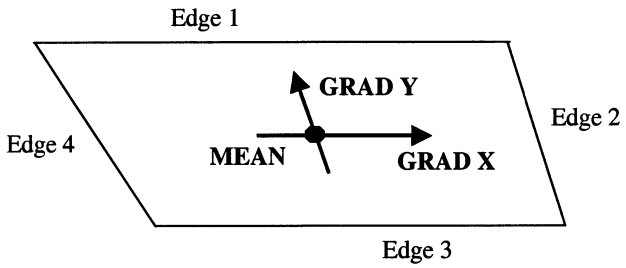

Fig. 3.18: Conventions for the beam element

Based on the temperature distribution obtained from the SAFIR calculations – where the element mesh has been much more refined - the mean temperatures along the four edges of the beam element have been determined as follows:

$$MeanTemperature(Edge\,X) = \frac{\sum_{node=2}^{NrNodesX} \frac{T_{node} + T_{node-1}}{2} \cdot (X_{node} - X_{node-1})}{X_{NrNodesX} - X_1}$$

where:

NrNodesX	is	the total number of nodes in the SAFIR model along edge X
X	is	distance measured along edge X

From the mean temperature along the edges, the temperature gradients has been determined:

$$\mathbf{GRAD\,X} = MeanTemperature(Edge\,2) - MeanTemperature(Edge\,4)$$

$$\mathbf{GRAD\,Y} = MeanTemperature(Edge\,1) - MeanTemperature(Edge\,3)$$

The mean value required in the input deck is defined as:

$$\mathbf{MEAN} = \frac{\sum_{elem=1}^{NrElements} T_{elem} \cdot A_{elem}}{\sum_{elem=1}^{NrElements} A_{elem}}$$

where:

NrElements	*is*	the total number of SAFIR elements in the area considered
T_{elem}	*is*	the mean temperature in the SAFIR element

$$T_{elem} = \frac{\sum_{node=1}^{NrNodes} T_{node}}{NrNodes}$$

with:

NrNodes	*is*	total number nodes in the SAFIR element
A_{elem}	*is*	area of the SAFIR element

The discrepancies between the 'real' temperature field and the 'assumed' one based on linear variation within the 'big' compartments are shown in Figs. 3.19 and 3.20. These figures apply to the temperature distribution over the cross section of a composite concrete slab exposed to natural fire conditions ('big' element nr.1). A perfect agreement between the CEFICOSS results and the linear temperature field would imply that all black lines in Figure 3.20 would fall within the two yellow curves. For a systematic review of the validation of the linearasation process, refer to Annex B. Although it follows from this analysis that the above condition is not always fulfilled, it has been decided that the approximation gained by the linearasation procedure is acceptable in view of the scope of this project.

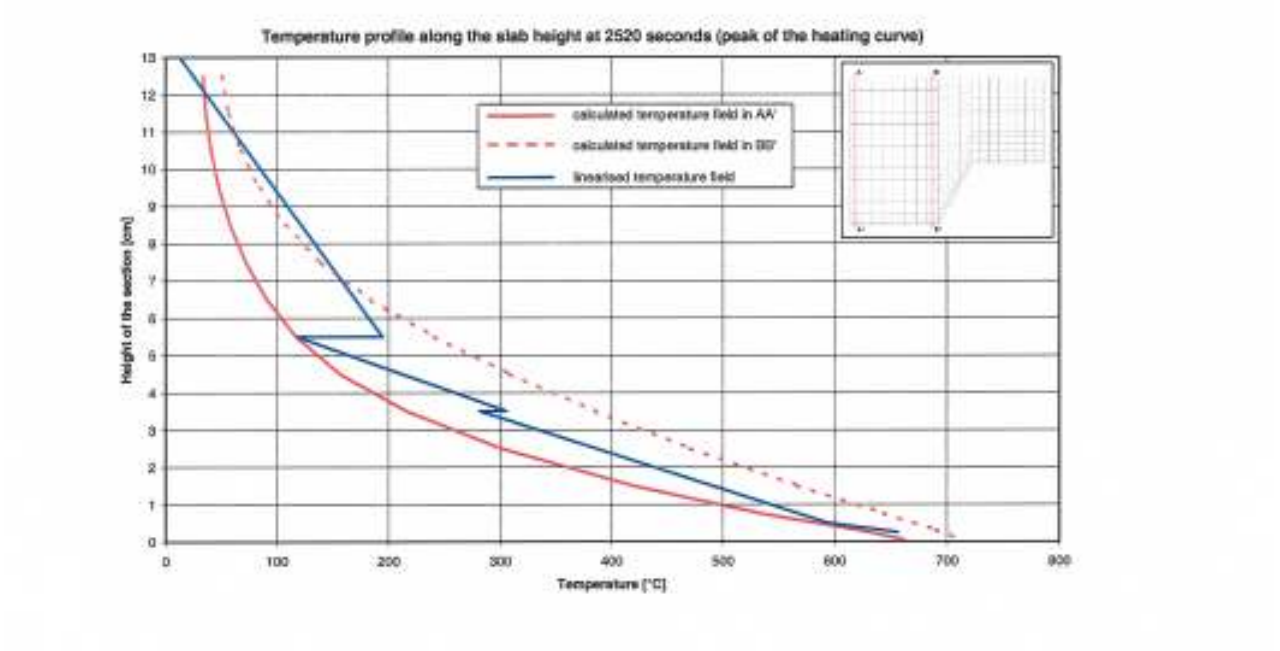

Fig. 3.19: Temperature profile along lines AA' and BB' of the cross section of a composite slab

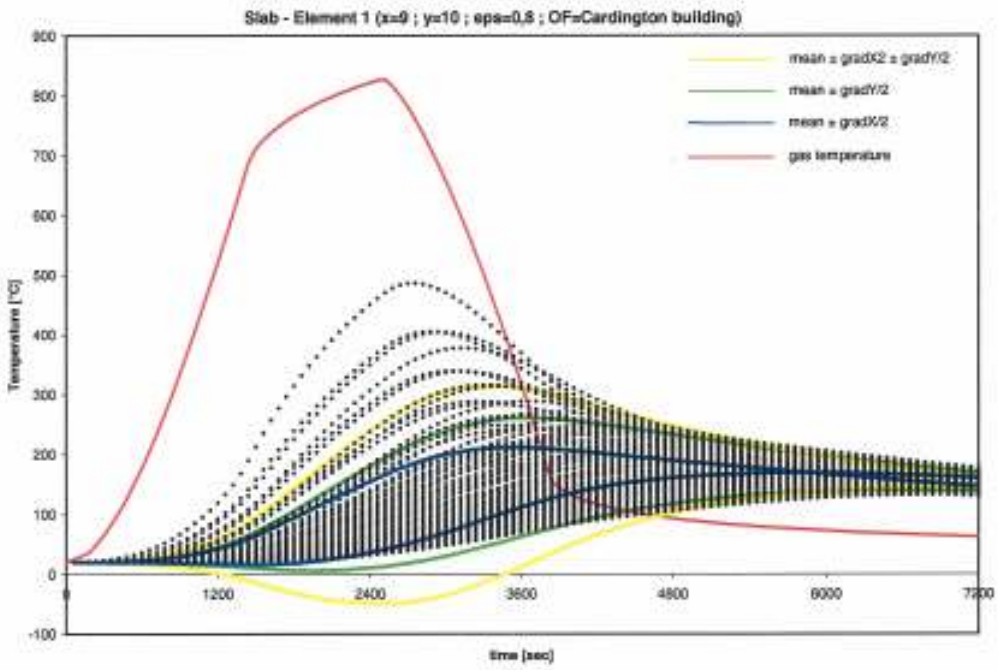

Fig. 3.20: Temperature distribution over "big" element 1 of the composite slab; black lines refer to CEFICOSS results

ad b: choice of adequate crack model for the concrete

With regard to the modelling of the cracking behaviour of concrete, the following options are available:

- Cracking is explicitly taken into account (smeared or discrete cracking).
- Cracking is implicitly taken into account (by adaptation of the friction angle of the yield contour).

To apply the explicit cracking option is very time consuming: factor 2 in terms of elapsed calculation time, bringing the total running time for a typical calculation case from 24 to 48 hours. In view of the need to reduce calculation time when entering the parameter study, it is at hand to use the implicit cracking option, if trustworthy. Another complication is that – whereas DIANA and ABAQUS can use both the implicit and the explicit cracking option – ANSYS is only equipped for the explicit option. Last but not least one has to realise that an exact interpretation of the results of the presently available explicit cracking models in terms of maximum strains in e.g. the steel reinforcement is not straightforward. In other words: the practical use of the additional information obtained from a explicit cracking model is very much in question.

To assess the effect of the cracking options on the overall structural behaviour, a series of calculations has carried out, with both the explicit crack model (smeared cracks) and the implicit crack model (reduced friction angle of the yield contour). The later model is taken identical to the one taken into account in ANSYS. Use is made of DIANA. For some results refer to Fig. 3.21. In this figure, the axial forces in the secondary beam of the CARDINGTON building (see Fig. 3.13), are presented, for certain periods of (well defined) natural fire exposure.

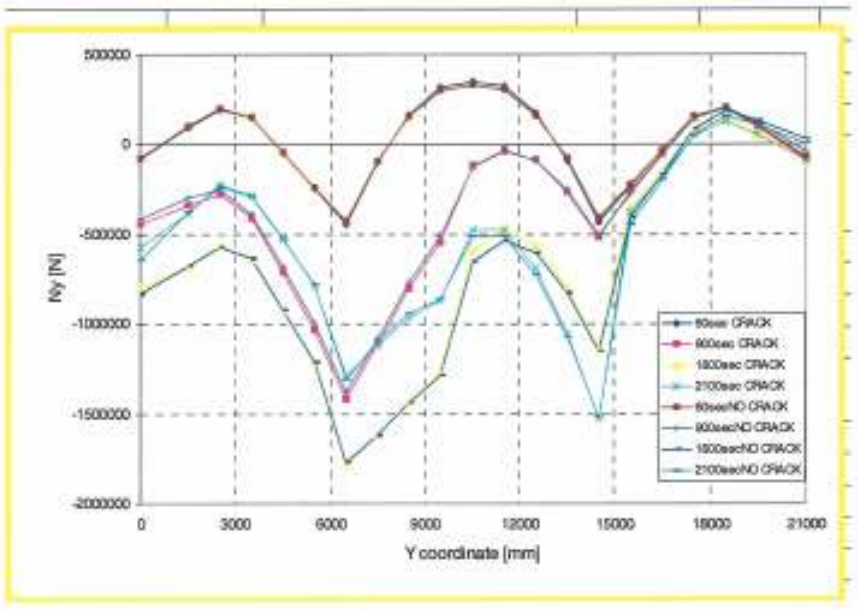

Fig. 3.21: Cracking vs. no cracking: comparison in terms of axial forces in the secondary steel beams

From the figure one can conclude that the effect of the chosen cracking option on the overall structural behaviour is relatively small. For this reason – and in view of the other arguments listed above it has decided to precede the remaining calculations on the basis of the implicit cracking model as available in the ANSYS code.

3.4 Consistency

In par. 3.2 it has been shown that the original versions of the available mechanical response models give consistent results when used to describe the mechanical performance of various structural systems under fire conditions.

To show consistency is felt to be of vital importance, not only for the models to be used as instruments in the parameter study, but also in the wider context of model use: without such consistency, the credibility of the advanced models in Fire Safety Engineering will invariably be called into questions. For these reasons, it has been decided to check – in addition to the above meant verification on consistency – the consistency of the streamlined models as well. For this purpose, a so called "calibration case" has been identified, representing a fire compartment with a floor area of 10.5 x 18 m in the CARD(1) building. See Fig. 3.22 for a plan of the fire compartment.

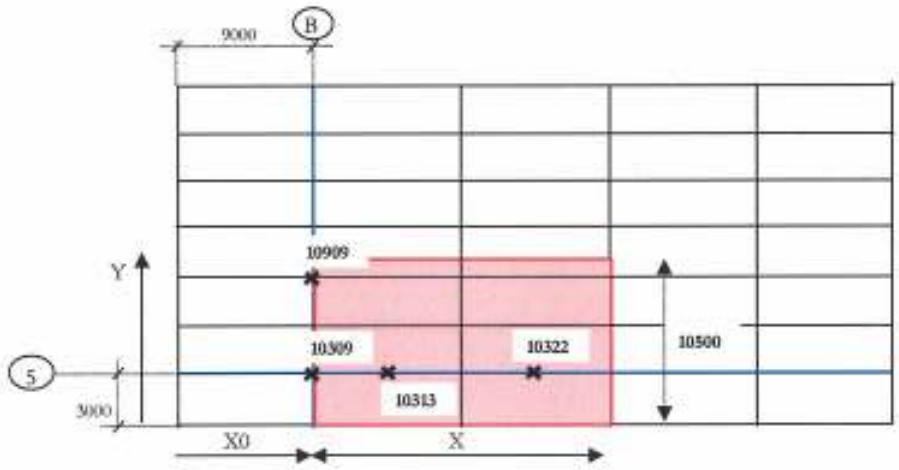

Fig. 3.22: Calibration case

Refer to Annex C for a detailed review of the specifications of the calibration case, including:
- Configuration.
- Mechanical loading.
- Material properties.
- Boundary conditions.
- Temperature fields.
- Integration scheme.
- Output format.

The fire development and the thermal response of the floors and beams in the fire compartment have been quantified by means of OZONE and CEFICOSS respectively. See also chapter 2.

The structural response is described in three different ways:
- Displacement U_z alongside lines 5 (Y = 3 m) and B (X = 9 m) as function of time.
- Normal force N_x along line 5 in the supporting beams, at certain times of fire exposure.
- Normal force N_y along line B in the supporting beams, at certain times of fire exposure.

For some results of the comparison, refer to Figs. 3.23, 3.24 and 3.25.

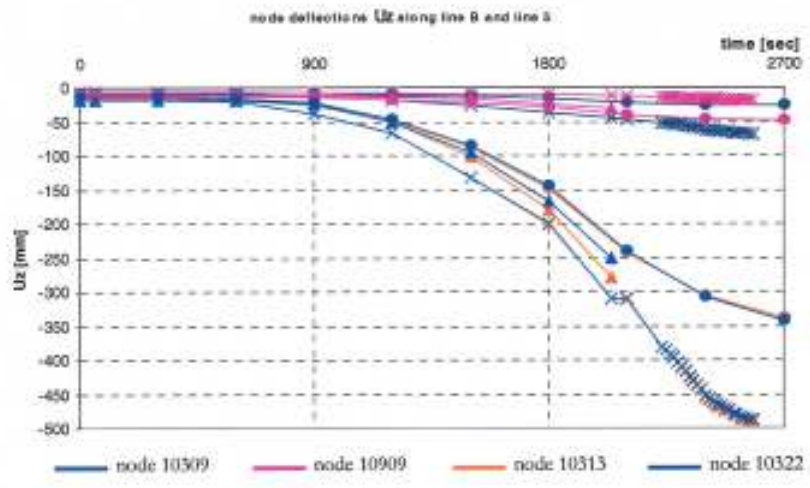

Fig. 3.23: Comparison of the calculation results in terms of node displacement history for line 5 (Y= 3 m).

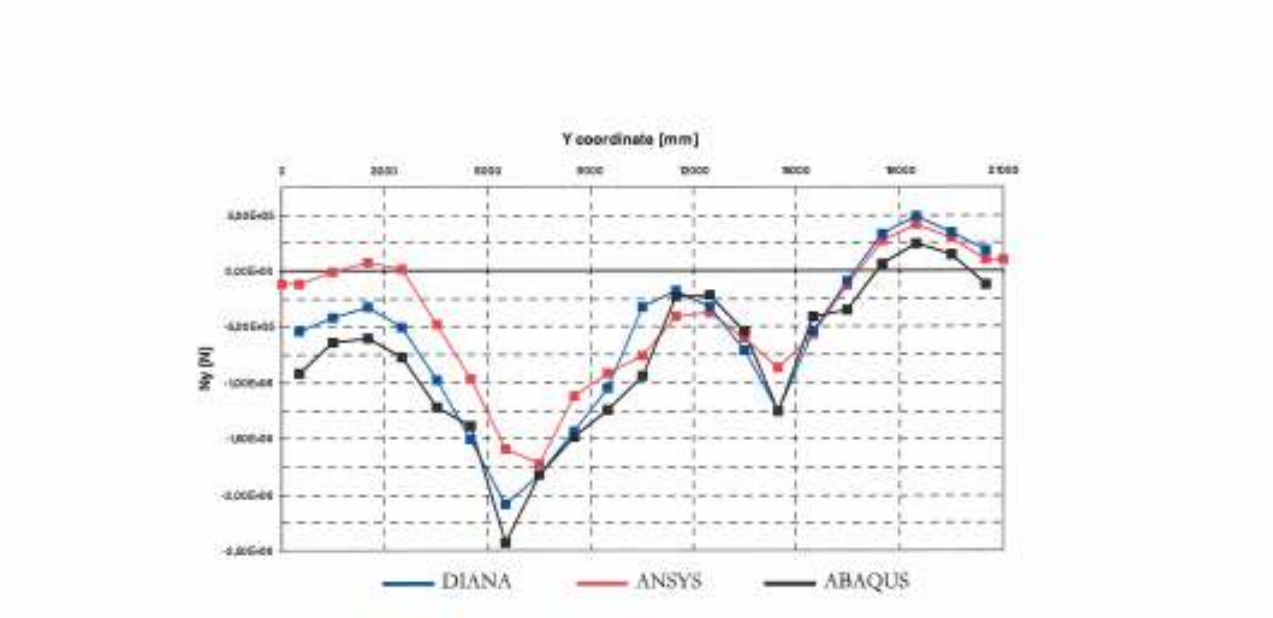

Fig. 3.24: Comparison of the calculation results in terms of normal forces N_z along line 5 (Y = 3 m) in supporting beams at a fire duration of 1800 secs.

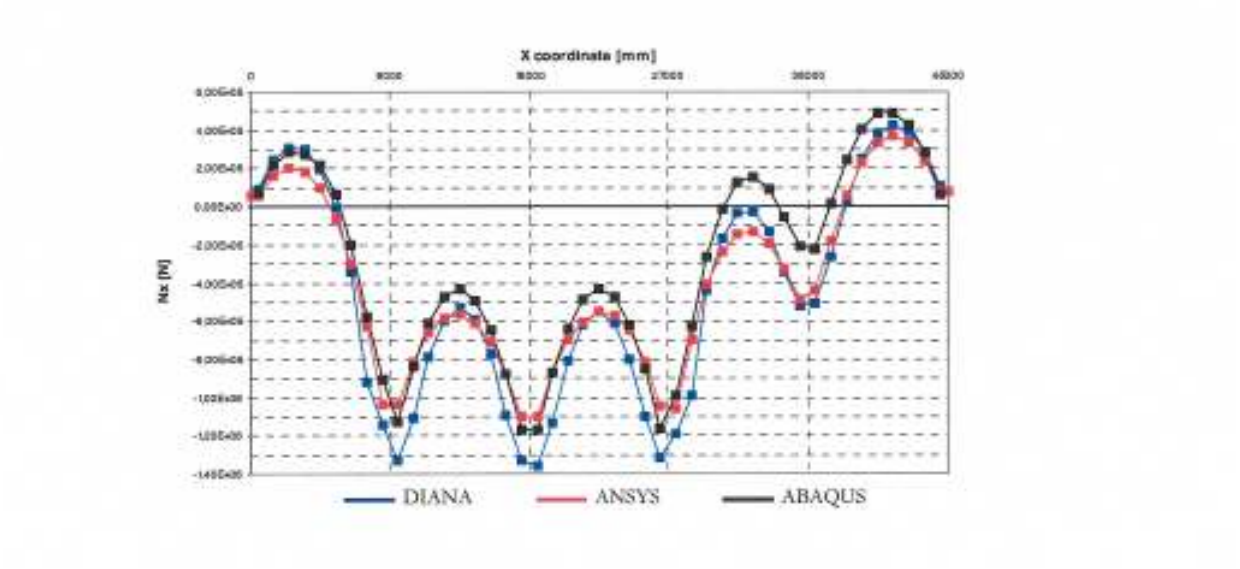

Fig. 3.25: Comparison of the calculation results in terms of normal forces N_y along line B (X = 9 m) in supporting beams at a fire duration of 1800 secs.

Comparison of DIANA, ANSYS and ABAQUS results show a reasonable agreement, both in terms of displacements and normal force distribution. It is therefore concluded that also the "streamlined" models show sufficient consistency.

4. Parametric study

4.1 Overview

As explained in the previous chapter, streamlining of the original mechanical response models (DIANA, ANSYS, ABAQUS), lead to versions, which nevertheless require significant calculation times (order of magnitude: 24 hours). Consequently, the number of cases to be considered in the scope of the parametric study had to be limited, compared to the initial plans. In this chapter, first the set up of the parametric study, as finally decided upon, will be presented. Hereafter, the major calculation results will systematically be discussed. Differentiation is made between the fire development and thermal response (where no important calculation time restraints hold) on one hand and the mechanical response (where due to the above calculation time restraints, the number of calculations had to be limited) on the other hand. For a further discussion on the practical implications, refer to the Design Guide [15].

4.2 Set up

In setting up the parametric study, first a limited number of basic cases are identified, each derived from the building configuration used in the CARD(1) project. Subsequently two sets of parameters are selected:

- Parameters which affect, for a given fire compartment size, the fire development in the compartment and/or the thermal response;
- Parameters, which for a given thermal response affect the mechanical response.

- ***Basic cases***

From tentative calculations it became evident, that – not only with regard to the fire development, but also with regard to both the thermal and the mechanical response, one of the main parameters is the fire compartment size. With a view to limit the number of calculations - and also to be in line with the actual fire safety design practice - only four compartment sizes are considered:

Type a: large fire compartment
Large fire compartment (A_{fi} = 45x21 = 945 m^2); the whole floor area is considered to form the fire compartment, i.e. no fire compartmentation is foreseen for the floor.

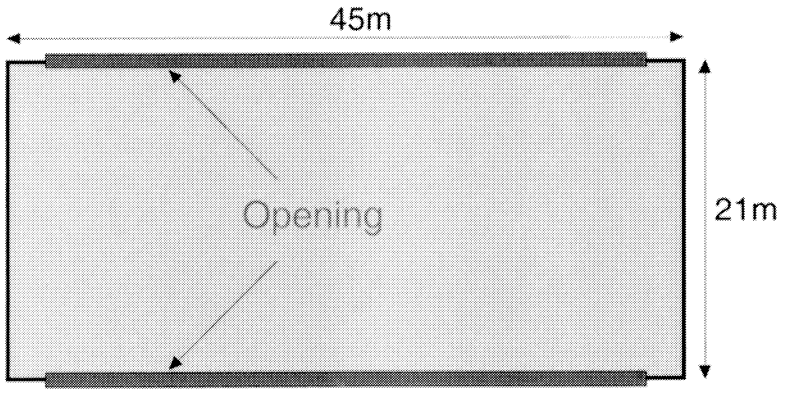

Fig. 4.1[a]: Type "a" fire compartment

Type b: medium size fire compartment
Medium size fire compartment with a firewall situated across the building (A_{fi} = 22x21= 462 m^2).

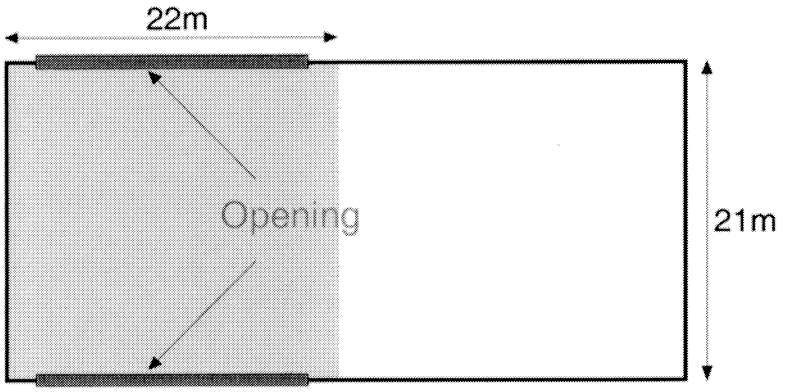

Fig. 4.1[b]: Type "b" fire compartment

Type c: medium size compartment
Medium size fire compartment with a firewall situated alongside the building (A_{fi} = 45x10 = 450 m^2).

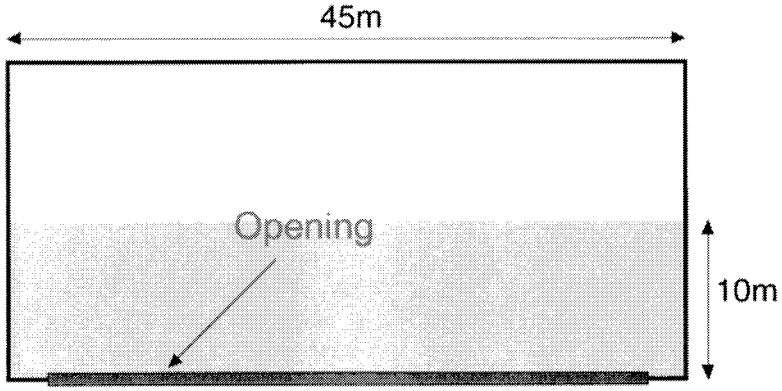

Fig. 4.1[c]: Type "c" fire compartment

Type d: small size compartment
Small size fire compartment situated halfway the floor (A_{fi} = 18x10 = 180 m^2).

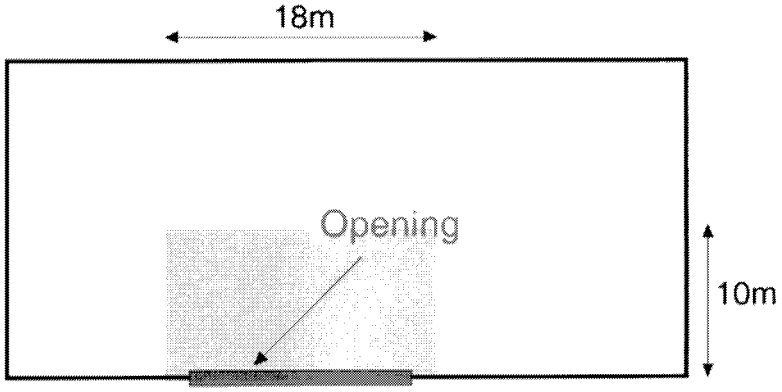

Fig. 4.1[d]: Type "d" fire compartment

- ***Additional parameters affecting the fire development and/ or the thermal response***

Main parameters belonging to this group are
(a) The fire load density.
(b) The height of the window opening.

Ad a: height of the window openings (h_w)
The height of the window openings varies between a minimum value (h_w = 0,5m) following acceptable working conditions inside the building to a maximum value h_w equal to 3,655 m. It will be assumed that - in each of the long facades of the building - there is only one window opening, the width of which equals 90% of the length of the building. In all cases, the height of the sill (h_i) was defined as equal to 0,5 m.

Table 4.1: Window geometry

	height of the window openings (h_w) [m]	width of the window opening [m]
Type a	The calculations were made for the following different heights : 0,5 ; 1,0 ; 1,5 ; 2,0 ; 2,5 ; 3,0 ; 3,655	40,5
Type b		19,8
Type c		40,5
Type d		16,2

Ad b: Fire load density
Starting point for the calculations is a 80% fractile value of the design fire load, representative for office buildings (= 511 MJ/m^2). Different design values for the fire load are derived, depending on the risk of activation (as function of the floor area of the fire compartment and the occupancy) and the active measures taken using the methodology developed in the NFSC-project [16][5]. For an overview, refer to Table 4.2. Note that in this way the maximum reduction of the design fire load is such that quite a large range of design fire loads is covered

The following properties are considered as typical for a building of the CARDINGTON type and are, therefore, not varied:

Floor: 11,7cm of Normal weight concrete (ρ = 2300 kg/m^3; c = 900 J/kgK; λ = 2,0 W/mK).
Ceiling: 11,7cm of Normal weight concrete[6] (ρ = 2300 kg/m^3; c = 900 J/kgK; λ = 2,0 W/mK).
Walls: 6cm Promasil 850/200 (ρ = 200 kg/m^3; c = 751 J/kgK ; λ = 0,0483 W/mK).
17,5cm Brick (ρ = 2000 kg/m^3; c = 1114 J/kgK; λ = 1,04 W/mK).

[5] For a practical explanation of the concept of the "design" fire load density, as introduced in the NFSC project, as well as some quantitative backgrounds, see also the Design Guide [15].
[6] In a later phase of the project it has been decided to analyse the effect of lightweight concrete. See also paragraph 4.4 and the Design Guide.

Table 4.2: Design values for the fire load density

	Design Fire Load $q_{f,d}$ [MJ/m²]			
	Type a	Type b	Type c	Type d
No Fire Active Measures	707	658	658	593
Off Site Fire Brigade	552	513	513	462
Off Site Fire Brigade + Automatic Fire Detection by Smoke	403	375	375	338
Off Site Fire Brigade + Automatic Fire Detection by Smoke + Automatic Alarm Transmission to Fire Brigade	351	326	326	294
Off Site Fire Brigade + Automatic Fire Detection by Smoke + Automatic Fire Detection by Heat + Automatic Water Extinguishing System	246	229	229	206

- **Additional parameters affecting the mechanical response**

In this group, the following parameters are identified:
- Mechanical loading.
- Reinforcement.
- Structural grid spacing.

Also, the effect of changing from normal weight concrete (NWC) to light weight concrete (LWC) has been investigated. For each of these parameters a practical range has been chosen. See paragraph 4.4.

With a view to systematically analyse the mechanical behaviour with a minimum input from the (time consuming) mechanical response models, the following procedure is applied:

(1) For various the 4 basic cases identified above and for a given value of the design fire load density, both the gas temperature development in the fire compartment and the thermal response is calculated for various values of the window height h_w. These calculations are carried out by means of OZONE.

(2) Step (1) is repeated for various values of $q_{f,d}$, to be chosen from the range given in the Table 4.2.

(3) The maximum temperature in the lower flange of the primary beam, resulting from the anticipated fire exposure, is taken as a reference temperature and is denoted as Θ_{ref}.

(4) By way of working hypothesis, the assumption is made that structural failure occurs, if the above reference temperature exceeds 800 °C.

(5) By systematically varying the fire load density, a situation is identified in which structural failure is assumed to take place (so-called "failure" situation)[7].

(6) The situation identified under step (5) is further documented in a way that it is accessible for the structural modellers.

[7] See Fig. 4.2 for a graphical illustration of this part of the procedure. Note that, on forehand, it is not sure that the reference temperature for small window heights is the same as for large window heights.

(7) By means of (one of) the mechanical response models, it is verified whether the selected situations really correspond to structural failure. If necessary some nearby situations are analysed to more precisely identify the "failure" situation

(8) The final "failure" situations are analysed by means of the mechanical response models to find out what the critical factors for failure are; e.g.: what is the effect of changing – within a practical range – the mechanical loading or the amount of reinforcement?

(9) An attempt will be made to generalise the results of step (8) in order to arrive at some design guidance.

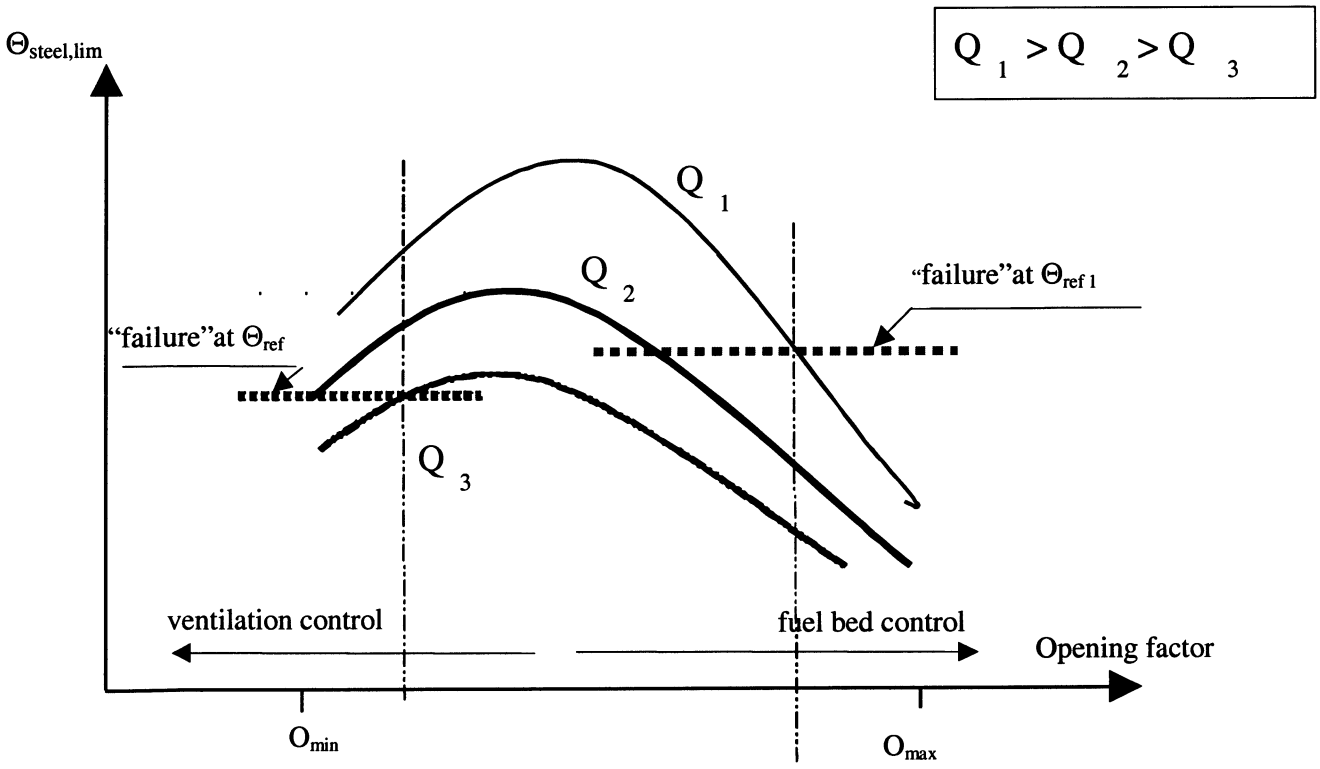

Fig. 4.2: Graphical representation of the procedure to analyse the mechanical response

For operational reasons, further to the above procedure, well-defined mechanical failure criteria have to be set. Two of such criteria have been identified:

- The plastic strain of the reinforcement should less or equal to 5%.
- The relative displacement of the floor beams should be less than 1/20th of the span.

The first mentioned criterion is introduced in view of the possibility of brittle fracture of the reinforcement. The second criterion has a mainly practical motivation and is in line with present practice in fire testing. See Annex D for some backgrounds. Note that both criteria can directly be assessed on the basis of the output of the mechanical response models.

4.3 Results of systematic calculations into the fire development and/or thermal response

For each of the basic cases identified in the previous paragraph, three figures are provided:

- Air temperature in the compartment as a function of the time for 35 cases (5 design fire loads * 7 window height h_w).
- Steel temperature as a function of the time for these 35 cases (section factor steel profile: A_m/V = 209 m^{-1}).
- Maximum steel temperature as a function of the window height h_w for the 5 design fire loads.

For basic case a, the results are – by way of illustration – presented in Fig. 4.3, 4.4 and 4.5 respectively. For a complete set of calculation results, refer to Annex E.

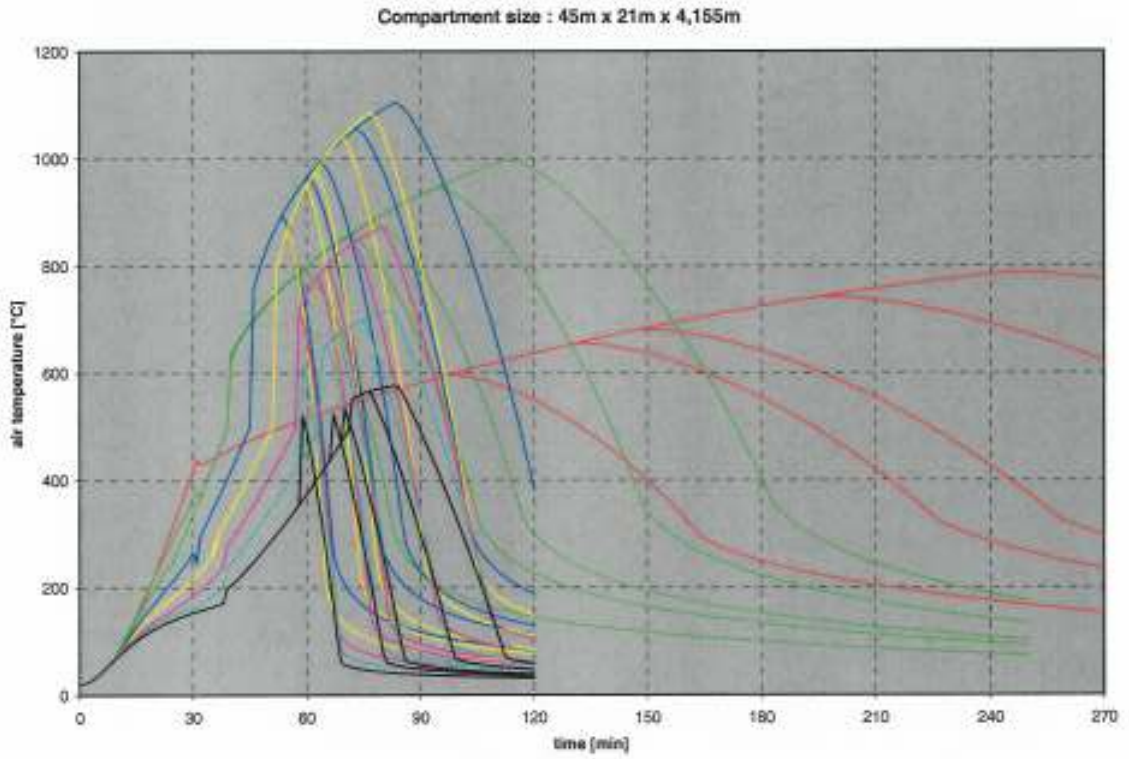

Fig. 4.3: **Development of gas temperature as (basic case a; various window heights and fire load densities)**

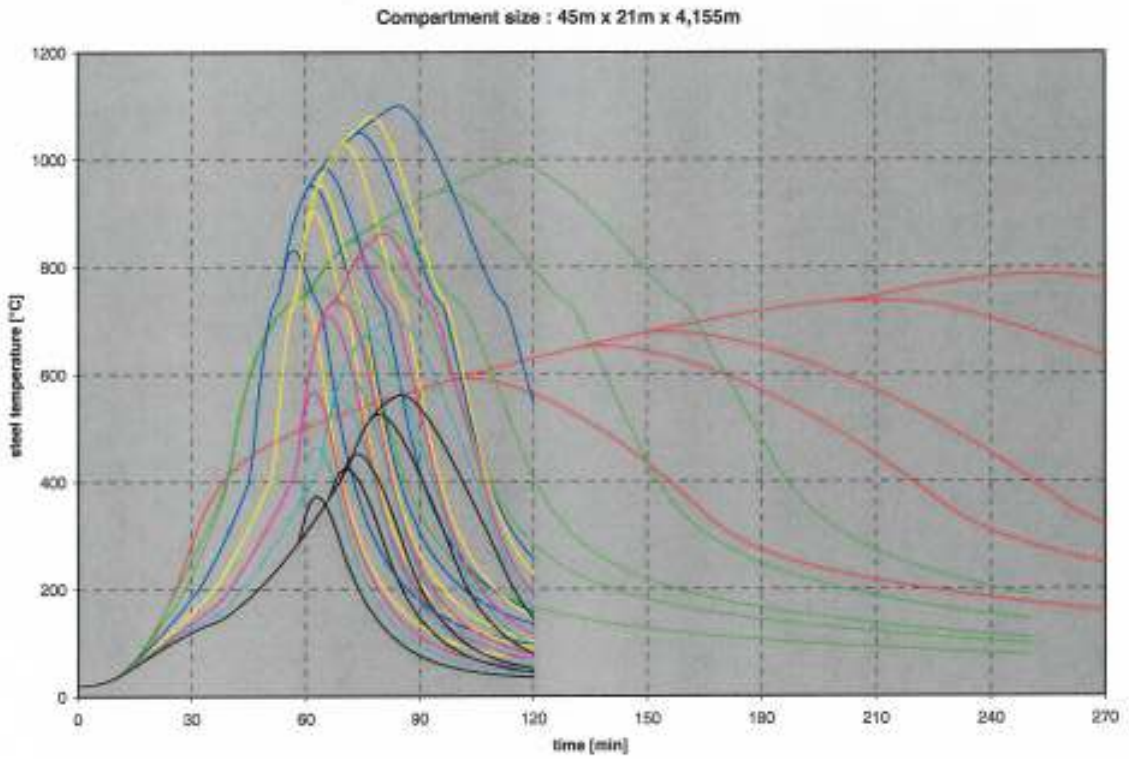

Fig. 4.4: **Development of gas temperature as (basic case a; various window heights and fire load densities)**

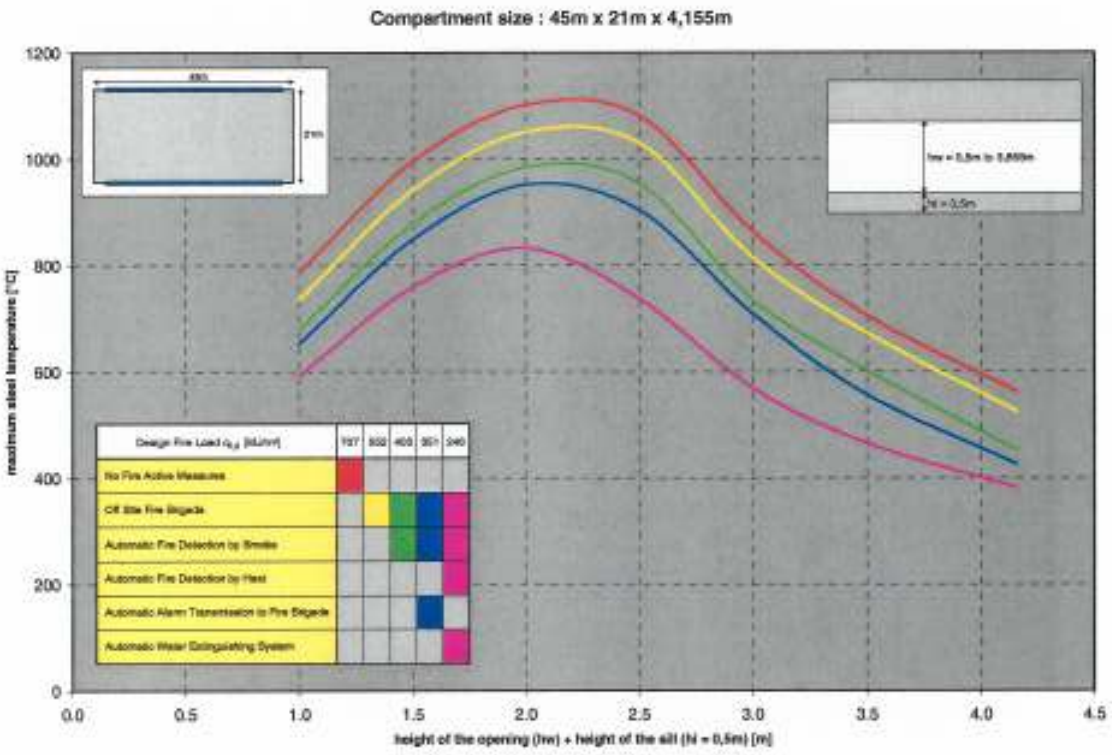

Fig. 4.5: **Maximum steel temperature as function of the height of the window opening for various values of the fire load density**

From the calculation results the prominent influence of both the window height and the fire load density becomes manifest. For relative high and for relative low window heights, in combination with not too high values of the fire load density, maximum steel temperatures of 700 °C and below are possible. Here the use of unprotected steel is feasible. For window height in between the maximum steel temperature reaches significant higher values: up to 1100 °C and – probably - steel beams and floors have to be protected. See Fig. 4.5. This is a typical feature for compartment fires, and can be recognised in the calculations results for the other basic cases. See Annex 6. The reason is that for low window heights, combustion is limited by limited oxygen supply (so-called "ventilation controlled" fire conditions). When the window height is increased, more oxygen becomes available, leading to a higher rate of heat release and higher gas (and steel) temperatures will result. Beyond a certain window height, however, there will be a surplus of oxygen, and further increasing of the ventilation beyond that point will not lead to a higher rate of heat release (so-called "fuel bed controlled" fire conditions). A side effect of increasing the window height is that the heat losses from the fire compartment via the window openings (radiation, convection) increase. Hence, further increasing of the window height results in a decrease of the gas (and steel) temperatures.

The curves of Annex E have been calculated for the various basic cases but for a certain façade design (i.e. variable window height, but a default value for the sill height equal to 0.5 m). The calculation results can be generalised as follows:

Effect of the sill height

For a practical situation (i.e. basic case b and fire load density of 500 MJ/m^2) and a window height of 1 m, the sill height has been varied from 0.5 to 3 m. For each of these combinations the maximum steel temperature has been calculated. For the results, refer to Table 4.3. As shown in this table, the effect of the sill height is negligible.

Table 4.3: Effect of the sill height on the maximum steel temperature

Sill height [m]	Maximum steel temperature [°]
0.5	909.7
1.0	909.5
1.5	909.4
2.0	909.3
2.5	909.8
3.0	909.1

Effect of the window height

In fact figures such as given in Fig. 4.5 are only valid for a certain fire compartment configuration. With a view to concentrate the information in an as small as possible number of diagrams, the concept of the so-called opening factor is introduced. The opening factor is given by:

$$A_w\sqrt{h_w} / A_t \qquad \ldots (4.1)$$

with:

A_w	is	the surface area of the opening;
h_w	is	the height of the opening;
A_t	is	the total surface area of the walls, including openings.

The advantage of using the opening factor concept is that it enables to account for different geometry's and different ventilation conditions with only one parameter. This is illustrated in Figs. 4.6[a,b].
Fig. 4.6[a] is similar to Fig. 4.5, however it holds for basic case b and is calculated for fire load densities of 200 to 700 MJ/m^2 in steps of 100 MJ/m^2. In Fig. 4.6[b] the same calculation results are represented, however on the horizontal axis now the opening factor is plotted instead of the window height.

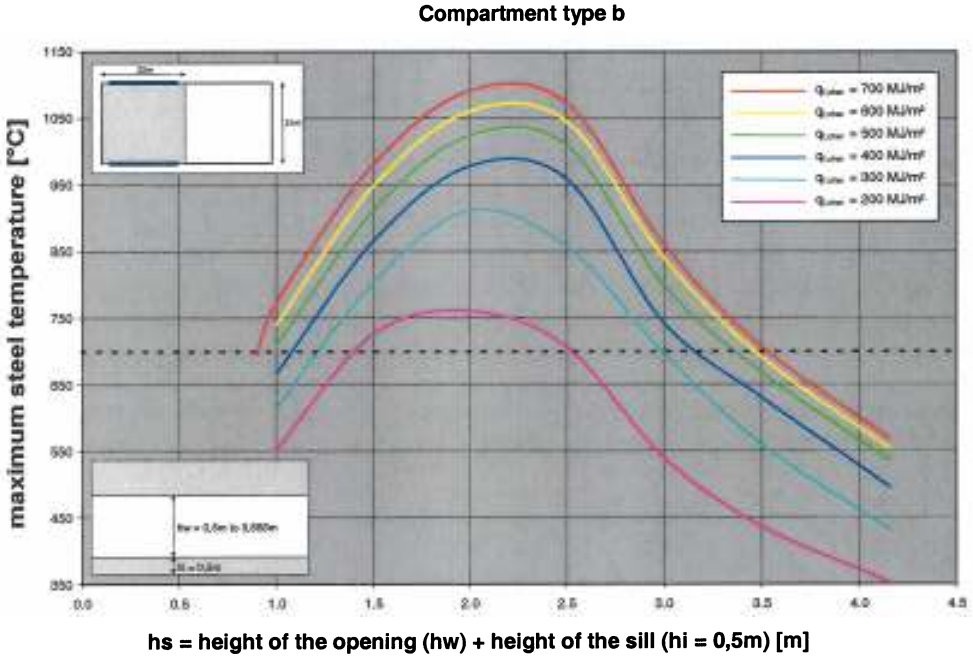

Fig. 4.6[a]: Maximum steel temperature as function of the window height for various values of the fire load density (basic case b).

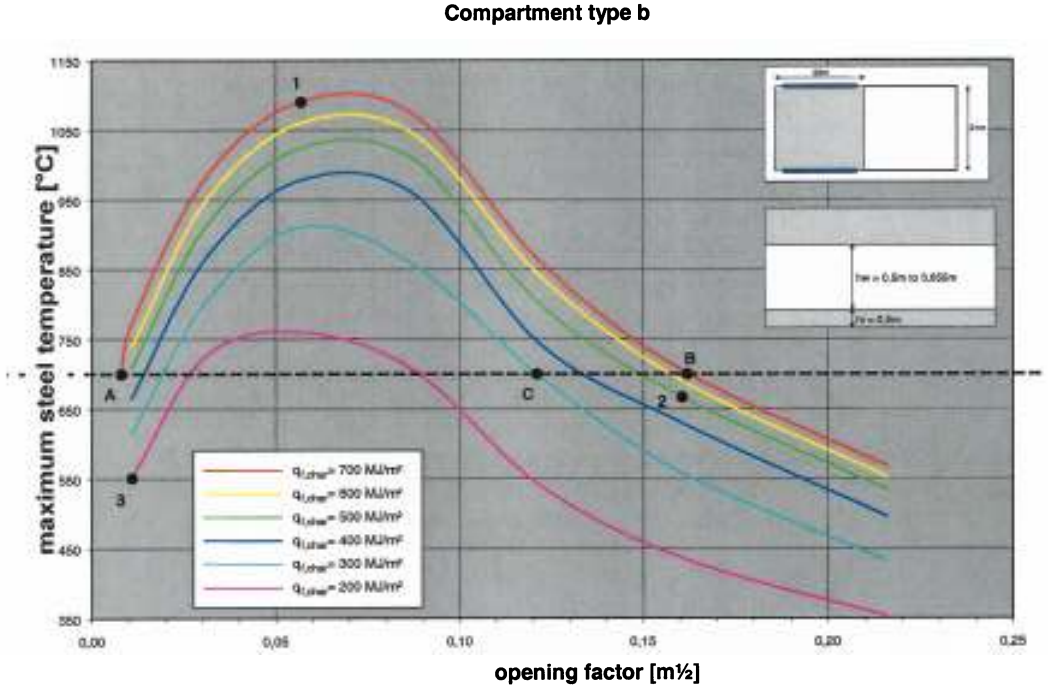

Fig. 4.6[b]: Maximum steel temperature as function of the opening factor for various values of the fire load density (basic case b).

In order to illustrate that the opening factor is really a key parameter, three representative points 1, 2 and 3 have been chosen. See Fig. 4.6[b]. For each point (1, 2 and 3), the size of the compartment (length L, width W and height H) has been varied, however keeping the opening factor constant by adapting the window height h_w. Refer to Table 4.4 some calculation results.

Table 4.4: Maximum steel temperatures for various fire compartment configurations

	L	0,9 * L	W	H	h_w	h_s	A_w	A_t	steel T°	A_v / A_t	O	A_f		
Point 1	$q_{t,d}$ = 700 MJ/m²													
ref.	22	19,8	21	4,155	1,500	2,000	59	1281	1090	0,3606	0,0568	462		
	11	9,9	21	4,155	1,636	2,136	32	726	1098	0,3173	0,0569	231		
	44	39,6	21	4,155	1,434	1,934	114	2388	1082	0,3869	0,0570	924		
	22	19,8	10,5	4,155	1,024	1,524	41	732	1110	0,3155	0,0561	231		
	22	19,8	42	4,155	2,245	2,745	89	2380	1073	0,3883	0,0560	924	ΔT°-	17
	22	19,8	21	3	1,408	1,908	56	1182	1078	0,3909	0,0560	462	ΔT°+	20
	22	19,8	21	5	1,565	2,065	62	1354	1098	0,3412	0,0573	462	ΔT°	37
Point 2	$q_{t,d}$ = 500 MJ/m²													
ref.	22	19,8	21	4,155	3,000	3,500	119	1281	667	0,3606	0,1606	462		
	11	9,9	21	4,155	3,266	3,766	65	728	614	0,3173	0,1606	231		
	44	39,6	21	4,155	2,862	3,362	227	2388	686	0,3869	0,1605	924		
	22	19,8	10,5	4,155	2,066	2,566	82	732	615	0,3155	0,1606	231		
	22	19,8	29	4,155	3,622	4,122	143	1700	678	0,3753	0,1606	638	ΔT°-	53
	22	19,8	21	3,5	2,912	3,412	115	1225	688	0,3771	0,1606	462	ΔT°+	21
	22	19,8	21	5	3,110	3,610	123	1354	641	0,3412	0,1604	462	ΔT°	74
Point 3	$q_{t,d}$ = 200 MJ/m²													
ref.	22	19,8	21	4,155	0,500	1,000	20	1281	551	0,3606	0,0109	462		
	11	9,9	21	4,155	0,531	1,031	11	728	556	0,3173	0,0106	231		
	44	39,6	21	4,155	0,470	0,970	37	2388	541	0,3869	0,0107	924		
	22	19,8	10,5	4,155	0,352	0,852	14	732	578	0,3155	0,0113	231		
	22	19,8	42	4,155	0,710	1,210	28	2380	524	0,3883	0,0100	924	ΔT°-	27
	22	19,8	21	3	0,467	0,967	19	1182	538	0,3909	0,0107	462	ΔT°+	27
	22	19,8	21	7	0,562	1,062	22	1526	571	0,3028	0,0109	462	ΔT°	54

Conclusion from Table 4.4[8] is that the variation in maximum steel temperature is relatively small: generally much less than 10% of the maximum steel temperature calculated for the reference configuration. On this basis it is concluded that the temperature variation is sufficiently small to consider the opening factor as a useful concept in the scope of this project.

4.4 Results of systematic calculations into the mechanical response

The following parameters have virtually no effect on the fire development, but may affect the mechanical response (and sometimes the thermal response):

- Mechanical loading (no effect on thermal response);
- Amount of reinforcement (no effect on thermal response);
- Structural gird spacing (some effect on thermal response).

The choice between normal weight concrete (NWC) and light weight concrete (LWC) for the floor slabs does not only affect both the thermal and mechanical response, but will - due to the different thermal resistance of the floors - also have an effect on the fire development. The latter effect will not be taken into account, since the influence of the thermal resistance of the floors of a fire compartment will be relatively small, compared to other factors such as ventilation conditions and fire load density.

In this paragraph, the effect of the above parameters will be discussed. Emphasis will be on the effect of the mechanical response, calculated by the streamlined models as described in par. 3.3.

- ***Mechanical loading***

The mechanical loading is based a situation corresponding to the test building of the CARD(1) project. In the analysis, the following values for the imposed have been chosen:

- 5,5 N/m^2 (maximum design value)
- 3.0 „ (normal value under fire conditions)
- 0.0 „ (hypothetical case, if no imposed load is present)

The load by own weight follows directly from the applied structural elements.

Starting point of the analysis is basic case b. The maximum temperature of the lower flange of the primary steel beams as function of the opening factor for various values of the fire load density is given in Fig. 4.6[b]. Further to the procedure for the systematic determination of the mechanical response - explained in par. 4.2. and Fig. 4.2 - two values of the opening factor, i.e.:

- 0.008 $m^{1/2}$ (in the ventilation controlled regime), and
- 0.16 $m^{1/2}$ (in the fuel bed controlled regime),

have been identified, for which – for a fire load density of 700 MJ/m^2 – a maximum temperature of 700 °C is obtained in the lower flange[9]. The points A and B in Fig. 4.6b represent these situations.

For the ventilation-controlled situation (point A in Fig. 4.6[b]), the maximum vertical displacement as function of time is given in Fig. 4.7[a]. The difference between normal load (3 kN/m^2) and no imposed load is not very large. Also for the fuel bed-controlled situation (point B of Fig. 4.6[b]), the difference between normal load and no imposed load is quite small. See Fig. 4.7[b]. However, the simulation with maximum imposed load (5.5 kN/m^2) shows a rapid increase in the vertical displacement between 45 and 60 minutes.

---

[8] In Table 4.4, $\Delta T°+$ is the increase value of the temperature regarding the reference case, $\Delta T°-$ is the decrease value of the temperature regarding the reference case, and $\Delta T°$ is the total temperature variation from the minimum to the maximum.

[9] Initially, the idea was that for a maximum steel temperature of 800 °C, failure conditions would occur. On basis of exploratory calculations (not shown here!), it became evident that for a high temperature failure could not be excluded.

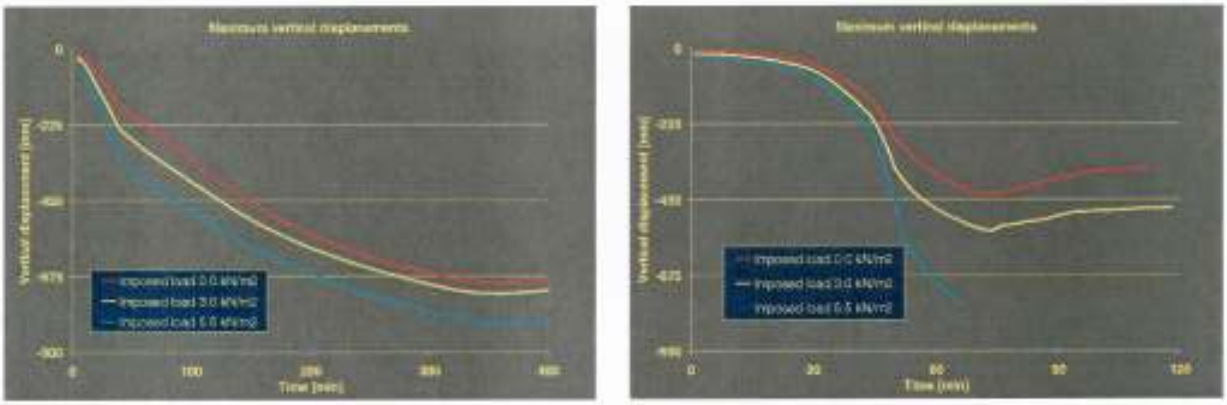

(a) ventilation-controlled (b) fuel bed-controlled

Figure 4.7: Maximum vertical displacements of the primary beam as function of time (basic case b; see also Fig. 4.6[a])

These calculation results have to be confronted with the failure conditions identified in par. 4.2, i.e.:

- *Relative* displacements, i.e. limiting value: L/20, taking into account the displacements of the beam supports (motive: in the context of this criterion, the deformation of the beam is relevant);
- Maximum plastic strain in the reinforcement of 5% (motive: rupture of the reinforcement is a failure mechanism to be accounted for).

As far as the maximum plastic strain is concerned, the calculations show that:

- For the fuel bed controlled fire: 2.0 %.
- For the ventilation controlled fire: 4.5 %.

Hence, in none of the two cases, the strain criterion is met.

For some results regarding the relative deflections, refer to Fig. 4.8[a,b].

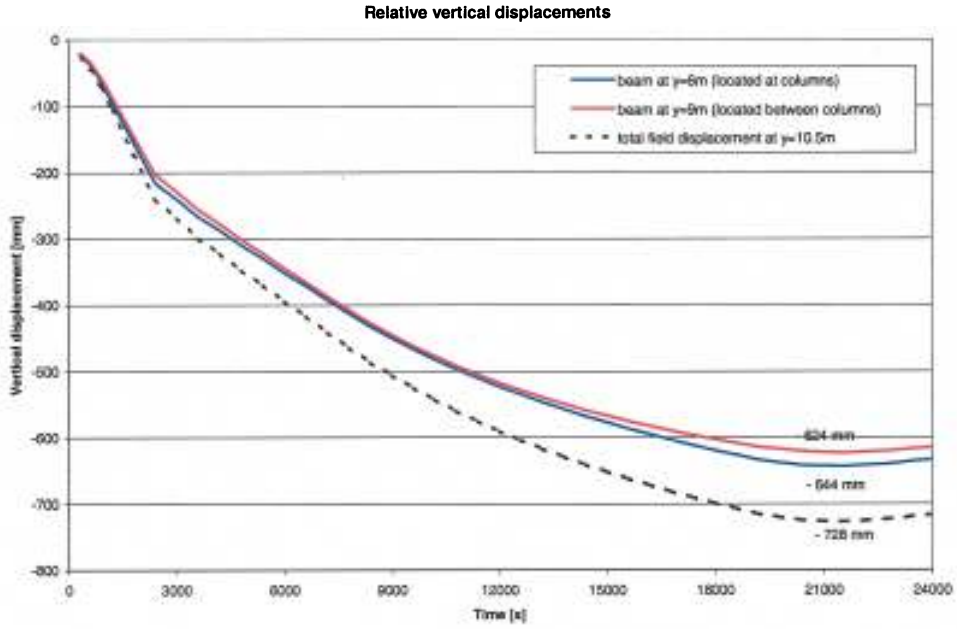

(a) Ventilation-controlled

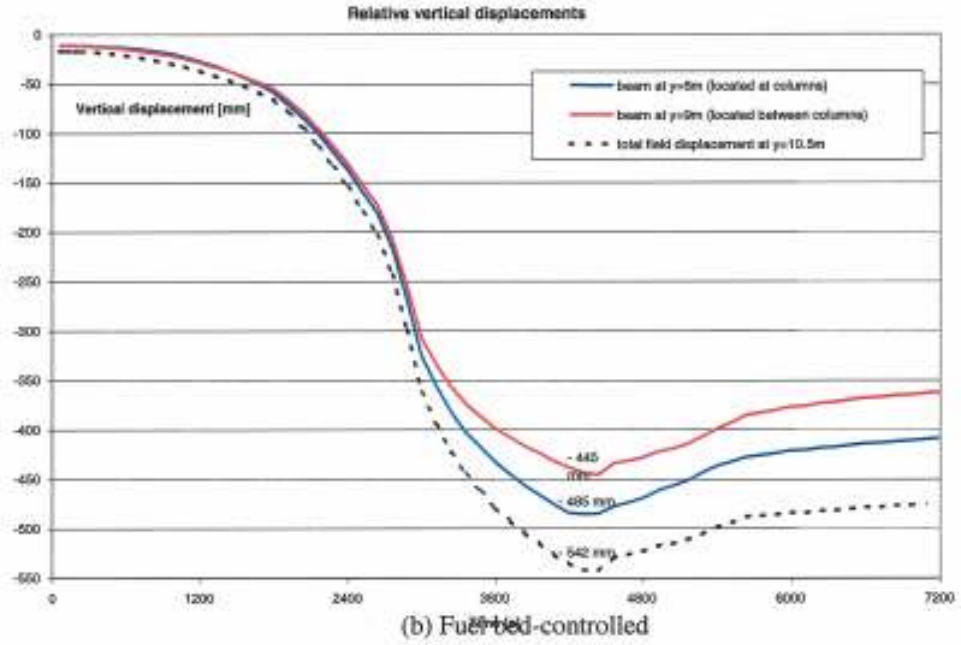

Figure 4.8: **Maximum relative vertical displacements of the primary beam as function of time (basic case b with fire load density of 700 MJ/m^2; see also point A, B of Fig. 4.6^b)**

For the maximum relative deflections according to the above interpretation of the deformation criterion, the following values hold:

- For the fuel bed controlled fire: 485 mm (i.e. app. L/19);
- For the ventilation controlled fire: 644 mm (i.e. app. L/14).

For the fuel bed controlled fire, the structure just fails the deformation criterion (= near to limiting deformation). For the ventilation-controlled fire, the deformation is well beyond acceptable limits, i.e. failure must be assumed to occur. The latter outcome is explained by the fact that, due to the extreme long fire duration, the construction is much more heated through than in the case of the fuel bed controlled conditions.

Fig. 4.9 illustrates the effect of the loading on the deformation. For the fuel bed controlled case a reduction of the variable loading to 2.15 kN/m^2 is necessary to meet all failure conditions; for the ventilation controlled case the loading is not a meaningful parameter to influence the failure behaviour

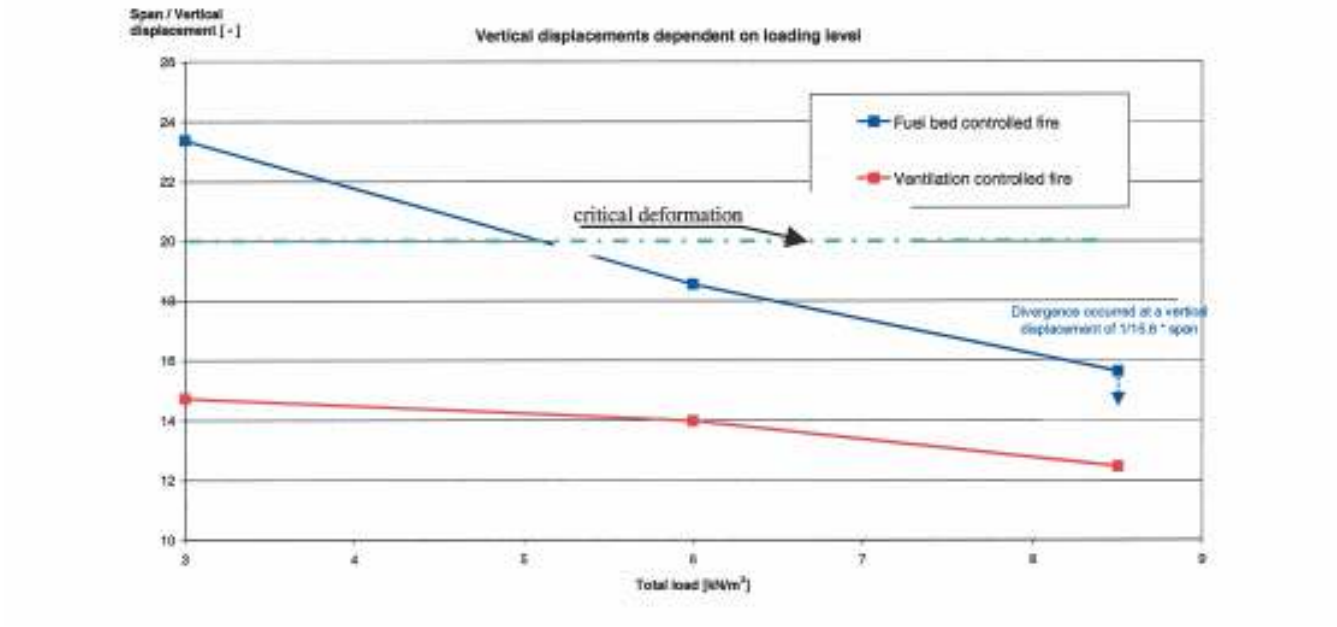

Fig. 4.9: Maximum relative vertical displacement as function of the loading.

For the fuel bed controlled situation, an additional analysis has been performed, now for a fire load density of 300 MJ/m^2. The value of the opening factor for which a maximum steel temperature of 700 °C is reached amounts 0.12 m$^{1/2}$. This situation is represented by point C in Fig. 4.6^b. The maximum relative deflections as function of time are presented in the Figs. 4.10^{a,b}. One can conclude from this Fig. that – again - for an imposed load of 3 kN/m^2, the floor is about to fail. For an imposed load of 5 kN/m^2 the failure criterion is just breached. In other words: the choice of 700 °C seems to be a fair estimate for the reference steel temperature Θ_{ref}, at least under fuel bed controlled conditions.

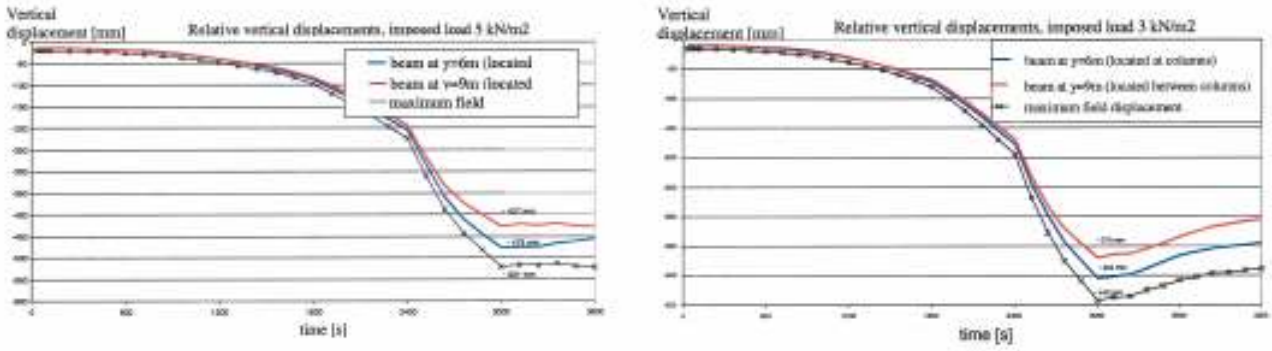

(a) Imposed load: 5 kN/m^2 (b) Imposed load 3 kN/m^2

Fig. 4.10: Maximum relative vertical displacements of the primary beam as function of time (basic case b with fire load density of 300 MJ/m^2 and fuel bed controlled conditions, see also point C of Fig. 4.6^a)

The above calculation results apply to basic case "b", i.e. a medium size fire compartment. With a view to investigate the effect of increasing compartment size, a similar analysis has been carried out for basic case "a" (large fire compartment). As in the previous analysis, two values of the fire load density have been chosen, i.e. 300 and 700 MJ/m^2 and two values of the imposed load: 3 and 5 kN/m^2. The analysis is limited to fuel bed controlled fire conditions. The procedure explained in par. 4.2 has been followed, taking Θ_{ref} = 700 °C.

All cases exhibit a similar behaviour, which will be explained hereafter by reference to the situation characterised by a fire load density of 300 MJ/m^2 and an imposed load of 3.0 kN/m^2 (ref.: case $a_{300,3}$)

The compartment analysed is illustrated in Fig. 4.10a. In this figure, also the position is indicated of some nodes of the secondary beams for which critical deformations occur.

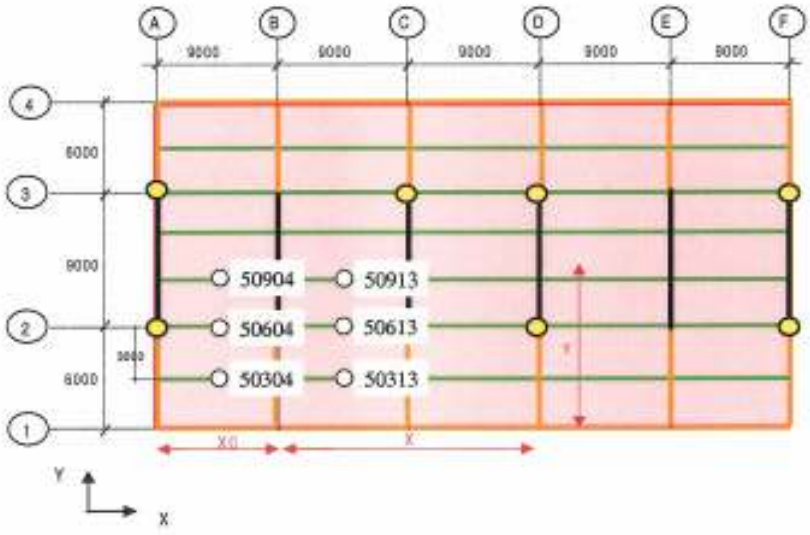

Fig. 4.10a: Position of nodes for relative vertical displacements of main secondary beams for case $a_{300,3}$

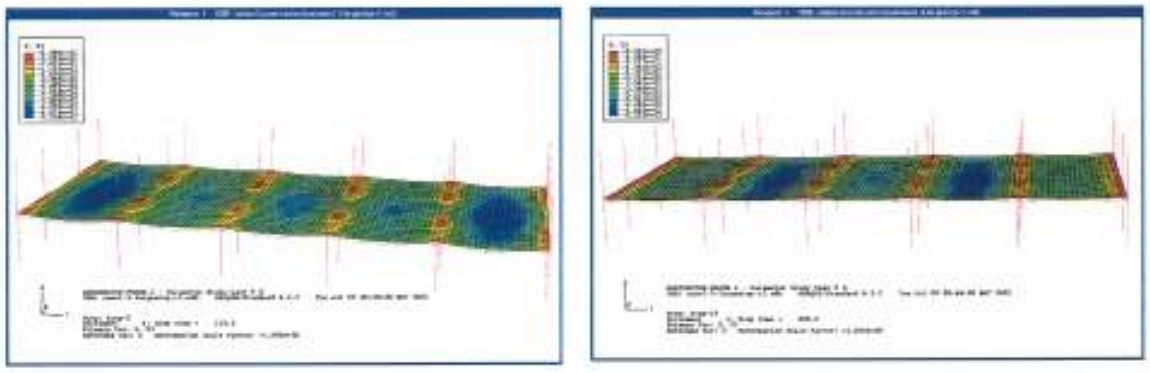

(a) at peak temperature (b) at end of analysis

Fig. 4.11: Vertical displacements of slab (case $a_{300,3}$)

Figure1.4.11[a] shows the deflected shape of the fire compartment at peak beam temperature (at ~3720 seconds). Note that the maximum deflections occur in the end bay and are of the order of 500mm. These deflections are total deflections and need to have secondary beam deflections subtracted to check relative deflection. Deflections in the middle bays are only of the order of 350mm. Figure 4.11[b] shows the deflected shape at the end of the analysis. Note that the deflections in the end bay have now decreased to around 150mm but deflections in second bay have increased to around 500mm, even though the entire structure is cooling down together. This must be due to the recovery of the strength of the main secondary and primary beams and locked in plastic strain in those beams, which occurs on heating. Relative deflections of the main secondary beams are shown in Fig. 4.12. For illustration, the deflection curves for a situation characterised by an fire load density of 300 and an imposed load of 5 kN/m^2 are also presented (ref.: case $a_{300,5}$). For case $a_{300,3}$, the maximum relative deflection criterion of 450mm (span/20) is about to be reached at 3600s for the secondary beam in the end bay between columns (node 50604 –Fig. 4.10) and at ~5400s, on cooling, for the secondary beam in the second bay between columns (node 50613 –Figure 4.10). The situation for case $a_{300,5}$ appears to be more critical: here the deformation criterion is breached.

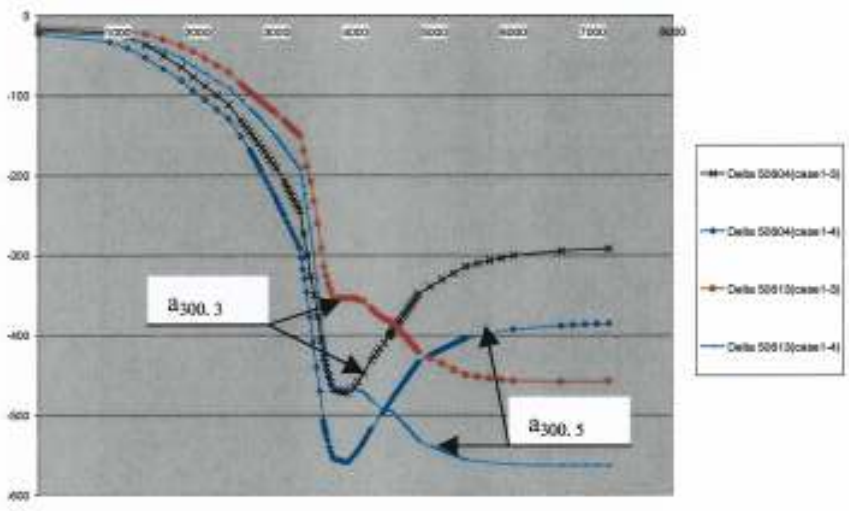

Fig. 4.12: Comparison of relative deflection of secondary beams for cases $a_{300,3}$ and $a_{300,5}$

The peak deflections are dependent on the degree of restraint to the relevant beam and the compatibility of the overall thermally strained shape of compartment. It also appears that for large compartments, the cooling phase needs to be considered as well as the heating phase. This implies that verification of how analysis programmes handle unloading behaviour needs to take place. For a more in depth discussion on the global distribution of stresses, force and moments and the consequences thereof, refer to Annex G.
The above analysis (including Annex G), illustrates that – if the fire is fuel bed controlled - also for a large fire compartment and for imposed loads in a practical range of 3 to 5 kN/m^2, 700 °C is a fair estimate for the reference steel temperature Θ_{ref} as defined in par. 4.2. It is, however, also shown that the actual value of the Θ_{ref} depends on many factors and cannot be given by a simple "rule of the thumb". In the design procedure, the concept of which is given in chapter 5, the assumption of 700 °C for the reference steel temperature is, therefore, proposed as a first estimate, useful for pre-design purposes. For a more detailed design, an in depth analysis is necessary, using an appropriate mechanical response model, such as the "streamlined" versions of DIANA, ANSYS and ABAQUS, developed in the scope of this project.

If the fire is ventilation controlled, the assumption of 700 °C for the reference steel temperature is too high. Further to a simplified approach, based on EC4-1.2, it can be shown that – under such conditions – 600 °C is a better estimate for the reference steel temperature. For details, refer to the Design Guide [15]. Also in this case, the validity of the assumption must be verified. See chapter 5.

- ***Amount of reinforcement***

The objective of the simulations is to investigate the sensitivity of the deflection of the floor to the amount of reinforcement.
Simulations have been carried out for different amounts of reinforcement. In these simulations the reinforcement in x- and y-directions was the same.
Additionally, simulations have been carried out with reinforcement oriented in only one direction.

The reinforcement in the CARDINGTON building is Ø6-200 (6mm diameter at distances of 200mm) in both x- and y-directions. In the simulations, reinforcements varying from Ø6-400 to Ø16-200 were used (6 simulations in total). It is very unpractical to use 16mm diameter reinforcement in the floor slab, however, the aim of the simulations is not to find a realistic reinforcement, but to provide a clear understanding of the sensitivity of the floor deflection to the amount of reinforcement.

Additional simulations with reinforcement in only one direction have been carried out with Ø6-200 and Ø8-200, one in x-direction and one in y-direction (4 simulations in total).

The other parameters were in line with the assumptions of basic case "b" (medium size fire compartment). The fire scenario was a 700 MJ/m^2 fire, with an opening factor of 0.177. See point B of Fig. 4.6[b]. The imposed load on the floor was 3.0 kN/m^2.

In Fig. 4.13 the relative deflection of the secondary beam in the first bay, located at y = 6m, is shown for different diameters of reinforcement bars.

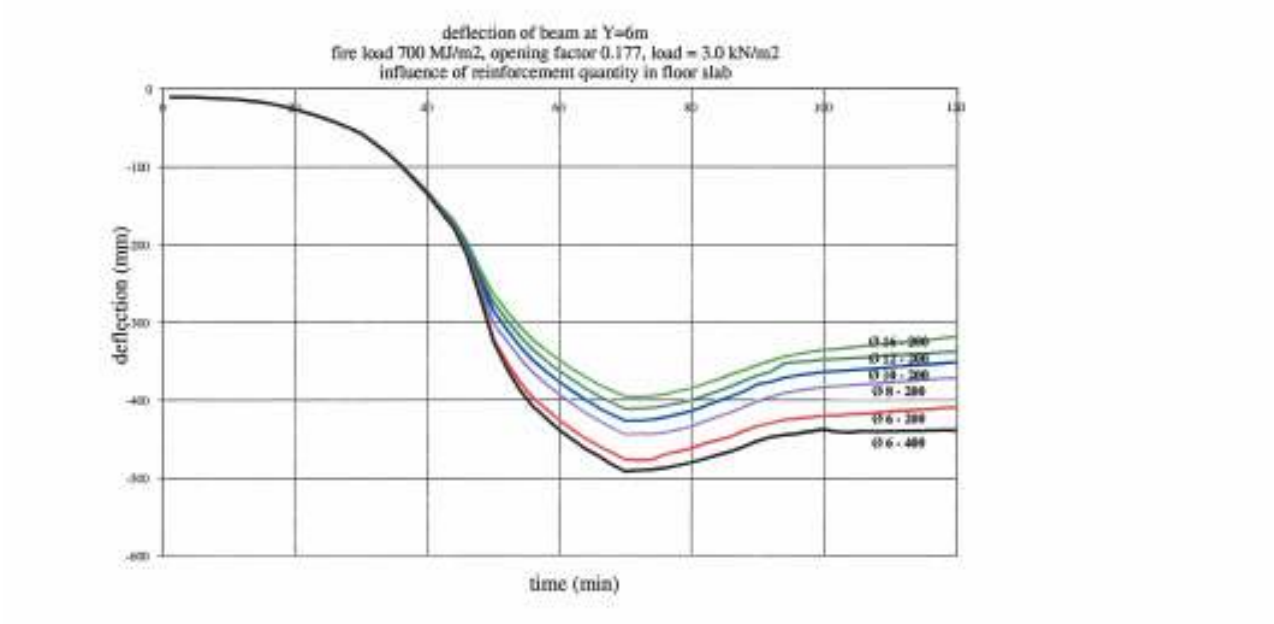

Fig. 4.13: Relative deflection for various amounts of reinforcement.

From the figure it becomes clear, that the influence of the amount of reinforcement is not very strong. This becomes clearer when figure 4.14 is considered. In this figure, on the vertical axis the maximum deflection of the beam is plotted. On the horizontal axis, the amount of reinforcement is represented by an equivalent reinforcement thickness. The equivalent reinforcement thickness is a simplified value in which all reinforcement bars are considered as a steel plate of a certain thickness. (e.g. Ø6-200 gives 5 bars of ¼π·6^2 mm^2 per 1000 mm; 5/1000 · ¼π·6^2 = 0.142 mm equivalent thickness).

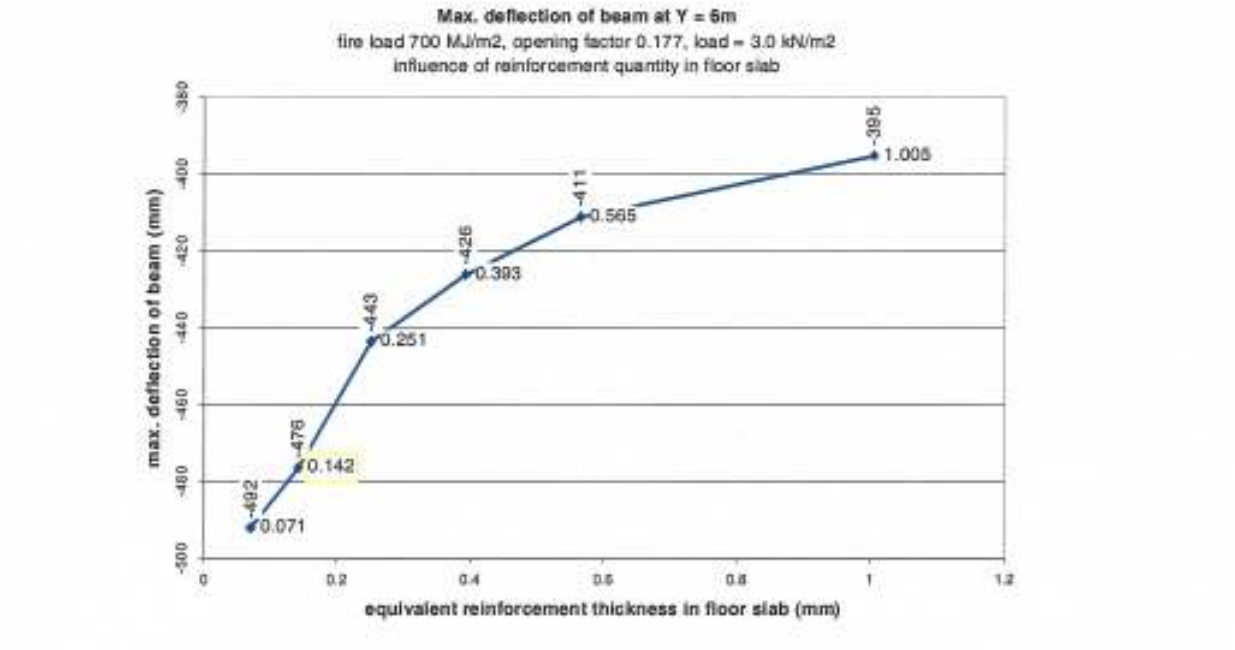

Fig. 4.14: Maximum relative deflection for various values of the equivalent reinforcement thickness.

The results show that replacing 6mm diameter bars by 16mm bars diameter (equivalent thickness 7 times higher) gives only a 17% decrease of the maximum deflection. However, the steepest part of the graph is from 0.142mm (=Ø6-200) to 0.251mm (=Ø8-200) equivalent thickness. In this range, the maximum deflection decreases 7%. If reinforcement of more than 0.251mm equivalent thickness is used, the improvement is negligible.

For the cases Ø6-200 and Ø8-200, simulations have been carried out with the reinforcement applied in only one direction. The results of these simulations are shown in Fig. 15[a,b].

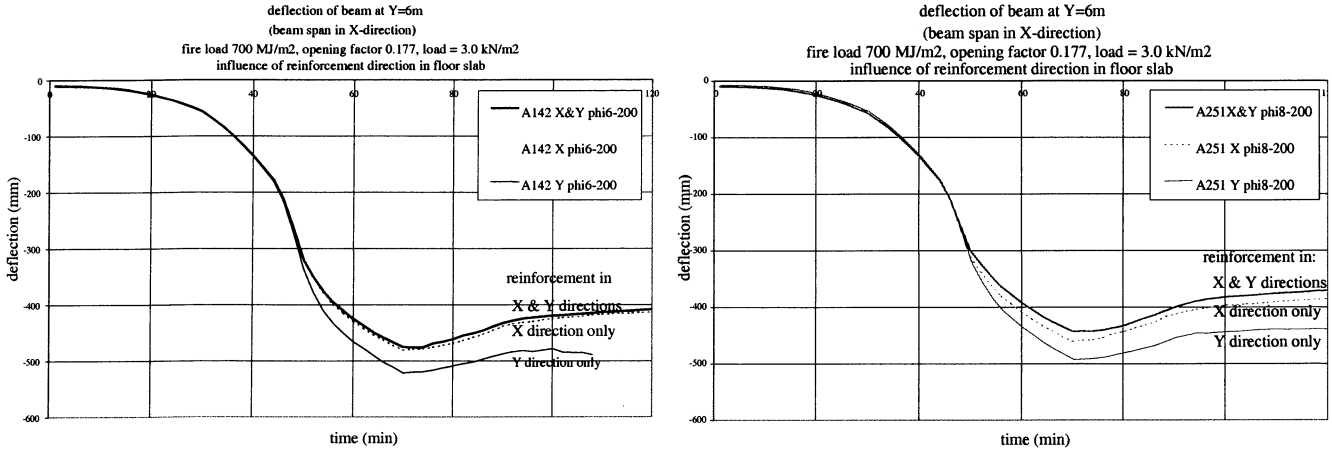

(a) Ø6-200 (b) Ø8-200

Fig. 4.15: Relative deflection for various amounts of reinforcement

The relative deflection of the secondary beam at y = 6m in the first bay is representative for the total deflection of the floor. Since this particular beam spans in x-direction, it is hardly surprising that the reinforcement in x-direction appears to be the most effective. If reinforcement in y-direction is omitted, this hardly influences the deflection.
In practice it is impossible to omit the reinforcement in one direction. However, the results of the simulations show that if there is any improvement to be realised by adding reinforcement, it is recommended to add Ø8-200 reinforcement in x-direction, and leave the y-direction at Ø6-200.

Although the influence of the amount of reinforcement on the maximum deflection is relatively low, the situation can be slightly improved by adding a little more reinforcement in the most effective direction.

- ***Structural grid spacing***

There is a lot of scope to consider different structural grid spacing. Two cases were chosen for analysis.

In previous analyses, grid spacing was based upon CARDINGTON building. Concrete slab is 130mm thick over secondary beams at 3m spacing. Column spacing across 21m direction are 6m-9m-6m respectively and across 45m direction are 5 x 9m bays. Refer to Fig. 3.13 for a plan of the CARDINGTON building.
The grid spacing to be considered in the present analysis has a concrete slab of 130mm thick over secondary beams at 3m spacing. Column spacing across 21m direction are 6m-9m-6m respectively and across 48m direction are 4 x 12m bays. Steel frame and floor slabs have been designed on the basis of practical, room temperature design considerations. Refer to Fig. 4.16 for the alternative plan and the selected steel profiles.

In addition to the above, also the mechanical loading (imposed mechanical load: 3.0 and 5.0 kN/m^2) and the fire load (300 and 700 MJ/m^2) have been decided to be varied in the calculations. For a review of the considered situations, refer to Table 4.5.

Table 4.5: Review of the parametric study into the effect of the structural grid spacing

imposed load ⇒ ⇓ fire load density	3 kN/m^2	5 kN/m^2
700 MJ/m^2	G-1	G-2
300 MJ/m^2	G-3	G-4

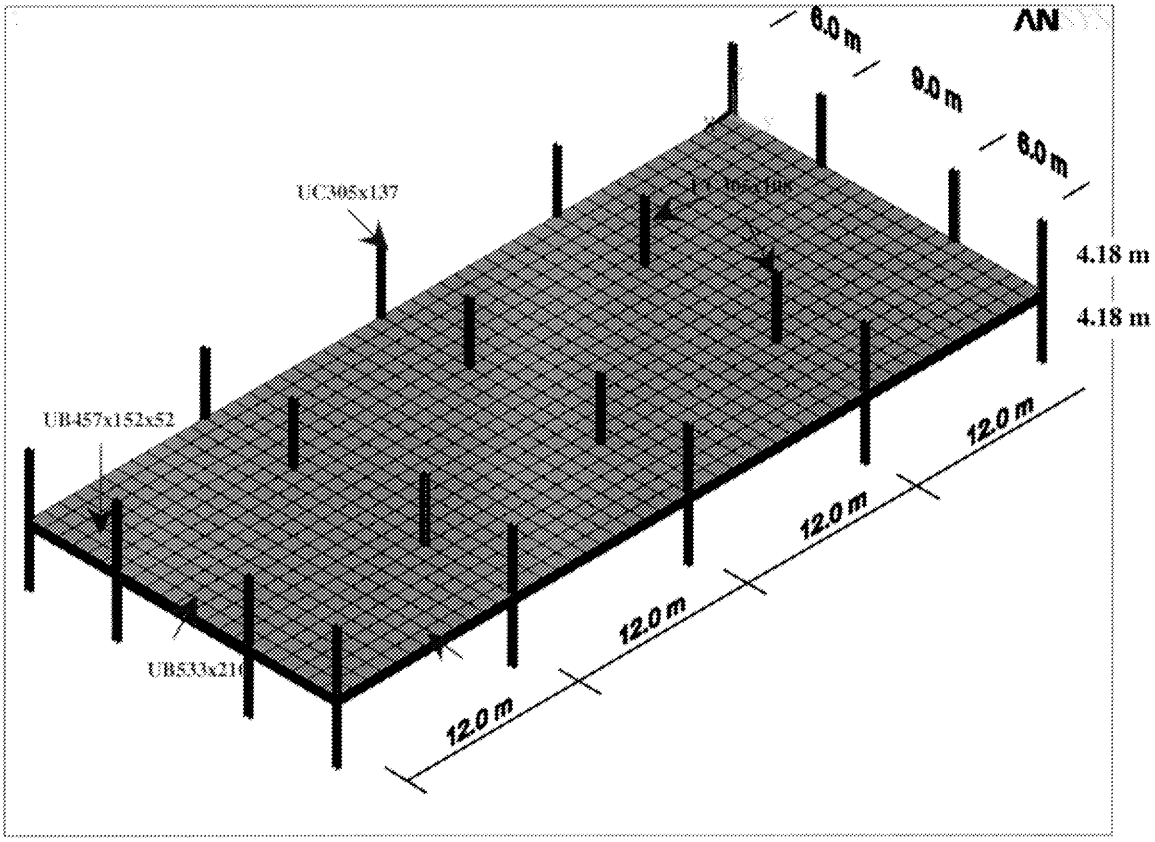

Fig. 4.16: Alternative structural grid spacing

For all calculations, basic case "b" applied (medium size fire compartment). As in earlier analyses, the opening factors were chosen such, that the maximum temperature in the lower flange of the primary beam was 700 °C. For some results in terms of relative deflection curves, refer to Fig. 17[a-d]

From Fig. 17 it may be concluded that in all four cases the criterion with regard to the relative deformation (in this case: $(\delta/L)_{rel} \leq 600$ mm) is not breached. Note that in the original design, breaching of the deformation criteria depends very much on the design values for the fire load density and the imposed load. See the discussion on the effect of the mechanical loading. Reason for this different result is that - by choosing practical steel profiles for the alternative grid spacing - a relatively low utilisation factor for the secondary beams is achieved when compared to the original design. The thermal response is hardly affected.

The analysis shows, that an unintended side effect of the room temperature design, may significantly influence the outcome of the structural fire safety design.

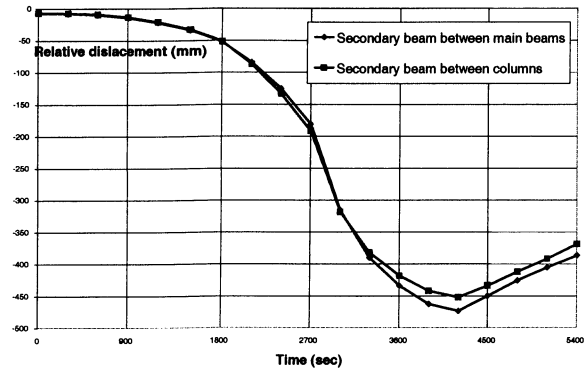

(a) case G-1 (300 MJ/m^2; 3 kN/m^2)

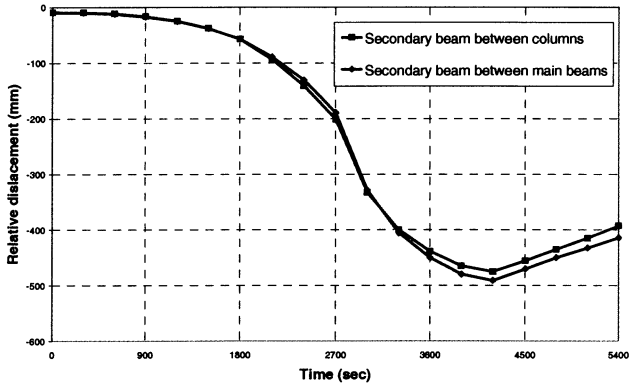

(b) case G-2 (300 MJ/m^2; 5 kN/m^2)

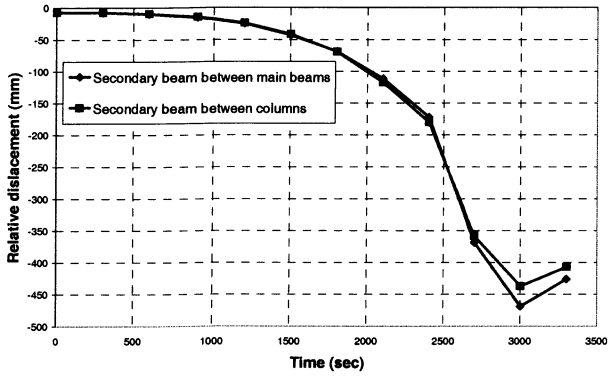

(c) Case G-3 (700 MJ/m^2; 3 kN/m^2)

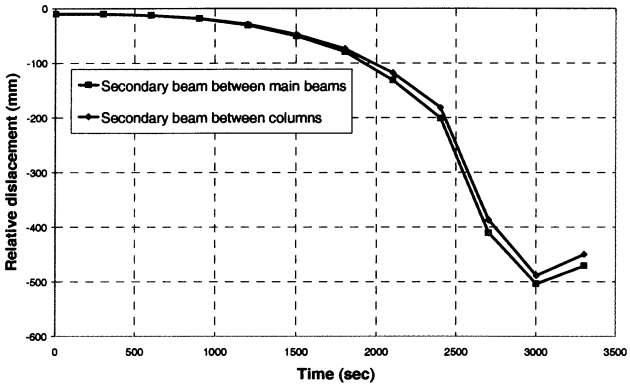

(d) Case G-4 (700 MJ/m^2; 5 kN/m^2)

Fig. 4.17: Deflection curves for the alternative structural grid spacing and various values for the fire load density and the imposed loading.

- ***Light weight concrete (LWC) vs. normal weight concrete (NWC)***

The objective of the simulations is to compare the behaviour of a construction with light weight concrete (LWC) floor slabs with the behaviour of a construction with normal weight concrete (NWC) floor slabs.
This comparison is focused on the relative deflection of secondary beams in the end bay of the floor.

The differences in material properties between normal weight concrete and light weight concrete are
- Thermal conductivity;
- Specific heat;
- Unit mass;
- Stiffness;
- Thermal expansion.

For these properties the values were taken according to the prEN1994-1-2 [12]. The tensile and compressive strength of LWC were assumed to be equal to the strength of NC. For simulation of the mechanical behaviour, the unit mass, stiffness and thermal expansion are of importance.

According to prEN1994-1-2, the unit mass of LWC "shall be in the range of 1600 to 2000 kg/m^3". A value of 1800 kg/m^3 was assumed for the simulation.
The stress-strain relationship is defined by the compressive strength and the strain at maximum compression. The compressive strength was assumed to be identical to the strength of NWC. The strain

at maximum compression "should be obtained from tests". A more practical approach has been followed by reducing the Young's modulus to 60% of the normal weight concrete value. Since the sensitivity of the maximum deflection to the Young's modulus is unknown, the simulation has also been done with a 100% Young's modulus.
The thermal expansion coefficient is taken as 8.0*10-6 K^{-1} for all temperatures.

The following scenarios were simulated with LWC floor slabs (as in earlier analyses):

- Imposed load: 3.0 and 5.0 kN/m2.
- Fire scenarios: 300 MJ/m2 (opening factor 0.14) and 700 MJ/m2 (opening factor 0.177).
- Basic type "b" fire compartment.

These scenarios, 4 in total, can be compared with the earlier simulation results for NWC with the same scenarios.

The first comparison is the deflection of the secondary beam in the first bay, located at y = 6m. The results for all scenarios with LWC are shown in Fig. 4.18[a,b].

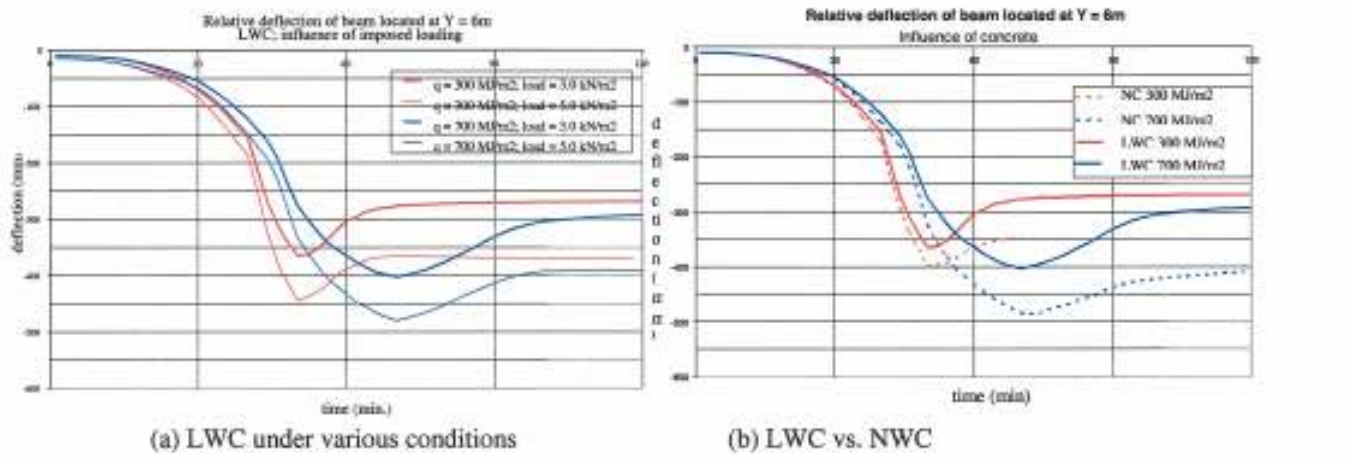

(a) LWC under various conditions (b) LWC vs. NWC

Fig. 4.18: Deflection curves of the secondary beam: LWC vs. NWC under ventilation controlled conditions (basic case "b"; various values for the fire load density and imposed load).

The figure shows a similar behaviour as the NWC simulations that were carried out earlier, i.e. a higher imposed loading results in a larger deflections. A comparison between the NWC and LWC simulations is shown in Fig. 4.18[b]. In this figure it becomes clear that the deflection with LWC is significantly less than with NC. For imposed loads of 5.0 kN/m^2 this is also the case.

Finally, simulations were carried out to investigate the sensitivity to the value of the Young's modulus. In Fig. 4.19 the results of this comparison are shown for the 300 MJ/m^2 fire scenario.

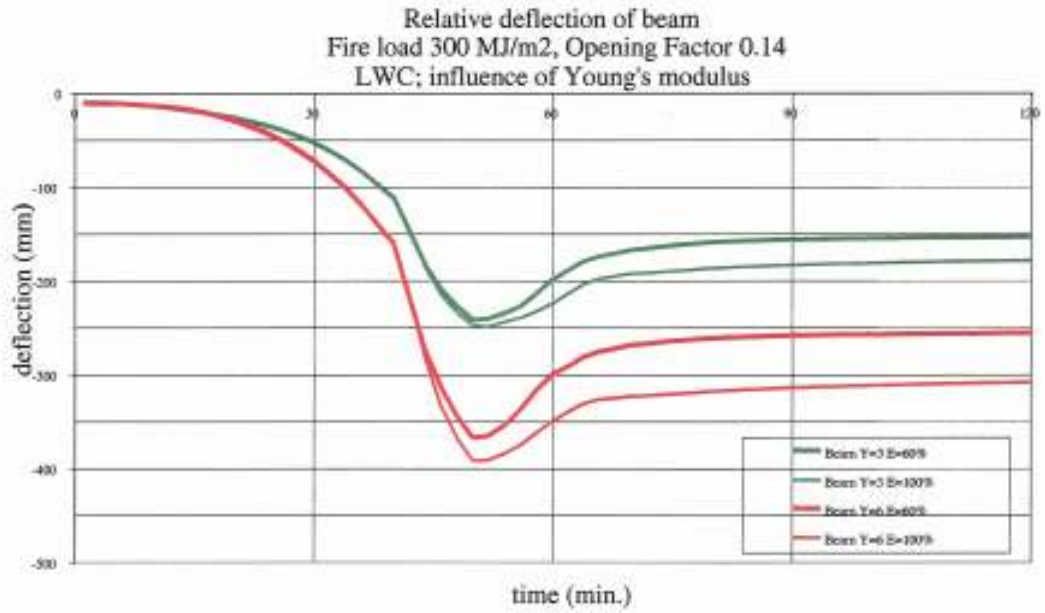

Fig. 4.19: Deflection of secondary beam with LWC floor slab for different Young's moduli.

From this figure it becomes clear, that a stiffer floor deflects more. This is remarkable because at ambient temperature the opposite will be the case. However, in fire conditions the thermal elongation of the floor plays an important role in the deflection. In this perspective it is logical that LWC causes less deflection than NWC, since the thermal expansion coefficient of LWC is lower. When the stiffness is less, the thermal elongation will cause less compression in the floor slab and therefore the deflection of the floor will be less. Of course, the compression in the floor is strongly dependent on the support conditions. If the thermal expansion is unrestrained, this effect will be absent. This can also be seen in the figure: for the beam at y = 3m the difference is much smaller than for the beam at y = 6m. The beam at y = 6m is fully restrained in horizontal direction in the model, while the beam at y = 3m is allowed to expand.

In conclusion: less deflection of lightweight concrete compared to normal weight concrete is caused by

- Lower unit mass.
- Lower Young's modulus.
- Lower thermal expansion.

The lower unit mass decreases the total load and therefore decreases the deflection as expected. Lowering the Young's modulus and thermal expansion causes a decrease of the deflection because the compressive stresses due to thermal expansion become less.

5. Design Procedure

5.1 Overview

In the scope of this research, an important objective of the structural fire safety design of composite steel framed buildings is to identify the conditions under which the steel beams can remain without fire insulation. In this chapter, a procedure is presented by which such conditions can be identified in a systematic manner, by using the design tools explored in the present project and discussed in the previous chapters. The procedure distinguishes between the following steps:

- Evaluation of the basic requirements.
- Performance of a pre-design.
- Performance of a detailed design.

In the subsequent paragraphs, each of the above steps is reviewed. The discussion will be limited to the main route. For details & evaluation refer to the Design Guide [15].

5.2 Basic requirements

The basic requirements follow from the anticipated occupancy and the required functionality of the building and are normally decided upon in the room temperature design. As such, the structural fire safety engineer has only limited influence on the basic requirements. Their relation with the input parameters of the structural fire design is presented in Fig. 5.1.

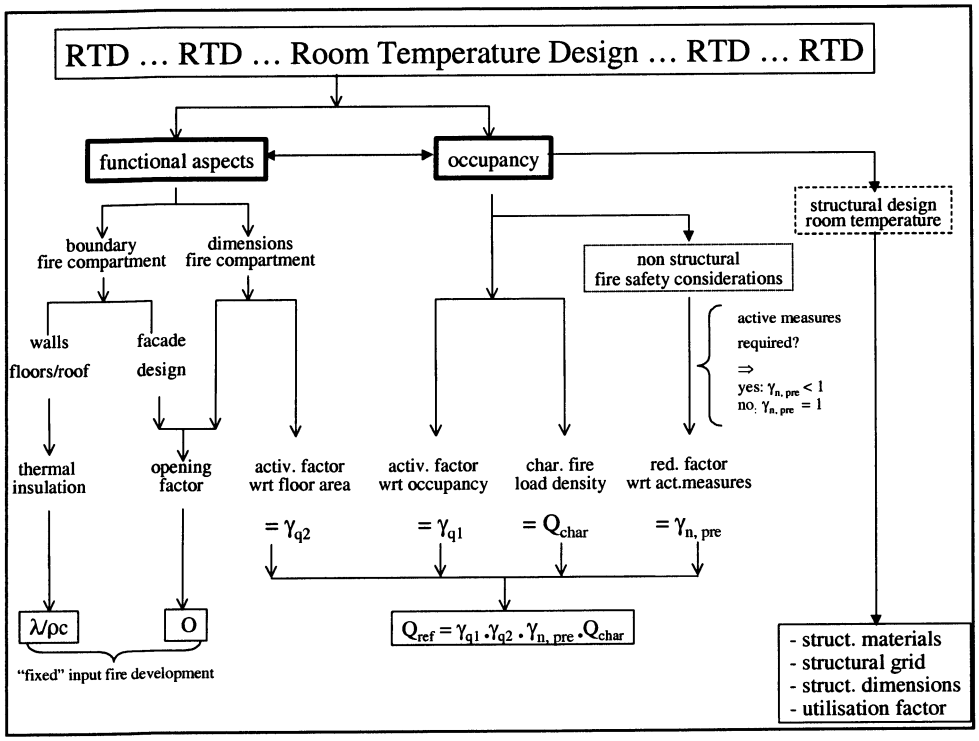

Fig. 5.1: Basic requirements for the Structural Fire Safety Design

The relationships shown in Fig. 5.1 can be elucidated as follows:

The functional aspects determine the dimensions of the fire compartment and its boundary conditions, in particular the façade design. By these factors the ventilation conditions (via the so-called "opening factor") and heat losses from the fire compartment are determined. Because these parameters follow directly from the basic requirements, they are denoted as "fixed" input for the structural fire design.

That means: modifying these factors will directly affect the room temperature design, hence the factors can not easily be changed.

As illustrated in the parametric study, also the fire load density is a factor which significantly influences the fire development (and consequently the structural behaviour) under natural fire conditions. Characteristic values of the fire load density follow directly from the occupancy, e.g. by means of statistical considerations. However, design values of the fire load density (i.e. values which are used as a basis for the structural fire engineering design) can strongly be influenced by active fire measures, such as sprinklers, detection etc. See the outcomes of the NFSC project [16]. These adaptation factors are denoted as γ_n-factors[10].

Other parameters, which – via the thermal and/or the mechanical response of the structural elements - affect the performance of structural systems under natural fire conditions, are:
- Mechanical loading.
- Reinforcement mesh.
- Column positions and beam sizes, e.g. by choosing a different structural grid spacing;
- Steel grade / concrete strength.
- Type of concrete (normal weight vs. lightweight concrete).

Some of these parameters (e.g. reinforcement mesh, steel grade/concrete strength and beams sizes) can be modified without major effect on the basics of the room temperature design. Others, such as the choice of concrete type and the structural grid spacing, may require substantial changes in the room temperature design and their feasibility is therefore doubtful. Note also that, as has been shown in the parametric study, the effect of these parameters is often rather limited.

Conclusion therefore is that - for various reasons – the fire load density is the main parameter by which structural fire safety design can be influenced in such a way that it is safe to apply unprotected steel beams[11]. The limiting value, for which this condition is just met, is denoted as the limiting value of the fire load density (= Q_{lim}). How to find Q_{lim} in a systematic manner is the aim of the structural fire safety design envisaged in the scope of the present research. Such a design is in two steps:
- *Pre design*, in which a first estimate of Q_{lim} is made; the pre-design must be "fast and easy" and is based on the fire model and (eventually) the thermal response models discussed in chapter 2;
- *Detailed design*, in which the estimated value of Q_{lim} should be verified and – if necessary – be adjusted; for this analysis also the (more time consuming) mechanical response models as evaluated in chapter 3 are necessary.

Design criterion for the steel beams to remain unprotected is that the limiting value of the fire load density is equal to or larger than the maximum value of the fire load density, following from the basic requirements and taking into account the appropriate γ-factors. See also Fig. 5.1.

For a review of the pre-design and the detailed design, refer to the paragraphs 5.3 and 5.4 respectively.

5.3 Pre-design

Aim of the pre-design is to make a motivated guess of the fire load density for which a steel framed, composite structural system is about to fail. This value is called the "limiting" value of the fire load density. The following steps are foreseen: (see also Fig. 5.2)

[10] Also the type of occupancy has – via the so-called activation factor γ_q an influence on the design values of the fire load density

[11] Note that for multi storey steel framed buildings, normally the columns have to be fire protected.

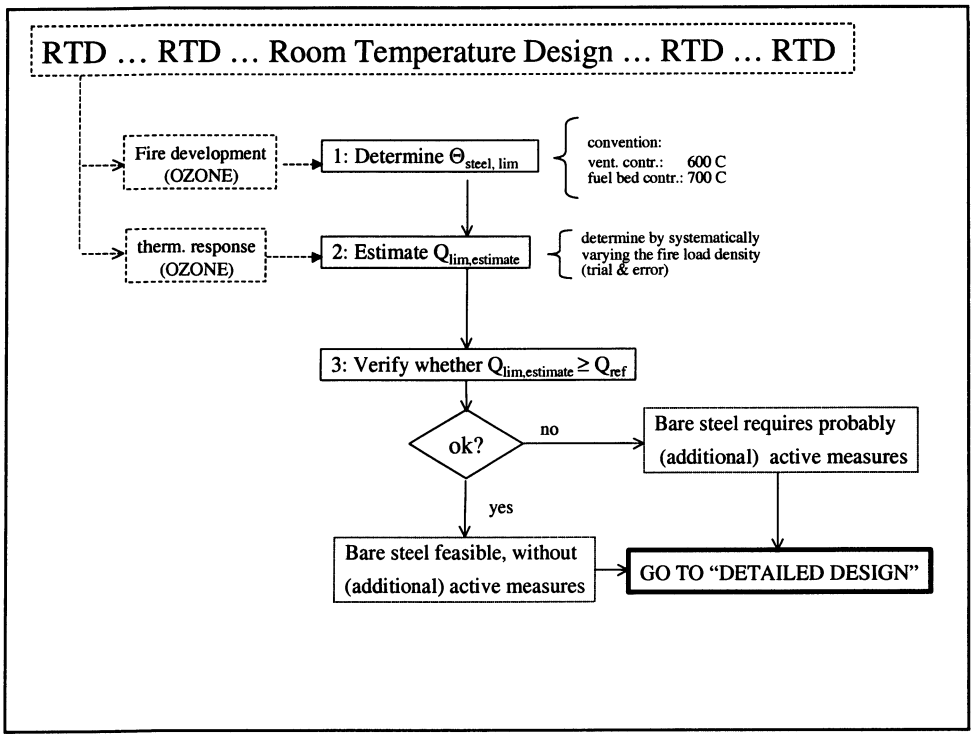

Fig. 5.2: The pre-design

step1: Determine the maximum value of the temperature of the lower flange of the primary steel beams for which failure is assumed to occur (notation: Θ_{lim}). The following conventions hold:
- Fuel bed controlled fire conditions: $\Theta_{lim} = 700$ °C.
- Ventilation controlled fire conditions: $\Theta_{lim} = 600.$ °C.

Which of the two above conditions holds, can easily be determined on basis of the rate of heat release development, which directly follows from e.g. an OZONE analysis into the fire development. In case of doubt, simply take the most conservative value, i.e. 600 °C. Rather than looking at the maximum steel temperature, one could base the assessment also on the maximum gas temperature, since the difference between maximum steel and gas temperature under fully developed fire conditions is only marginal. Compare e.g. Figs. 4.3 and 4.4.

step 2: Estimate the value of the fire load density, for which the above identified value of Θ_{lim} is just met. Notation: $Q_{lim,estimate}$. This assessment is carried out by systematically varying the fire load density in a fire development calculation, eventually followed by a thermal response calculation. Such an analysis can be performed in a "fast and easy" way by e.g. Ozone.

step 3: Verify whether the condition $Q_{lim,estimate} \geq Q_{ref}$ is fulfilled. If so, bare steel is feasible without (additional) measures; if not, bare steel requires probably (additional) measures.

Unless it is decided to apply fire insulation on the steel beams, it necessary to perform a more precise analysis in order to check whether for the estimated value of $Q_{lim,estimate}$ failure conditions are indeed not breached. This is the aim of the "detailed" design. See par. 5.4.

5.4 Detailed design

Aim of the detailed design is to verify in detail whether the criterion for the safe use of unprotected steel beams and floors, i.e. $Q_{lim} \geq Q_{ref}$, is actually met and to decide on additional fire safety measures, if any. Use is to be made of the calculation model discussed earlier (see chapter 2 and 3) including the FEM models on mechanical response. The models belonging to the last mentioned category are still rather time consuming: calculation time approximately 24 hours. Therefore, alternative – however: more conservative – options are offered. See also Fig. 5.2.

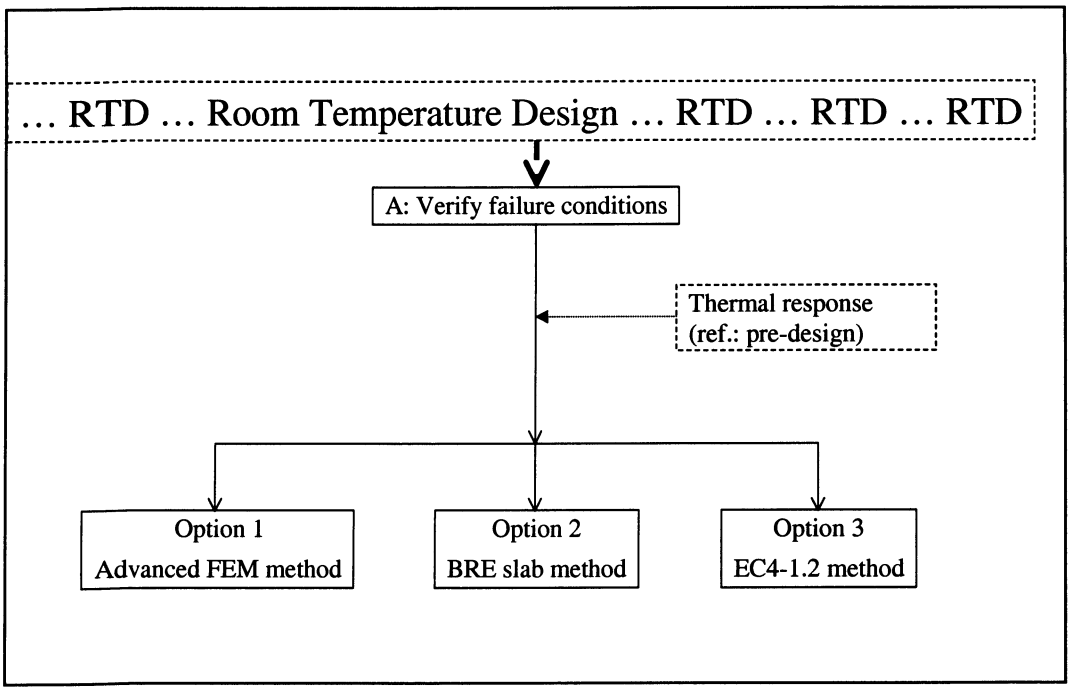

Fig. 5.3: Various options for the assessment of the mechanical response.

In order of hierarchy, the following options are distinguished:
- Streamlined FEM models (highest level);
- BRE slab method;
- EC4-1.2 method.

The EC4-1.2 method is directly based on the fire part of the Eurocode for composite structures [12] and ignores the interaction of the various elements in the structural system (member analysis). Generalized information based on natural fire conditions is provided, using the fire and thermal response models discussed in this Final Report. For some backgrounds, refer to Annex H. Practical information, including design tables and graphs, is given in the Design Guide [15].

The BRE slab method is based on a combination of yield line and membrane action and has been developed by BRE in the UK for standard fire conditions [17]. It does take into account – although in a conservative manner – the interaction between the different elements of a structural system. In the scope of the underlying research, the field of application has been extended into the area of natural fire conditions, using the fire and thermal response models discussed in this Final Report. For some backgrounds, refer to Annex G. Practical information, including design tables, is given in the Design Guide [15].

The streamlined models are based on advanced FEM models for the mechanical response and do take full account of the interaction between the various elements of the structural system. The models are extensively discussed in chapters 2 and 4. The detailed design procedure, based on these models, is summarized in Fig. 5.4.

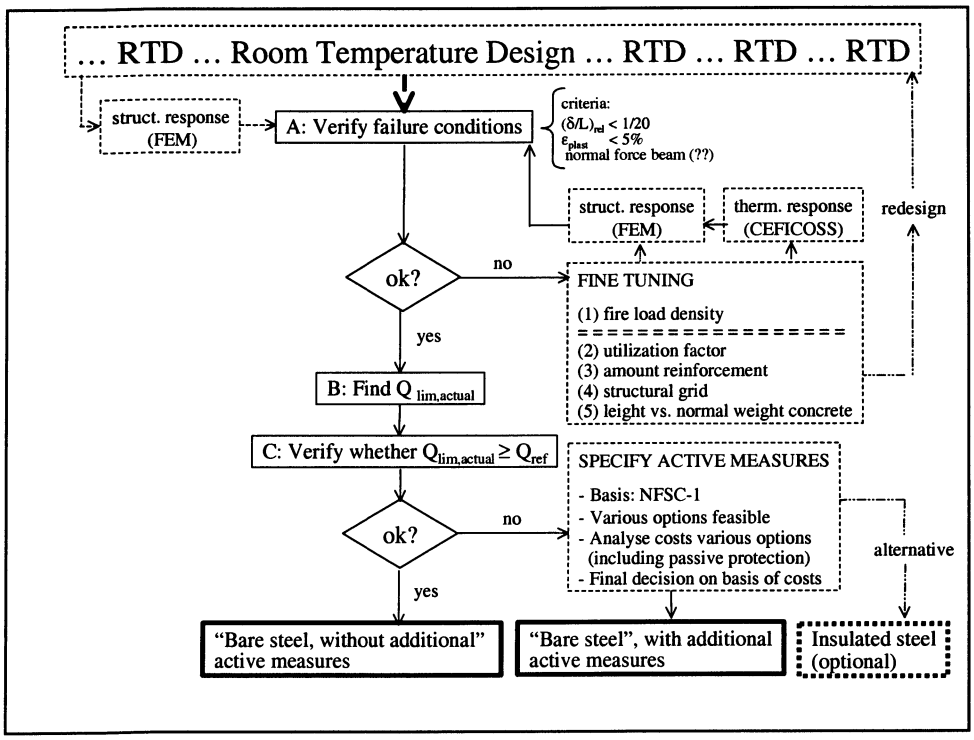

Fig. 5.4: Detailed design procedure

Three main steps are distinguished:

Step A: Verify failure conditions: Starting point is the thermal response under the limiting value of the fire load density and other conditions determined in the pre-design. Verification whether the failure conditions are met, is by means of the mechanical response models (FEM). For the time being, two failure criteria are identified (see also par. 4.2 and Annex D):

- The plastic strain of the reinforcement should less then or equal to 5%;
- The relative displacement of the floor beams should be less than 1/20th of the span.

In addition, one has to check the ability of the structural system (including connections) to be able to transmit the moments and forces in any phase of the fire exposure. See Annex E.

Step B: Find the actual value of the limiting fire load density: If the failure conditions are met, a (safe) value for the limiting fire load density is found (notation: $Q_{lim,act}$). If not, fine tuning of the analysis is necessary. For some suggestions, refer to the results of the parametric study (chapter 4). If fine tuning does not give the desired (practical) results, one could consider the option of re-discussing basic requirements (redesign).

Step C: Verify whether additional measures are necessary in order to leave the steel beams unprotected. This verification is in the fire load density domain, i.e.:

$$Q_{lim,act} \geq Q_{ref}$$

With:

- $Q_{lim,act}$ is the actual value of the limiting fire load density identified above;
- Q_{ref} is the maximum fire load density, following the basic requirements.

If the above condition is met, unprotected steel beams can be used without additional measures. If not additional active measures have to be selected, such that the "gap" between $Q_{lim,act}$ and Q_{ref} is closed. If, for any reasons (costs, practicality) this appears not to be possible, one could as yet decide to apply fire insulation on the steel beams.

For some practical considerations regarding the above detailed design procedure, based on the findings of the present research, refer to the Design Guide [15].

References

[1] Broadgate Phase 8 Fire, London, 1990.

[2] Martin, D. et al: "The Behaviour of Multi-storey Steel Framed Buildings in Fire". British Steel PLC, Swinden Technology Centre, UK, 1999.

[3] BHP William Street Fire Tests, Melbourne, Australia, 1999.

[4] Ozone 2.2.2, University of Liege, Liege, 2002

[5] CEFICOSS 12.0, ARBED, Luxembourg, 1997

[6] SAFIR, University of Liege, Liege, 2002

[7] F.C. de Witte: "DIANA User's Manual, Release 7.2". TNO, 1999.

[8] Swanson Analysis Systems, Inc. "ANSYS User's Manual for Revision 5.0 - Volume IV – Theory". Houston U.S.A., 1992.

[9] Hibbit, Karlsson and Sorensen Inc.: "ABAQUS/Standard Users's Manual – Version 6.2". Pawtucket, USA, 2001.

[10] Both, C.: The fire resistance of composite steel-concrete slabs, PhD-Thesis, Delft University of Technology, 1998.

[11] CEN TC250: ENV1993-1.2: "Eurocode on the Fire Design of Steel Structures". CEN, Brussels, 1995.

[12] CEN TC250: ENV1994-1.2: "Eurocode on the Fire Design of Composite Steel Concrete Structures". CEN, Brussels, 1994.

[13] Proposal by Y. Anderberg, Lund, Sweden, 1998 (private communication)

[14] Arnault, P., Ehm, H. and Kruppa, J.: "Résistance au feu des systèmes hyperstatiques en acier (poutres et portiques)". CTICM, , Doc CECM 3 - 74/6 F, mai 1974

[15] Newman, G. et al: "Design recommendations for composite steel framed building in fire". SCI Publication RT943, March 2003

[16] Schleich, J-B. et al: "Competitive steel buildings through natural fire safety concepts". EU, Directorate General for Research, Brussels, 2002.

[17] Bailey, C. and Moore, D.B.: " The structural behaviour of steel frames with composite floor slabs subject to fire; *Part 1: Theory & Part 2: Design*" The Structural Engineer, Volume 78/No 11, June 6, 2000.

List of Figures (Main text)

List of Tables (Main text)

Annex A: Stress strain diagrams of steel at elevated temperatures according to EC3 and Anderberg

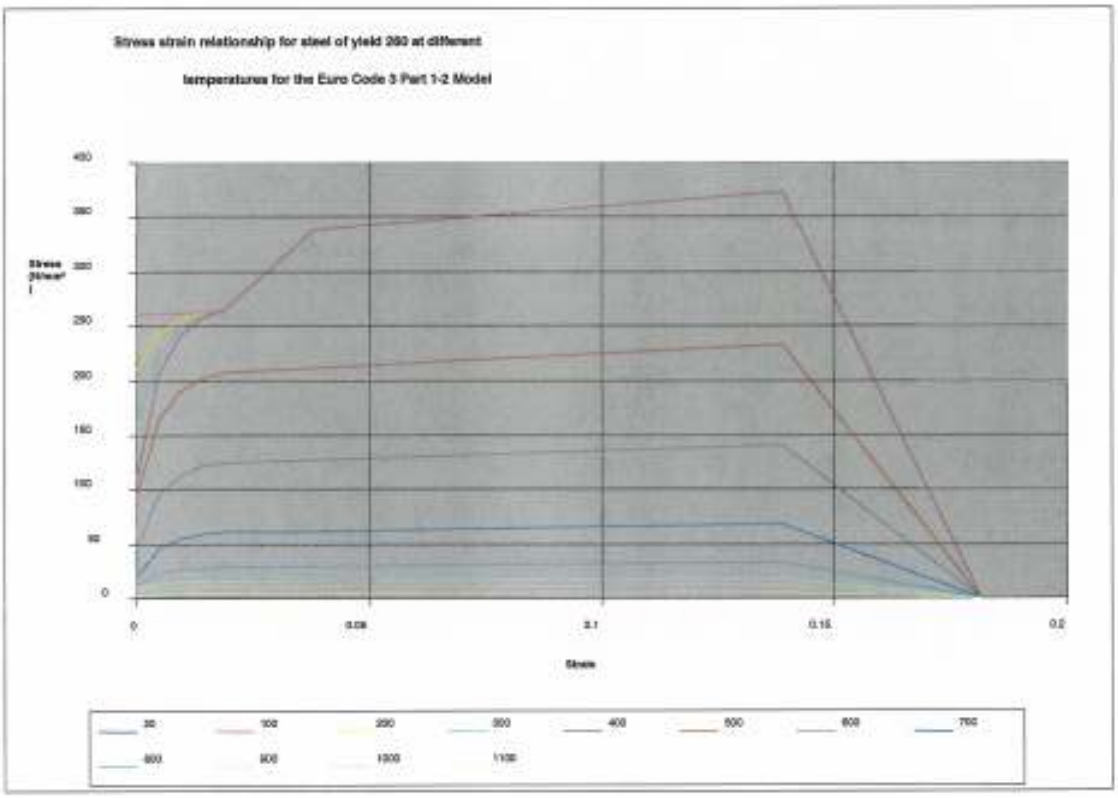

Fig. A-1: **Stress strain relationship at elevated temperatures for Fe 260 according ENV1993-1.2 [11]**

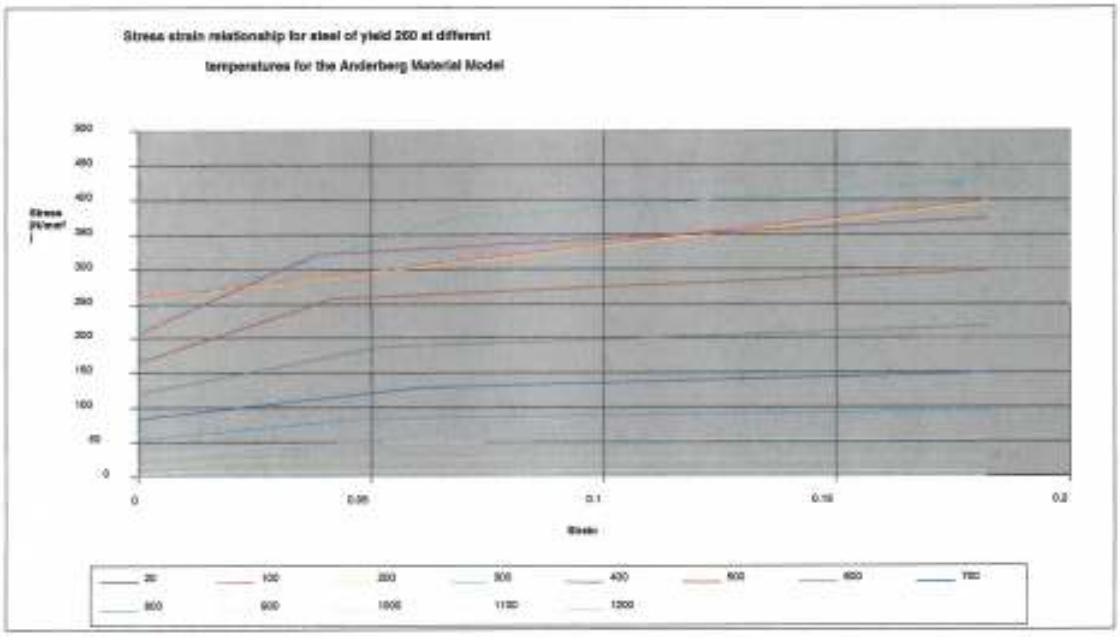

Fig. A-2: **Stress strain relationships at elevated temperatures for Fe 260 according to Anderberg [13]**

Annex B: Evaluation of the linear temperature distribution

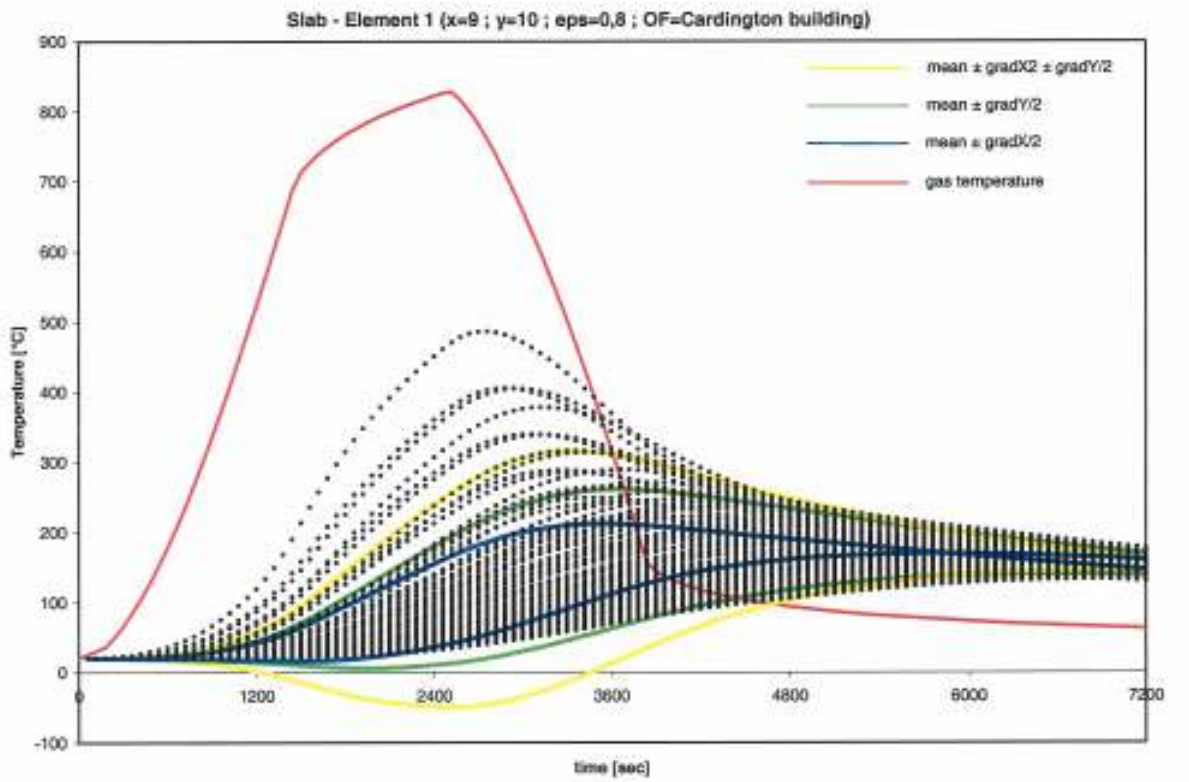

Fig. B.1: Composite concrete slab alone - Big element 1

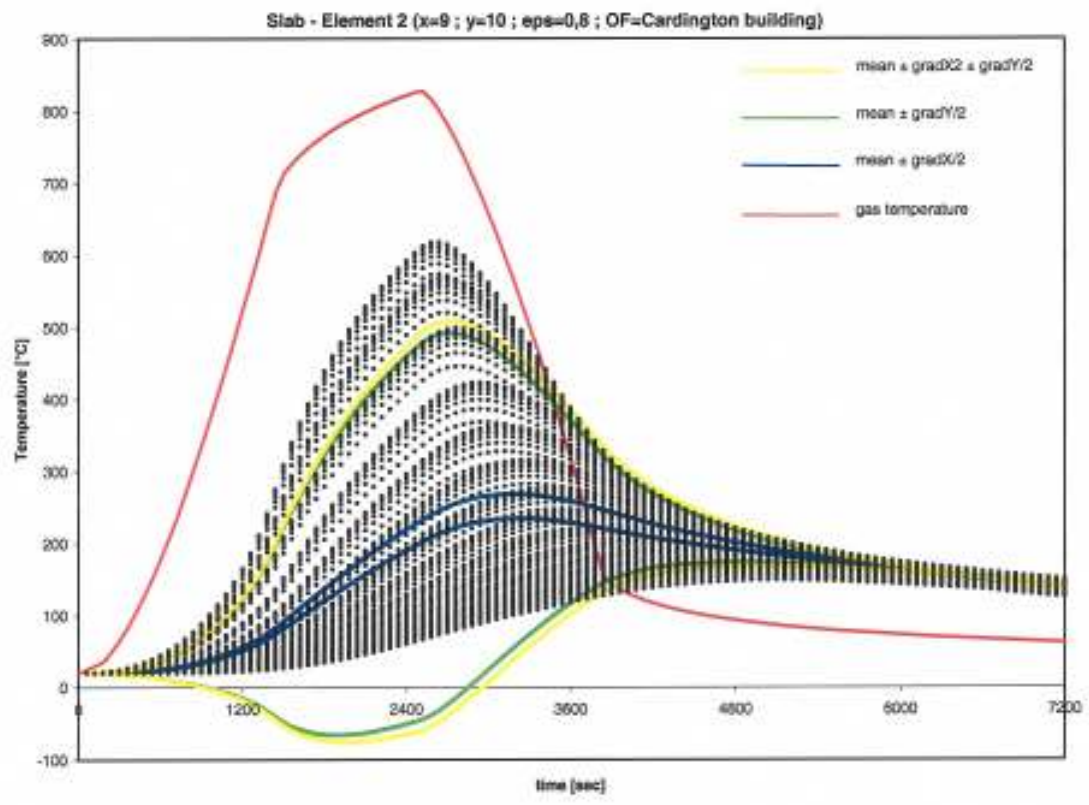

Fig. B.2: Composite concrete slab alone - Big element 2

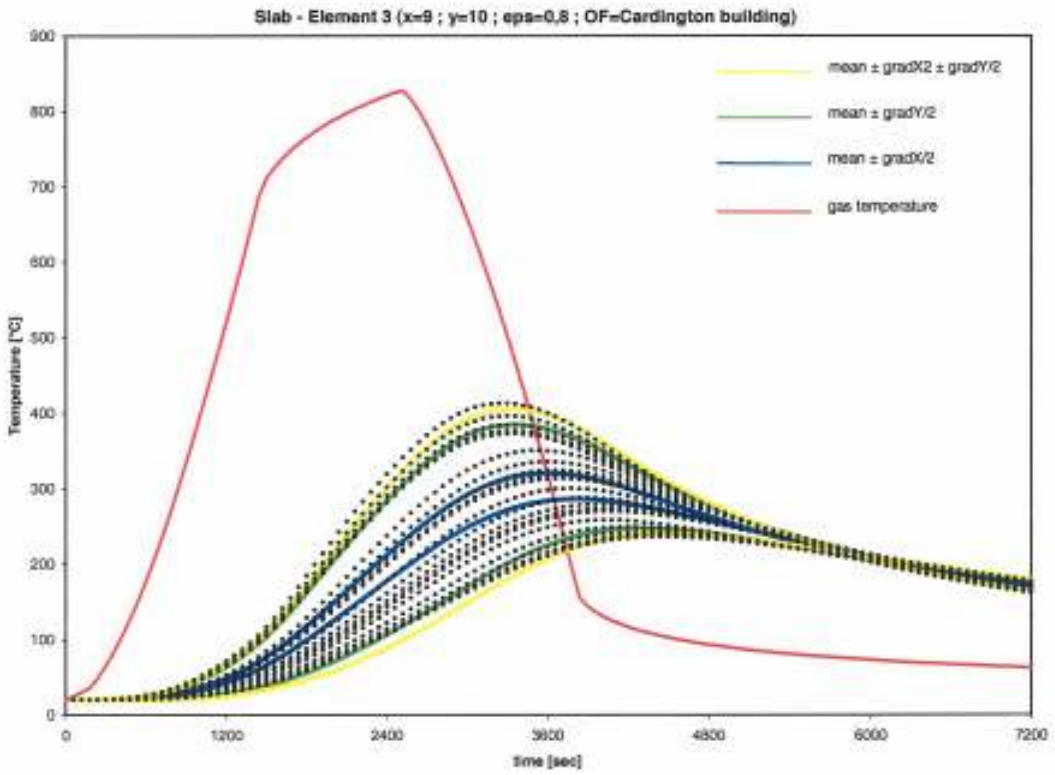

Fig. B.3: Composite concrete slab alone - Big element 3

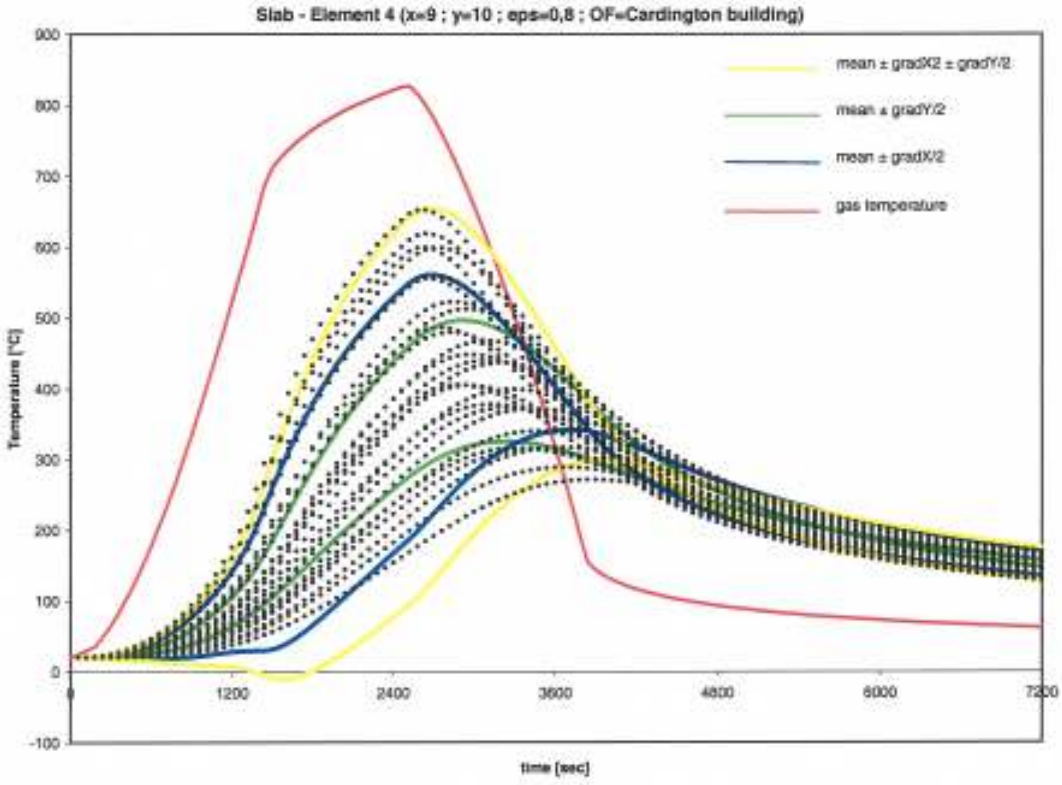

Fig. B.4: Composite concrete slab alone - Big element 4

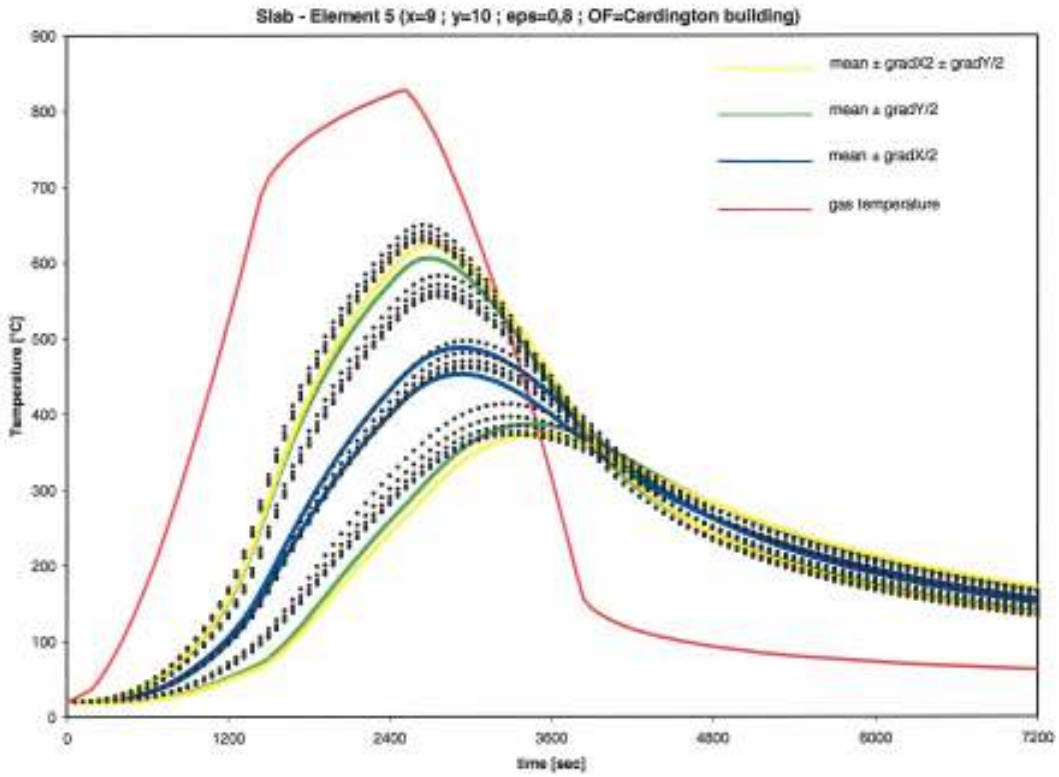

Fig. B.5: Composite concrete slab alone - Big element 5

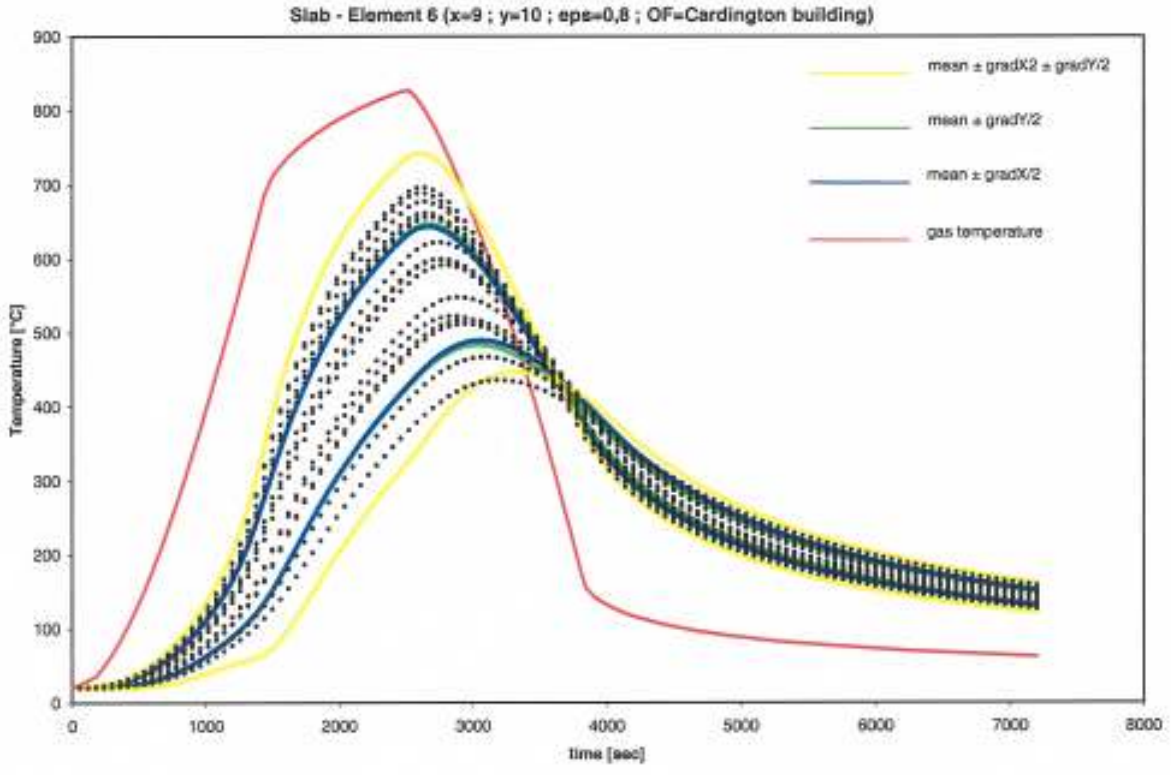

Fig. B.6: Composite concrete slab alone - Big element 6

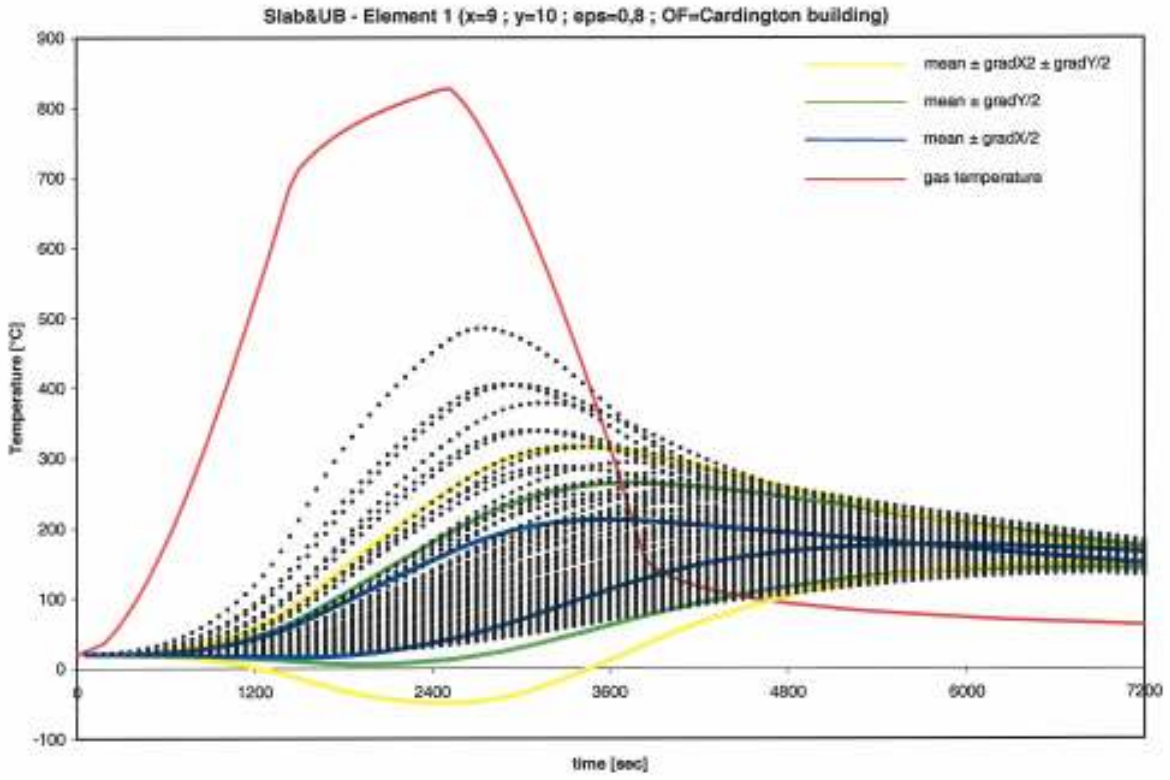

Fig. B.7 : **Steel profile under a composite concrete slab alone with ribs parallel to the beam - Big element 1**

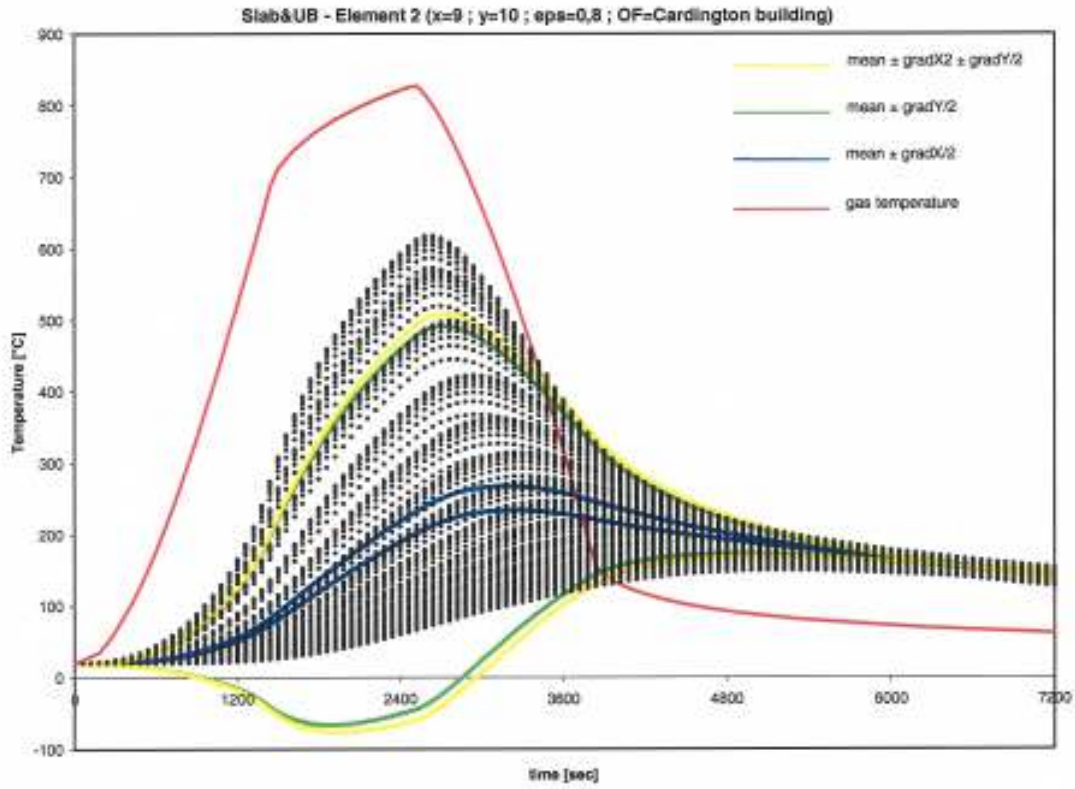

Fig. B.8: **Steel profile under a composite concrete slab alone with ribs parallel to the beam - Big element 2**

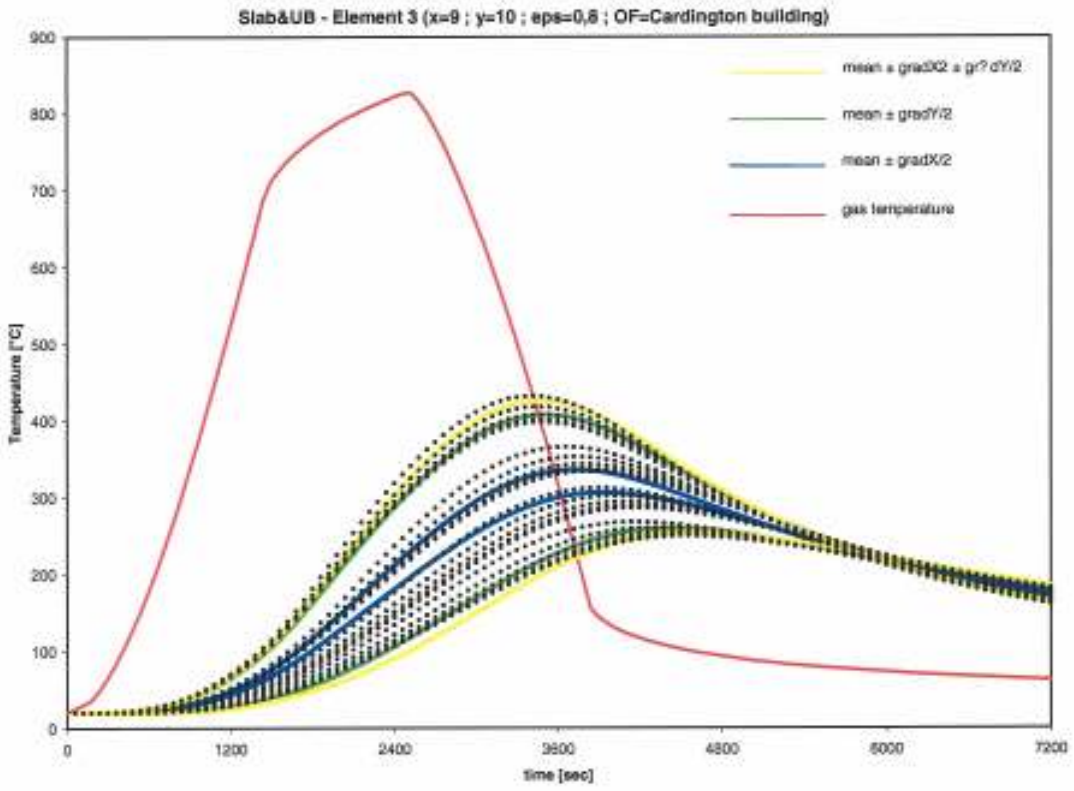

Fig. B.9: **Steel profile under a composite concrete slab alone with ribs parallel to the beam - Big element 3**

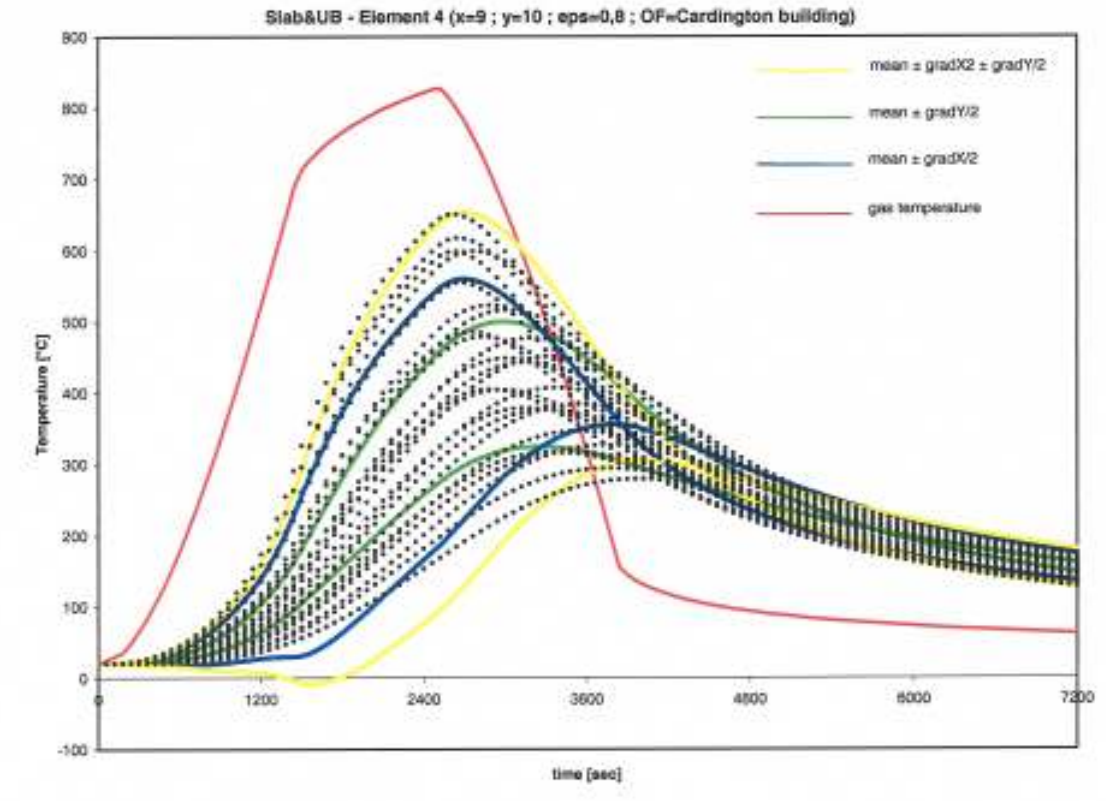

Fig. B.10: **Steel profile under a composite concrete slab alone with ribs parallel to the beam - Big element 4**

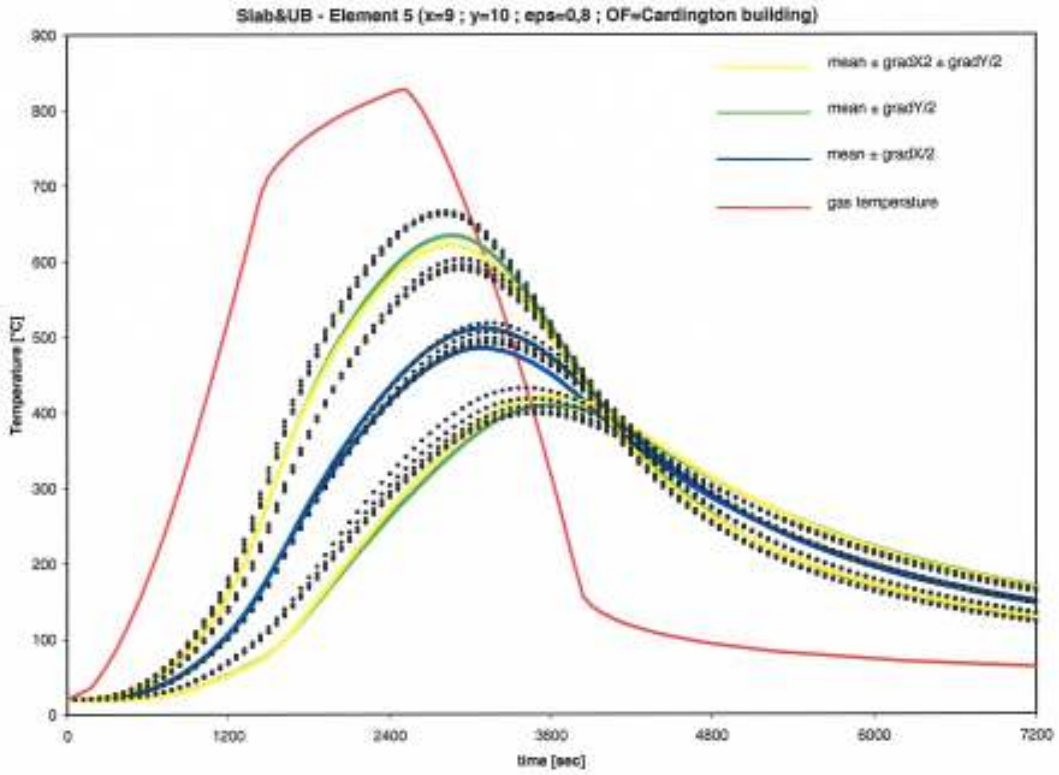

Fig. B.11: **Steel profile under a composite concrete slab alone with ribs parallel to the beam - Big element 5**

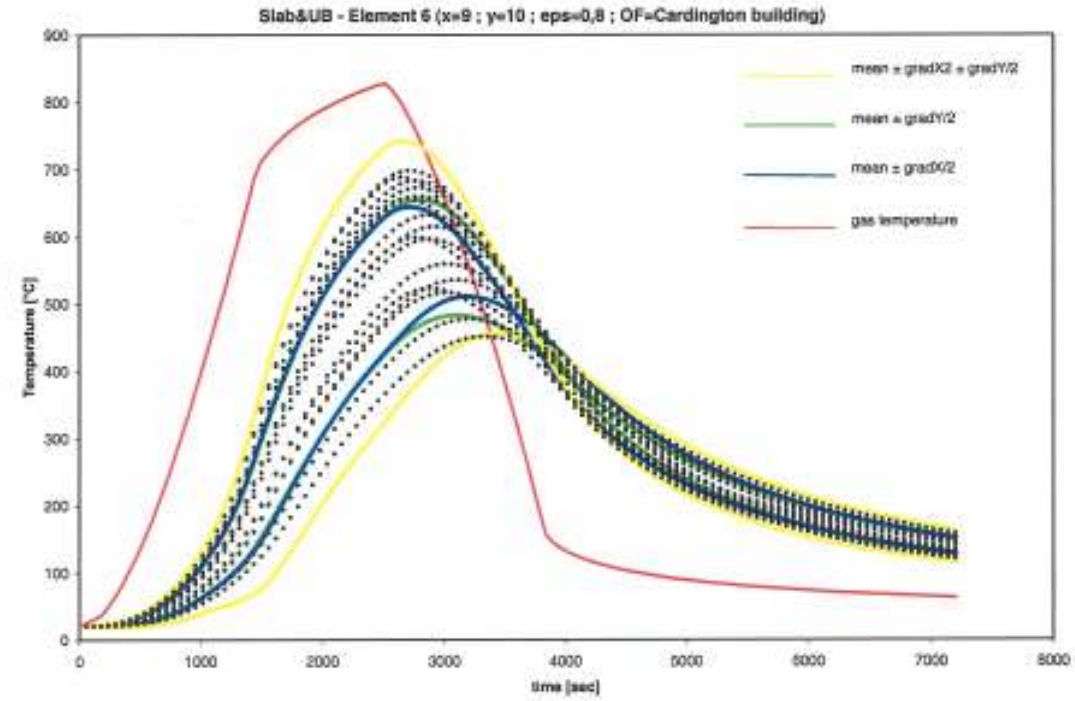

Big element 5

Fig. B.12: **Steel profile under a composite concrete slab alone with ribs parallel to the beam - Big element 6**

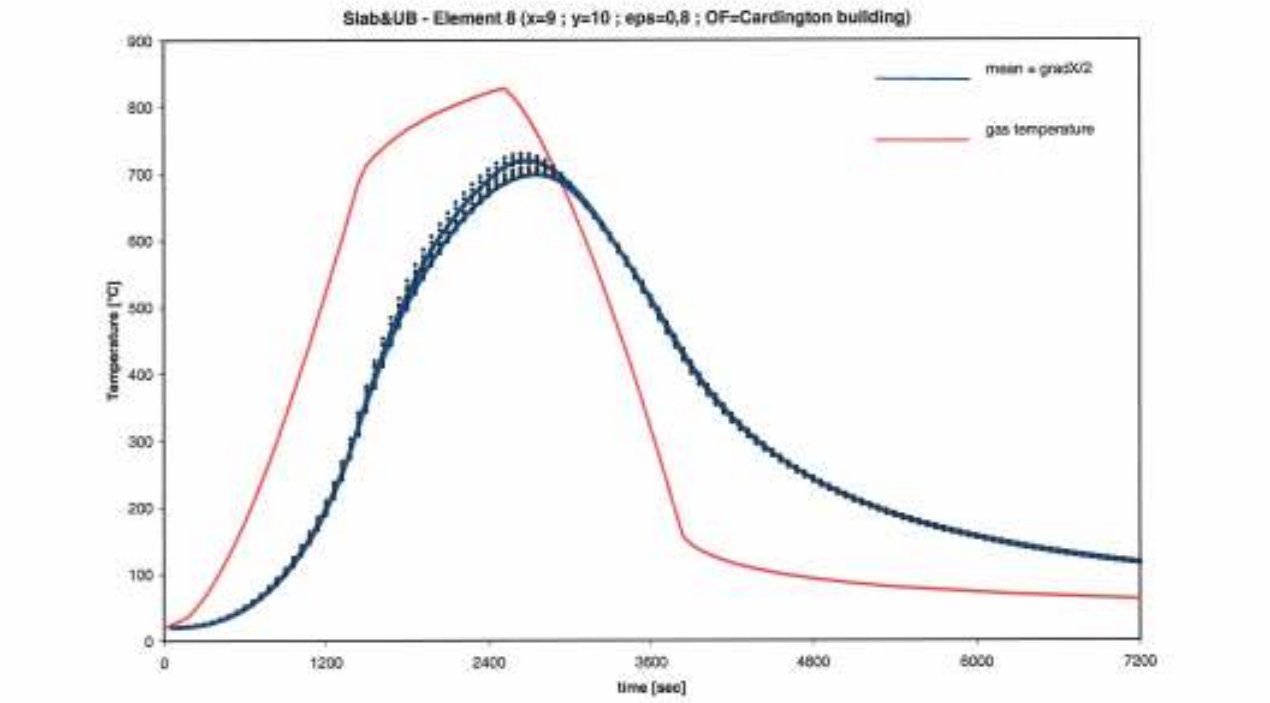

Fig. B.13: **Steel profile under a composite concrete slab alone with ribs parallel to the beam - Big element 8**

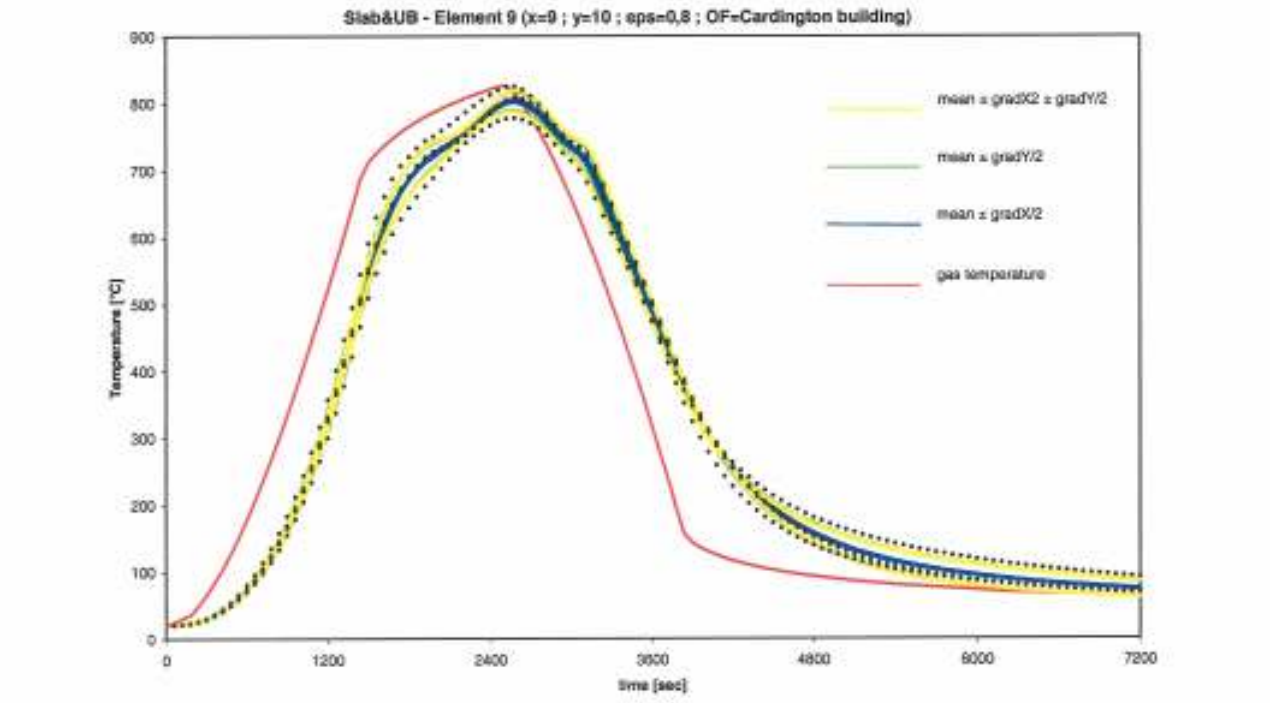

Fig. B.14: **Steel profile under a composite concrete slab alone with ribs parallel to the beam - Big element 9**

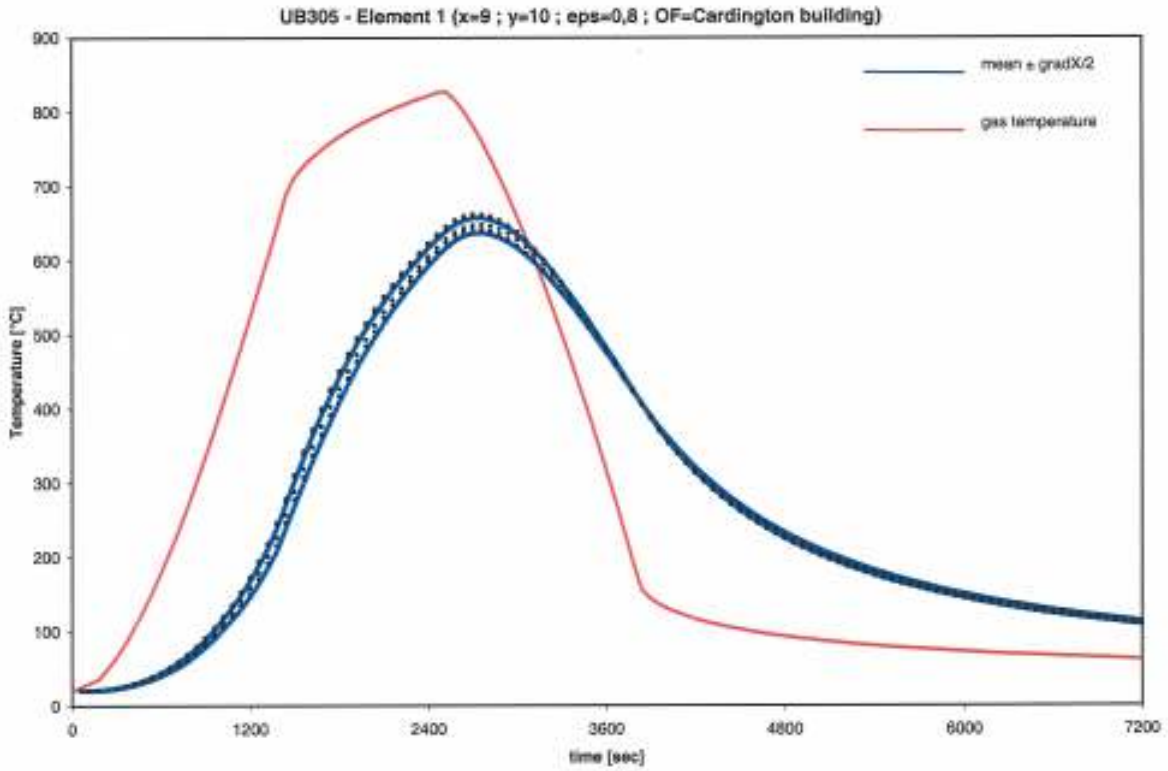

Fig. B.15: **Steel profile under a composite concrete slab alone with ribs perpendicular to the beam - Big element 1**

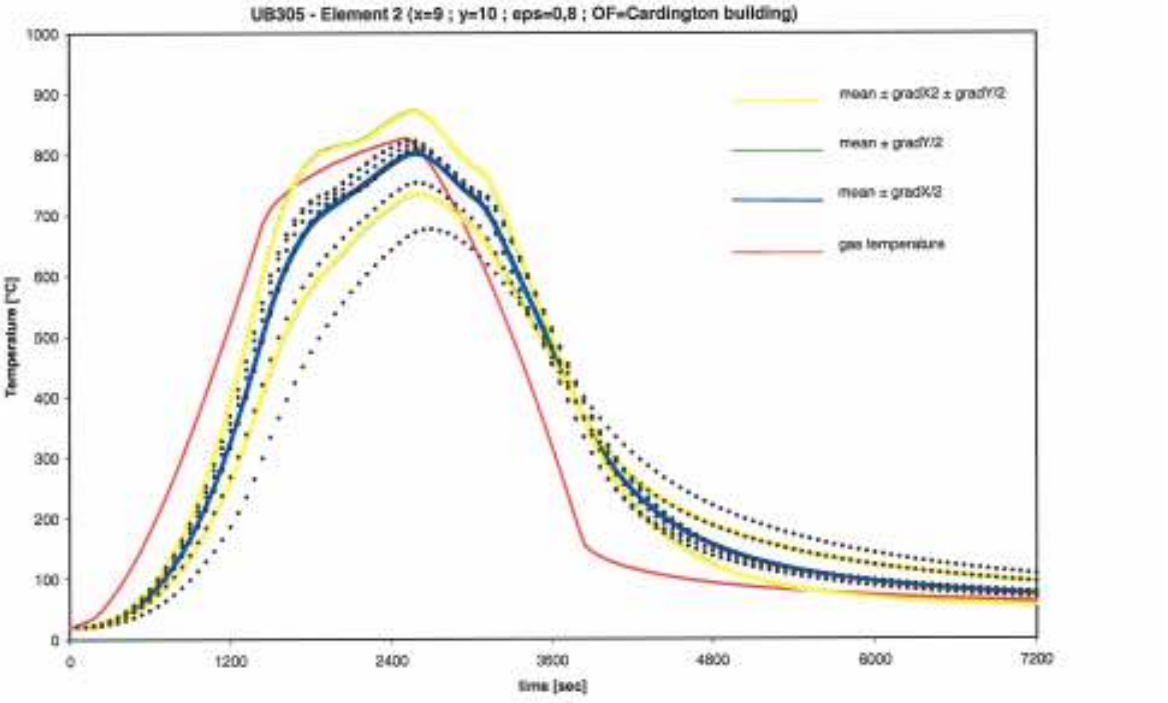

Fig. B.16: **Steel profile under a composite concrete slab alone with ribs perpendicular to the beam - Big element 2**

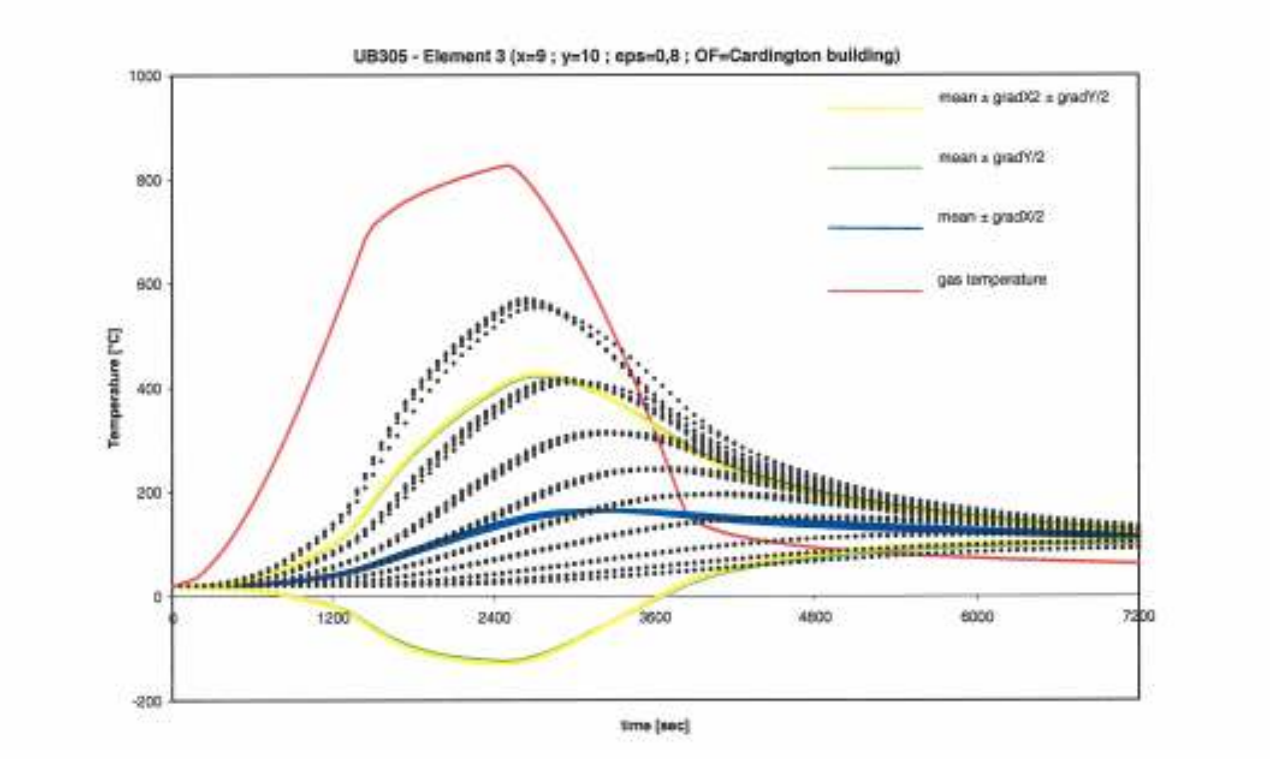

Fig. B.17: **Steel profile under a composite concrete slab alone with ribs perpendicular to the beam - Big element 3**

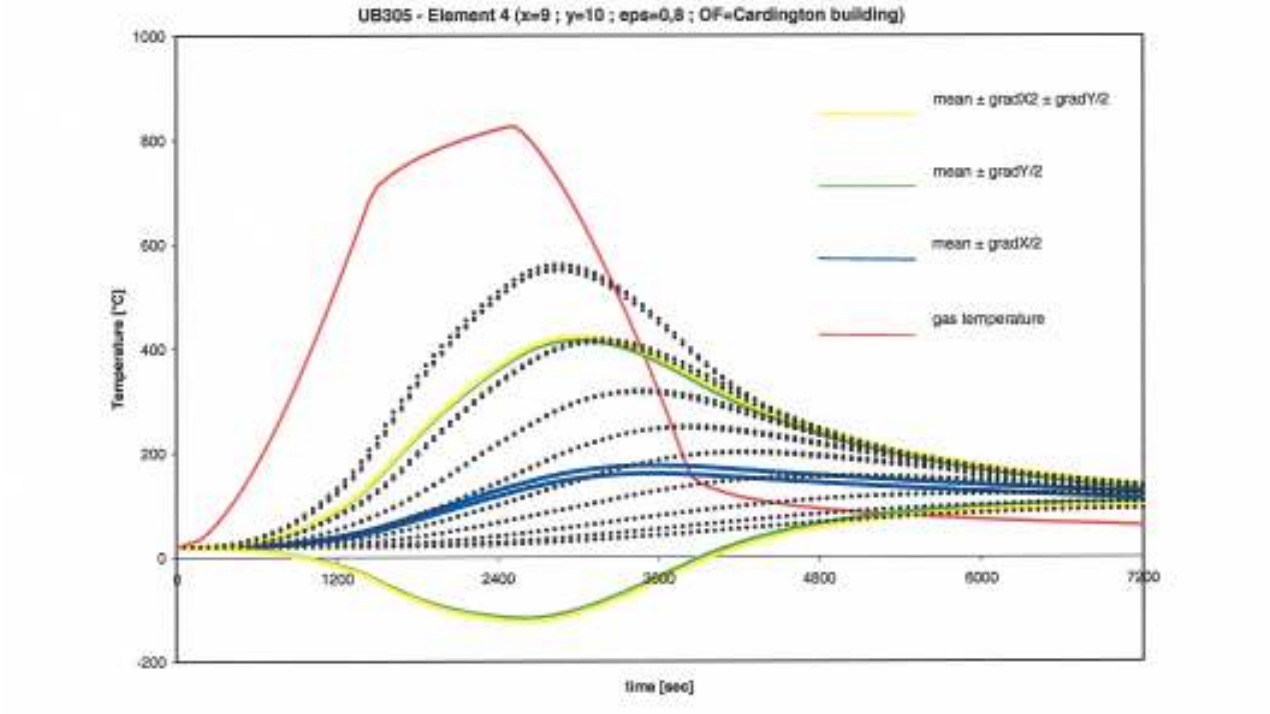

Fig. B.18: **Steel profile under a composite concrete slab alone with ribs perpendicular to the beam - Big element 4**

Annex C: Specification calibration case

C.1 Configuration

- The fire compartment: see the shaded area in Fig. C.1.

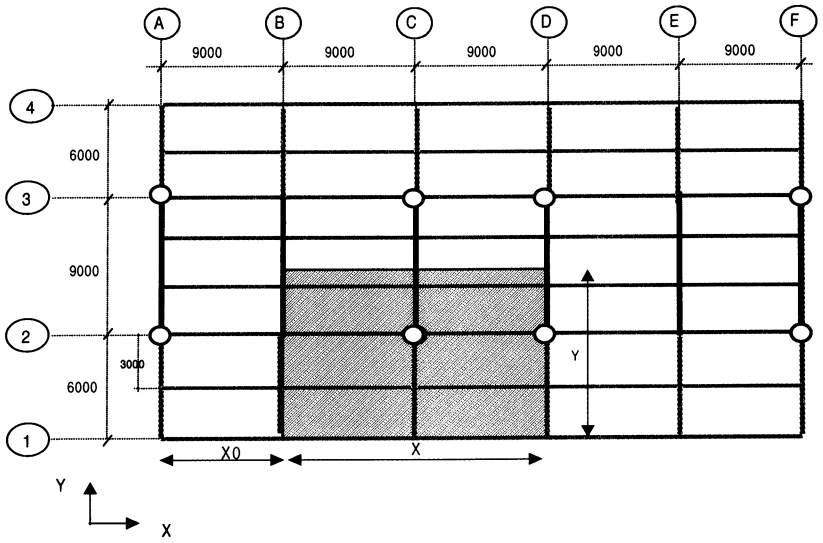

Figure C.1: Plan of the building

- Cross-section of beams and columns:
  primary beams
  -side bay beams: 356 X 171 X 51 UB
  - middle bay beams: 610 X 229 X 101 UB
  secondary beams: 305 X 165 X 40 UB
  columns: 305 X 305 X 198 UC

- Configuration for the ribs:

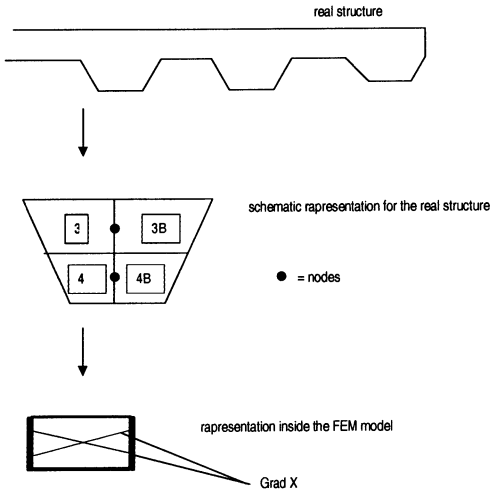

Figure C. 2: Configuration of the ribs

Note: The GradX in the elements 3 and 4 is = -GradX in the elements 3B and 4B, respectively.

C.2 Mechanical Loading

- 2 cases:

'**normal** load' = { self weight + ; **3 kN / m²** distributed on the floor + ; **2.0 * 10^6 N** nodal load on top of the columns connecting to the floor above }

[Distributed load = { 0.8 [raised floor + services + ceiling] + ; 2.5 * 0.5 [imposed load under fire conditions] + ; 1.0 [partitions] } = 3.05 kN/m² ~ 3.0 kN/m²]

'**maximum** load' = self weight + ; **5.5 kN / m²** distributed on the floor + ; **2.8 * 10^6 N** nodal load on top of the columns connecting to the floor above

[Distributed load = { 0.8 [raised floor + services + ceiling] + ; 5.0 * 0.7 [imposed load under fire conditions] + ; 1.0 [partitions] } = 5.3 kN/m² ~ 5.5 kN/m²]

- Density values to be used for calculating the self weight:
  - steel : 7850 kg / m^3
  - concrete : 2300 kg / m^3 (excluding the reinforcement)

C.3 Material properties

- Properties at room temperature:

Steel members (columns and beams):
Steel grade S275
Poison's ratio 0.3
Young's modulus 210000 N/mm^2
Yielding strength 275 N/mm^2

Steel decking:
Steel grade S355
Poison's ratio 0.3
Young's modulus 210000 N/mm^2
Yielding strength 355 N/mm^2

Reinforcement:
Steel grade S500
Poison's ratio 0.3
Young's modulus 210000 N/mm^2
Yielding strength 500 N/mm^2

Concrete:
C30/37
Poison's ratio 0.2
Compressive strength 30 N/mm^2
Tensile strength 3 N/mm^2

- Properties at elevated temperatures

  For steel (steel members, steel decking), reinforcement and concrete, the mechanical and thermal properties are taken in accordance with the Eurocodes Fire [11], [12].

C.4 Boundary Conditions

column ends at the floor level below the heated floor: fully fixed.

column ends at the floor level above the heated floor: fully fixed, except for vertical displacement.

stiff cores in the construction are modelled as follows (ONLY in the nodes identified in Fig. C.1):
nodes marked in Fig. C.1: fixed for translations in X and Y directions, rotations are free.
other nodes: free.

C.5 Temperature fields

- Input deck: temperatures in the element are defined in increments of 5 minutes.
- Protected beams and columns: temperature development to be taken on the basis of a fixed fraction of the temperatures for the reference beam as follows:
  - Internal protected beams: 60% of mean and gradients of reference beam.
  - Edge beams: 80% of mean and gradients of reference beam.
  - Columns: 40% of mean temperature of reference beam (no gradients considered):
  - $T_{mean\text{-}columns} = 0.4 * (T_{mean\ upperflange} + T_{mean\ web+lower\ flange})/ 2$
- Since four elements are considered for the (complete) rib, the mean temperature and the gradients are calculated as follows (see also Fig. C.3):

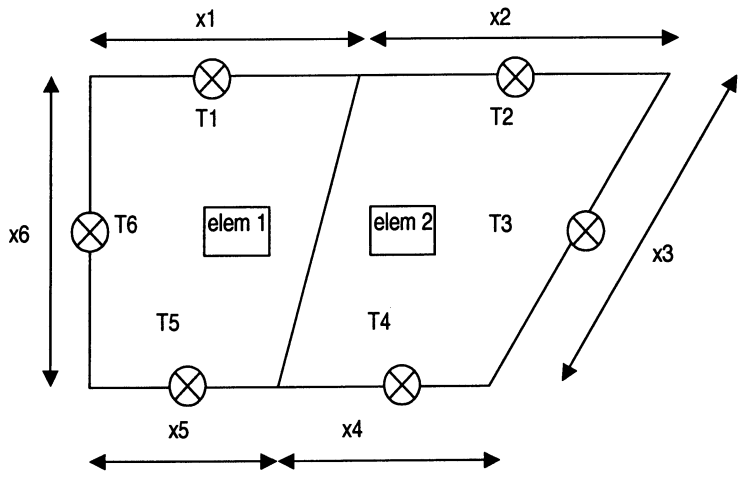

Figure C..3: Temperature distribution in the ribs

$$Tmean = \frac{\sum_{elem=1}^{2} T_{elem} A_{elem}}{\sum_{elem=1}^{2} A_{elem}}$$

$$GradX = T_3 - T_6$$

$$GradY = \frac{\sum_{i=1}^{2} T_i x_i}{\sum_{i=1}^{2} x_i} - \frac{\sum_{i=4}^{5} T_i x_i}{\sum_{i=4}^{5} x_i}$$

- According to data provided by ARBED some elements at some time steps meet the condition that the lowest temperature in the element ($T_{lowest} = T_{mean} - ABS(GradX / 2) - ABS(GradX / 2)$) is lower than 20°C or eventually negative.
  If this occurs, the values for GradY (and eventually for GradX) are adapted such the temperature is not lower than 20°C. In this procedure, T_{mean} is not changed.

C.6 Integration scheme

- The following integration scheme is used (Gauss integration rule is adopted):
  - Slabs at ribs: 2 x 2 in plane (the element area $\xi\eta$).
  - 3 integration points in the thickness (ζ direction).
  - Slabs between ribs: 2 x 2 in plane.
  - 5 points in the thickness.

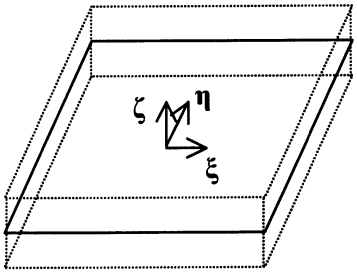

- Ribs: - 3 x 3 in the area of the cross-section
  - 2 points along the beam axis
- Upper flange of supporting beams:
  - 2 x 2 in the area of the cross-section
  - 2 points along the beam axis
- Web and lower flange of supporting beams:
  - 2 x 2 in the area of the cross-section of the web
  - 2 x 2 in the area of the cross-section of the flange
  - 2 points along the beam axis

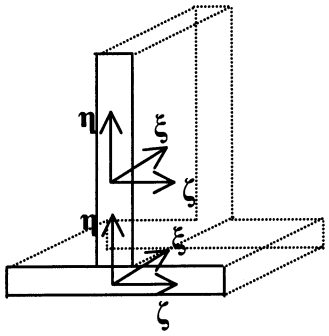

- Steel decking:
  - 2 x 2 in the area of each of the three quadrileral zones of the cross-section;
  - 2 points along the beam axis.

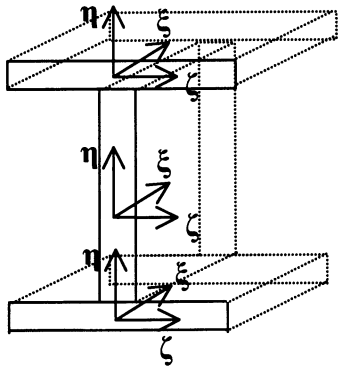

- Columns:
  - 2 x 2 in the area of the cross-section;
  - 2 points along the column axis.

C.7 Output Format

- The following plots are to be produced (refer to Fig. C 4 for notation):
  - Vertical displacement U_z [mm] along line B (at X=Xo+9000mm) against Y, with Y = 0 ÷ 21000 mm.
  - The graph presents different curves for the following time steps:
    0, 900, 1800, 2700, 3600, 4500, 5400, 6300, 7200 sec.
  - Vertical displacement U_z [mm] along line 5 (at Y=3000mm) against X, with X = 0 ÷ 45000 mm.
  - The graph presents different curves for the following time steps:
    0, 900, 1800, 2700, 3600, 4500, 5400, 6300, 7200 sec.
  - Vertical displacement U_z [mm] in midspan-nodes along line 5 against time [sec].
    The displacement to be presented for the following in five nodes:
    10304 10313 10322 10331 10340.

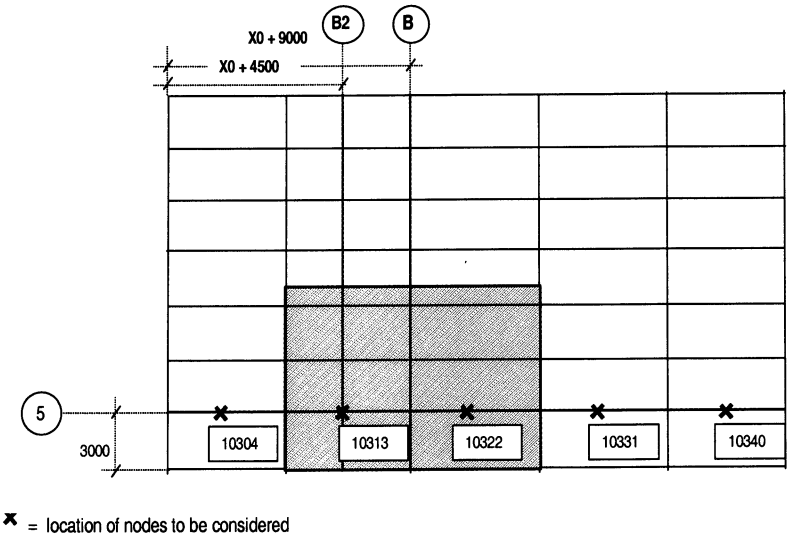

Fig. C. 4: Conventions for output format

- Normal force N_y [N] along line B against Y, with Y = 0 ÷ 21000 mm.
  The normal forces to be calculated in the supporting beams (contributions by the upper flange, the web and the lower flange to be taken together).
  Distribution of forces to be presented for the following time steps:
  0, 900, 1800, 2700, 3600, 4500, 5400, 6300, 7200 sec.
- Normal force N_x [N] along line 5 against X, with X = 0 ÷ 45000 mm.
  The normal forces to be calculated in the supporting beams (contributes by the upper flange, the web and the lower flange to be taken together).
  Distribution of forces to be presented for the following time steps:
  0, 900, 1800, 2700, 3600, 4500, 5400, 6300, 7200 sec.
- Stresses σ_{yy} [MPa] along line B2 (at Xo=X+4500mm) against Y, with Y = 0 ÷ 21000 mm.
  The stresses to be calculated in reinforcement
  Distribution of stresses to be presented for the following time steps:
  0, 900, 1800, 2700, 3600, 4500, 5400, 6300, 7200 sec.
- Stresses σ_{xx} [MPa] along line 5 against X, with X = 0 ÷ 45000 mm.
  The stresses to be calculated in the reinforcement
  Distribution of stresses to be presented for the following time steps:
  0, 900, 1800, 2700, 3600, 4500, 5400, 6300, 7200 sec.

Annex D: Deformation criteria

Aim of any structural fire safety analysis is to determine whether, for a specified period of time, the fire-exposed structure will fail or not. In a design based on classification, the required fire resistance time refers to the standard fire curve. In the natural fire safety concept, often a complete burnout is considered (i.e. the effect of active fire safety measures is implicitly taken into account via the design fire load density [16]). If it is not necessary for the building to survive a complete burnout, the required time is related to the time necessary for inspection by the fire services and evacuation of the occupants.

In either case it is necessary to specify objective and functional performance criteria for failure.

Under standard fire conditions (i.e. monotonically rising gas temperature) and for structural components in which no geometrical non-linearity's do apply, a typical "run-a-way" situation will occur, provided unlimited deformation capacity is available. See Fig. D.1. The failure conditions follow from:

$$\lim_{t->tf} [d\delta/dt] = \infty \qquad \ldots (1)$$

With:

t	is	time;
t_f	is	fire resistance time;
δ	is	deflection.

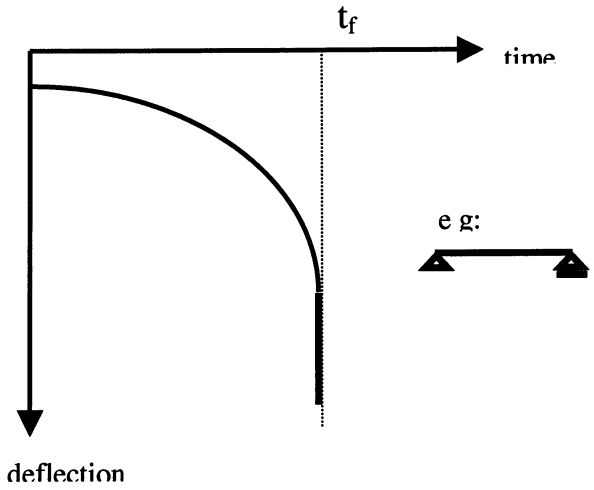

Fig. D.1: A typical run-a-way situation

In standard fire tests it is not possible to measure an infinitive high rate of deflection. Therefore an arbitrary (but relatively high) limit is set to the rate of deflection (= $L^2/900h$, with L is span and h is depth of the member). If the (measured) maximum value of $(d\delta/dt)_{max}$ is beyond the limiting value, the load bearing capacity of the structural element under consideration is assumed to be exhausted. In order to avoid that any "dip" in an early stage of the deflection history must be considered as "failure", breaching condition (1) has no effect as long as the relative deformation δ/L is less than L/30.

In calculations, the temperature field for which the above condition is fulfilled follows from an analysis of the structural element at elevated temperatures. Such analyses do not necessarily give information on the state of deformation of the structure. The so-called "simple" calculation methods in EC 3 & 4, parts 1.2 ("structural fire design") for steel and steel concrete structures are based on plasticity theory and follow this approach.

When the above conditions hold, both the interpretation of standard fire tests and the outcomes of theoretical analyses confirm that "run-a-way" occurs very suddenly. Setting an additional limit to the

deformation - which may be necessary for practical reasons – has, under such conditions, only a marginal effect on the fire resistance and may be ignored.

However, there are situations in which "run-a-way" will be suppressed or will not occur at all. A well known example is a beam or slab, with fixed supports, under standard fire test conditions. When deflection increases, membrane forces will develop and the load bearing capacity will gradually transform from bending into membrane action. See Fig. D.2.

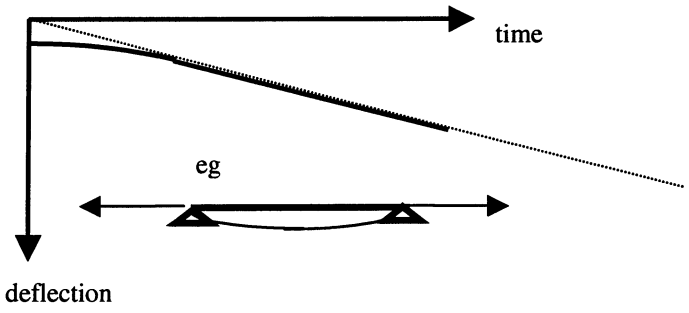

Fig. D.2: Effect membrane action

Such a beam/slab may reach extreme large deflections, without breaching failure condition (1). This may lead to unacceptable situations in practice, such as malfunctioning of fire partitions, occurrence of gaps in joints between floor slabs, damage to structural fire protection etc. Hence, for interpreting the results of standard fire tests, in addition to condition (1), a limit to deformations is set (symbols as defined above):

$$\delta = L^2/400h \qquad \ldots (2)$$

When analysing a structural system under natural fire conditions, similar complications occur. First of all, the analysis is not limited to one single member exposed to fire – as in the case of standard fire tests – but applies to a structural system, parts of which are exposed to fire, other parts are not. This means that membrane action may – depending on the design features – play an important role and undo any run-a-way effects. Also, since natural fire exposure is considered, the gas temperature is not continuously increasing – as in the case of standard fire conditions - but will, during the decay period of the fire, decrease. Consequently, the temperatures in the structure will, with some delay, go down too. This effect is of special importance when the structural behaviour during the complete burnout is relevant. When the construction cools down, the deformations will (party) recover.

For some typical time-temperature and time-deflection curves resulting from an analysis of a structural system under natural fire conditions, refer to Figs D.3 and D.4.

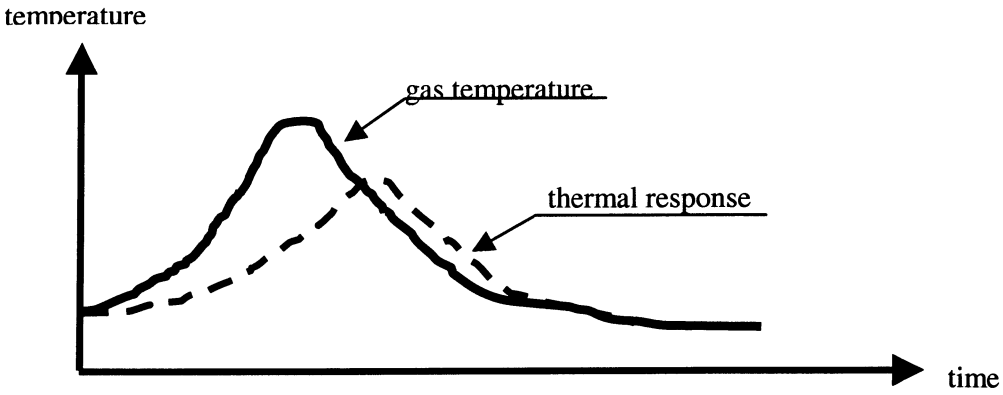

Fig. D.3: Gas temperature and thermal response in a natural fire analysis

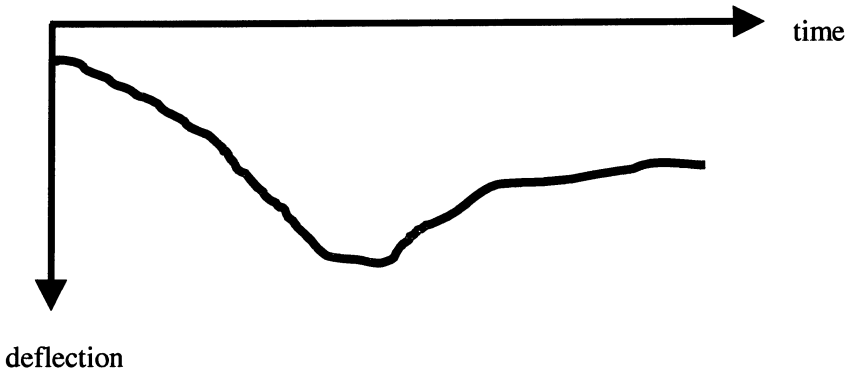

Fig D..4: Mechanical response in a natural fire analysis

As for the simple beam under membrane action, the structural system may undergo extreme deformation without breaching the failure condition (1), since no run-a-way occurs. As indicated before, this is not acceptable and the introduction of a deformation criterion is necessary. For practical reasons, in this Design Guide, the same limiting value will be used as has been agreed upon for the interpretation of standard fire testing, however with the following modification: δ is the relative deflection of the structural member under consideration (with reference to its supports) and *not* the absolute value, as when interpreting standard fire test results. Reason is that the deformation of the member is the significant aspect and not so much its maximum displacement. For the interpretation of the result of a standard fire test this is not of importance, since during a test the member is rigidly supported on the furnace wall. Hence, the following deformation criteria is adopted:

$$\delta_{rel} = L^2/400h \qquad \ldots (2)$$

with

δ_{rel}	is	maximum relative deflection of the member, with reference to the supports;
L	is	span of the member;
h	is	depth of the member.

With $L/h \approx 20$ for hot rolled steel beams, condition (x+1) can be simplified to:

$$\delta_{rel}/L = 1/20 \qquad \ldots (3)$$

Finally, emphasis is on the fact that the above limiting value has an arbitrary character only. It has been introduced because of the need to avoid, for practical reasons, extreme deformations in fire exposed structural systems. By choosing a value identical to the one on which international agreement has been reached in the adjacent field of fire testing, hopefully the probability of acceptance will increase.

Annex E: Fire development and thermal response curves for the basic cases

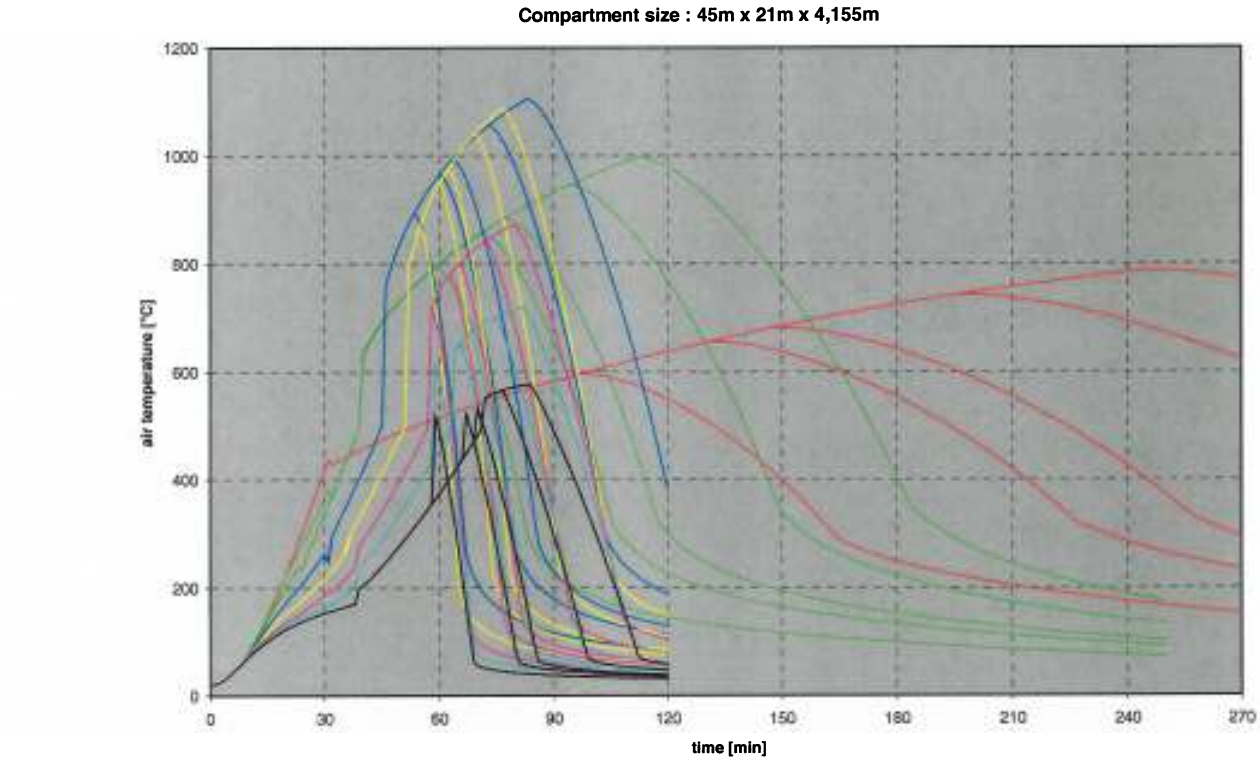

Fig. E.1[a]: Gas temperatures, compartment "a"

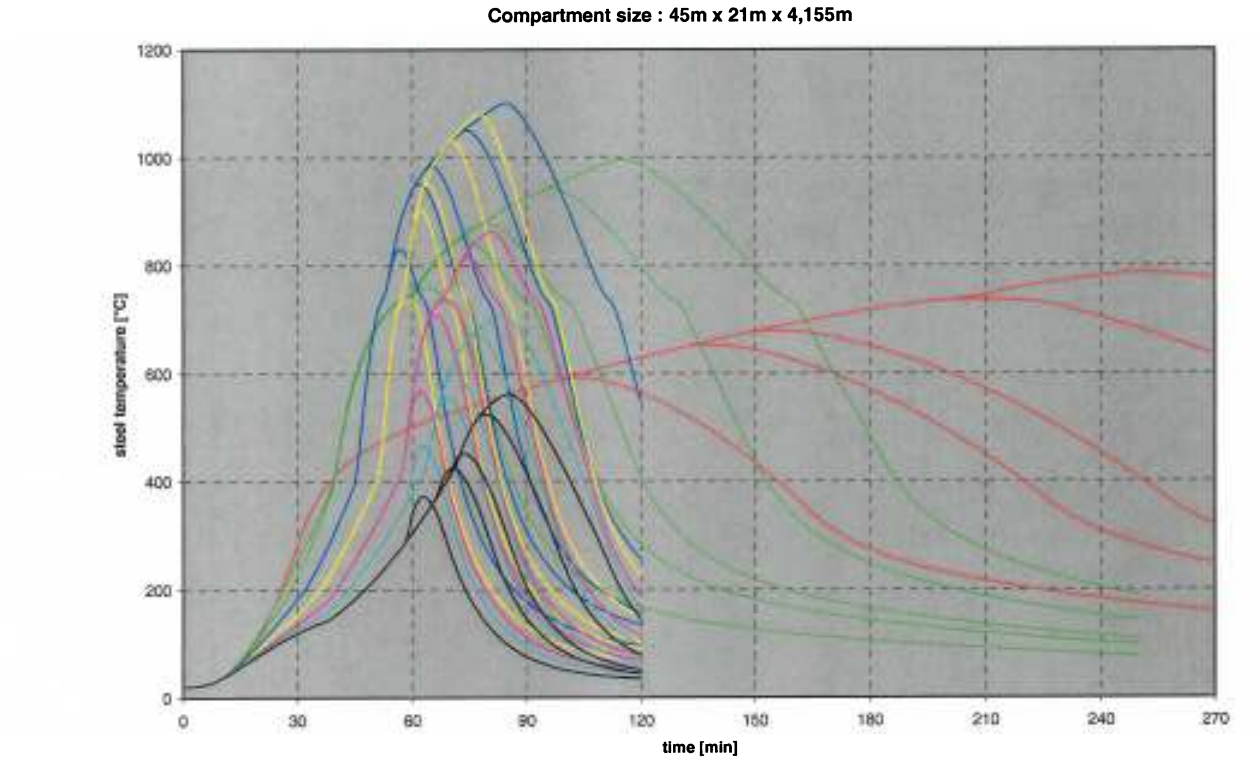

Fig. E.1[b]: Steel temperatures, compartment "a"

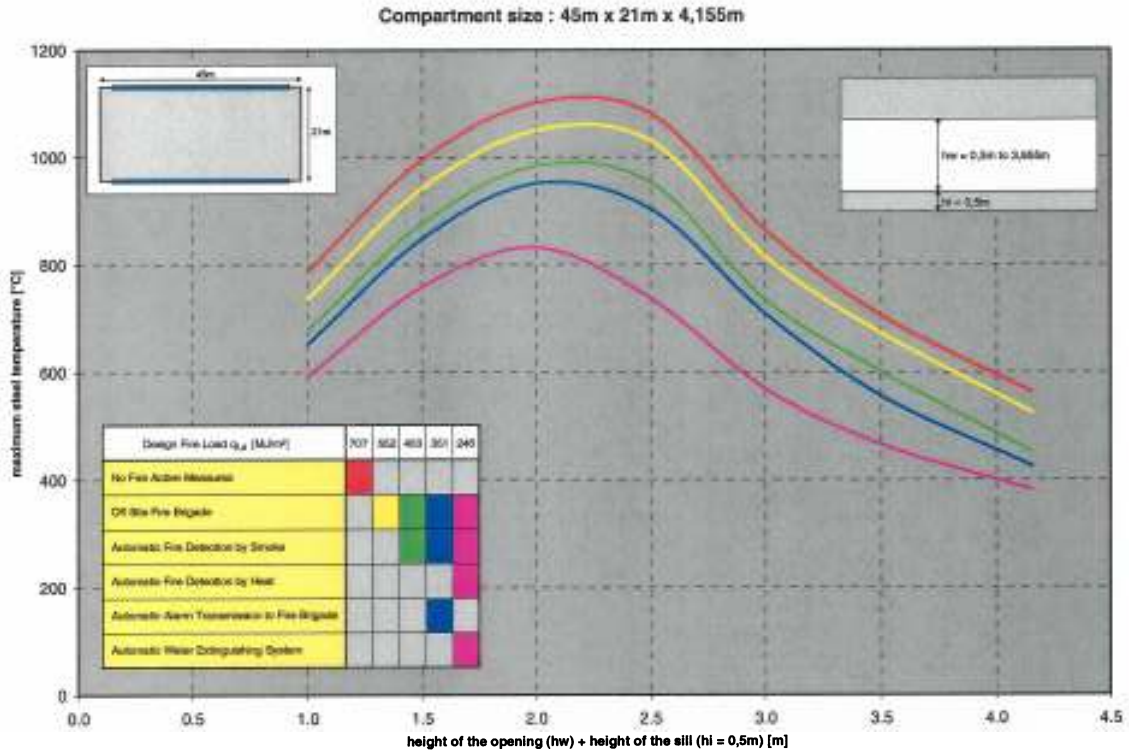

Fig. E.1[c]: Maximum steel temperatures , compartment "a"

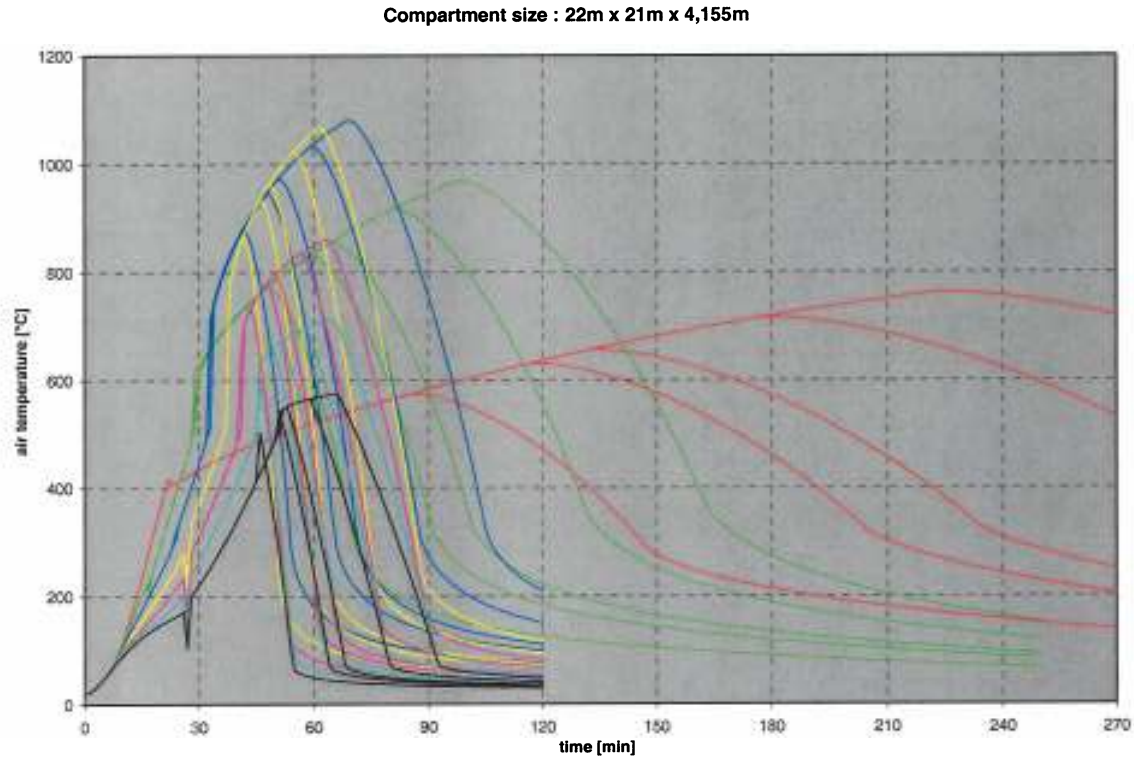

Fig. E.2[a]: Gas temperatures, compartment "b"

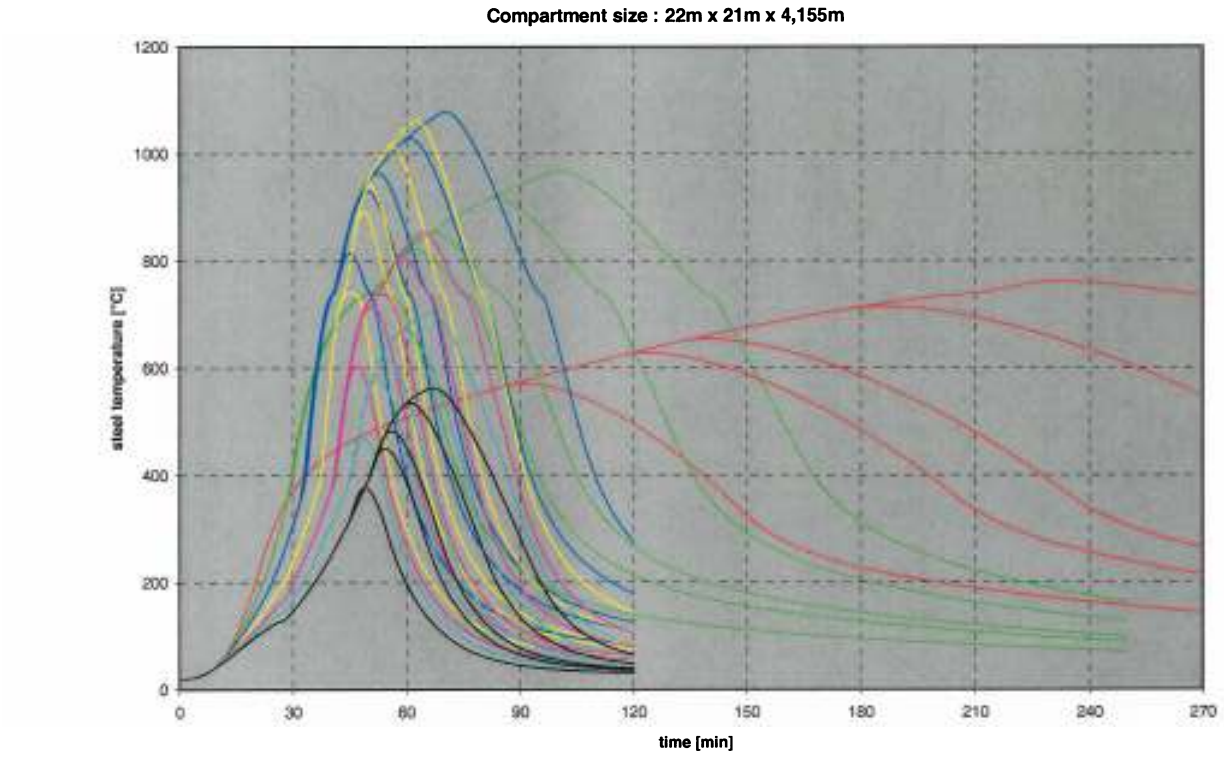

Fig. E.2[b]: Steel temperatures, compartment "b"

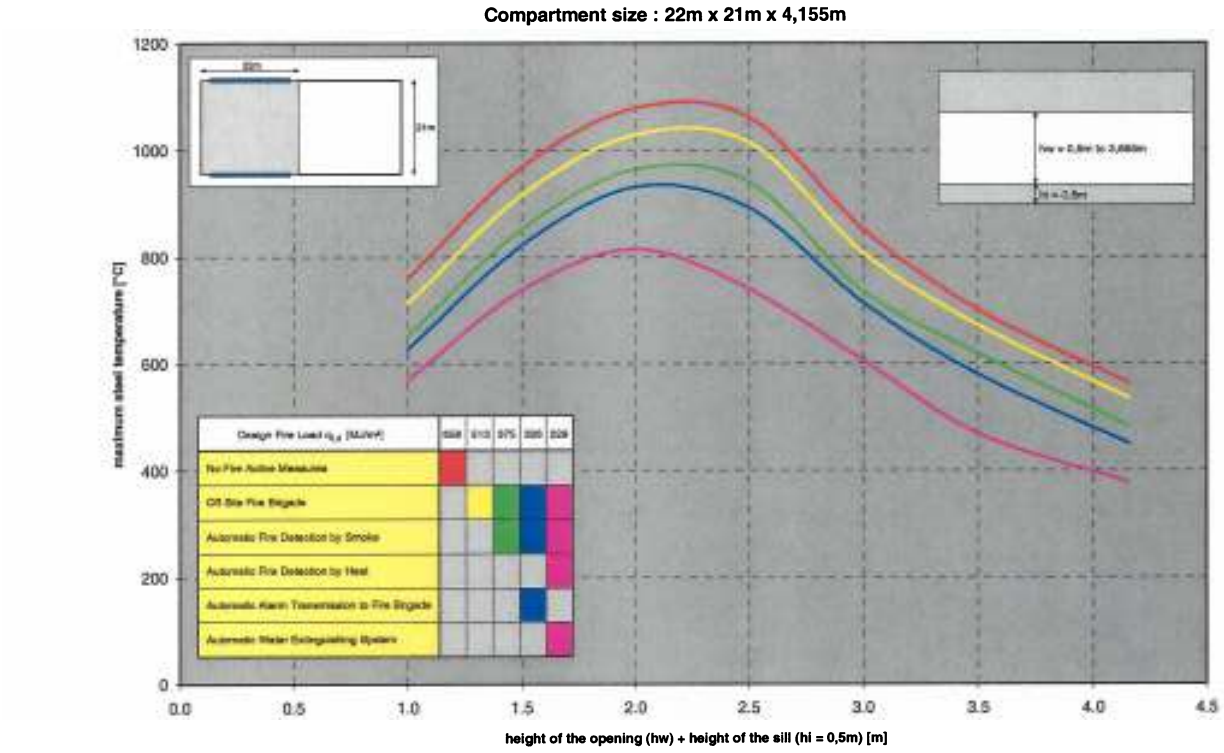

Fig. E.2[c]: Maximum steel temperatures , compartment "b"

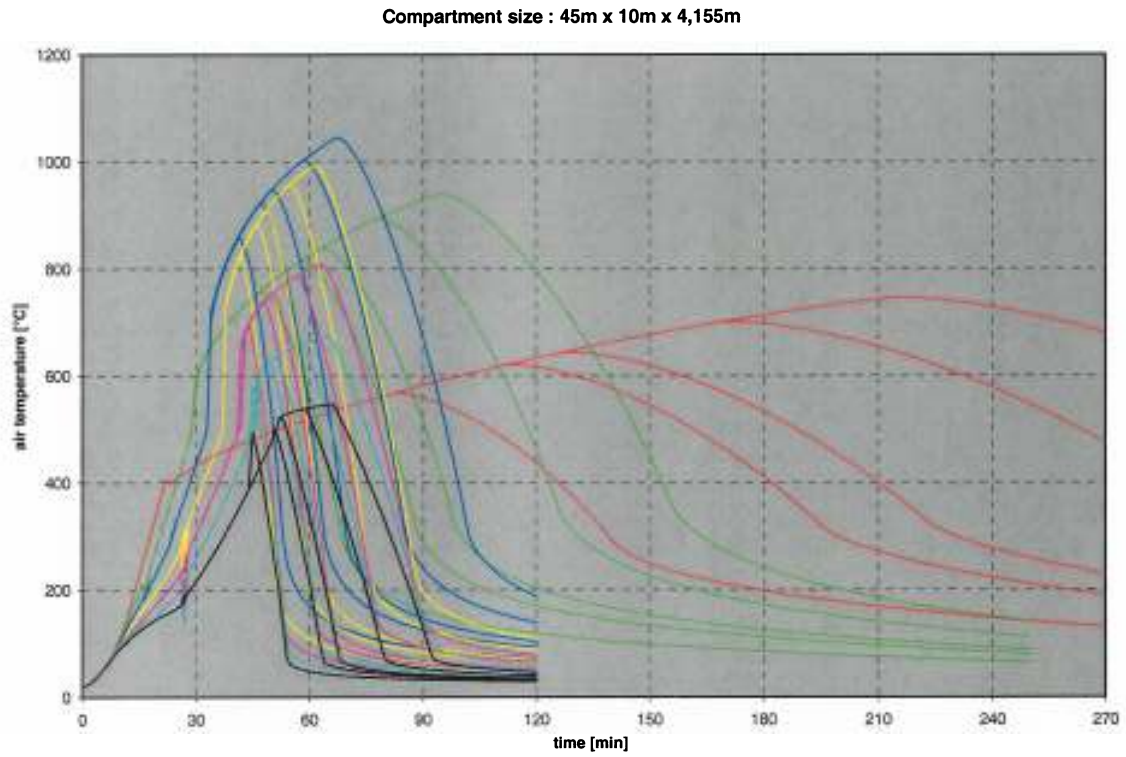

Fig. E.3[a]: Gas temperatures, compartment "c"

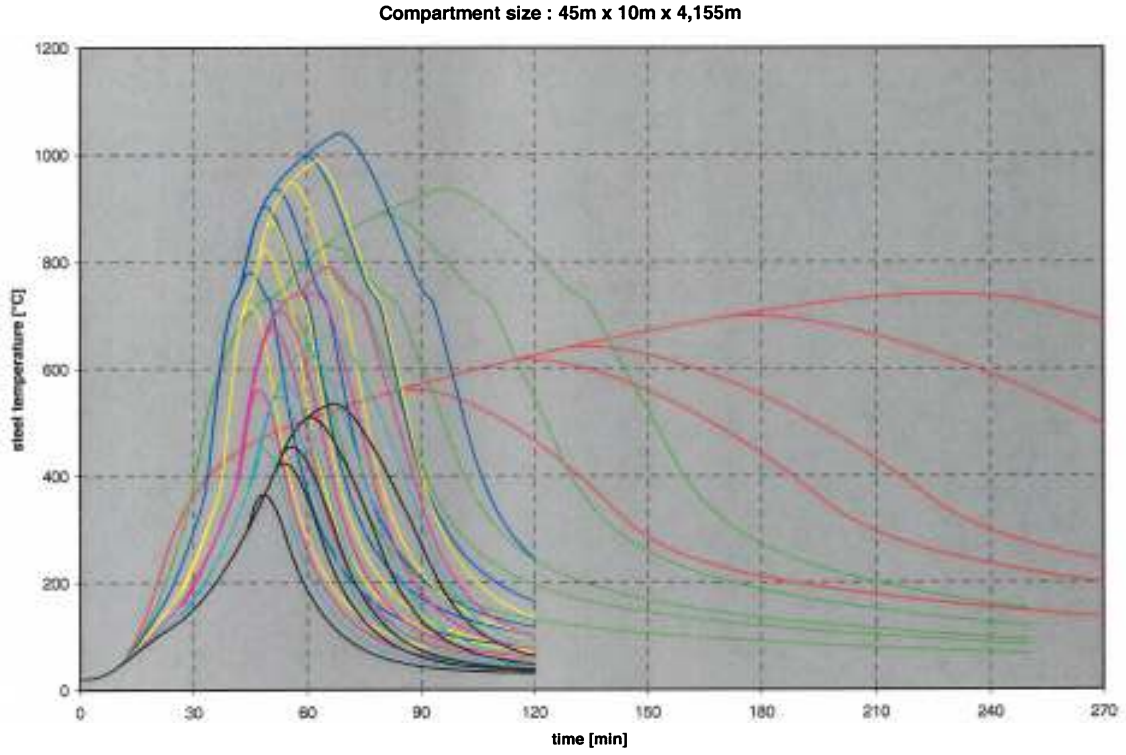

Fig. E.3[b]: Steel temperatures, compartment "c"

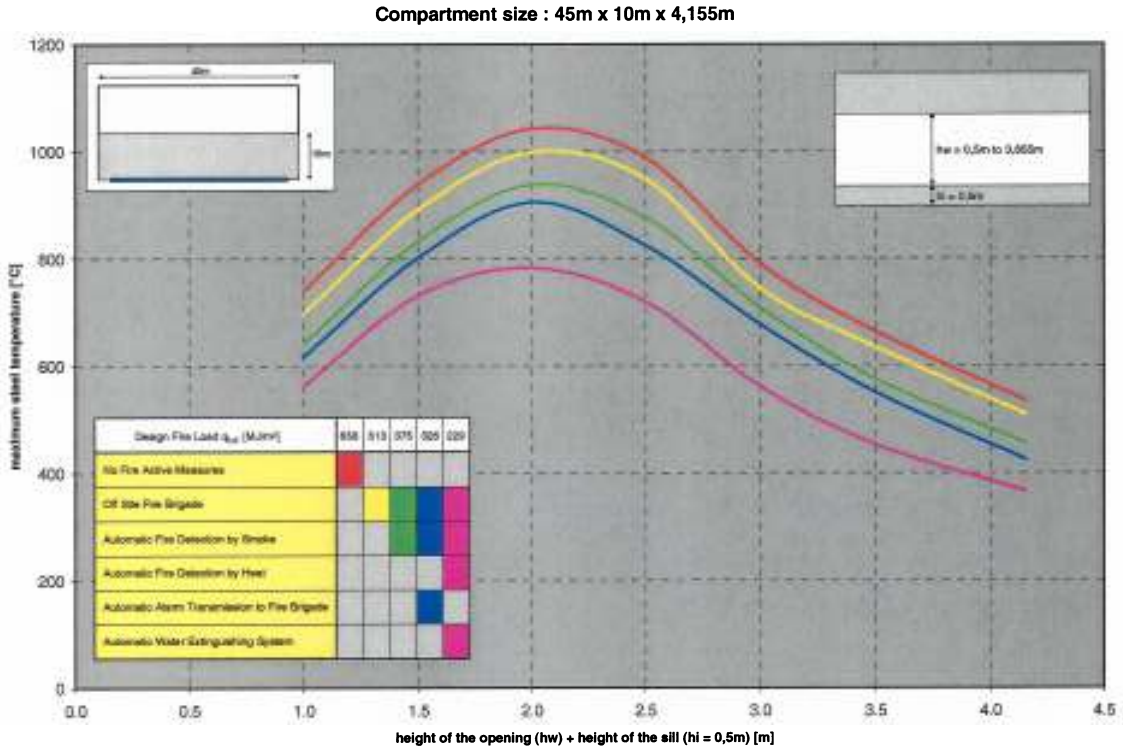

Fig. E.3[c]: Maximum steel temperatures , compartment "c"

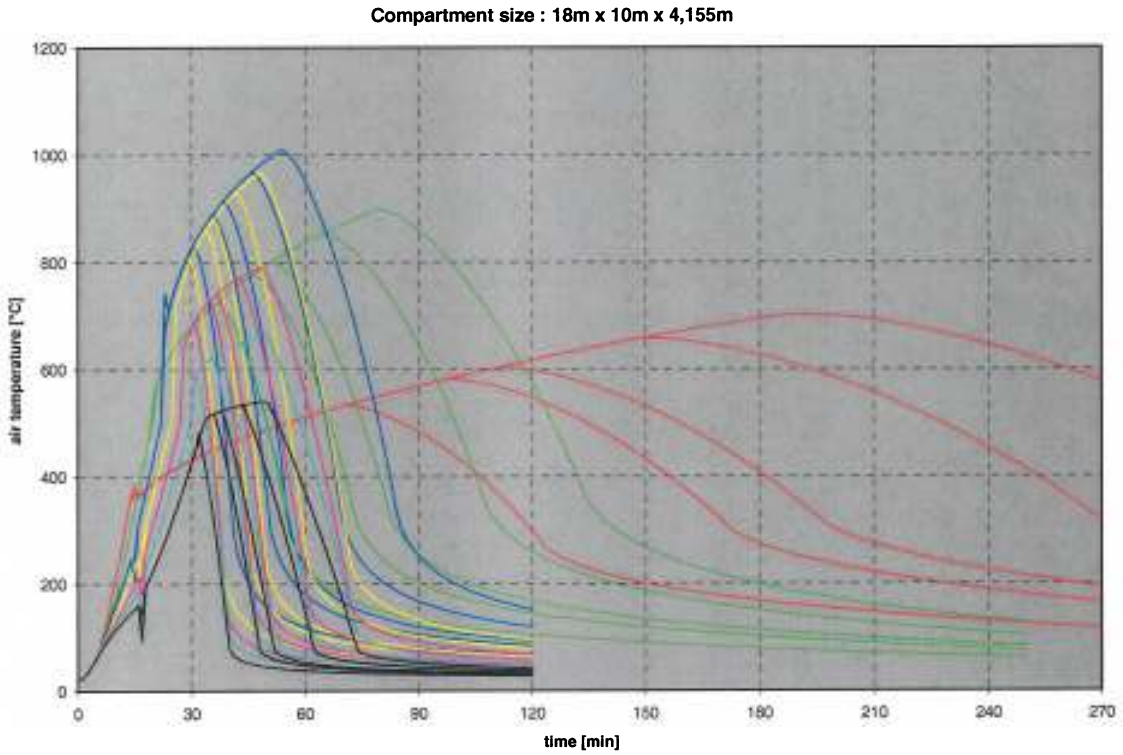

Fig. E.4[a]: Gas temperatures, compartment "d"

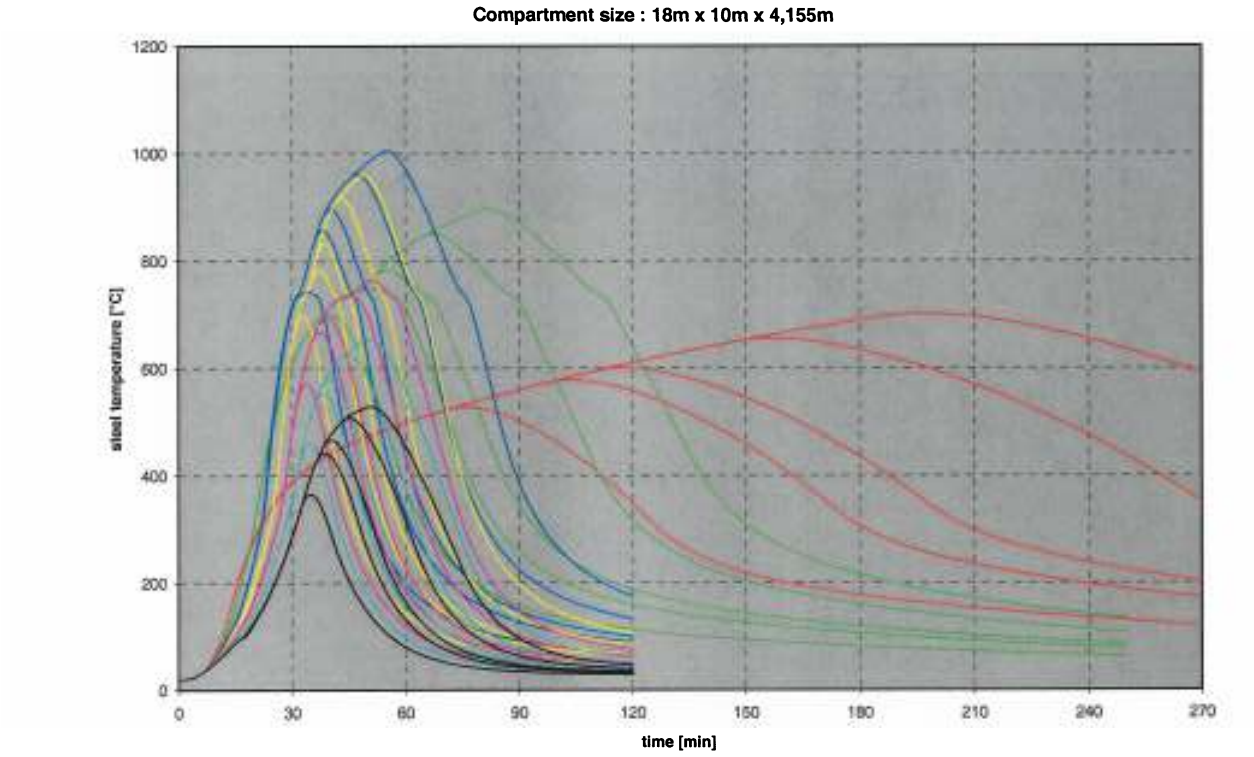

Fig. E.4[b]: Steel temperatures, compartment "d"

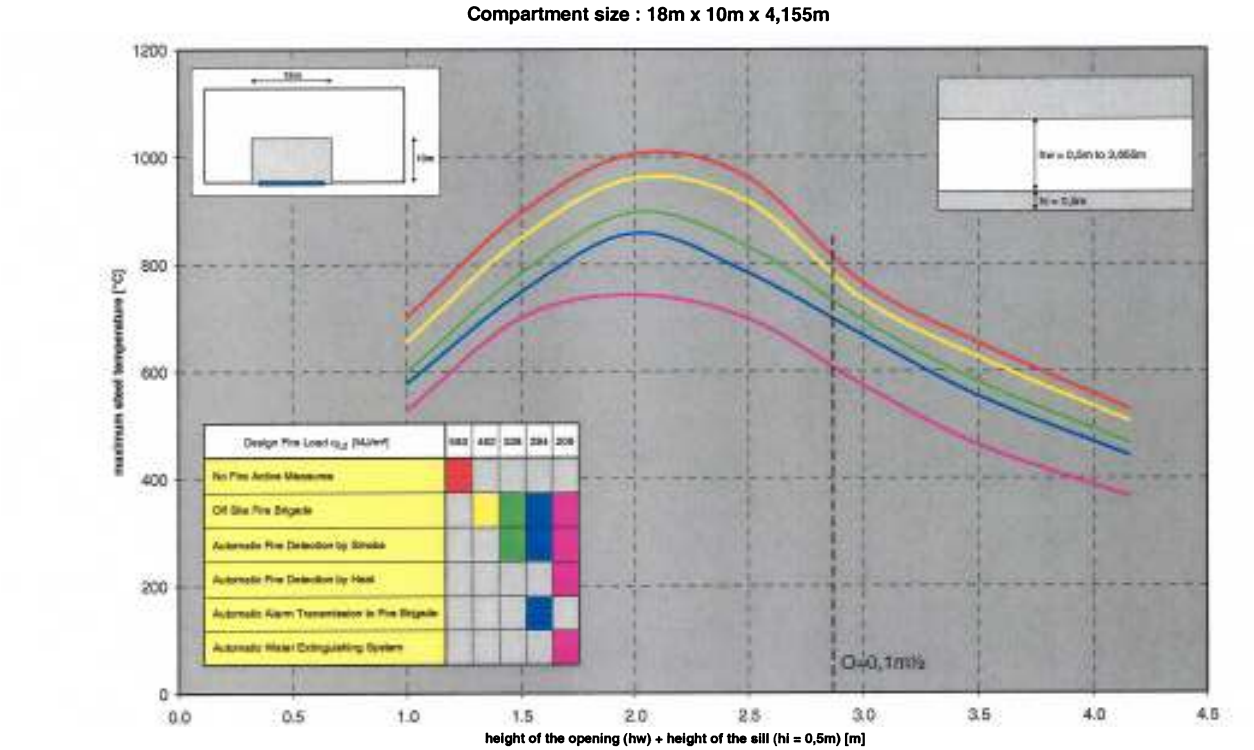

Fig. E.4[c]: Maximum steel temperatures , compartment "d"

Annex F: Distribution displacements, forces and moments in 3D composite steel frames under natural fire conditions

With a view to analyse more in depth the structural performance of 3D composite steel framed buildings exposed to natural fire conditions, basic case "a" (large fire compartment) as introduced in the main text and assuming ventilation controlled fire conditions and a fire load density of 300 MJ/m^2, the distribution of displacements, forces and moments, has been considered more in detail. The case to be analysed is chosen such, that the maximum steel temperature in the lower flange of the primary steel amounts 700 °C. For a review of calculated the peak steel temperatures as function of time, refer to Fig. F. 1. For orientation, in figure the steel maximum temperature for a fire load density of 700 MJ/m^2 has been presented as well.
For relevant node locations, refer to Figs. F. 2 to F.7.

To try to add further light on the behaviour of the deflected shape of the slab, in-plane slab longitudinal displacements are plotted. Figure F. 8 shows in-plane displacements at peak temperature. This illustrates that the structure expands away from the central braced core area of the floor slab (denoted by the central lateral restraints in Figure 4.10 of the main text) in the heating phase of the fire. Restraints at edge of structure ensure that peak displacements occur in the end bay. Figure F.9 shows in-plane displacements at the end of the analysis to illustrate that deflections have now moved the other way with the structure pulling back in on itself, probably due to the effect of locked in plastic strain.

Fig. F.10 and F.11 illustrate the column base shears at the bottom of the fire compartment in the longitudinal and transverse direction respectively (Fig. F.2 gives node locations). A number of events can be discerned within these plots at different times and these will probably relate to structural events in the different beams during the analysis. Peak base shears occur firstly before peak temperature is reached at ~3000 seconds and then at the end of the analysis on cooling. Peak shears of ~170kN are recorded.
Vertical forces are probably the most interesting as they show major redistribution of load carrying behaviour during the analysis. Vertical forces are given in Fig. F.12. Variations in the reactions are of the order of 5% of the initial load carried and are therefore not that significant as this variation can be easily accommodated but again this gives a good illustration of changing structural events. Interestingly, the major load redistributions tend to take place in the cooling phase of the fire.

Checks on the plastic strain at the level of the reinforcement in the slab at peak temperature and the end of the analysis in longitudinal direction are given in Figs. F.13 and F.15 respectively. At peak temperature, maximum tensile strains are highly localised around columns and are of the order of 2% strain. The same pattern is seen at the end of the analysis, with maximum tensile strains increasing to around 3% strain. Similar patterns can be seen in the transverse direction (Fig. F.14 and F.16) although the strain levels are a lot lower at around 1 to 1.5%. This is logical as the majority of the straining will be due to restrained thermal elongation, which is greater in the longitudinal direction than the transverse direction due to the greater length of structure that is heated. It is surprising that the strains only increase marginally in the cooling phase of the fire as the effect of locked in plastic strains was expected to be much greater. To try to get a better picture of the structural events that are occurring in the main composite beams during the analysis, the axial forces in the main primary and secondary steel beams are plotted throughout the analysis. The axial forces are plotted at the ends and centre of the beams at the locations illustrated in Figs. F.3 to F.7

The axial force of the secondary beams between gridlines 1 and 2 is plotted in Fig. F.17. Initially, we expect to see the initial end forces in the steel beam as compressive as the composite beam will be acting under a hogging (negative) moment. The central forces will be tensile, as the composite beam will be acting under a sagging (positive) moment. Note that the end force at the edge of structure is a lot lower than the end forces at the columns and this illustrates that the degree of restraint provided by the rotational stiffness of the edge beam that is supporting the secondary beam is not high enough to sustain a sizeable composite moment at this location.
The axial capacity at both yield stress and ultimate tensile stress of the steel section in compression and tension is also plotted in Fig. F.17. This axial capacity is adjusted throughout the analysis depending on the peak temperature of the steel beam. For comparison purposes, the forces in the same beam have

the same shape marker with solid black for the central axial force and open blue and red markers for the two end forces.

The first force examined is at edge of structure (node 6100). The axial force remains negligible meaning that edge restraint is not enough to generate significant axial force due to restrained thermal expansion. Elsewhere, the beam forces can be seen to go into compression due to the effect of restrained thermal expansion. As end forces start off compressive, these approach the yield capacity of section first, at around 1800 seconds. The beam temperature at this stage is around 150°C. Note that we are only plotting axial force here and bending moments will mean that the actual axial force achievable is less than the pure axial squash load illustrated on the plot. Beam forces are then constant following the axial capacity envelope. This means that all the thermal elongation with increasing beam temperature is going into plastic straining and greater slab vertical deflections. At around 3300 seconds, at a beam temperature of ~ 400 °C , significant material degradation starts to take place and the axial force in the beam starts to reduce. Beam forces continue to follow the axial capacity envelope down rapidly reducing in force. These structural events in the beam can be seen to coincide with major changes in the relative deflections of the secondary beams (Fig. 4.12 of the main text.) and the changes in reaction forces (Figs.F.10 to F.12).

The peak steel temperatures are reached at 3720 seconds. See Fig. F.1. Axial forces stabilize for a short period until around 4000 seconds. This coincides with the peak temperatures in some of the concrete ribs although temperatures in the slab elements in the troughs peak about 100 seconds later and in the slab elements above the ribs at around 6000 seconds. At this stage, axial forces start to reverse and rapidly go into tension as the axial capacity of the steel sections starts to increase due to the steel strengthening as it rapidly cools down. The tensile force rapidly reaches the order of 1400 kN, the axial capacity of the steel beam at room temperature. This is logical as all the plastic straining that is taking place on cooling will be irrecoverable and this will give rise to increasing tensile forces.

However, the connection capacity will be significantly less than this. For example, calculation of the tensile design capacity at room temperature gives a tying force of ~168kN for the fin plate connection at the end of these beams and therefore we must assume that the connection would have failed very soon after cooling starts although if the connection itself is hot then it would be considerably more ductile. These failure criteria are not covered in the model and the effect needs to be investigated. This behaviour should not be a surprise as connection failures in tension were observed in the fire tests at Cardington.

All the other beams, both secondary and primary, follow the same pattern of behaviour (Figs. F.18 to F.21. There are some minor differences that can be explained by the different thermal regimes and the different restraint conditions for these beams. For example, edge beams have 80% of the temperature of internal beams, therefore failing in end squash capacity at a later stage of the analysis and some beams are more restrained than others, therefore failing slightly earlier.

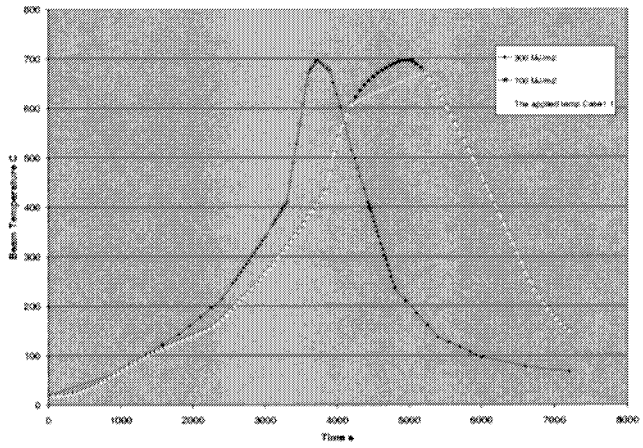

Fig. F.1: **Peak beam temperatures for the basic cas "a" and two values of the fire load density.**

2.: **Position of nodes for column base forces**

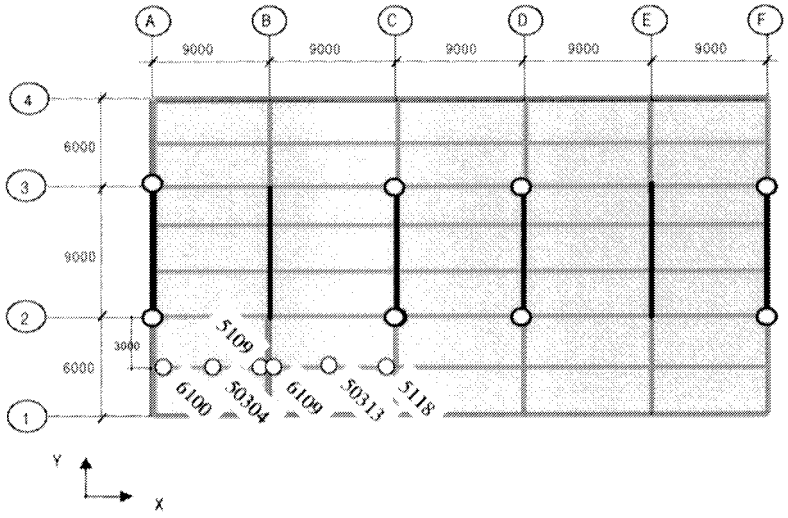

Fig. F.3: **Position of nodes for axial forces in secondary beams – 305x165x40UB – Gridline 1-2**

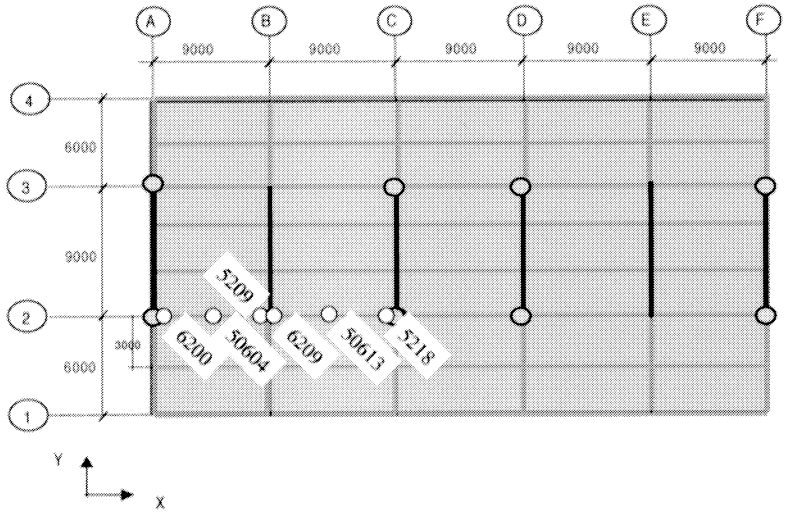

Fig. F.4: Position of nodes for axial forces in secondary beams – 305x165x40UB – Gridline 2

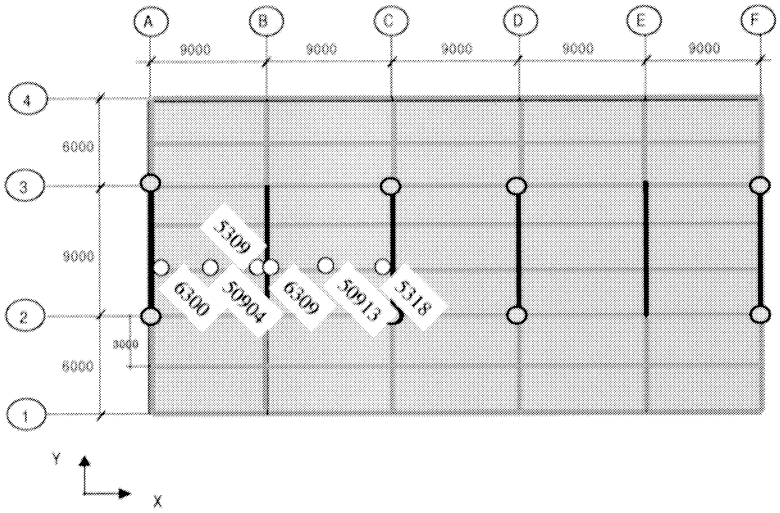

Fig. F.5: Position of nodes for axial forces in secondary beams – 305x165x40UB – Gridline 2-3

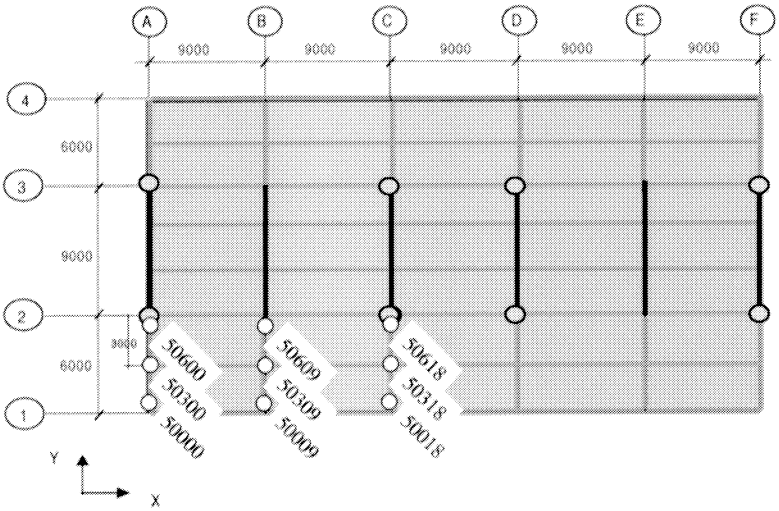

Fig. F.6: Position of nodes for axial forces in primary beams – 356x171x51UB

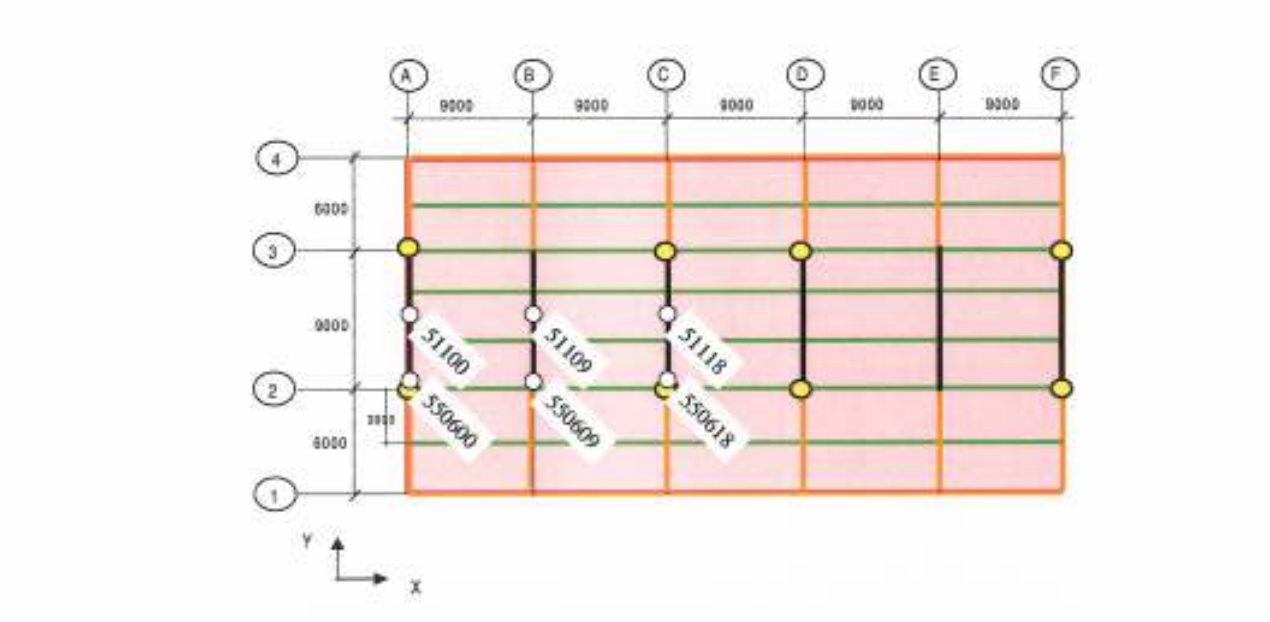

Fig. F.7: Position of nodes for axial forces in primary beams – 610x228x101UB

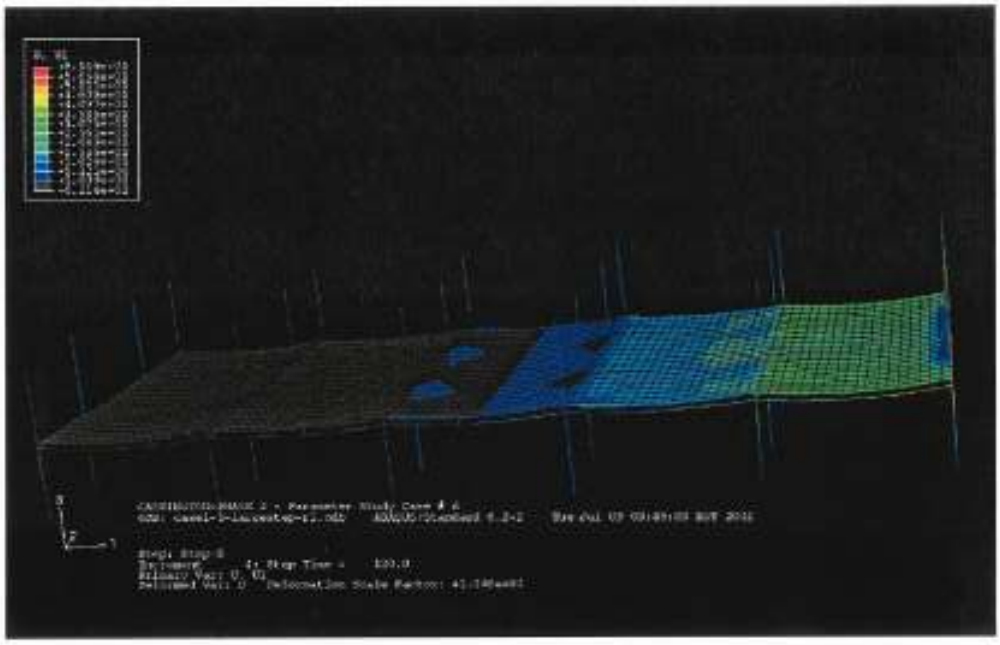

Fig. F.8:Longitudinal in-plane displacements of slab at peak temperature

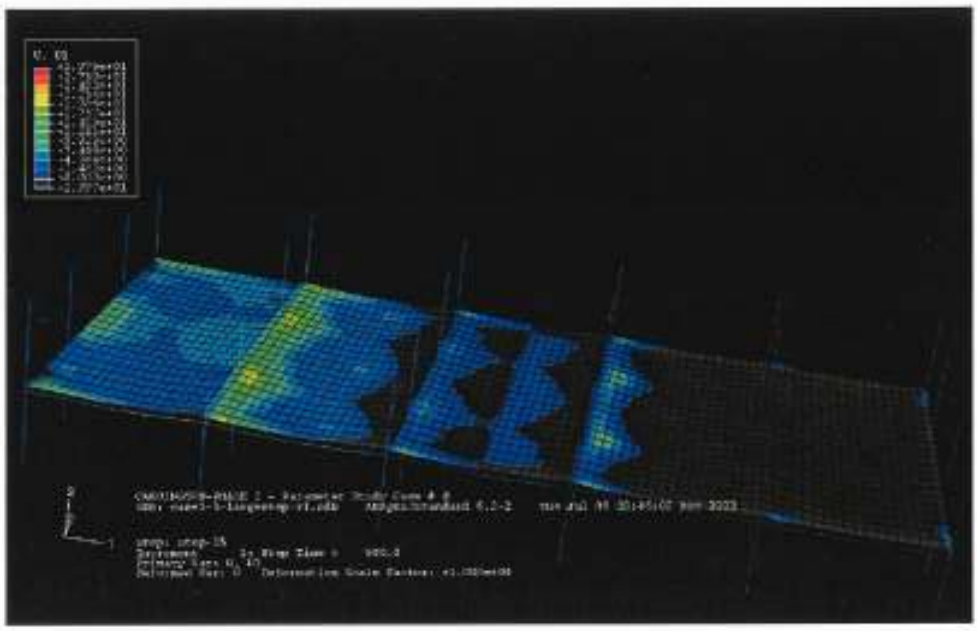

Fig. F.10: Column base shears in longitudinal direction

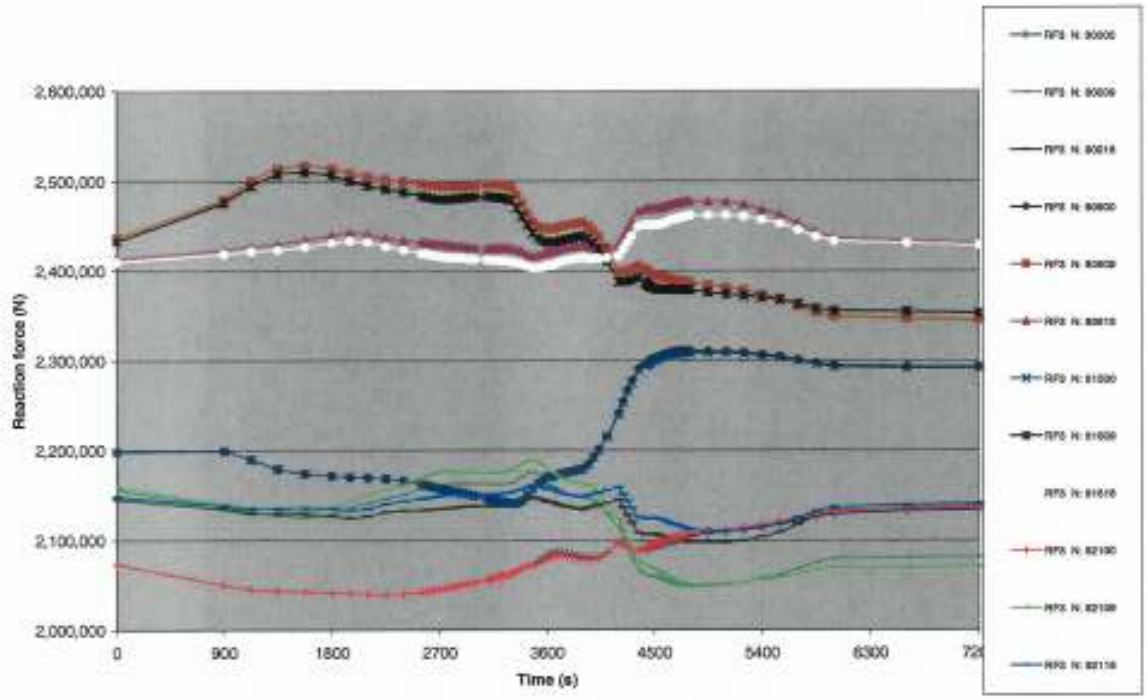

Fig. F.11: **Column base shears in transverse direction**

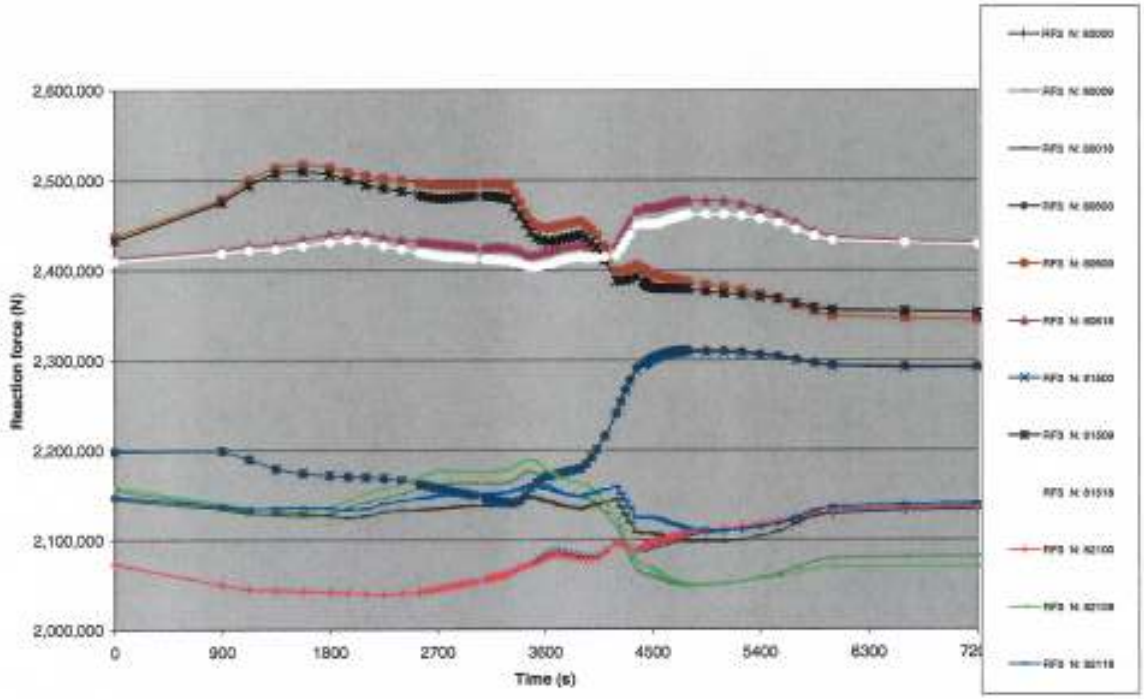

Fig. F.12: **Column reaction forces in vertical direction**

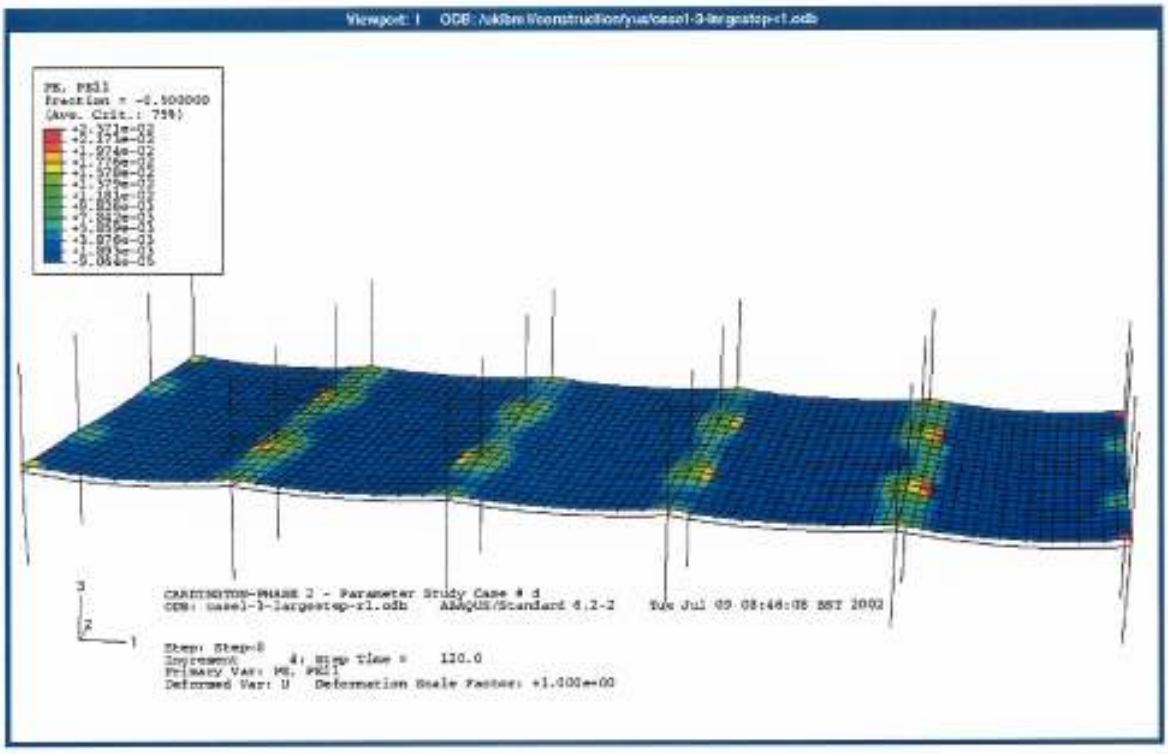

Fig. F.13: **Plastic strain in slab in longitudinal direction at peak temperature**

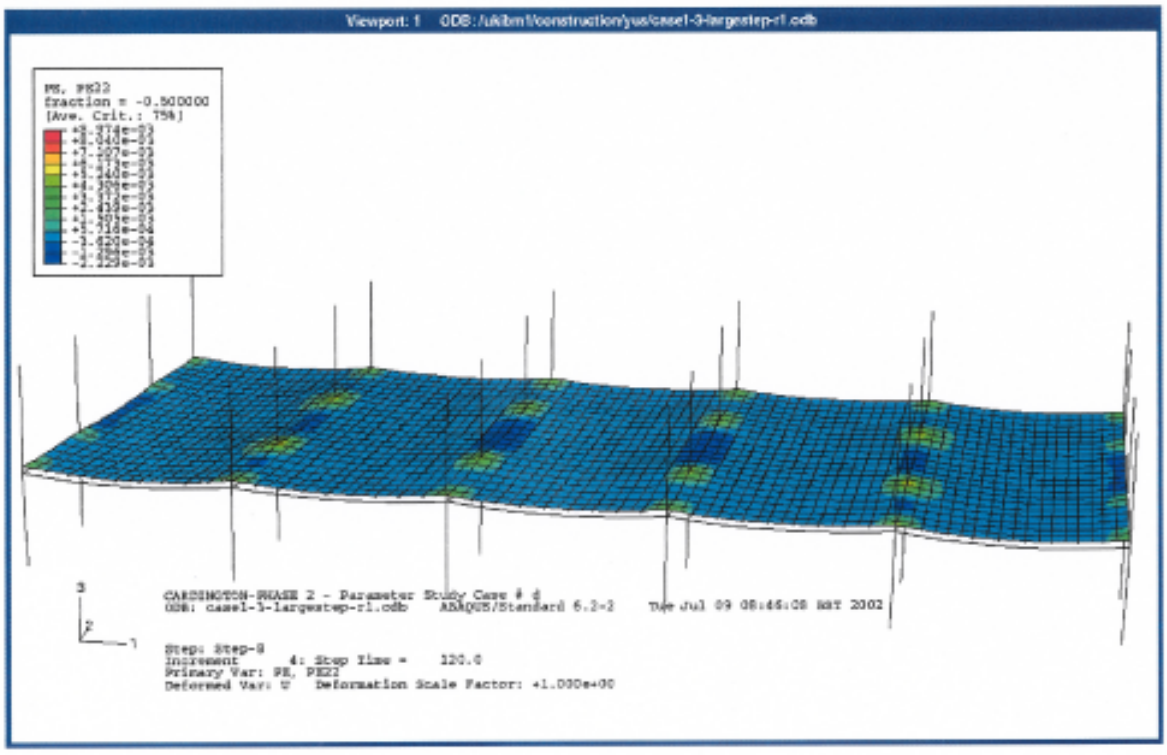

Fig. F.14: **Plastic strain in slab in transverse direction at peak temperature**

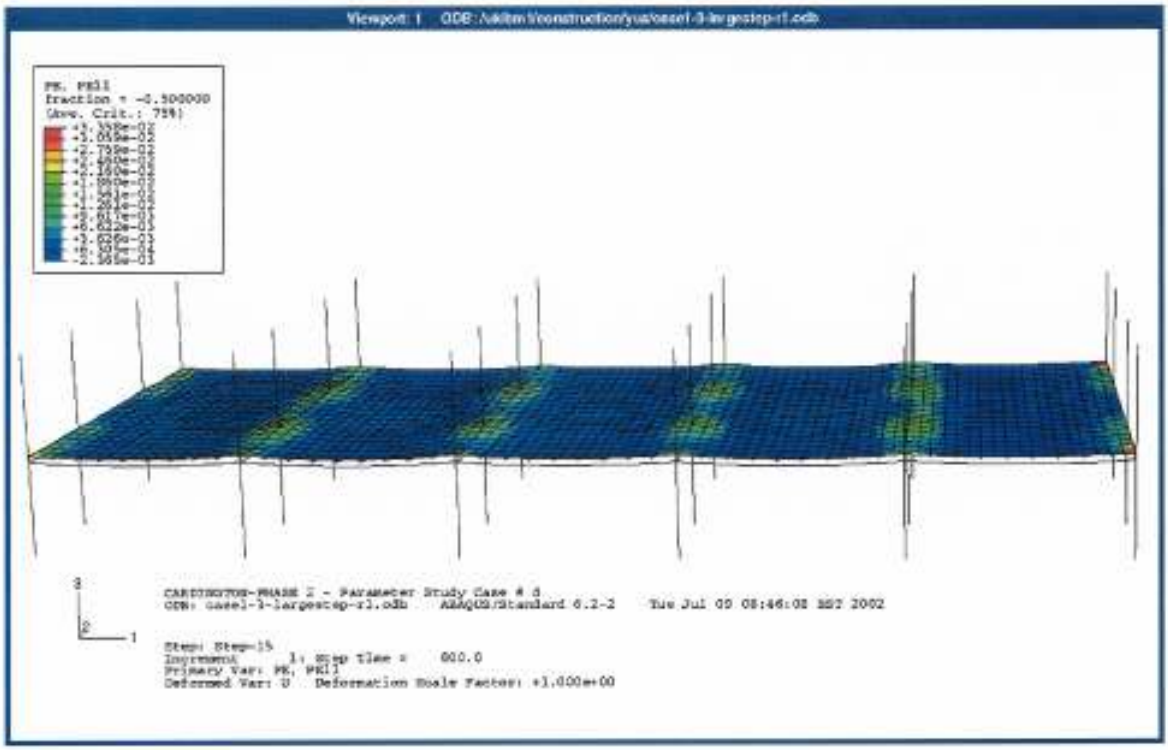

Fig. F.15: Plastic strain in slab in longitudinal direction at end of analysis

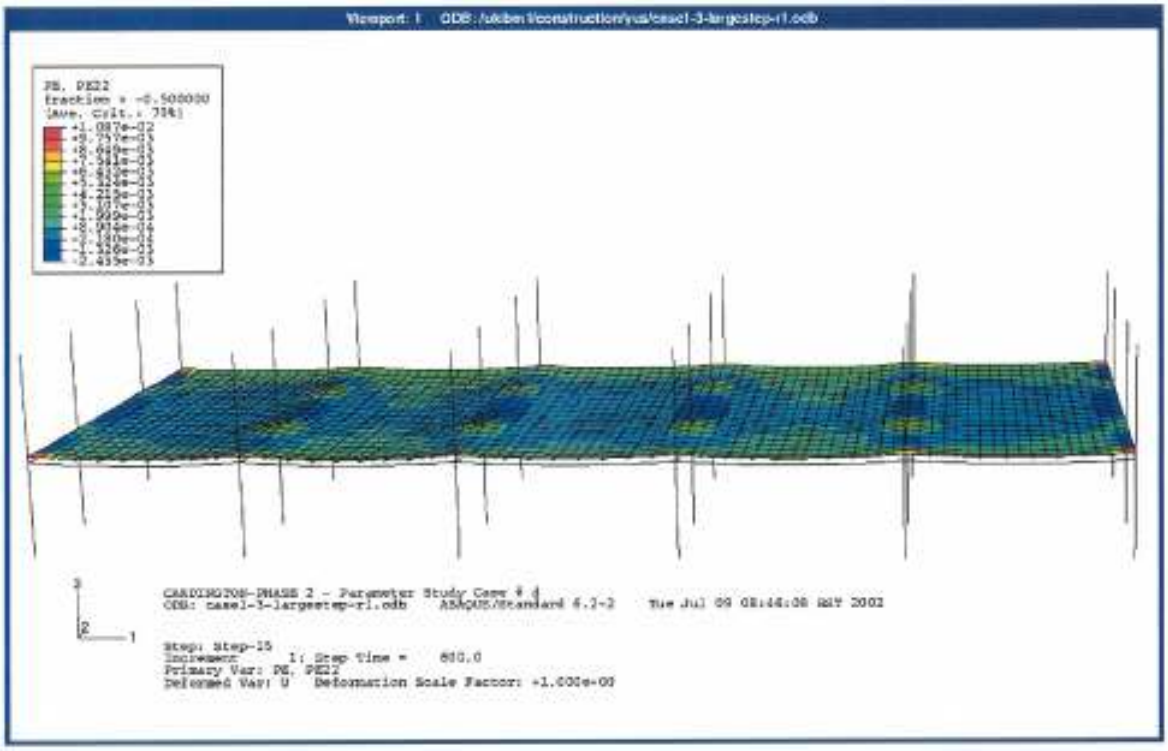

Fig. F.16 Plastic strain in slab in transverse direction at end of analysis

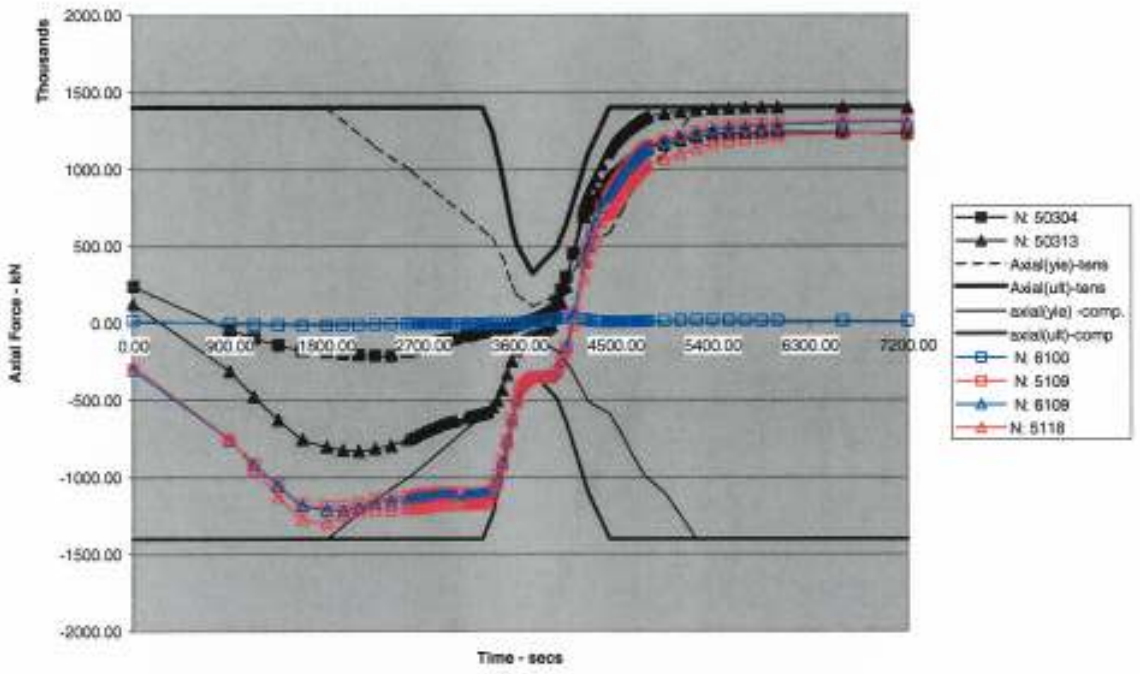

Fig. F.17: **Axial force in secondary beams – 305x165x40UB – Gridline 1-2**

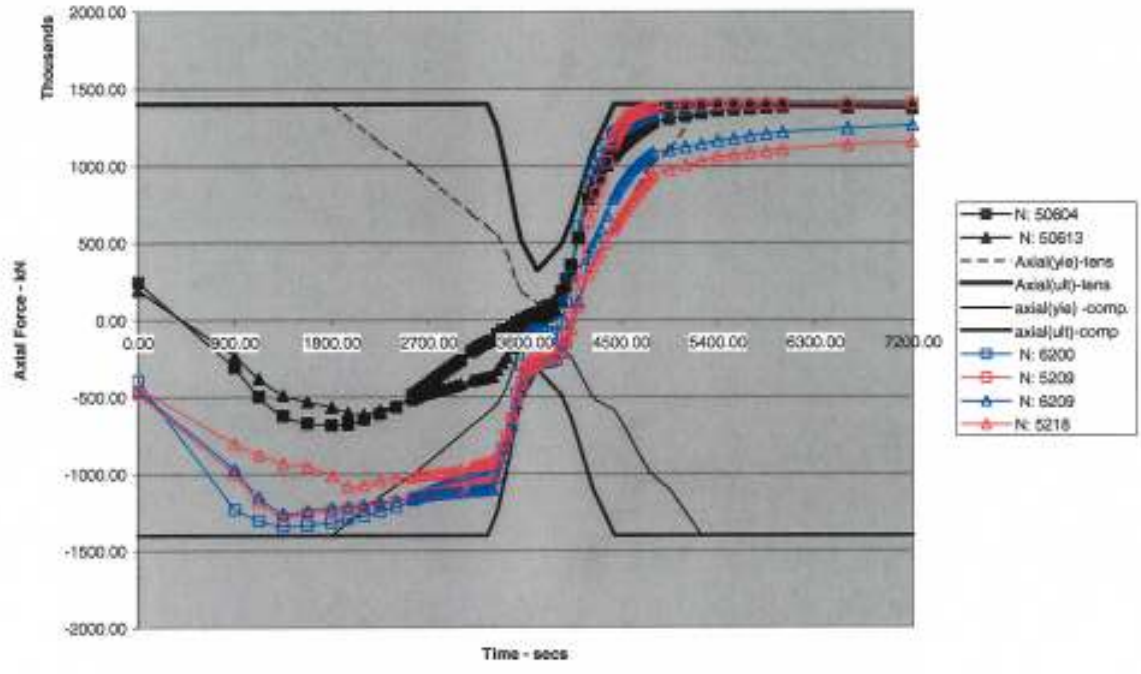

Fig. F. 18. **Axial force in secondary beams – 305x165x40UB – Gridline 2**

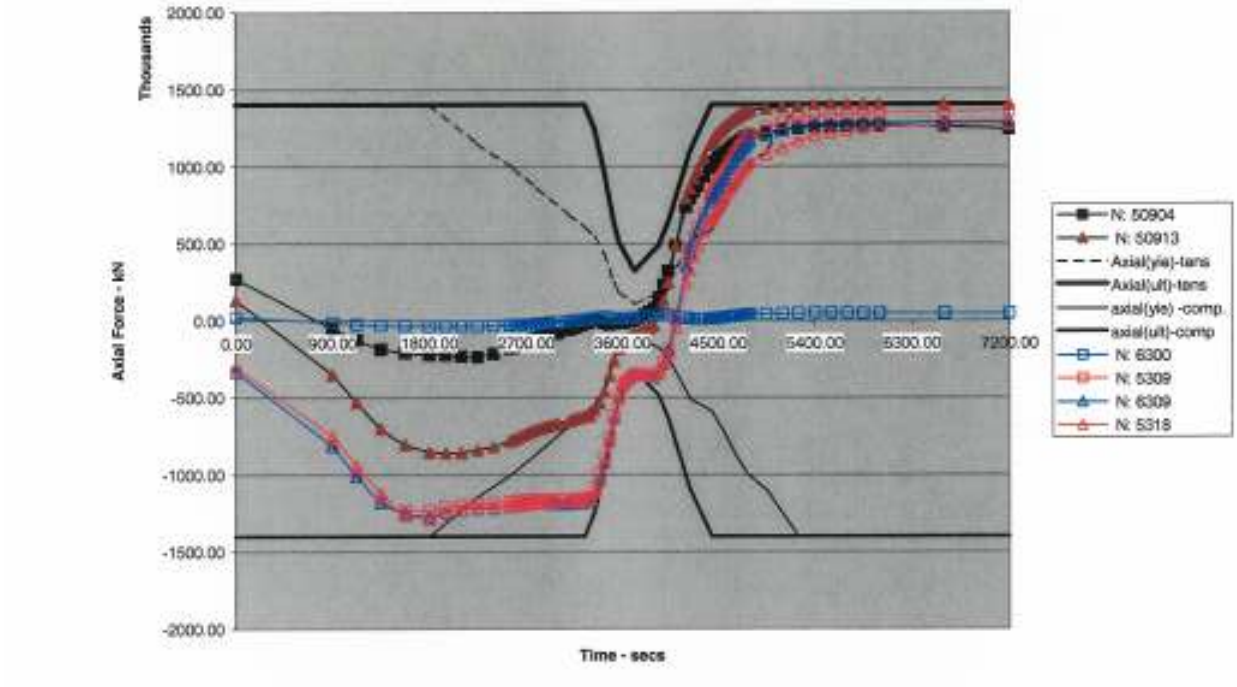

Fig. F.19: **Axial force in secondary beams – 305x165x40UB – Gridline 2-3**

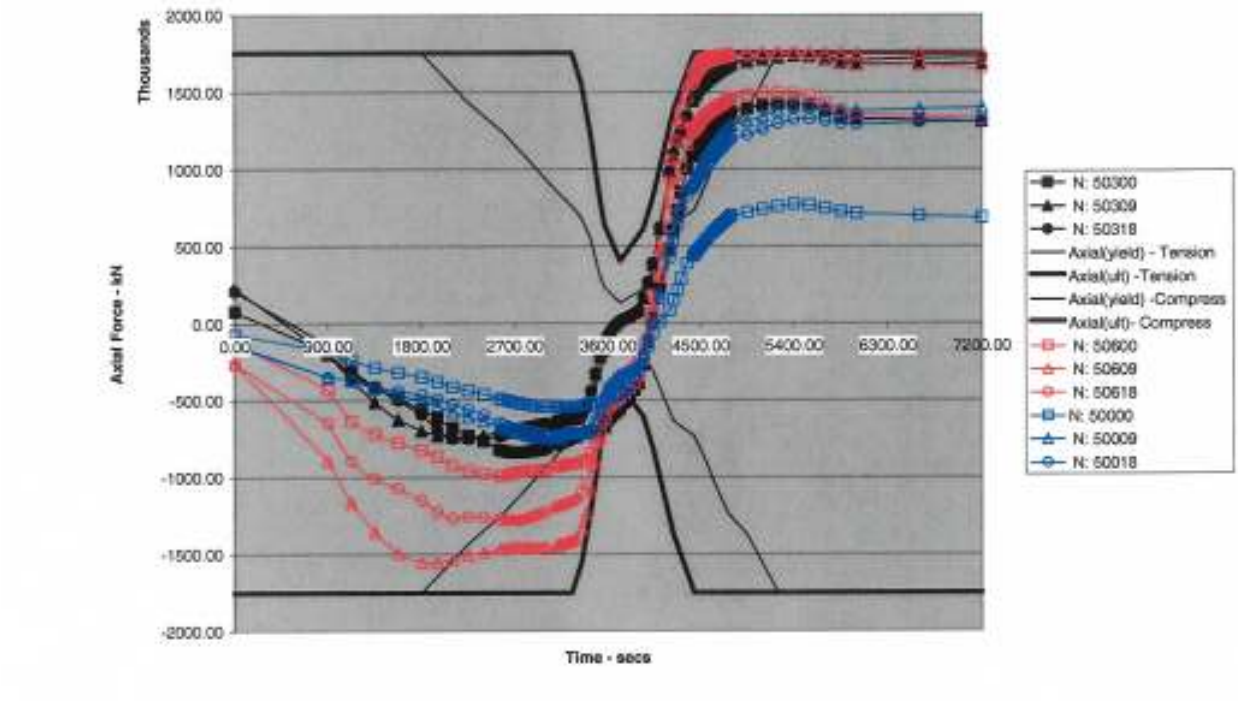

Fig. F.20: **Axial force in primary beams – 356x171x51UB**

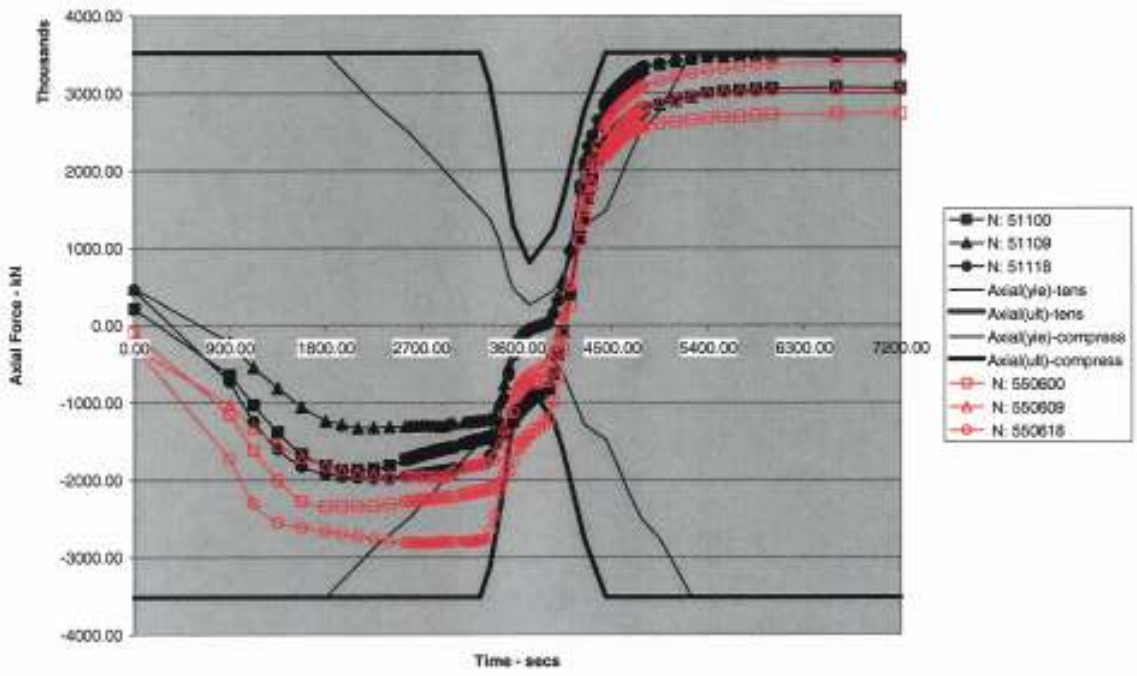

Fig. F.21: Axial force in primary beams – 610x228x101UB

Annex G: The BRE slab method

Following the UK research at Cardington, a method of assessing the strength of a system of composite beams acting with a composite floor slab was developed by the UK engineering consultancy of BRE. The advantage of the method is that it is more easily adapted to different building geometries and hence the method can be used in situations where no information is available from the finite element modelling.
The model developed by BRE combines the residual bending resistance of the composite beams with the contribution of the composite slab, calculated using a combined yield-line and membrane action.

The model is most easily described by considering the behaviour of an isolated floor slab supported rigidly on knife supports at its edges. As load is applied to the slab, it will initially resist the load by bending action and, as the load is further increased, yield lines will form as plastic hinges develop (Fig. G.1) .

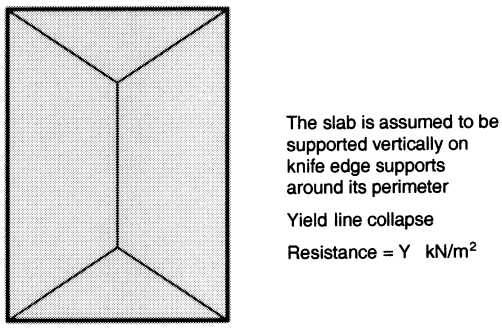

Fig. G.1: Formation of yield lines in simply supported slab

As the load is increased further, the structural mechanism within the slab changes from bending action to membrane action as tensions and compression build up. A pattern of internal forces develops in which the centre of the slab is in tension and the outer parts are in compression (Fig. G.2). All applied loads are balanced by vertical reactions at the perimeter. The slab fails when the reinforcement mesh fractures across the centre of the slab.

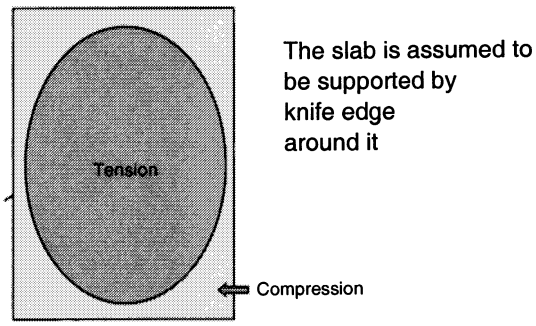

Fig. G.2: Tensile membrane action with tensile and compression zones

In the BRE model, the bending resistance (yield line) is first computed and then an enhancement factor is computed based on membrane behaviour. This factor is applied to the bending resistance to obtain the final slab resistance. For simplicity, the small residual bending resistance of the beams is added to form a total resistance of the slab and beam system. For simplicity, the small residual bending resistance of the beams is added to form a total resistance of the slab and beam system.

$$\text{Total resistance} = Y \times E_{fac} + B$$

Where:
Y is the load at which the yield line pattern develops

E_{fac} is the enhancement factor for membrane action
B is the total resistance of any beams spanning across the slab (kN/m^2)

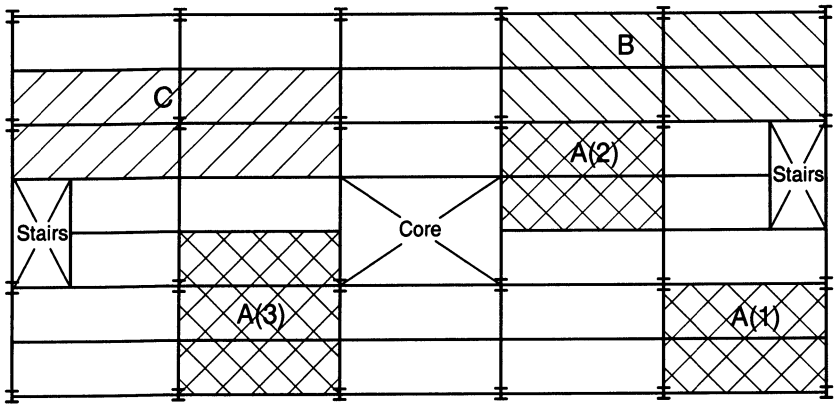

Key to figure A: Permitted area within scope of the guide
B: Permitted area outside scope of the guide
C: Not permitted – contains columns

Fig. G.3: Possible floor design zones

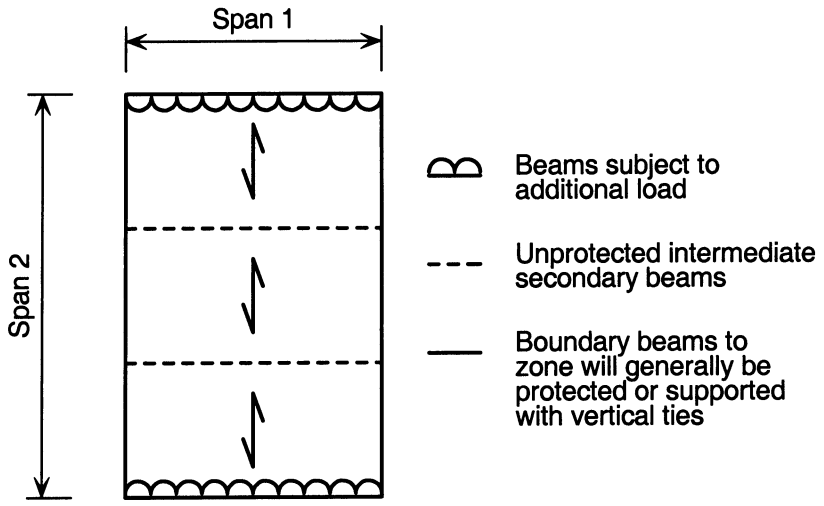

Fig. G.4: Definition of span 1 and span 2 and beam lay out

The design information has been generated for a range of fire loads and ventilation conditions. Design imposed loads are given which have been reduced by the EC1-1 load combination factor, $\psi_{1,1}$, of 0.5. Thus, for an applied load of 3.5 kN/m^2, the load used in calculations is 1.75 kN/m^2.

Fire loads range from 200 to 700 MJ/m^2. A wide range of ventilation conditions is covered to enable maximum use to be made of the recommendations.

Design recommendations are presented in 17 design tables. Many of the tables are appropriate to more than one fire condition (0).

Table G.1: Relationship between design cases and design tables

Fire load (MJ/m^2)	Window height (m), Opening factor ($m^{1/2}$)						
	0,5	1,0	1,5	2,0	2,5	3,0	3,655
	0,011	0,031	0,057	0,087	0,122	0,161	0,216
200	B	1	2	1	B	B	B
300	B	3	4	5	6	B	B
400	9	5	7	7	8	B	B
500	9	4	10	10	3	9	B
600	9	11	12	10	13	6	B
700	9	14	15	16	17	1	B

In many cases, but generally where the ventilation is either very high or very low, it was found that the unprotected beams spanning across the design zone were adequate in themselves to support the applied loads and it was not necessary to take into account any membrane action in the floor slab. These cases are marked as "B" in 0 and the full design table is not presented. Where "B" is indicated, the beams are adequate on the basis of a simple EC4-1-2 check.

A sample of a design table is shown here as Table G.2.

Table G.2: Extract from design table 7 of the Design Guide

Imposed load 3.5 kN/m^2					
	Span 1	Mesh/Extra Load (kN)			
Span 2	6	**>>7<<**	8	9	10
6	6x200 / 0	6x200 / 4	6x200 / 7	7x200 / 11	7x200 / 15
7	6x200 / 3	6x200 / 7	6x200 / 11	7x200 / 16	7x200 / 21
8	6x200 / 5	6x200 / 9	6x200 / 15	6x200 / 20	7x200 / 27
>>>> 9	7x200 / 6	**7x200 / 12**	6x200 / 18	6x200 / 25	7x200 / 32
10	7x200 / 8	7x200 / 14	7x200 / 21	7x200 / 28	7x200 / 36

For span 1 of 7m and span 2 of 9m the reinforcing mesh required is 7x200 and the additional loading to the edge beams parallel to span 1 is 12kN per beam.

Annex H: The EC4-1.2 method

EC4-1-2 contains a method by which it can be shown that, in some circumstances, the unprotected can support all applied loads. The method is simple to use but is very conservative as it ignores any interaction between the beams and the floor slab. It can only be used if the intensity of the fire is low.

The fire part of Eurocode 4 (EN1994-1-2) contains simple rules for the design of composite beams. Using these methods, in a limited number of circumstances, when the fire exposure is low, the use of unprotected steel may be justified.

The design can be justified using 4.3.4.2.3 (from EN1994-1-2):

4.3.4.2.3 *Structural behaviour - critical temperature model*

(3) *The critical temperature, θ_{cr} may be determined from the load level, $\eta_{fi,t}$, applied to the composite section and from the strength of steel at elevated $f_{amax,\theta cr}$ temperatures according to the relationship:*

For R30 (or less), $0{,}9\ \eta_{fi,t} = f_{amax,\theta cr} / f_{ay,20°C}$

In any other case, $1{,}00\ \eta_{fi,t} = f_{amax,\theta cr} / f_{ay,20°C}$

where,

$f_{amax,\theta cr}$ *is the steel strength corresponding the maximum steel temperature*

$f_{ay,20°C}$ *is the strength of steel at 20 °C*

$\eta_{fi,t}$ *determined from the load level*

For a simply supported composite beam the load level is the maximum applied moment in the fire condition divided by the moment resistance used in normal design.
An unprotected beam will normally have a fire resistance of less than R30 so for the natural fire case the R30 case can safely be assumed. Therefore,

$$0{,}9\ \eta_{fi,t} = f_{amax,\theta cr} / f_{ay,20°C}$$

The maximum temperatures calculated using the natural fire model can be converted directly into a maximum load level on any beam. For all the cases considered in the maximum beam temperatures and corresponding load levels are presented in Table H.1and graphically in Fig. H.1.

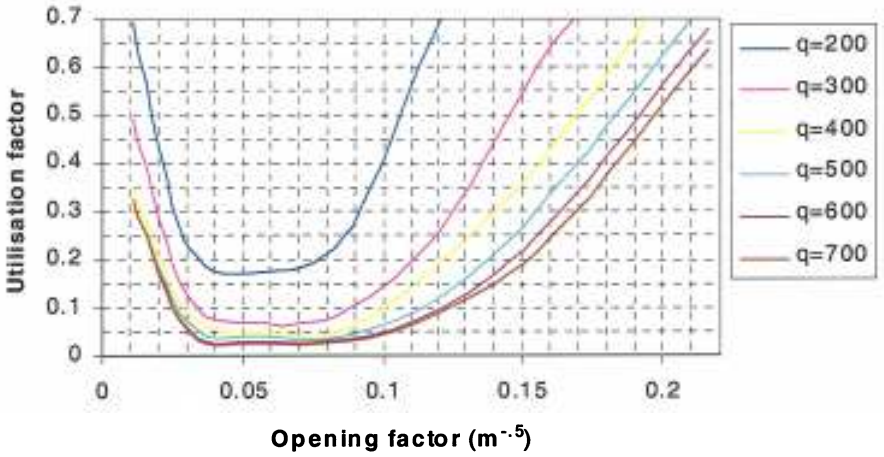

Fig.H.1: Load level factor vs. opening factor

Table H.1: Beam temperatures and load levels

Fire load (MJ/m^2)	Window height (m) and Opening factor ($m^{1/2}$)						
	0,5 0,011	1,0 0,031	1,5 0,057	2,0 0,087	2,5 0,122	3,0 0,161	3,655 0,216
200	551/0,691	723/0,225	760/0,176	706/0,248	546/0,708	443/1,00	358/1,00
300	612/0,490	800/0,122	906/0,065	855/0,092	695/0,269	563/0,650	435/1,00
400	665/0,349	864/0,087	975/0,050	955/0,054	741/0,201	632/0,437	498/0,872
500	674/0,325	909/0,065	1022/0,040	1006/0,043	798/0,125	668/0,341	536/0,743
600	674/0,325	947/0,056	1059/0,031	1043/0,035	838/0,101	690/0,282	554/0,681
700	674/0,325	979/0,049	1089/0,025	1071/0,029	858/0,090	705/0,249	567/0,636

It can be seen in the table that, in many cases, the maximum beam temperature results in very low, impractical load levels and, in some cases, the load level is sufficient high to justify unprotected steel without further calculation.
The load level may be expressed as:

$$\eta_{fi} = \frac{(\gamma_{GA} + \psi_{1,1}\zeta)}{(\gamma_G + \gamma_Q \zeta)}$$

where

γ_G	is the partial safety for permanent loads
γ_{GA}	is the partial safety for permanent loads in fire
γ_Q	is the partial safety for variable loads
$\psi_{1,1}$	is the load combination factor
ξ	is the ratio between the main variable and permanent actions

For offices the load level is normally about 0,53 corresponds to a maximum steel temperature of 598°C. However, because the full strength of a beam is rarely utilised, load levels of 0.4 are not uncommon.

List of Figures (Annexes)

List of Tables (Annexes)

FOREWORD

This SCI report is presented in the form of a design guide and contains recommendations which will allow many of the beams in multi-storey buildings to be designed without any applied fire protection. The recommendations have been derived following a major study of the behaviour of composite steel framed buildings. The project built on earlier UK and ECSC projects into the behaviour of complete buildings in fire, including studies of actual buildings following real fires, full-scale fire tests at Building Research Establishment, Cardington (UK) and at BHP, Melbourne, Australia. In particular, this project was concerned with the modelling of buildings using advanced finite element techniques.

This publication was prepared as part of an ECSC sponsored project, *Design tools for the behaviour of fire exposed multi-storey steel framed buildings, 7210 PA, PB, PC, PD112.*

The project team comprised:

L Twilt	TNO (Netherlands)
C Both	TNO (Netherlands)
A Breunese	TNO (Netherlands)
D O'Callaghan	Corus (United Kingdom)
M O'Connor	Corus (United Kingdom)
M Rotter	University of Edinburgh (United Kingdom)
A Usmani	University of Edinburgh (United Kingdom)
L-G Cajot	PROFILARBED Recherches (Luxembourg)
B Zhao	CTICM (France)
G M Newman	Steel Construction Institute (United Kingdom)

Report prepared by G M Newman, Steel Construction Institute (United Kingdom)

SUMMARY

This design guide has been prepared following extensive research into the behaviour of composite steel framed buildings in fire. It contains procedures and recommendations which will allow buildings to be constructed with a large number of floor beams unprotected. Columns are always required to have protection. In all cases, the fire is assumed to be a real or natural fire that might occur in a building, and not the standard fire, used for fire resistance testing, which building regulations are based on.

This publication is in 10 chapters. Following the introduction, Chapters 2, 3 and 4 contain general information on how real fires were modelled and how finite element techniques might be used. Chapters 5, 6, 7 , 8 and 9 contain design recommendations. Chapter 10 contains references.

In detail:

Chapter 2 contains information on the methods used to model the real fire behaviour.

Chapter 3 contains guidance on the thermal response modelling of composite structures in fire.

Chapter 4 contains guidance on the use of finite element modelling of composite structures in fire

Chapter 5 contains general recommendations relating to building stability and compartmentation.

Chapter 6 contains design procedures and guidance on available options.

Chapter 7 contains design procedures and recommendations based on advanced FE modelling.

Chapter 8 contains design recommendations using a more conservative simple analysis method developed by the Building Research Establishment in UK.

Chapter 9 contains design recommendations based on the direct application of the simple analysis techniques of EC4-1-2.

The Guide contains, in Chapter 6, general guidance on the best procedure that should be adopted in using the tools described in Chapters 2, 3 and 4. The effects of the main parameters for the structural behaviour of composite steel framed building exposed to natural fires are quantitatively discussed on the basis of the parametric study, performed in the scope of the present research. For details, reference is made to the final project report. Alternative methods, using more conservative tools are introduced. They are further explained and quantified in Chapters 8 and 9.

The recommendations in Chapter 8 are based on a much simpler structural model than a full finite element model and are therefore more conservative. The advantage of the method used is that it is more easily adapted to different building geometries and hence the method can be used in situations where no information is available from the finite element modelling.

The recommendations in Chapter 9 are based on a simple beam model. They are simple to use but are very conservative as they ignore any interaction between the beams and the floor slab. They will only be useful if the intensity of the fire is low.

Part 2: Design recommendations for composite steel framed buildings in fire

Table of contents

1 INTRODUCTION

1.1 General

The elements of structure of multi-storey buildings are required by Building Regulations to have fire resistance. The fire resistance is established from performance in a standard fire resistance tests. In a standard test, single, isolated and unprotected I or H section beams can only be expected to achieve 15 to 30 minutes fire resistance. It has thus been normal practice to protect steel beams and columns with of fire resisting boards, sprays or intumescent coatings, or, in slim floor or shelf angle floor construction, by encasing the structural elements within floors or by partially encasing sections in concrete.

Large-scale real or natural fire tests carried out in a number of countries have shown consistently that the fire performance of steel framed buildings is much better than the standard test would suggest. Evidence from these fires indicates that the amount of protection being applied to steel elements may be excessive and, in some cases, unnecessary.

This publication contains recommendations which will allow many of the beams in multi-storey buildings to be left without any applied fire protection. It has been prepared as part of an ECSC funded research project. The project builds on earlier UK and ECSC projects into the behaviour of complete buildings in fire, including studies of actual buildings following real fires, full-scale fire tests at Building Research Establishment, Cardington (UK) and at BHP, Melbourne, Australia. In particular, this project was concerned with the modelling of buildings using advanced finite element techniques.

The recommendations apply to braced composite frames using composite slabs and shallow decking (Figure 1.1 and Figure 1.2).

1.2 The Cardington Tests

In September 1996, a programme of fire tests was completed in the UK at the Building Research Establishment's Cardington Laboratory. The tests were carried out on an eight-storey composite steel-framed building that had been designed and constructed as a typical multi-storey office building. The purpose of the tests was to investigate the behaviour of a real structure under real fire conditions and to collect data that would allow computer programs for the analysis of structures in fire to be verified.

A detailed description of the tests has been published[1]. The complete test data, in electronic form with accompanying instrument location maps, is available for Tests 1, 2, 3 and 6 from Corus RD&T (Swinden Technology Centre, UK) and for Tests 4 and 5 from BRE (UK).

A design guide containing simple recommendations based on the Cardington research has been published in UK by The Steel Construction Institute[2].

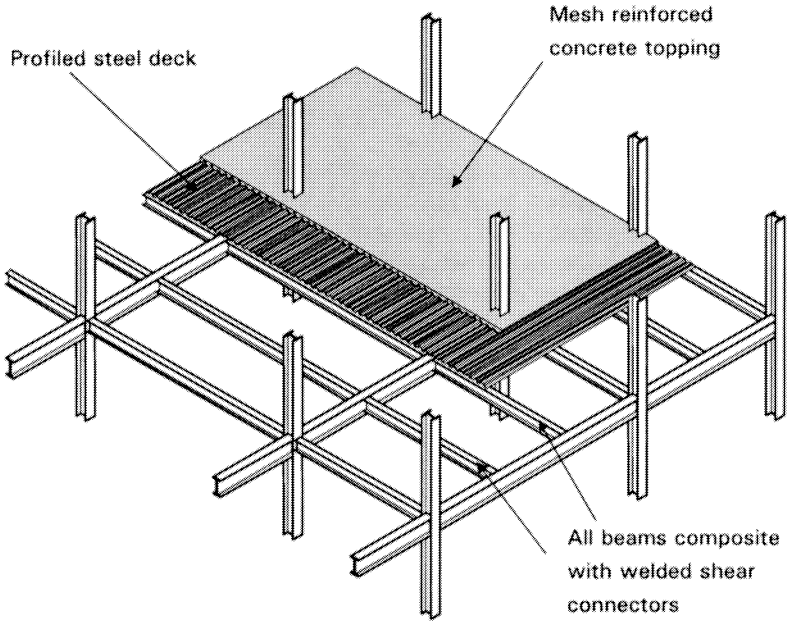

Figure 1.1 *Schematic of composite steel framed building*

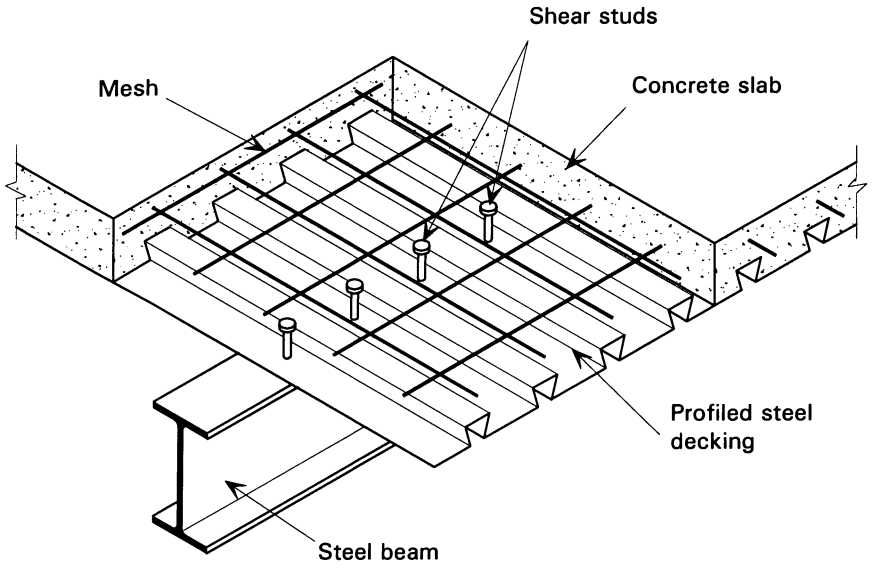

Figure 1.2 *Schematic of composite floor and composite beam*

The test building (see Figure 1.3) was designed to be a typical example of both the type of braced structure and the load levels that are commonly used for office buildings in the UK. In plan, the building covered an area of 21 m x 45 m and had an overall height of 33 m. Normally a building of this type would be required to have 90 minutes fire resistance. The beams were designed as simply supported acting compositely with a 130 mm floor slab. Fin-plates were used for the beam-to-beam

connections and flexible end plates for the beam-to-column connections (Figure 1.4). The structure was loaded using sandbags distributed over each floor to simulate typical office loading.

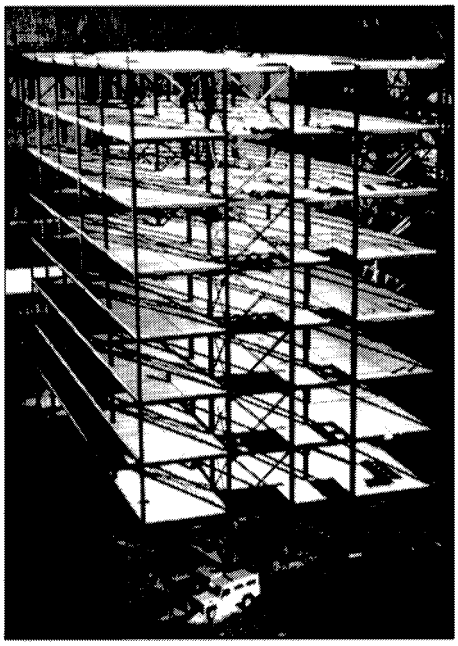

Figure 1.3 *Cardington test building prior to the concreting of the floors*

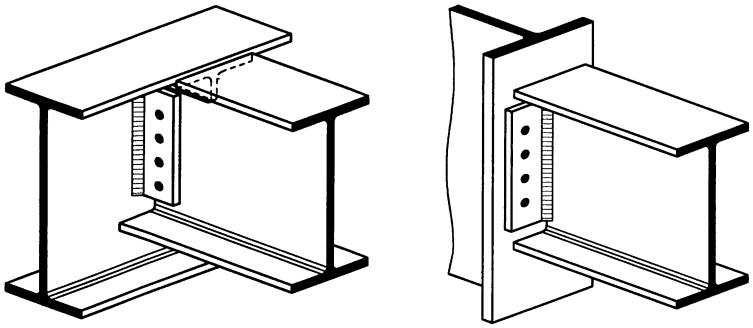

Figure 1.4 *Fin plate and flexible end plate connections*

There were two projects in the research programme. One project was funded by Corus (formerly British Steel) and the European Coal and Steel Community (ECSC), and the other was funded by the UK Government via the Building Research Establishment (BRE). Other organisations involved in the research programme included Sheffield University (UK), TNO (The Netherlands), CTICM (France) and The Steel Construction Institute (UK). Fire tests took place between January 1995 and July 1996. The tests were carried out on various floors; the location of each test is shown on the floor plan in Figure 1.5.

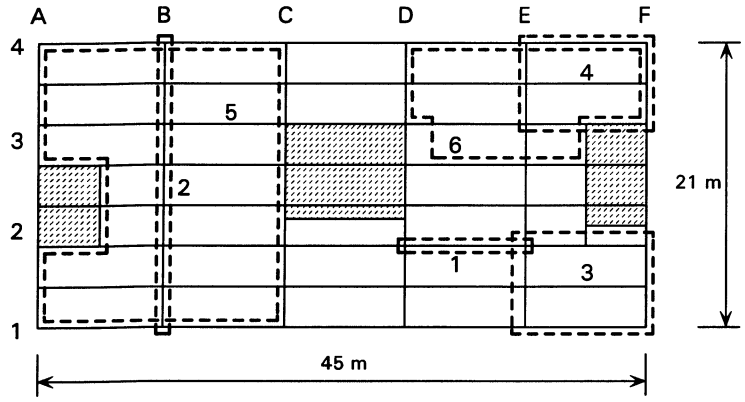

Figure 1.5 *Test locations*

Key to figure

1.	Restrained beam (ECSC)	2.	Plane frame (ECSC)
3.	Corner (ECSC)	4.	Corner (BRE)
5.	Large compartment(BRE)	6.	Office demonstration (ECSC)

Test 1 involved a single secondary beam and the surrounding floor slab which was heated by a purpose-built gas-fired furnace. Test 2 was also heated using gas, and was conducted on a plane frame spanning across the building on one floor; the test included primary beams and associated columns. Tests 3, 4 and 5 involved compartments of various sizes subjected, in each case, to a natural fire fuelled by timber cribs. The columns in these tests were protected up to the underside of the floor slab and the beams and floor slab were left unprotected. The last, and most severe, test was a demonstration using furniture and contents typically found in modern offices.

1.3 Design Principles

The proposed design recommendations have been prepared with a number of considerations in mind.

- The risk to life safety of occupants, fire fighters and others in the vicinity of the building shall be no less than that implied by existing National Building Regulations.

- On the floor exposed to fire, excessive structural deformation will not cause failure of compartmentation, i.e. the fire is contained within its compartment of origin and should not spread horizontally.

- The guidance applies only to composite steel framed buildings of the general form tested at BRE, Cardington and illustrated in Figure 1.3. That is to say:

    - The structure is a braced, non-sway frame designed as simple. That is to say that all the beam were designed as simply supported and horizontal forces were assumed to be resisted by the bracing system.

    - The floor slabs are composite, comprising steel decking and normal or lightweight concrete.

    - The floor beams are down-stand I or H sections and are designed to act compositely with the floor slab via welded shear connectors.

The building should have at least two bays in each direction.

1.4 About this publication

This publication is in 9 chapters. Following the introduction, Chapters 2, 3 and 4 contain general information on how real fires were modelled and how finite element techniques might be used. Chapters 5, 6, 7 , 8 and 9 contain design recommendations. Chapter 10 contains references.

In detail:

Chapter 2 contains information on the methods used to model the real fire behaviour.

Chapter 3 contains guidance on the thermal response modelling of composite structures in fire.

Chapter 4 contains guidance on the use of finite element modelling of composite structures in fire

Chapter 5 contains general recommendations relating to building stability and compartmentation.

Chapter 6 contains design procedures and guidance on available options.

Chapter 7 contains procedures and guidance for using FE modelling although, because the complexity of FE models, it was not found to be possible to include specific design information that can be directly used.

Chapter 8 contains design recommendations using a more conservative simple analysis method developed by the Building Research Establishment in UK.

Chapter 9 contains design recommendations based on the direct application of the simple analysis techniques of EC4-1-2.

The guide contains no specific recommendations which have been developed from studies using finite element methods. It was found impossible, within the scope of the project, to generalise the findings. Instead, Chapter 6 contains general guidance on the best procedure that should be adopted in using finite element models and how the more conservative methods described in Chapters 7 and 8 might be used.

The recommendations in Chapter 7 are based on a much simpler structural model than a full finite element model and are therefore more conservative. The advantage of the method used is that it is more easily adapted to different building geometries and hence the method can be used in situations where no information is available from the finite element modelling.

The recommendations in Chapter 8 are based on a simple beam model. They are simple to use but are very conservative as they ignore any interaction between the beams and the floor slab. They will only be useful if the intensity of the fire is low.

Diagrammatically, the possible approaches to the design of structures in fire are illustrated in Figure 1.6. In the figure the differences between the normal regulatory fire resistance approach and the methods on which the recommendations described in this publication can be seen. In this publication, methods based on natural fires are proposed. The principle design method proposed, based on finite element modelling, is the least conservative approach. The BRE method cannot be seen as a simple elemental approach but is not a whole structure model. It is more conservative than the finite element approach. The EC4 approach is the most conservative approach and is based on a simple elemental behaviour.

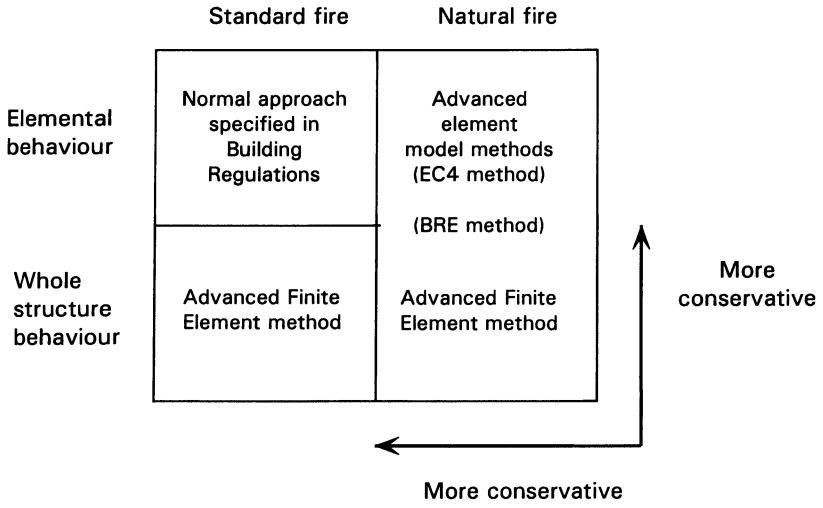

Figure 1.6 *Schematic of fire engineering approaches*

2 FIRE MODELLING

2.1 Introduction

The recommendations in this publication are based on natural fires and not the commonly used standard fire. The fire model used was developed in a recent ECSC project, which looked at fires, the probabilities of fires occurring, and the effects of active fire safety measures such as sprinklers. The project developed what has become known as "The Natural Fire Safety Concept".

In the "Natural Fire Safety" approach the fire safety design is based on physically determined thermal actions. In contrast with the conventional fire design (based on the standard fire and fire resistance), parameters like the amount of fire load, the rate of heat release and the amount of ventilation play an important role in the natural fire design. The specification of appropriate design fire scenarios (i.e. the course of a fire with respect to time and space) is a crucial aspect of fire safety design. The assumptions made with regard to these factors, have major influence on the conditions in the compartment and have a significant impact on the fire design.

The design fire scenarios used for the analysis/development of a building fire have to be deduced from all the possible fire scenarios. In most buildings the number of possible fire scenarios is infinite and need to be reduced to enable analysis and calculation.

The starting point for calculating thermal actions (modelling) is the fire in the enclosure where the fire starts. The fire (scenario) depends on the ignition source, the amount and type of fuel, the size of the enclosure, the amount of ventilation, the growth rate, the rate of heat release etc. Starting with a small growing fire, growing to flashover and dying after the available fire load is consumed.

Design fire scenarios for analysis should be based on the "credible worst case fire scenario". That is to say that more onerous fire scenarios have an acceptably low probability of occurring and that the consequence of those scenarios would need to be borne by society. It is desirable that regulatory authorities are involved in the selection of the design fire scenarios.

One of the main parameters of the design fire scenario is the design fire. A design fire is an idealisation of real fires that may occur in the building and represents a credible worst case of possible fires[3].

2.2 Rate of Heat Release

To simulate a fire in a building and its effect on the structure of this building, you need to define the rate of heat release (RHR) given in kW as function of time. At the beginning the fire starts small and produces little heat. It then grows and begins to spread. The fire-spread velocity depends on the type of building and its use. The buildings are classified into four categories according to the fire-spread velocity: low, medium, fast and ultra-fast (see Figure 2.1 and Table 2.1).

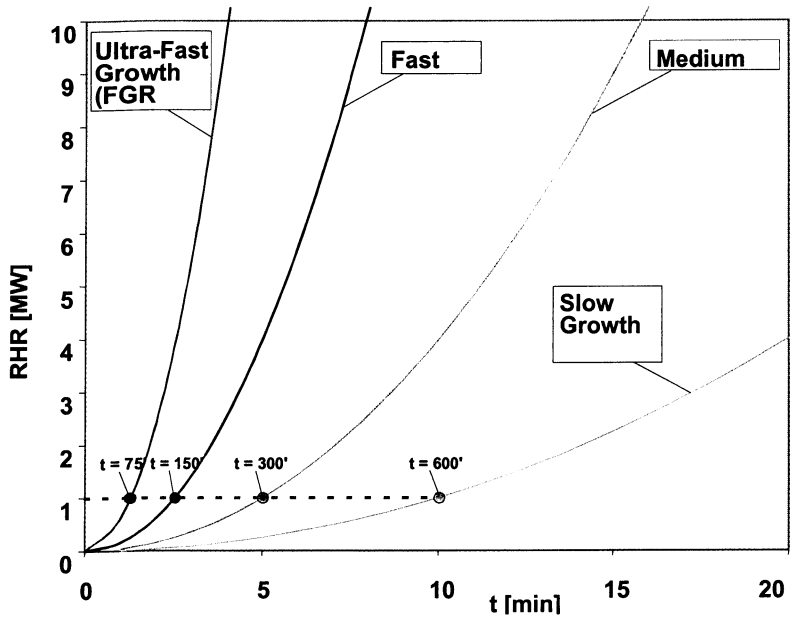

Figure 2.1 *Rate of Heat Release in the growing phase*

Table 2.1 *Fire Growth Rate, Fire Loads and RHR_f for different buildings*

Occupancy	Fire growth rate	RHR_f (kW/m^2)	Fire load $q_{f,k}$
Dwelling	Medium	250	948
Hospital (room)	Medium	250	280
Hotel (room)	Medium	250	377
Library	Fast	500	1824
Office	Medium	250	511
School	Medium	250	347
Shopping Centre	Fast	500	730
Theatre (movie/cinema)	Fast	250	365
Transport (public space)	Slow	250	122

The fire power increases up to a maximum which corresponds to the RHR maximum per m^2 which depends on the building type (see Table 2.1), multiplied by the fire area (see Figure 2.2).

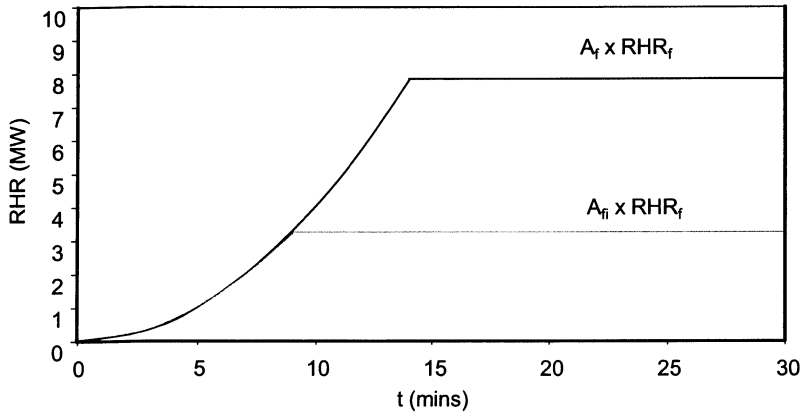

Figure 2.2 *Rate of Heat Release in the fire development phase*

This surface is the whole compartment area (A_f) or, in some cases, it is only the surface where the fire load is localised (A_{fi}). In railway stations, car parks, and large compartments with a non-uniformly distributed fire load, the fire may remain localised.

However, generally, the fire does not remain localised. For instance, in an office building, the fire spreads and finally engulfs the whole compartment.

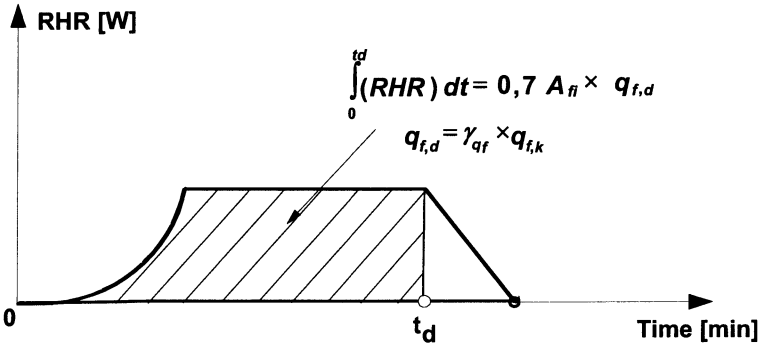

Figure 2.3 *Design Rate of Heat Release Curve. Stationary state and decay phase*

At the end of the growing phase, after that the whole compartment has been involved in the fire, the fire reaches a stationary state corresponding to the horizontal plateau of the RHR curve. The value of this plateau can be equal to the area of the compartment multiplied by the RHR_f corresponding to a fuel controlled fire or the value of this plateau is fixed by the oxygen content in the compartment. In this last case the fire is called ventilation controlled. Following this steady rate of burning, when about 70% of the fuel has been consumed, the fire begins to decline.

The fire load defines the available energy but the gas temperature in a fire is more dependent on the rate of heat release. The same fire load burning very quickly or smouldering can lead to completely different gas temperature curves.

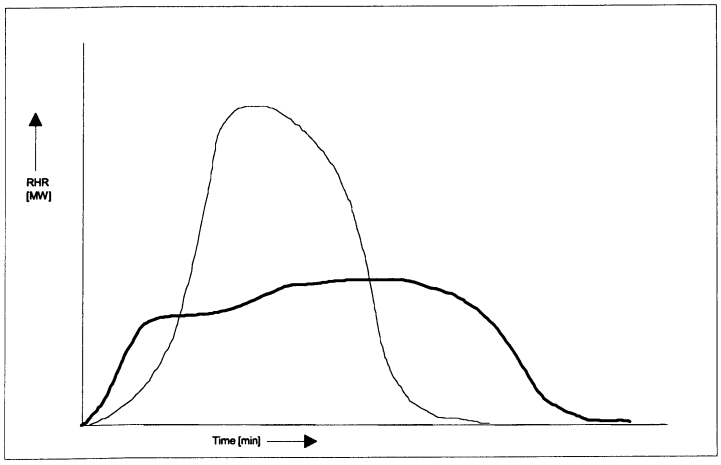

Figure 2.4 *Two RHR curves corresponding to the same amount of fire load, as the surface beneath both curves is the same*

The RHR is the source of the gas temperature rise, and the driving force behind the spreading of gas and smoke. A typical fire starts small and goes through a growth phase. Two things can then happen depending whether during the growth process there is always enough oxygen to sustain combustion. Either, when the fire size reaches the maximum value without limitation of oxygen, the RHR is limited by the available fire load (fuel controlled fire). Or, if the size of openings in the compartment enclosure is too small to allow enough air to enter the compartment, the available oxygen limits the RHR and the fire is said to be ventilation controlled. Both ventilation and fuel-controlled fires can go through flashover (Figure 2.4).

Flashover is an important phenomenon that marks the transition from a localised fire to a fire involving all the exposed combustible surfaces in the compartment. The two regimes are illustrated in Figure 2.5, which presents graphs of the rate of burning vs. the ventilation parameter $A_w \sqrt{h}$, with A_w being the opening area and h being the opening height. Graphs are shown for different fire load densities. Starting on the left side of the figure in the ventilation controlled regime, with increasing ventilation parameter the rate of burning grows up to the limiting value determined by the fire load density and then remains approximately constant (fuel controlled region).

As noticed when analysing more than 80 tests made in laboratory which have been gathered during the previous research[4], the power of the fire starts to decrease when 70% of the fire load has been consumed. The fire load to be considered in the design is the characteristic fire load corresponding to 80% fractile multiplied by a differentiation factor γ_{qf} (see 0). This differentiation factor γ_{qf} has been established using Annex E of EC1-1-2[5] which is the basis of the differentiation factors on static loads and the safety factors on the materials properties.

[Note, EC1-1-2 now uses the symbol δ and not the symbol γ used here.]

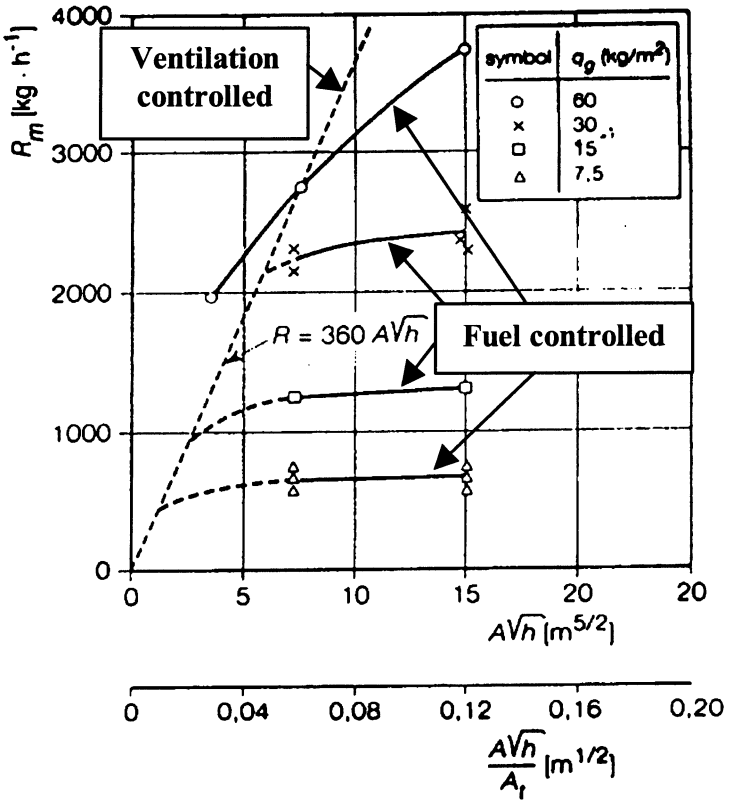

Figure 2.5 *Mass rate for different fire load densities*

Table 2.2 *Fire probabilities depending on occupancy*

Occupancy	Probability	
	Fire Occurrence or Starting Fire p_{fi}^{st} (1/m^2 per year)	Failure of Occupants and Standard Firemen in stopping fire $p_{O\&SFB}^{fail}$ (-)
Industrial building	10 x 10^{-6}	0,05 to 0,1
Office	10 x 10^{-6}	0,02 to 0,04
Dwellings	10 x 10^{-6}	0,0125 to 0,25

This differentiation factor γ_{qf} is based on probability ignition, fire spread and failure of active fire fighting measures (see Table 2.3). These probabilities have been deduced from fire statistics gathered in the department of BERNE in Switzerland (39104 fires from 1986 to 1995), in Finland (2109 fires in 95), in France (82179 in 95) and from existing standards in Germany[6] and in UK[7]. This work has been performed by the Working Group 4 (WG4) under the leadership of Prof. M. Fontana (ETH)[8].

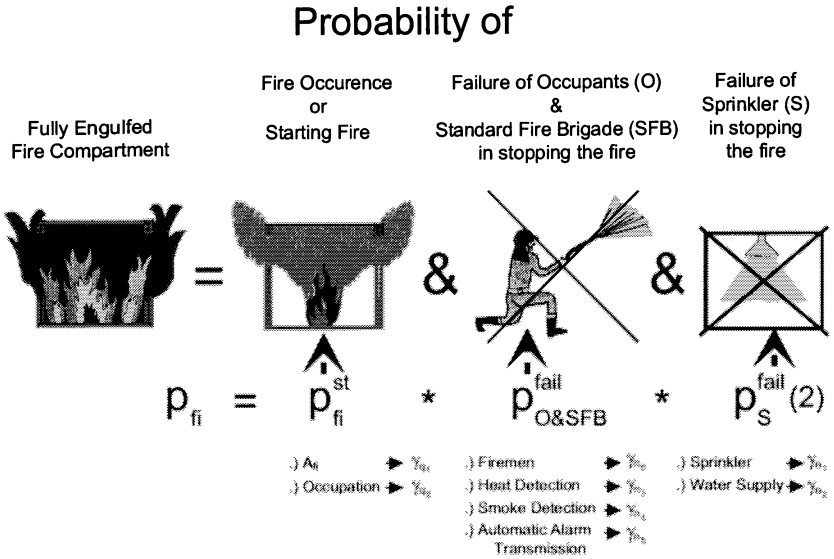

Figure 2.6 *Subcoefficients*

The differentiation factor γ_{qf} has been divided into subcoefficients γ_{q1}, γ_{q2} and γ_{ni} (see Table 2.3) to take into account the compartment size, the building type and the different active fire fighting measures, like sprinklers. In order to perform a calculation, you have to combine the data concerning the fire spread, the maximum rate of heat release per m^2, the characteristic fire load, the compartment size, the building use and the active fire fighting measures. The design fire load can then be calculated.

2.3 Air temperature calculation

A simulation tool to determine the gas temperature has been developed in the scope of previous ECSC research projects [9,10,11] and is called "OZONE". It consists of a two-zone model at the beginning of the fire which may switch to a one-zone model if the 4 conditions described in Figure 2.7 are met.

An example of the use of Ozone is given in Annex A.

Table 2.3 *γ factors*

Compartment floor area $A_f[m^2]$	Danger of Fire Activation γ_{q1}	Danger of Fire Activation γ_{q2}	Examples of Occupancies
25	1,10	0,78	art gallery, museum, swimming pool
250	1,50	1,00	residence, hotel, paper industry
2500	1,90	1,22	manufacturing for machinery & engines
5000	2,00	1,44	chemical laboratory, painting workshop
10000	2,13	1,66	manufacturing of fireworks or paints

γ_{ni} **Function of Active Fire Safety Measures** (factors from NFSC proposal)										$\gamma_n^{min} = \gamma_{n1} \cdots \gamma_{n10}$
Automatic Fire Suppression		**Automatic Fire Detection**			**Manual Fire Suppression**					$\gamma_n^{maxs} = \gamma_{n4} \cdot \gamma_{n7}$
Automatic Water Extinguishing System	Independent Water Supplies	Automatic fire Detection & Alarm		Automatic Alarm Transmission to Fire Brigade	Works Fire Brigade	Offsite Fire Brigade	Safe Access Routes	Fire Fighting Devices	Smoke Exhaust System	
	0 | 1 | 2	by heat	by smoke							
γ_{n1}	γ_{n2}	γ_{n3}	γ_{n4}	γ_{n5}	γ_{n6}	γ_{n7}	γ_{n8}	γ_{n9}	γ_{n10}	
0,61	1,0 | 0,87 | 0,7	0,87 or 0,73		0,87	0,61 or 0,78		0,9 or 1 / 1,5	1,0 / 1,5	1,0 / 1,5	0,15 / 0,57

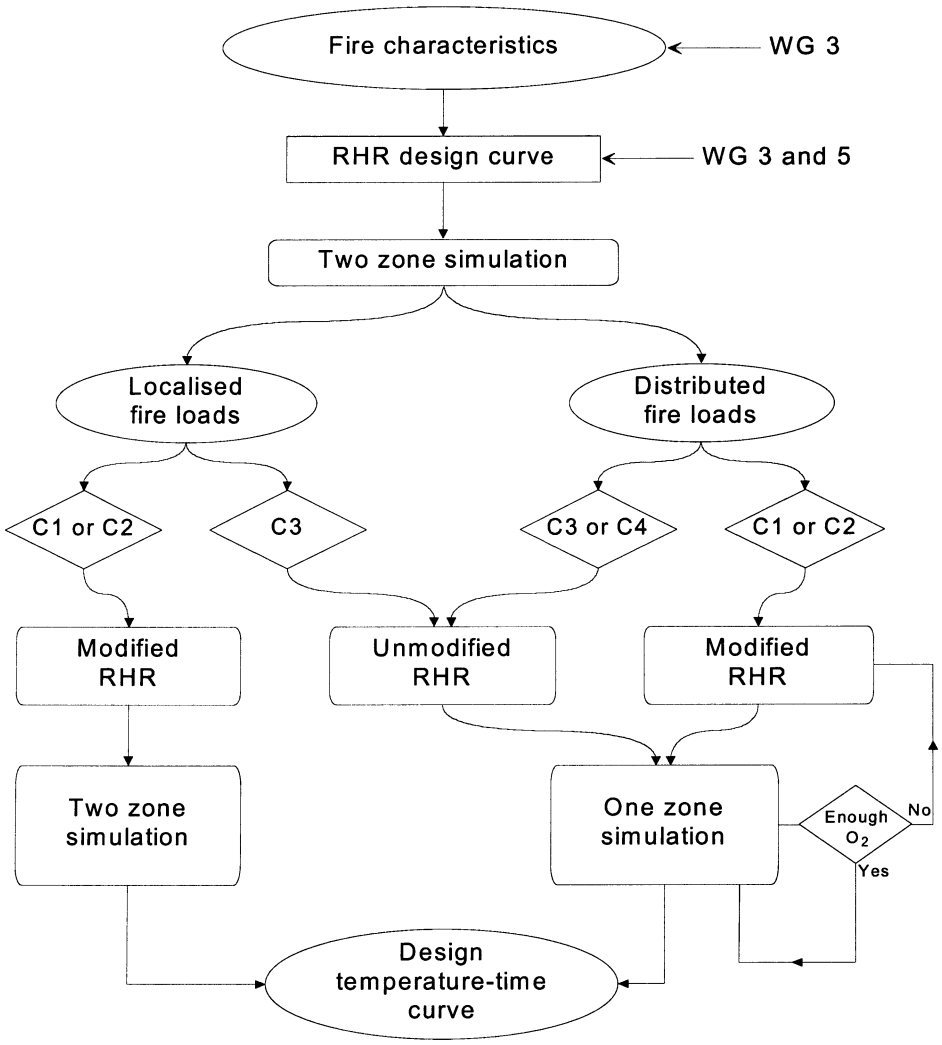

Figure 2.7 *Determination of the design temperature-time curve*

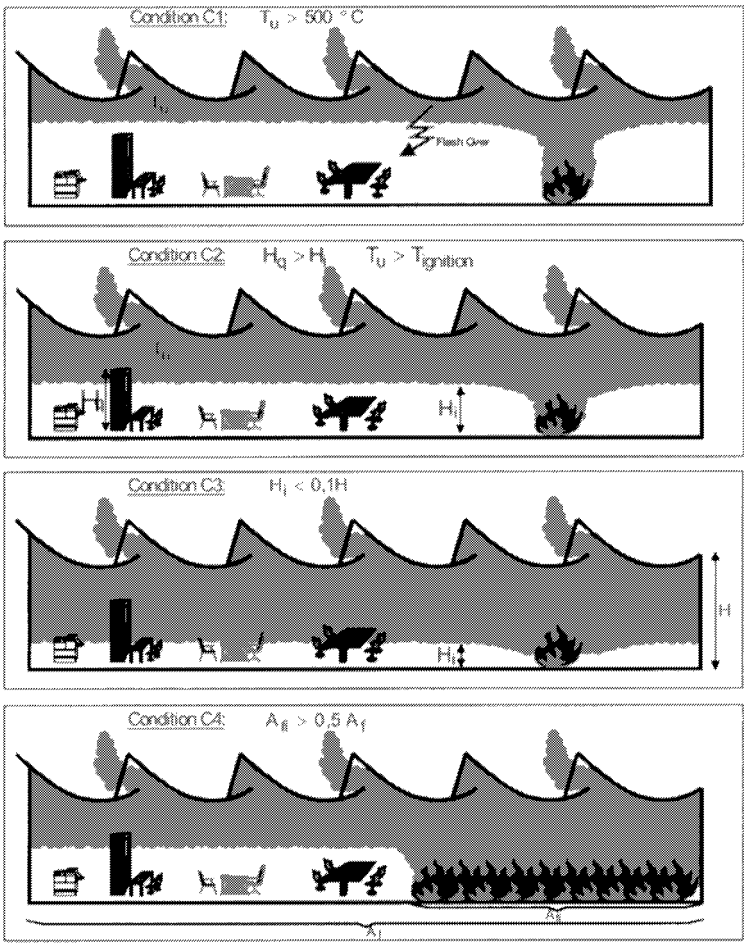

Figure 2.8 *Different stages of a fire*

3 THERMAL RESPONSE MODELLING

3.1 Introduction

In this Chapter, the different steps required to determine the temperature distribution in the cross section are described. First, the air temperature distribution in the compartment is determined by using OZONE or a similar fire modelling program (see Chapter 2). This air temperature field is used as boundary conditions to calculate the heating of the cross section itself. In this project, the program SAFIR was used. The resulting temperature field is then simplified in terms of mean temperatures and gradients in order to be dealt with by the advanced structural simulation models like ANSYS, ABAQUS and DIANA. This simplification is called "linearisation of the temperature distribution".

3.2 Determination of the temperature distribution in the compartment

This calculation has been done using the compartment fire model "OZONE". It is based partially on the natural fire approach NFSC [12, 13, 14].

The active fire fighting measures were not included in the design fire load. The fixed values 200, 300, 400, 500, 600 and 700 MJ/m² have been considered as "a priori" design fire loads.

3.3 Calculation of the temperature field in the section

Two computational models have been used. CEFICOSS is a first generation program which uses the finite difference method and the more advanced SAFIR, a second generation, finite element, program.

The main part of the results has been provided by SAFIR because the complex cross section, including trapezoidal steel sheet, is best modelled using the finite element method.

3.3.1 CEFICOSS

CEFICOSS[15,16,17] stands for Computer Engineering of the Fire resistance of Composite and Steel Structures. This two-dimensional numerical program performs a step-by-step simulation of the behaviour of columns, beams or plane frames submitted to the fire.

The thermal part of the program calculates the temperature distribution in the cross-sections of the structure for different instants. As the sections are discretized by rectangular meshes, it is possible to analyse various shapes of pure steel, reinforced concrete or composite steel-concrete sections. The transient conductive equations are solved by an explicit finite difference scheme, the time step of which being automatically calculated in order to ensure convergence with the shortest computing time. As thermal conductivity and specific heat of the building materials are temperature dependent, this time step varies during the calculation.

The boundary conditions are convection and radiation or symmetry. The outside world is represented by the temperature of the gases with various possibilities: ambient temperature, ISO curve or any other time-temperature curve including a cooling down phase. Evaporation and moisture movement in 'wet' materials is considered.

3.3.2 SAFIR

SAFIR[18]is a special purpose computer program for the analysis of structures under ambient and elevated temperature conditions. The program, which is based on the Finite Element Method, can be used to study the behaviour of one, two and three-dimensional structures.

The thermal analysis is usually performed while the structure is exposed to fire and allows the temperatures in the section to be determined (see Figure 3.1). For a complex structure, the sub-structuring technique is used, where the total structure is divided into several substructures and a temperature calculation is performed successively for each of the substructures. This kind of situation arises in a structure where the members are made of different section types, or made of sections subject to different fire exposures. The thermal analysis is made using 2-D solid elements, to be used later on cross sections of beam elements or on the thickness of shell elements.

a) Temperatures in beams

The temperature is non-uniform in the sections of the beam, but there is no heat transfer along the axis of the beams.

b) Temperatures in shells

The temperature is non uniform on the thickness of the shell, but there is no heat transfer in the plane of the shell. The temperature analysis is performed on a section having the thickness of the shell and a unit width.

In this research, no structural calculation with beam or shell elements has been used. Only the thermal module has been activated and has provided 2D-temperature field in the cross section of the structural elements. For each node, the temperature is calculated (Figure 3.2).

The following parameters where used for the thermal calculation :

Concrete:
- Water content = 40 l/m^3
- Convection coefficient on hot surface = 25 W/m² °C
- Convection coefficient on cold surface = 9 W/m² °C
- Relative emissivity = 0,56

Steel (steel sheet and profile)
- Water content = 0 l/m^3
- Convection coefficient on hot surface = 25 W/m² °C
- Convection coefficient on cold surface = 9 W/m² °C
- Relative emissivity = 0,50
- View factor = 1,0

SAFIR is based on the finite element method. For each node, the temperature is calculated (Figure 3.2). Due to the complexity of the discretized section, it is not possible to introduce into the advanced models, used to predict structural behaviour, the temperature field produced by SAFIR. The structural models can deal only with linear gradient and mean temperature and, for this reason, linear temperature distributions have been used in the structural analysis.

3.4 Linearisation of temperature distribution

The cross sections is divided into 9 "big" elements (2 floor elements, 4 rib elements, 1 sheet element and 2 profile elements, Figure 3.3). The corresponding mean temperature and gradient are deduced from the "real" calculated temperature field provided by SAFIR according to the following steps.

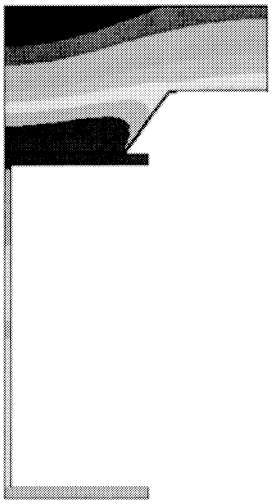

Figure 3.1 *Temperature distribution in a composite beam*

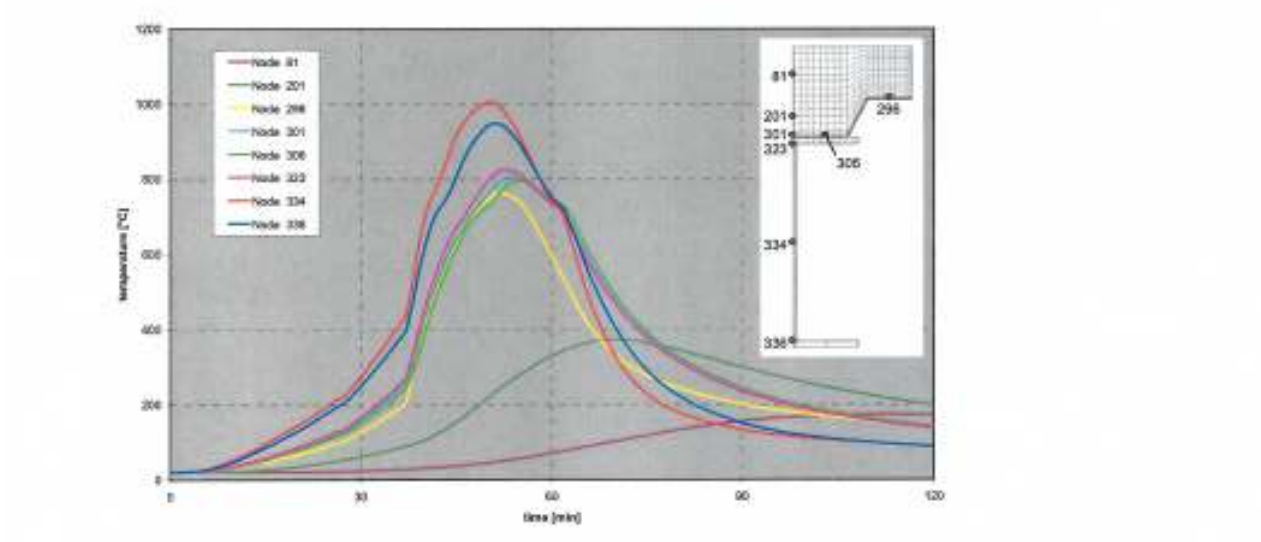

Figure 3.2 *Nodes and elements and temperatures in finite element model*

Mean values and gradients of the temperature in the ribs are defined in Figure 3.4.

Based on the temperature distribution obtained from the SAFIR calculations, the mean temperatures along the four edges of the beam element are determined as follows:

$$MeanTemperature(Edge\,X) = \frac{\sum_{node=2}^{NrNodesX} \frac{T_{node} + T_{node-1}}{2} . (X_{node} - X_{node-1})}{X_{NrNodesX} - X_1}$$

where:

NrNodesX = the total number of nodes in the SAFIR model along edge X

and,

X = distance measured along edge X

From the mean temperature along the edges, the temperature gradients are determined as follows:

$$\textbf{GRAD X} = MeanTemperature(Edge2) - MeanTemperature(Edge4)$$

$$\textbf{GRAD Y} = MeanTemperature(Edge1) - MeanTemperature(Edge3)$$

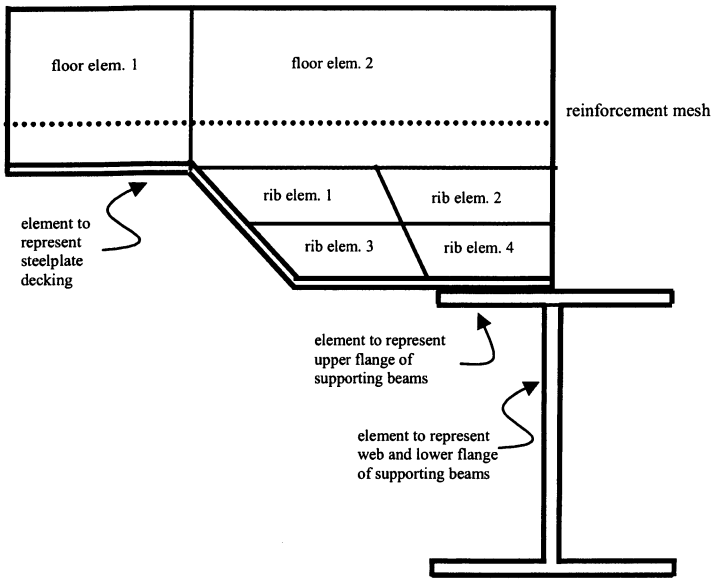

Figure 3.3 *The finite element representation of the floor and supporting beams*

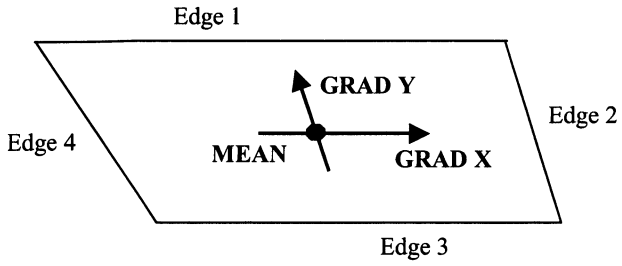

Figure 3.4 *Typical beam element in a rib*

4 FINITE ELEMENT MODELLING OF COMPOSITE STRUCTURES IN FIRE

4.1 Introduction

One possible method of assessing a composite structure's ability to withstand a given fire event is finite element (FE) modelling. This chapter describes the modelling procedures that need to be adopted to adequately represent composite structural behaviour in fire. Firstly, the key structural aspects to be modelled are discussed before the modelling principles adopted to capture these aspects are outlined. The chapter concludes with a discussion of the variables that should be monitored to assess whether a model of a particular compartment has failed under a given fire scenario.

4.2 Key Structural Aspects of Composite Structures

In conventional design, the behaviour of the structural frame under static loading is simplified. At the fire limit state, these simplifications would lead to incorrect predictions of structural behaviour. Therefore, it is important to make the distinction between the actual behaviour and the simplified behaviour as 'actual' behaviour needs to be modelled at the fire limit state.

A typical composite floor layout is given in Figure 4.1 illustrating the assumed main load carrying mechanisms. The key structural points to note are:-

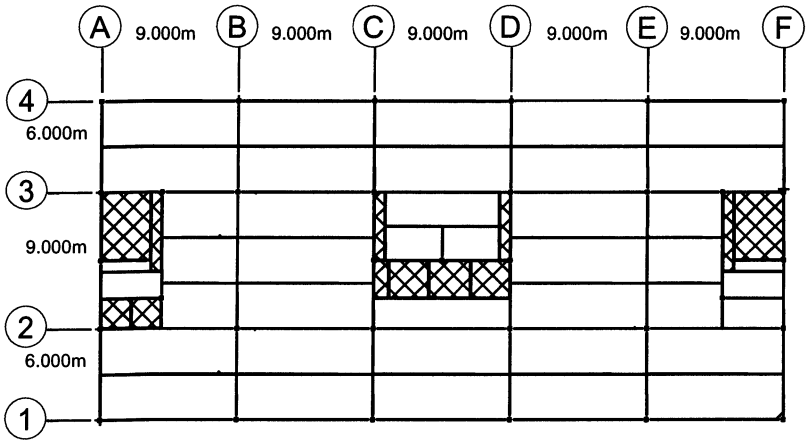

Figure 4.1 *Floor Layout of Typical Composite Structure*

- Braced cores provide lateral stability
- The floor slab carries load to secondary beams.
- Secondary beams span between columns and primary beams
- Primary beams predominantly carry secondary beam concentrated loads to columns.

In conventional design, the key points to note are:-

- The beams are design as isolated members.
- The slab is assumed to carry the floor load as a continuous or simply supported beam spanning between the secondary beams.

- Secondary beams are assumed to be simply supported and to carry half of the slab load either side of the beam.
- Secondary beams are assumed to have an effective width of slab acting compositely with the beam. This is usually the half span of the slab either side of the beam or a quarter of the secondary beam span, whichever is the less.
- The secondary beam loading translates to a concentrated load on the primary beam which is assumed to be simply supported.
- The primary beam has the same structural assumption for the effective width of the slab acting compositely with the beam as the secondary beam.

This means that conventionally the structure is assumed to act as two mutually independent and largely determinate load carrying systems for design purposes. The first is the slab spanning between the secondary beams carrying the load to the secondary beams and the second is the composite secondary beam carrying the slab load back to the columns and composite primary beams. However, in reality these two mechanisms are neither determinate nor independent. To examine this we must look at some key structural details.

4.2.2 Composite Primary and Secondary beams

A typical connection detail at the internal end of a secondary beam spanning between primary beams is illustrated in Figure 4.2. This connection is usually assumed to be a simple connection, i.e. shear transfer takes place but no moment transfer. However, due to acting compositely with the slab, force transfer will take place in tension through the slab and in compression through the beam. The compression force can be generated due to the stiffness of the beam on the other side of the connection. This gives rise to some moment being transferred at the connection, meaning that in reality the connection is really semi-rigid, at least initially. Moreover, and particularly important for behaviour in fire, the end of the beam is heavily restrained against translation.

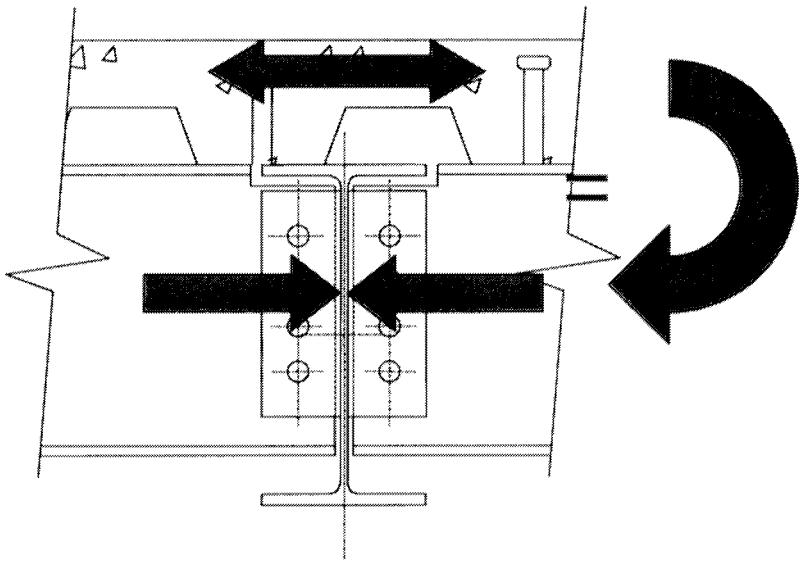

Figure 4.2 *Internal connection detail at the end of secondary beam*

Figure 4.3 shows the connection detail at the external end of a typical secondary beam spanning between the primary beams. Again, this connection is usually assumed to be a simple connection. However, due to composite action with the slab, force transfer will take place in tension through the

slab and compression through the beam. The actual compression force generated will be dependent upon the stiffness of primary beam resisting the compression force. In this case, this stiffness is dependent upon the lateral flexural and torsional stiffness of the primary beam. This gives rise to a limited moment being transferred at the connection dependent on the degree of stiffness, meaning that in reality the connection is really semi-rigid and that the end of the beam will be translationally restrained to some degree.

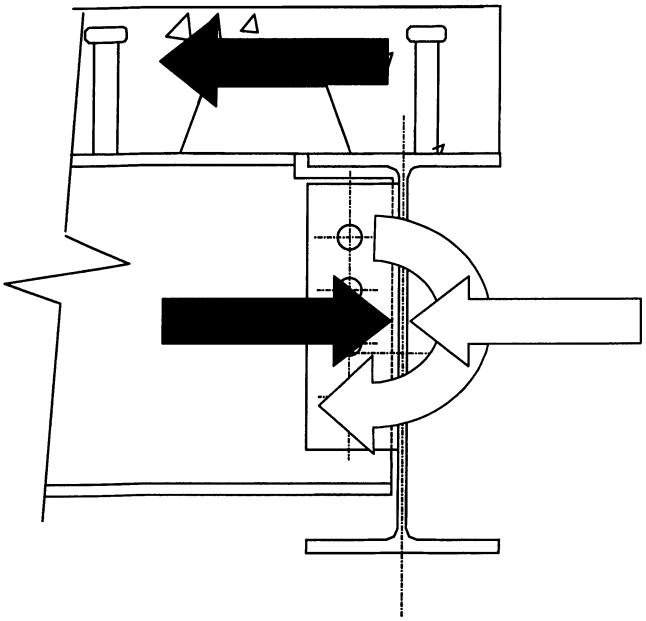

Figure 4.3 *External connection detail at end of secondary beam*

Primary beams usually span between columns. The connections to the columns are usually assumed to be a simple, pinned, connection. Composite action between the slab and beam leads to the same kind of moment resisting behaviour as observed for the previous two cases. This occurs at both the internal and external connections. The actual compression force generated will depend upon the stiffness of the columns and the adjacent composite beam (for internal columns). At external columns, it will depend upon the degree of connectivity of the slab with the column and perpendicular edge beams in the same plane. Clearly these beam-column connections are also semi-rigid. Translationally, the beams are heavily restrained by the columns and adjacent composite beams.

This means that in reality, the amount of load transfer that can take place at composite beam ends under static conditions will be dependent upon the relative stiffness of the support structures and the composite beam. Conventional design assumptions are that these effects are negligible however, under the fire conditions this will not be the case.

4.2.3 Composite slabs

The composite concrete slab can be isotropic or anisotropic due to the presence of the downstands in the spanning direction. Anisotropic slabs are predominantly one way spanning and this behaviour needs to be captured if the correct load transfer mechanisms are to be captured. A cross-section through a typical anisotropic slab at the centreline of the secondary beam is given in Figure 4.4. In terms of the actual behaviour of these slabs, the slabs are vertically supported by the secondary beams. However, the slab is also translationally restrained by the rest of the slab internal to the structure and by edge beams at the edge of the structure. This degree of restraint will be dependent upon the

strength and stiffness of the continuity internally and by the lateral and torsional stiffness and strength of the edge beam. In terms of the slab itself, the flexural and membrane stiffnesses are obviously important parameters which influence the behaviour of the slab.

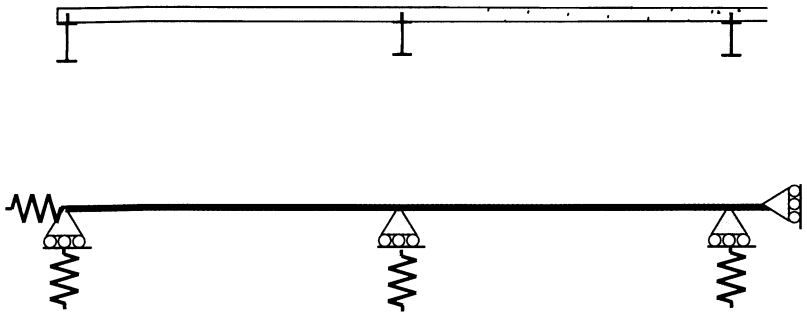

Figure 4.4 *Cross-section through typical composite slab and structural representation*

4.2.4 Whole composite frame behaviour

The above view of actual structural behaviour tries to isolate individual element behaviour. However, the structural elements do not act in isolation. Secondary beams are supported off primary beams and the slab is supported off the secondary beams. By considering the support mechanism, i.e. degree of restraint, to each structural member, the degree of interaction between the various structural members can be contemplated.

Under static conditions, the simplifying assumptions of isolated determinate members leads to safe and conservative structures under both vertical and lateral loading. However, in reality, the structure will have a high degree of redundancy arising from these assumptions.

Under fire conditions, the predominant structural responses arise from thermally induced expansions and curvatures of the main structural elements. This will give rise to complex interacting mechanisms due to the thermal performance of one member affecting the support conditions of other structural members. It is important that these interactions are captured to adequately represent any changing load carrying mechanisms that may arise under a given compartment size and fire loading.

4.3 Modelling Principles

The primary considerations in modelling the behaviour of composite structures in fire are now outlined. Little knowledge of finite element techniques is assumed and the steps taken in building models which represent the key structural behaviour are outlined. Building models that adequately reflect the key structural behaviour is dependent upon making the right choices and assumptions at each level of the analysis.

To ensure a successful analysis, the following basic objectives should be achieved by the analyst:-.

- The identification of the main load carrying mechanisms
- Adequate representation of those load carrying mechanisms
- Correct representation of the stiffness of the structure as well as strength, including temperature dependence
- Accurate representation of the heating induced strains (thermal expansion, thermal curvature, transient thermal creep etc.)

- An assessment of the sensitivity of developed models to key variables
- Qualitative, as well as quantitative, validation against hand calculations of assumed behaviour at the static limit state.

Of these, the most important are stiffness of the structure and its response to heating. If the representation of these parameters in the model is correct then the response of the model to the various applied loads (including fire) will also be correct. This point is important, as most engineers tend to concentrate on strength rather than stiffness due to the discipline of design and the use of codes.

The basic steps in building a finite element model are listed below.

- Meshing of the structure
- Finite element selection
- Material modelling
- Boundary conditions
- Loading (including thermal loads)
- Analysis procedure

The steps will be taken one by one and the most important choices made at each stage illustrated.

4.3.1 Meshing of the structure

Meshing is illustrated by reference to a corner of a composite frame as it includes most of the typical structural details. A plan view of such a typical frame with a schematic representation of the mesh is given in Figure 4.5.

In terms of meshing, the centreline spacing of the normal grid system is usually taken. Column elements are usually represented with line elements. The columns are meshed so that a column node exists at the level of the main structural steelwork (see Figure 4.7). Beams are also usually modelled using line elements. Beams can have separate nodes where they meet columns or be directly connected using pinned connections. Having separate nodes gives flexibility to include spring representations (rotational and translational) for the connections or the ability to include various constraint conditions to connect beams to columns.

After the steelwork has been meshed, a representation of the slab is included. This is best achieved using planar shell elements. The slab mesh density will normally be the same mesh density as the supporting steelwork. To achieve the correct degree of thermal restraint, the slab representation should be at an appropriate level above the supporting steelwork (see Figure 4.7). The slab elements can usually be connected to the beam elements using constraint equations to achieve the desired composite effect. It is usually permissible to assume full composite connection between the beam and slab during fire scenarios.

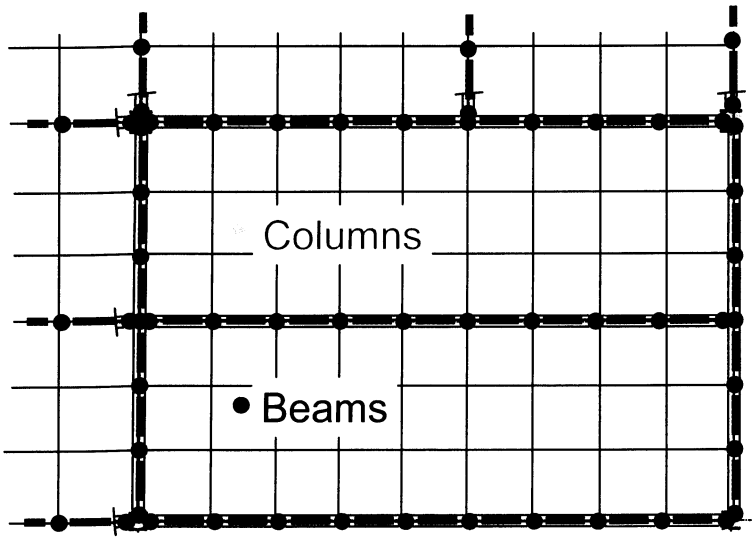

Figure 4.5 *Plan view of corner of typical composite frame showing meshing details*

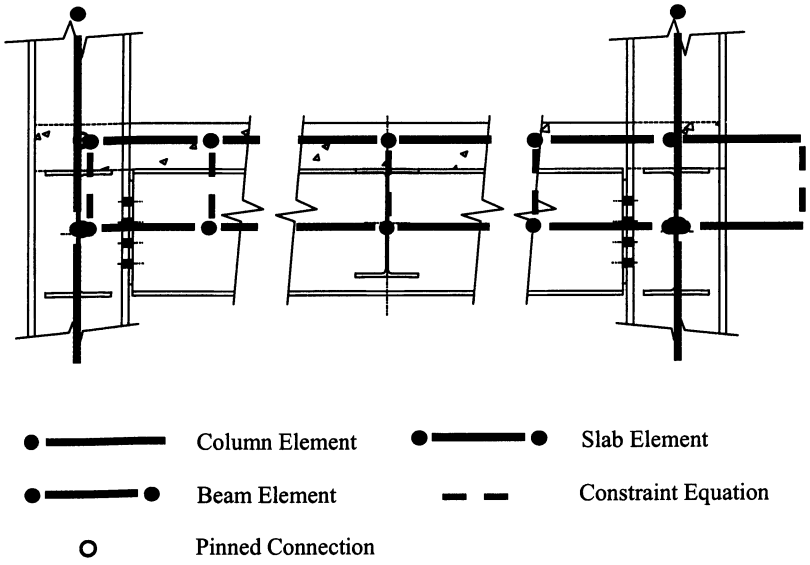

Figure 4.6 *Elevation through typical composite frame showing meshing details*

4.3.2 Finite element selection

The basic finite element sets used to represent the structural members in the composite frame are given below. Solid elements are omitted as they are numerically too expensive for representing large extents of frameworks.

- Shell elements are planar elements which include both membrane and flexural terms. Through thickness properties are included by integrating through several layers. Each layer is assumed to be in a two dimensional plane stress state.
- Beam elements are linear elements which include both axial and flexural terms. Plane sections are assumed to remain plane in bending. Cross-sectional variations are included by integrating at several points across the appropriate cross-section with a one-dimensional stress state assumed at each point.
- Spring elements represent the strength and stiffness between two points which are assumed to be nearly coincident.

Columns and beams can be adequately modelled in fire using non-linear beam elements. Connections between beams and columns can be assumed to be pinned or included using appropriate spring elements. The concrete slab should be modelled using planar, non-linear shell elements. Any anisotropic properties of the slab can be included by representing the downstand (bottom trapezoid) of the slab using beam elements, Figure 4.7. These elements can use the same nodes as the slab or separate nodes that are adequately constrained to the slab shell elements. In either case, the downstand elements should be offset by the correct amount to achieve the correct slab properties.

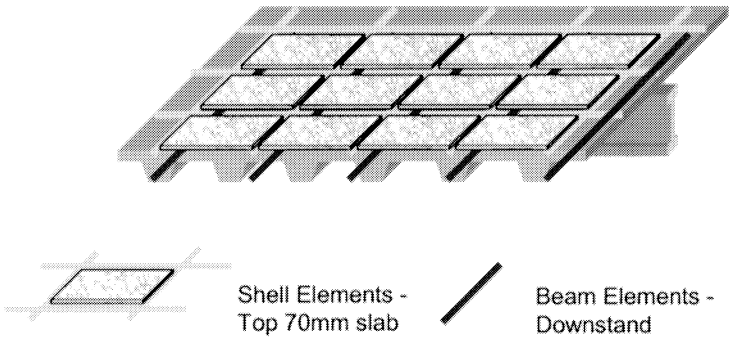

Figure 4.7 *Shell representation of concrete slab including anisotropic properties*

4.3.3 Material Modelling

Steel beams and columns should be modelled using an elasto-plastic material model. A von Mises yield criterion may be used with an associated plastic flow rule. Stress-strain curves and their variation over the full temperature range should be included. The structural modelling and recommendations in this guide are based on the material laws given in EC3-1-2[19] including the enhanced strain hardening effect above 400°C, if desired.

Concrete should be modelled using an appropriate material model to represent concrete's low tensile (cracking) strength. Full degradation of concrete material properties with temperature should be included. Reinforced concrete properties should be included by adequate representation of the steel reinforcement.

The above can be achieved using either a concrete cracking or a Drucker-Prager material model. Reinforcement can be specified in terms of layers or individual bars with an appropriate steel elasto-plastic material model as outlined above within concrete elements. The reinforcement layers are usually assumed to be one-dimensional only acting purely in tension or compression. Some approximations to the transfer of load from cracking concrete to reinforcement can be included within concrete cracking models. The structural modelling and recommendations in this guide are based on the material laws for concrete and reinforcement given in EC4-1-2[20].

4.3.4 Boundary conditions

As the predominant response of the structure arises from restraint to thermal expansion, it is important that close attention is paid to applying the correct boundary conditions in the model. This becomes doubly important when analysing sub-models of a complete frame as placing boundaries too close to a particular compartment can lead to inaccuracies. Boundary conditions can be split into two types, fixity boundary conditions which are applied to assumed structural boundaries (at appropriate locations) and symmetry boundary conditions which are applied where a plane of structural symmetry exists and therefore represent some of the 'stiffness' of the structure beyond the sub-model boundary.

It is usually assumed that a compartment is confined to one floor. The main fixity boundary conditions assumed, therefore, are usually that the bases of the columns in the floor structure are fully restrained in all directions and that the tops of the columns are translationally restrained in the horizontal directions. These boundary conditions simulate the continuity of the columns at the base of the structure and the fact that the floors on top of the floor modelled provide lateral restraint to the top of the columns as well as loading the columns from floors above the fire compartment floor.

A typical symmetry boundary condition for a half floor model is illustrated in Figure 4.8. The symmetry boundary in this case is lateral restraint in the longitudinal direction and rotational restraint about the other two lateral directions. Care does need to be exercised in the application of symmetry boundary conditions particularly when the fire compartment is close to the model boundary. In these cases two fire tests on either side of the symmetry boundary will be simulated with the consequent effect on the degree of restraint provided to the compartment of interest. When this occurs, supermodels of the other half of the floor ,i.e. representing the 'stiffness' of the other half of the floor but not the loading applied to it, should be used.

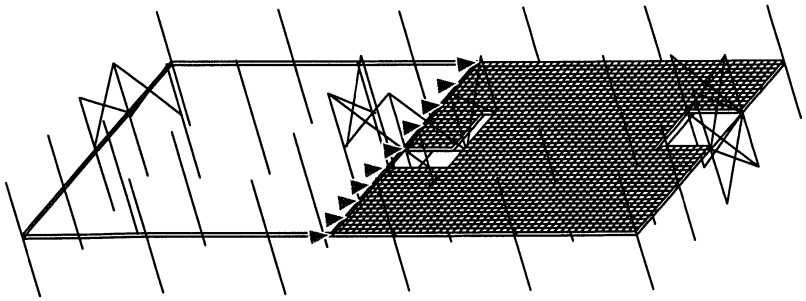

Figure 4.8 *Symmetry boundary condition applied to typical composite frame*

4.3.5 Loading

The main loads to be applied to the structure are the static loads at the fire limit state and the changing temperatures of the main structural elements. The static loads applied should conform with the recommendations of the appropriate design code. Loads from floors above the fire compartment can be applied at the top of the appropriate column element. Temperature variations of the main structural members with time can be taken from any approved method of determining such temperatures (Refer to Chapter 3). Temperature gradients through the main structural members should also be included. The sensitivity to possible variations in temperatures applied to the main structural members should be investigated.

4.3.6 Analysis

Various analytical techniques can be used within FE packages to obtain solutions to a variety of structural problems. Most of these techniques have been derived to deal with buckling type problems

where sudden bifurcations in structural behaviour lead to unloading of key structural members. However, all these techniques assume that the program has control of the loading so that unloading can take place on reaching bifurcation. In this case, though, the loading - the temperature applied to the structure - is imposed on the structure and cannot be unloaded, therefore such techniques, e.g. arc length method, cannot be used. This is unfortunate because in this case the restraint to thermal expansion gives rise to quite complex bifurcation type problems in both the slab and beam elements. The only technique the analysis package has is to cut back the solution increment size leading to quite lengthy solution times.

The most important part of any analytical technique is geometric nonlinearity. High axial forces due to restraint to thermal expansion coupled with the large deflections due to large thermal strains mean that geometric nonlinearity and P-delta effects are extremely important. Any package that does not take this into account will not be able to represent the desired structural behaviour.

4.4 Assessment of failure

In interpreting the results of FE analysis, care should be taken to ensure that none of the limits of applicability of the elements are breached as defined in the relevant user manual for the FE package considered. Additionally, a number of practical limitations in terms of the assumptions made within the representation of the key structural behaviour should also be adhered to. For example, the concrete modelling adopts a smeared crack approach and therefore plastic tensile straining within the mesh reinforcement should be restricted to a low elongation value.

Generally, the structure can be considered to be safe under the applied fire scenario, if:

- The maximum deflections are within the range of deflections that would arise from the induced thermal strains and compatibility
- The tensile plastic strains (mechanical strains, after excluding the elastic and thermal strains) in the concrete slab reinforcement, in the supports and midspan region, do not exceed 5%.
- The deflections of beams at the compartment boundaries do not exceed a value that may cause partition failure and consequent breach of compartmentation.

Within this project, for the first criterion, a structure is assumed to have failed if the maximum displacement of a floor beam, relative to its end supports, exceeds the beam span/20. This is the same as in standard fire resistance testing and is a measure which would be familiar to checking authorities. This further discussed in Annex B.

5 GENERAL RECOMMENDATIONS

In Chapters 6 8 and 9, the conditions are described when it is considered safe to omit the fire protection from certain beams. However, there are other building parameters which must be taken into account to ensure satisfactory performance in fire. These include overall building stability, maintenance of compartmentation, design of edge beams, fire protection of connections and correct installation of reinforcing mesh. Where reliance has been placed on active measures such as sprinklers (see Chapter 2), these should be properly installed to the appropriate national standards.

5.1 Overall building stability

In order to avoid sway collapse, the building should be braced by shear walls or bracing systems. Masonry or reinforced concrete shear walls should be constructed with the appropriate fire resistance.

Bracing plays a major part in maintaining the overall stability of the building and should be protected to the appropriate standard.

In two-storey buildings, it may be possible to ensure overall stability without requiring fire resistance for all parts of the bracing system. In taller buildings, all parts of the bracing system should have the appropriate fire resistance.

One way in which fire resistance can be achieved without applied protection is to locate the bracing system in a protected shaft such as a stairwell, lift shaft or service core. It is important that the walls enclosing such shafts have adequate fire resistance to prevent the spread of any fire. Steel beams, columns and bracing totally contained within the shaft may be unprotected. Other steelwork supporting the walls of such shafts should have the appropriate fire resistance.

5.2 Compartmentation

Building Regulations require that compartment walls separating one fire compartment from another shall have stability(R), integrity(E) and insulation(I) for the required fire resistance period.

Stability is the ability of a wall not to collapse. For loadbearing walls, the loadbearing capacity must be maintained.

Integrity is the ability to resist the penetration of flames and hot gases.

Insulation is ability to resist excessive transfer of heat from the side exposed to fire to the unexposed side.

5.2.1 Stability

Walls that divide a floor into more than one fire compartment must be designed to accommodate expected structural movements without collapse (*stability*). For walls which are directly below and in line with beams, even the deformation of unprotected beams may be small and the normal allowance for deflection should be adequate. In other cases, the deflection of the structure in fire may be large and, for this reason, fire compartment walls should ideally be positioned directly below and in line with beams possible.

For walls which are not directly below and in line with beams a deflection allowance must be considered. This may take the form of a sliding joint. In other cases, the potential deflection may be large and some form of deformable blanket or curtain may be required, as illustrated in Figure 5.1.

Most building regulations require compartment walls to be full height so any device used to accommodate deformation should have the required integrity and insulation.

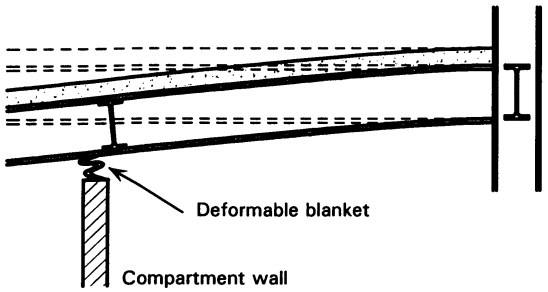

Figure 5.1 *Deformation of beams crossing wall*

5.2.2 Insulation and Integrity

Steel beams above fire compartment walls are part of the wall and are required to have the same separating characteristics as the wall. The combined wall/beam separating element must have adequate insulation and integrity as well as stability.

The temperature of the unexposed face of unprotected beam heated on one side will rise rapidly and will quickly be considered to have failed *insulation.* It is therefore recommended that all beams at compartment boundaries should be fire protected, as shown in Figure 5.2. In this regard, beams protected with intumescent coatings require additional, non-intumescent, insulation because the temperature on the non-fire side is likely to exceed the limits required in the fire resistance testing standards before the intumescent process starts.

A steel beam without penetrations will have *integrity.* However, any service penetrations must be properly fire stopped and all voids above composite beams should also be fire stopped.

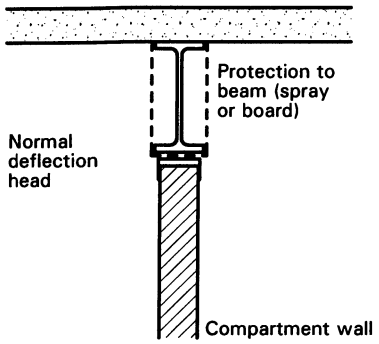

Figure 5.2 *Beams above fire resistant walls*

The Cardington tests demonstrated that unprotected beams above and in the same plane as separating walls, which are heated from one side only, do not deflect to a degree that would compromise compartment integrity, and normal movement allowances are sufficient.

5.3 Reinforcing Mesh

To ensure membrane action in the slab, care must be taken to ensure that the reinforcing mesh is properly lapped. This is especially important in the region of unprotected beams and around columns. Ideally, mesh should be specified with the perimeter wires omitted to allow longitudinal wires to correctly lap with adjacent meshes to eliminate build up at laps

The mesh reinforcement should conform to the ductility limits of ENV 10080 for type B reinforcement. These limits are consistent with 12% elongation at failure.

5.4 Connections

In cases where both structural elements to be connected are fire protected, the protection appropriate to each element should be applied to the parts of the plates or angles in contact with that element. If only one element requires fire protection, the plates (or angles) in contact with the other unprotected elements may be left unprotected.

5.5 Edge Beams

It is common practice for beams at the edge of floor slabs to be designed as non-composite. This is because the costs of meeting the requirements for transverse shear reinforcement are more than the costs of installing a slightly heavier non-composite beam. However, for fire design, it is important that the floor slab is adequately anchored to the edge beams. For this purpose, if edge beams are designed as non-composite they must have shear connectors at not more than 300 mm centres and the reinforcing mesh must be hooked over the shear connectors.

Edge beams serve the dual function of supporting both the floors and the cladding. It is important that the deformation of edge beams should not affect the stability of cladding as it might increase the danger to fire fighters and others in the vicinity. (This does not refer to the hazard from falling glass that results from thermal shock, which can only be addressed by use of special materials or sprinklers.) Excessive deformation of the façade could increase the hazard, particularly when a building is tall and clad in masonry, by enabling bricks to be dislodged. As an alternative to fire protection, vertical ties or wind posts in the façade above the fire compartment may be used to provide support and limit deformation.

The Cardington tests showed consistently that edge beams above windows were not heated to the same extent as internal beams. Typically, the temperature rise of the edge beam was 25% lower than the highest internal beam temperature rise. In view of this, it is conservatively recommended that, if protection to edge beams is required, the fire protection to edge beams, can be assessed for a limiting temperature 50°C above that which would normally be used. For example, if, based on the applied load, the limiting temperature of a beam was 600°C, the protection thickness could be based on 650°C. Depending on the method of protection, this may lead to a reduced thickness of fire protection.

5.6 Columns

Columns should be able to withstand a burnout of the contents of any compartment. This may be ensured by a number of means

- The column may be designed to have fire resistance as required by national building regulations for the size and use of the building. This may result in the application of applied fire protection or the column may be designed compositely so that it can achieve the required fire resistance without applied protection.

  or,

- The column may be designed using advanced methods to withstand a natural fire. This may also result in fire protection being applied or in some form of composite design.

6 DESIGN PROCEDURE FOR STRUCTURAL FIRE SAFETY

The Cardington pilot project[1,2] has shown that it is not always necessary to apply passive fire protection on composite steel framed buildings. The design procedure developed in this Design Guide aims at a systematic identification of the conditions under which such a solution is acceptable from a fire safety point of view. However, a review of the costs implications is outside the scope of this study. The starting point of the procedure is the room temperature design. More in particular, attention will be paid to the challenges (and limitations) for the structural fire safety engineer, resulting from room temperature design considerations. See Figure 6.1.

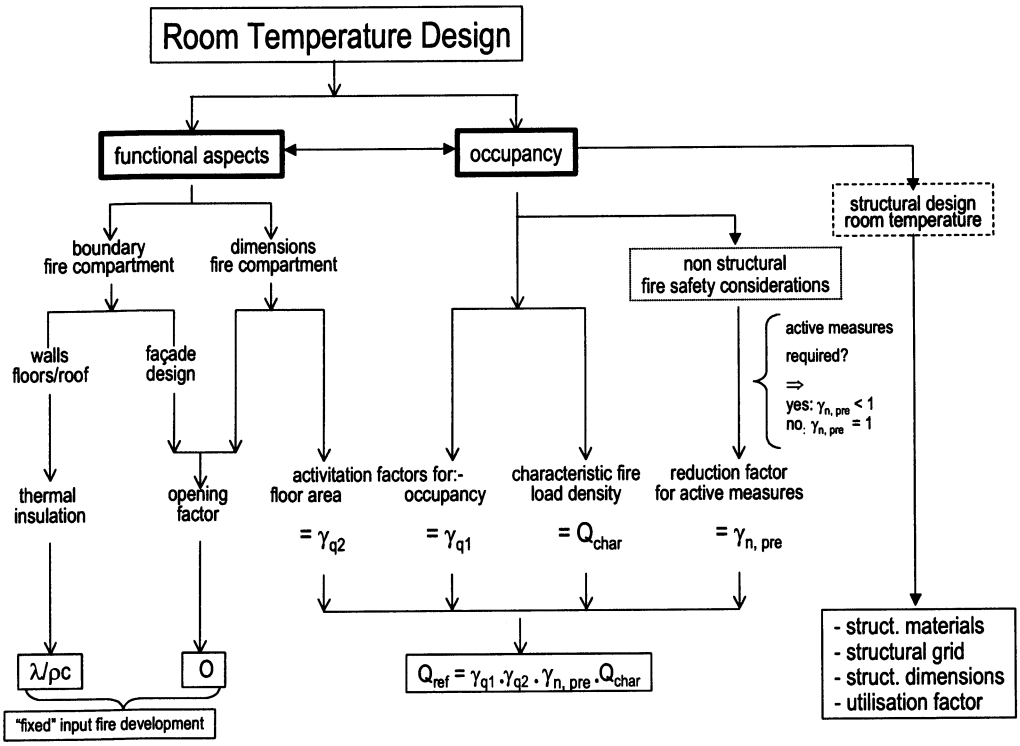

Figure 6.1 *Basic requirements for the Structural Fire Safety Design.*

The main aspects governing building design are occupancy and functionality of the space created. Both aspects, which are obviously closely related, are defined by the owner/user/architect in an early stage of the design and imply a series of basic requirements for the structural fire design which are more or less "fixed".

The following parameters tend to be fixed by these design decisions and are therefore outside the control of the fire safety engineer.

- dimensions of the fire compartment;
- boundaries of the fire compartment;

- fire load density

Normally, a fire compartment is confined to one storey only: the floors above and below form the horizontal boundaries. The vertical boundaries are formed by the facades and by (internal) walls. The compartment boundaries shall be such that a fire in the compartment will not spread to other parts of the building. This means that floors and walls (including doors, penetrations, joints etc.) should have sufficient resistance to fire and should be designed and executed accordingly. As a result, fire walls can not be moved easily after completion of the building. Hence fire compartmentation interferes with the need of a flexible building design, which is of particular interest in modern buildings such as offices, schools, hospitals etc. From a functional point of view, fire compartments should, therefore, be taken as large as possible. On the other hand, the size of fire should be limited. In order to control the spread of fires. National fire regulations normally set upper limits to the maximum floor area of fire compartments, e.g. 1000 m^2. For fire compartments which do not comply with such conditions, additional (compensating) requirements are often necessary, e.g. the use of sprinklers.

For facades, the requirement is that a fire should not spread to fire compartments above or to the side, leading to minimum requirements with regard the fire performance of parapets and piers (including joints) and the minimum height or width thereof. Note, in this respect that the facade design is a key element in the architectural concept and is mainly determined on the basis functionality under normal conditions of use (aesthetics, labour conditions, costs). In here, structural fire safety plays only a minor role, if any role at all.

Nevertheless, the choice of the construction elements bounding the fire compartment and the dimensions of the fire compartment have a significant impact on the development of the gas temperatures during a fire. This especially holds for the facade design since, not only the (radiative) heat losses, but also the ventilation conditions during a compartment fire, depend largely on the window openings, since glass will break under fire conditions. The window openings, in combination with the dimensions of the fire compartment, define the so-called opening factor. This factor is a practical parameter to describe the above effects of the facade design in a simple manner and is used as an input parameter in fire development calculations. See also Chapter 2.

The construction of the walls and floors bounding the fire compartment has a significant influence on the gas temperature development during fire, because of the effect of conductive heat losses from the fire compartment. Relevant properties are the thermal conductivity (λ) and the heat capacity (c) in combination with the density (ρ) of the applied materials as well as the dimensions of the elements. As for the facade, also for floors and walls, room temperature design considerations are normally indicative.

In conclusion, the functional requirements of a building design have, because of the size of the fire compartment and its boundary constructions, an important impact on the development of the gas temperature during a compartment fire. However, the extent to which the structural fire safety engineer can influence these design decisions is only marginal. The challenge is therefore to provide adequate solutions, taking the above parameters as primary input data.

A very important factor for the gas temperature development during a compartment fire is the fire load density. This quantity is basically determined by the anticipated occupancy and is ideally based on statistical information (e.g.: characteristic value based on a 80 % fractile). For some suggestions regarding characteristic values of the fire load density, refer to Table 6.1. Note that the values given are indicative only and may need to be adapted on the basis of national or local statistical information.

Table 6.1 *Characteristic values for the fire load density*

Occupancy / Activity	Fire Load q_f,k80% fractile [MJ/m²]
Dwelling	948
Hospital (room)	280
Hotel (room)	377
Library	1.824
Office	511
School	347
Shopping Centre	730
Theatre (movie/cinema)	365
Transport (public space)	122

However, design values of the fire load density can be influenced by adaptation factors applied to the characteristic value of the fire load density. (See 0). There are two main considerations to introduce such adaptation factors:

(a) level of activation risk

The level of activation risk is determined by the occupancy (dangerous vs. less dangerous activities) and the floor area of the fire compartment (the larger the floor area, the higher the activation risk). Adopting the notation used in 0, the corresponding adaptation factors are denoted as $\gamma_{q,1}$ and $\gamma_{q,2}$ respectively.

(b) level of active fire safety measures

The level of active measures is determined by the (combination) of various active measures applied (automatic fire suppression, detection, etc.) and additional provisions (type of water supply, signal transmission to fire brigade, etc.). Again, adopting similar notation, the corresponding adaptation factors are denoted as $\gamma_{n,i}$.

For convenience 0 is reproduced here as Table 6.2.

Table 6.2 *γ factors*

Compartment floor area $A_f[m^2]$	Danger of Fire Activation γ_{q1}	Danger of Fire Activation γ_{q2}	Examples of Occupancies
25	1,10	0,78	art gallery, museum, swimming pool
250	1,50	1,00	residence, hotel, paper industry
2500	1,90	1,22	manufacturing for machinery & engines
5000	2,00	1,44	chemical laboratory, painting workshop
10000	2,13	1,66	manufacturing of fireworks or paints

γ_{ni} Function of Active Fire Safety Measures (factors from NFSC proposal)										$\gamma_n^{min} = \gamma_{n1} \cdot \ldots \cdot \gamma_{n10}$
Automatic Fire Suppression		**Automatic Fire Detection**			**Manual Fire Suppression**					
Automatic Water Extinguishing System	Independent Water Supplies	Automatic fire Detection & Alarm		Automatic Alarm Transmission to Fire Brigade	Works Fire Brigade	Offsite Fire Brigade	Safe Access Routes	Fire Fighting Devices	Smoke Exhaust System	$\gamma_n^{maxs} = \gamma_{n4} \cdot \gamma_{n7}$
	0 | 1 | 2	by heat	by smoke							
γ_{n1}	γ_{n2}	γ_{n3}	γ_{n4}	γ_{n5}	γ_{n6}	γ_{n7}	γ_{n8}	γ_{n9}	γ_{n10}	
0,61	1,0 | 0,87 | 0,7	0,87 or 0,73		0,87	0,61 or 0,78		0,9 or 1 / 1,5	1,0 / 1,5	1,0 / 1,5	0,15 / 0,57

Note:

For normal fire fighting measures, which should be almost always present, such as the Safe Access Routes, the Fire Fighting Devices and the Smoke Exhaust System in staircases, the corresponding factor should be taken as 1,5 in case those measures are either unsatisfactory or do not exist.

It can be shown that the combined effect of the activation risk and the active fire safety measures can be accounted for by simply multiplying the various (partial) adaptation factors. Hence:

$$Q_{design} = \gamma_{q,1} \cdot \gamma_{q,2} \cdot \gamma_{n,1} \cdot \gamma_{n,2} \cdot \ldots \cdot \gamma_{n,i} \cdot Q_{char}$$

Just like the opening factor (See Chapter 2) and the thermal resistance of the construction elements bounding the fire compartment ($\lambda/\rho c$), the adaptation factors $\gamma_{q,1}$ and $\gamma_{q,2}$ follow directly from room temperature design considerations and can only marginally be influenced by the structural fire safety engineer.

In the national regulations in Europe, the emphasis is on passive fire protection. This does not mean that, under all circumstances, no active measures will be required, for example with a view to compensate for (too) large fire compartments. If active fire protection is required on basis of non structural fire safety considerations, the corresponding adaptation factor is denoted as $\gamma_{n,pre}$. Hence the

maximum design value of the fire load density to be taken into account for the structural fire design (notation: Q_{ref}) follows from:

$$\gamma_{q,1} \cdot \gamma_{q,2} \cdot \gamma_{n,pre} \cdot Q_{char} \quad (= Q_{ref})$$

where

Q_{char}	follows from the anticipated occupancy of the building;
$\gamma_{q,1} \cdot \gamma_{q,2}$	follow from the basic design assumptions with respect to fire compartmentation and occupancy respectively
$\gamma_{n,pre}$	follows from the active measures, required on basis of non-structural fire safety considerations.

If no active fire safety measures are foreseen at this stage of the design, obviously $\gamma_{n,pre} = 1$.

Finally, there is a number of design parameters, normally also determined in scope the structural design under normal conditions of use, which have an impact on the thermal and/or the structural response of the building. The following are mentioned:

- *Overall-floor height:* normally fixed in the room temperature design
- *Mechanical loading.* This may not normally not be changed, because it is directly related to the anticipated occupancy; however varying the load bearing structure (e.g. by modifying beam sizes or slab depth), will influence the utilization factor of the load bearing structure and thus the structural performance under fire conditions. Such changes in the load bearing elements can be interpreted as changes in mechanical loading;

  Note:

  If the failure mechanism under normal conditions is different from the one under fire conditions (e.g. in case of transfer from bending to membrane action) the utilization factor (defined as the ratio between the relevant mechanical loading and the load bearing capacity under fire conditions) can not be interpreted directly in terms of structural performance.
- *Reinforcing mesh size:* may be changed without important functional consequences
- *Column positions:* may sometimes be changed, leading to an alternative structural grid
- *Beam sizes:* may be changed in some locations (necessary if the structural gird is changed)
- *Steel grade/concrete strength:* may be changed without important functional consequences; such changes may be interpreted as changes in the mechanical loading.
- *Type of concrete (normal weight vs. lightweight):* change from room temperature assumptions only in exceptional cases; such changes have an impact both in terms of thermal and mechanical response.

It is the challenge of the structural fire safety engineer to quantify the effect of the various design parameters and to present a solution within the margins provided by occupancy and functionality requirements, taking due account of the normal conditions of use. After a review of these basic requirements, the design procedure consists of two main steps:

- performance of a "pre design" on structural fire, leading to a global identification of the conditions under which the floors and beams may remain unprotected;
- performance of a "detailed design" on structural fire safety, leading to a final identification of the conditions under which the floors and beams may remain unprotected.

The main feature of the "pre design" is that this should be possible with very limited efforts, provided adequate tools are available. These tools refer basically to a computer program by which, using

minimum effort, the development of a compartment fire and the primary thermal response of structural steel can be quantified.

In the "detailed design", the mechanical failure conditions postulated in the "pre design" shall be verified. For an in-depth analysis of this nature, an adequate insight in the temperature distribution in the various structural elements (beams and slabs) and the structural response are required. With the present state of knowledge and computer programs, an in-depth analysis of the thermal response is a matter of routine and does not hinder an efficient design procedure. However, a detailed analysis of the structural performance of composite steel framed building systems under fire conditions is still very elaborate (calculation time: 24 hours or more), when use is made of advanced FE modelling. Therefore, in this Design Guide, the following options for a mechanical analysis are offered (order of hierarchy):

- Advanced FE model (highest level);
- BRE slab method;
- EC4-1.2 method (lowest level).

The lower the hierarchy, the less elaborate (but also: the more conservative) the assessment method is. This is schematically indicated in Figure 6.2.

The above methods are described in detail in chapters 7, 8 and 9 of this Design Guide.

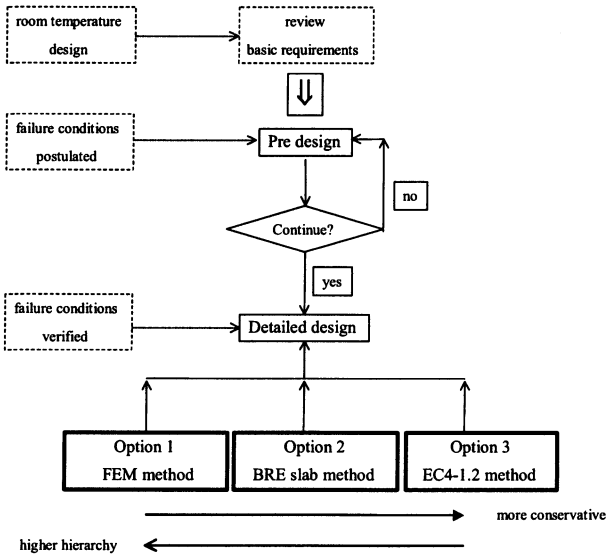

Figure 6.2 *Design procedure*

7 DESIGN PROCEDURE & RECOMMENDATIONS BASED ON THE ADVANCED FEM METHOD

7.1 Pre-design

The starting point of the pre-design is that the floors and beams of the building are unprotected and that all general recommendations given in chapter 5 are fulfilled. For a schematic review of the proposed "pre design" procedure, refer to Figure 7.1.

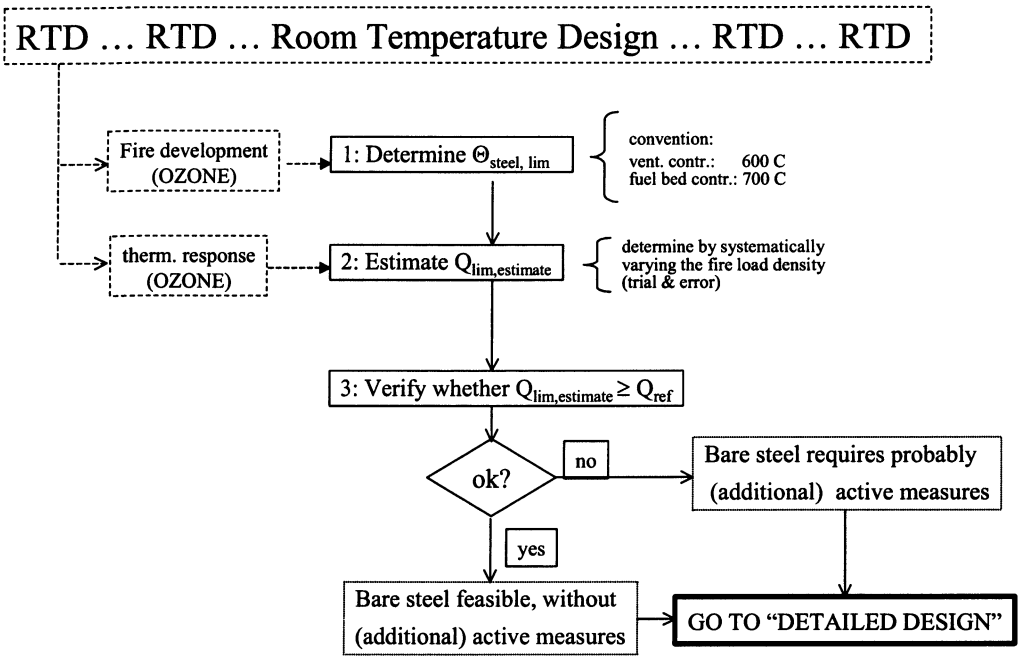

Figure 7.1 *Structural Fire Safety: "Pre-design"*

In the "pre design" it is assumed that the failure conditions of a floor in a composite steel framed building in fire can be expressed in terms of a maximum steel temperature attained in the lower flange of the primary steel beam. This temperature is called: "limiting temperature" (notation: $\theta_{steel,\,lim}$).

The maximum temperature attained by (unprotected) structural steel under fully developed fire conditions follows closely the gas temperature and depends, therefore, mainly on:

- fire load density;
- opening factor;
- thermal resistance of the boundary construction of the fire compartment.

As explained in the previous chapter, the last two parameters should be considered as more or less fixed by the room temperature design (basic requirements). It is therefore at hand to use the fire load density as the design parameter, at least in this stage of the structural fire safety design.

For a certain fire compartment configuration, the effect of the fire load density on the maximum steel temperature is presented in Figure 7.2 for a practical range of opening factors.

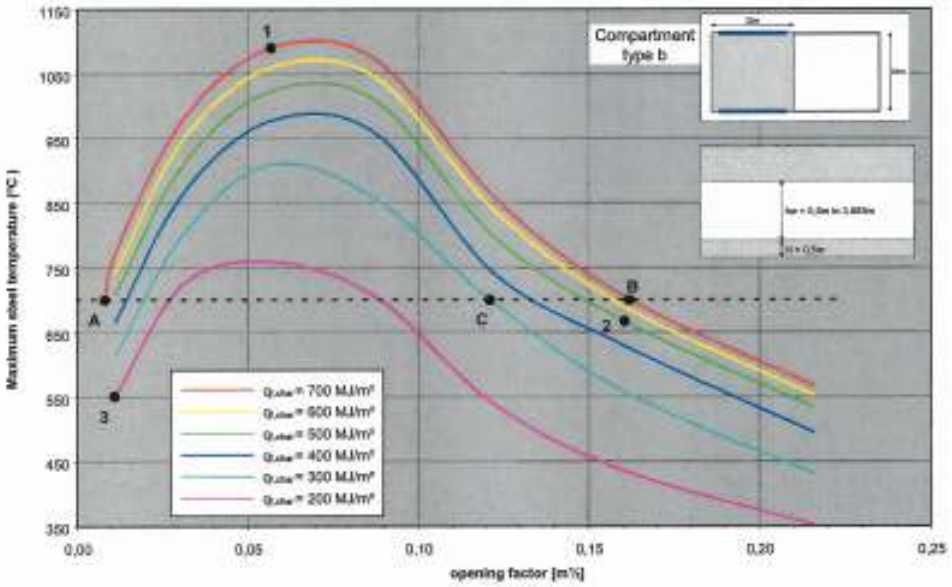

Figure 7.2 *Maximum steel temperatures in the lower flange of primary steel beams for different values of the fire load density and a practical range of opening factors*

The fire load density for which the maximum steel temperature equals $\theta_{steel,lim}$ is an estimate for fire load density at which failure of the floor is about to occur. This value is called the "limiting" value of the fire load density (notation: $Q_{lim,estimate}$). Within the scope of the assumption made, one would expect structural failure for fire load densities higher than $Q_{lim,estimate}$.

The next and final step in the pre-design procedure is to check whether the failure condition (now expressed in terms of fire load densities) is met. This condition reads:

$$Q_{lim,estimate} \geq Q_{ref}$$

where:

$Q_{lim,estimate}$	is the above defined limiting value of the fire load density;
Q_{ref}	is the maximum value of the fire load density on basis of the basic requirements (see chapter 6).

From tentative calculations, carried out within this project, one may conclude that under fuel bed controlled fire conditions (i.e. large window openings (opening factors) and hence a relative short fire) 700 ° C is a fair estimate for $\theta_{steel,\ lim}$. For ventilation controlled fires (i.e. small opening factors and hence a relative long fire duration) significantly lower values for $\theta_{steel,\ lim}$ hold. The reason is that a long fire duration will result in more "thorough" heating of the floor construction and hence in lesser structural performance then a short fire, also if the longer fire will lead to similar maximum steel temperatures in the primary beam as the shorter one. The suggested value for the limiting steel temperature for fires in the ventilation controlled regime is 600 °C. For a graphical presentation of the above conventions, refer to Figure 7.3.

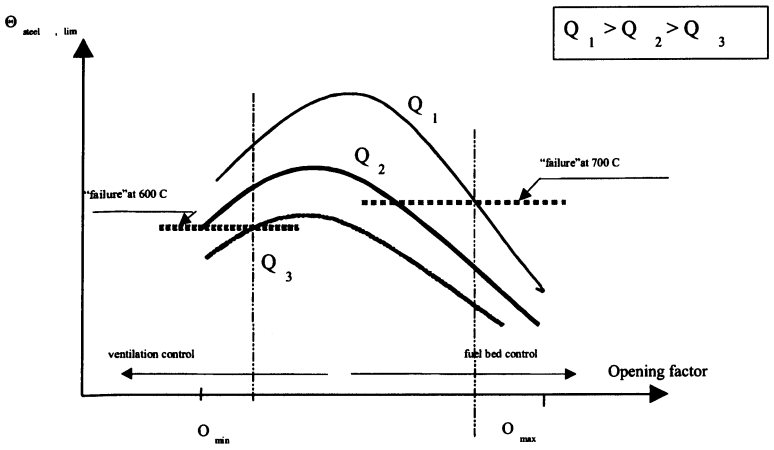

Figure 7.3 *Conventions for the "pre-design"*

A first point to clarify when performing the pre-design, is whether the fire is ventilation or fuel bed controlled. This feature follows from the analysis of the fire development, more in particular from the factors determining the Rate of Heat Release (RHR) level in the stationary stage of the fire. (See also the RHR, Figure 2.1). If this RHR level is fixed by the oxygen content in the fire compartment, the fire is ventilation controlled, otherwise the fire is fuel bed controlled. By applying the Ozone computer code to model the fire development, this information is directly available to the user. Based on this information a decision is taken on the value of $\theta_{steel,lim}$ to work with: 600 or 700°C. If in doubt, simply take the lower value.

The next step is to determine the value of the fire load density for which $\theta_{steel,lim}$ is just reached. This value (= $Q_{lim,estimate}$) is calculated by systematically varying the fire load density. Also here, the use of Ozone is recommended, because one of the options of Ozone is to calculate the temperature of (unprotected) structural steel under natural fire conditions. One could approximate the maximum steel temperature in the lower flange of the primary beam by maximum gas temperature attained during the fire development, since the differences are only small and the approximation is on the safe side. Compare Figure 7.4 and Figure 7.5 in which for a certain fire compartment configuration, the maximum steel and gas temperature is given for various window height and fire load densities.

The final step of the pre-design is the comparison of the identified value of $Q_{lim,estimate}$ with the maximum value of the fire load density (= Q_{ref}), following the room temperature design assumptions (= basic requirements), taking into account the appropriate γ-values. See Table 6.2.

If $Q_{lim,estimate} \geq Q_{ref}$, it is feasible that no passive fire protection is needed for the composite steel framed building to withstand natural fire exposure without additional active fire protection measures (i.e. active measures above those already decided upon, independent from structural fire safety considerations). If the above condition is not met, it is probably that additional active measures (or deviations from the room temperature design) are necessary. The "gap" between $Q_{lim,estimate}$ and Q_{ref} is an indication how far the preferred solution (i.e. non-insulated) is away. See also Table 6.2.

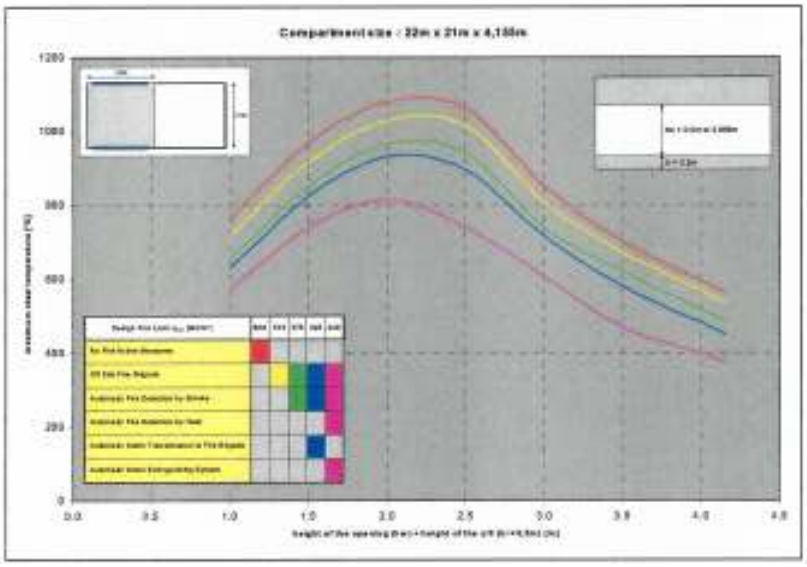

Figure 7.4 *Maximum steel temperatures in a certain fire compartment as function of the opening factor for various values of the fire load density.*

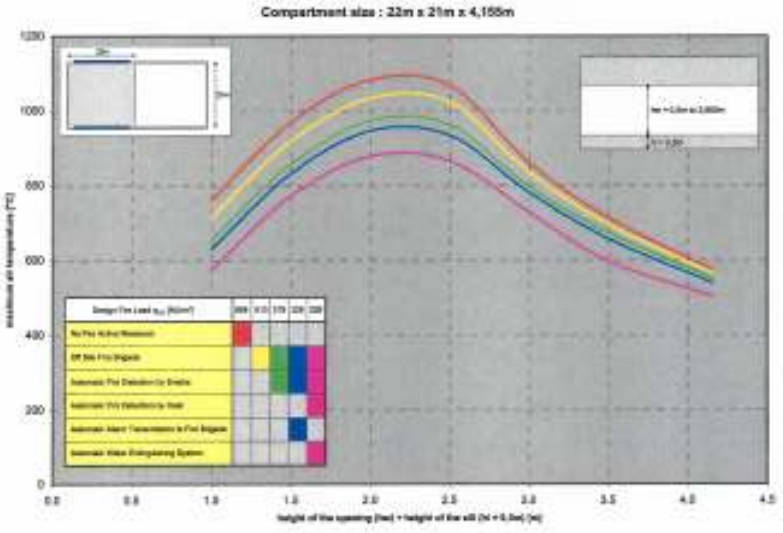

Figure 7.5 *Maximum gas temperatures in a certain fire compartment as function of the opening factor for various values of the fire load density.*

However, in view of the global character of the pre-design assumptions, it is necessary – in both situations! – to carry out a further analysis. This is the subject of the "detailed design".

7.2 Detailed design

The aim of the "detailed design" is to verify whether for the limiting value of the fire load density, estimated in the scope of the pre-design, failure conditions are met indeed. The analysis described in this paragraph is based on an advanced FEM method for the mechanical response, in combination with detailed analysis of the thermal response. For a schematic review of the proposed detailed design procedure, refer to Figure 7.6. More approximate design procedures are given in Chapters 8 and 9.

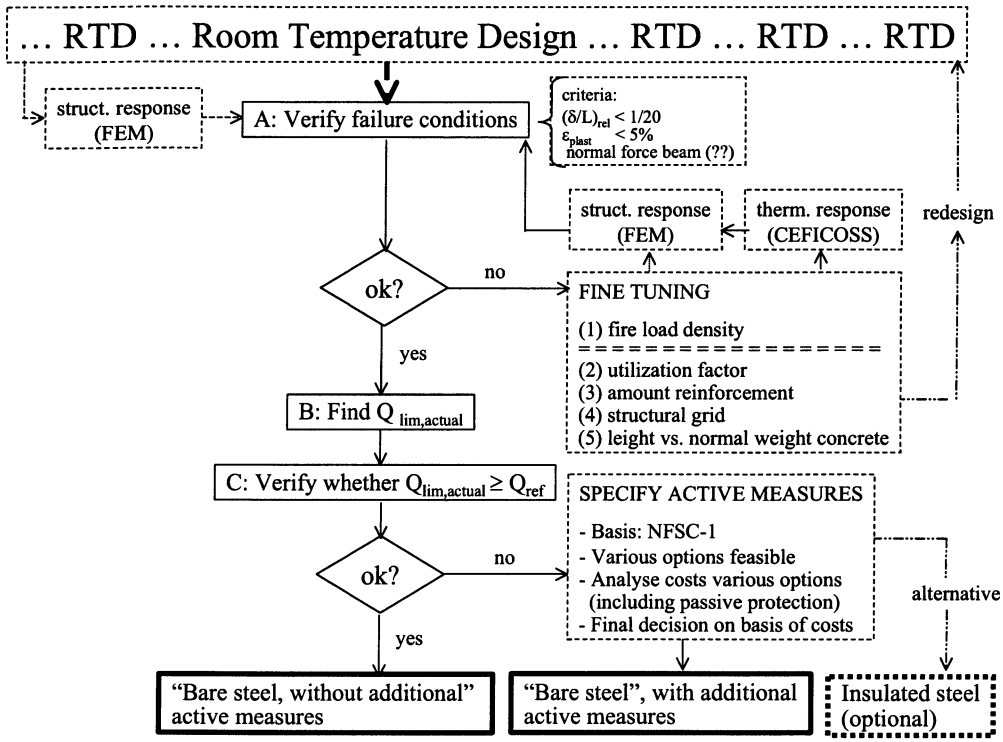

Figure 7.6 *Structural Fire Safety: "Detailed design", based on FEM method*

Starting point of the verification procedure is the temperature response of the composite floor (steel beams). In principle, many computer codes are available, (e.g. CEFICOS, DIANA, etc.) and the calculation of the temperature distribution in a composite steel concrete cross section is a matter of routine. See Figure 7.7 for a typical example.

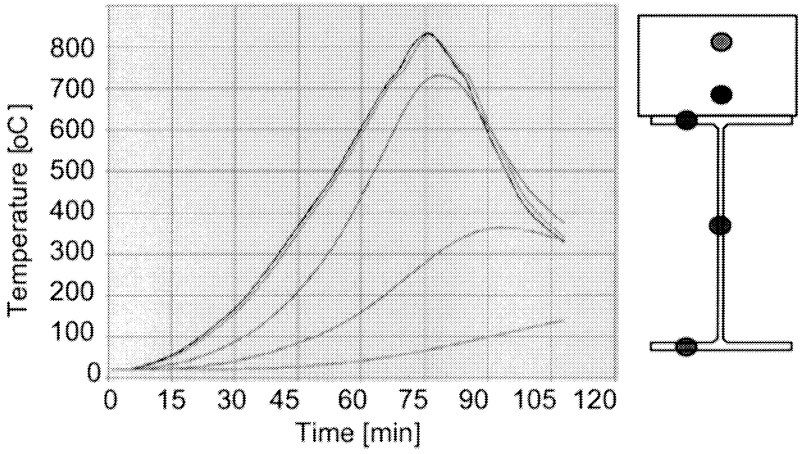

Figure 7.7 *Thermal response*

However, applying the advanced FE models, necessary for mechanical response analysis, can deal only with linear temperature gradients and a mean temperature for each element. Due to the complexity of the discretized section, it is not possible to introduce in the advanced structural FE models the temperature field as it is. Therefore, in the scope of this project, a limited number of elements have been selected for the concrete slab and steel beams and a procedure has been developed to linearise the temperature distribution over these sections. For details, refer to chapter 3. It has been shown that the thus "streamlined" FE models provide a fair representation of the actual mechanical behaviour of the structural system, while also the necessary calculation time remains within reasonable limits, i.e. around 24 hours for one calculation run. For details on the FE modelling, refer to chapter 4. As explained in this chapter, the advanced FE-model calculations provide detailed information on:

- displacements
- stress and strains distribution (total, thermal, plastic)
- axial force in primary and secondary beams
- reaction forces

Output options to facilitate the interpretation of the calculation results are available. This is illustrated in Figure 7.8 and Figure 7.9. In Figure 7.8 the maximum vertical displacements are presented for the primary beams, calculated for a certain fire compartment configuration of the Cardington building (medium sized fire compartment, with a floor area of 450 m^2, opening factor 0,16 $m^{1/2}$ and fire load density 700 MJ/m^2). For a 3-D representation of the field of vertical displacements, refer to Figure 7.9.

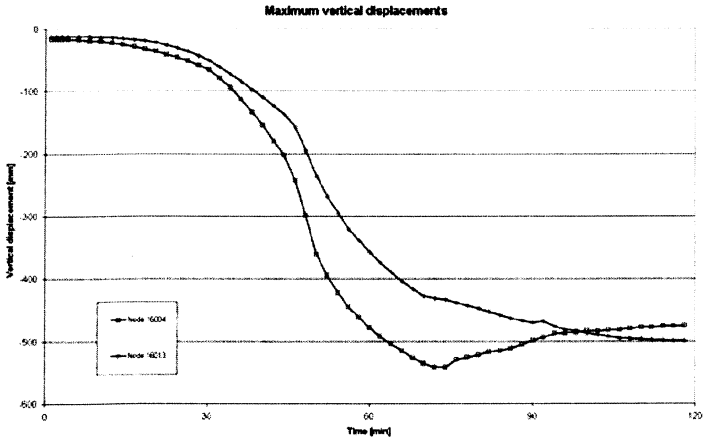

Figure 7.8 *Maximum vertical displacements of the primary beam as function of time (case B: fuel bed controlled)*

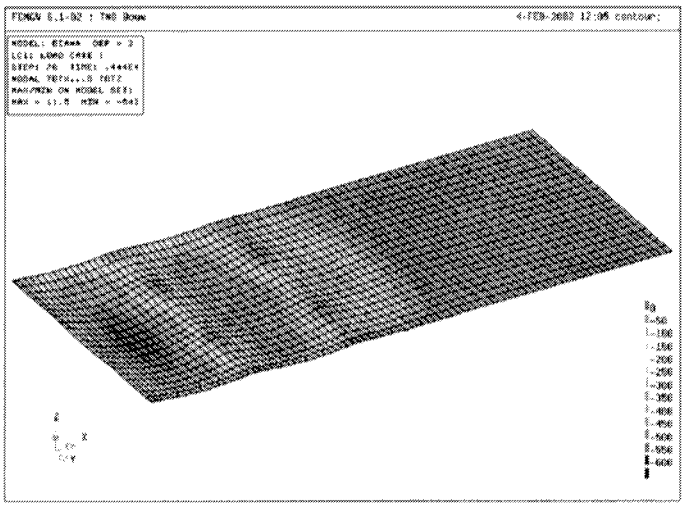

Figure 7.9 *Vertical displacements of slab at peak temperature*

For practical reasons, it is necessary to specify failure conditions. These refer to: (see also Chapter 4 and Annex B)

- The maximum relative displacement: $(\delta/L)_{rel}$ 1/20
- The maximum plastic strain: $\varepsilon_{plast} \leq 5\%$

In addition the above, one has to check the ability of the structural system (including connections) to be able to transmit moments and forces in any phase of the fire exposure. See, in particular, Annex F of the Final Report [21].

On the basis of an advanced FE analysis it can now be verified whether for the estimated value of the limiting fire load density (= $Q_{lim,estimate}$), the failure conditions are not breached. If so, the calculations have to be repeated under modified assumptions ("fine tuning", see also Figure 7.6) until it is shown that the that the failure conditions are met. The corresponding value of the fire load density is denoted as $Q_{lim,actual}$.

From tentative calculations, one may conclude that the most important option for "fine tuning" is modifying the value of the fire load density. This is illustrated in Figure 7.2. Depending on the opening factor, maximum steel temperatures in a range from 700 to 450°C (and below) can be attained by varying the fire load density between 700 and 200 MJ/m^2, which is feasible by choosing higher levels of active fire safety. See Table 6.2. Within this temperature range, it will be possible to identify conditions under which the failure conditions are just reached. Note that choosing an alternative value for the fire load density requires not only a new thermal response analysis, but often also new mechanical response calculations.

If the failure conditions are nearly met, or if the consequences of choosing a higher level of active fire safety measures are not acceptable, it is recommended to look at alternative tools for "fine tuning". The following are mentioned:

Mechanical loading

Choosing an alternative mechanical loading does not influence the thermal response. Also the input for the mechanical response model needs only minor adaptation. It is therefore recommended to

analyse – for a practical range of mechanical load values - the effect of the mechanical loading by way of a standard procedure.

From the tentative calculations carried out in the scope of this project, one may conclude however, that the effect of this design parameter is only limited. This is illustrated in Figure 7.10.

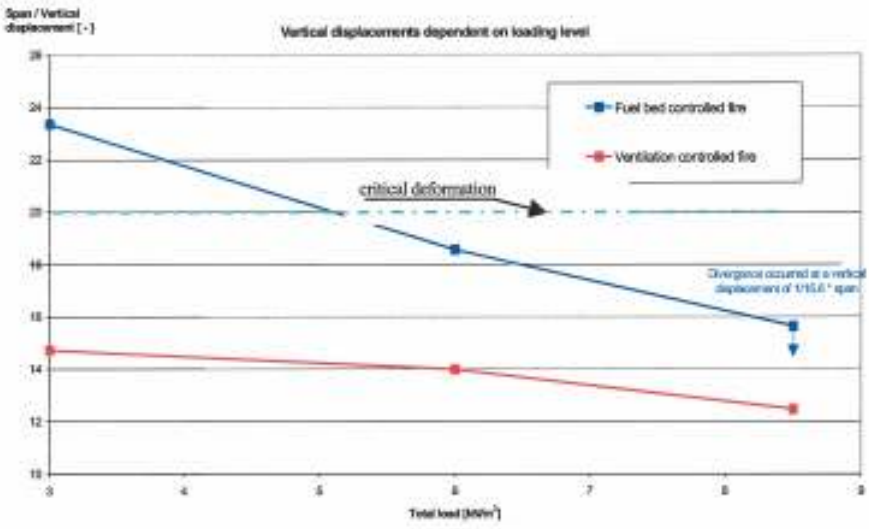

Figure 7.10 *Maximum relative displacements as function of the loading*

In this Figure, the maximum vertical displacements of the primary beams are presented as function of the applied imposed loading for a typical composite steel framed building configuration. Two design values for the opening factor are chosen, one leading to a ventilation controlled fire regime, the other to a fuel bed regime. On the horizontal axis, the total load (own weight + imposed load) is plotted. The value of 3 kN/m^2 corresponds to the dead load; the maximum allowable load under room temperature conditions is 8,5 kN/m^2. The critical displacement, based on a critical deformation of $(\delta/L)_{rel} = 1/20$, is also indicated.

For the fuel bed controlled case, a reduction of the variable loading by 50% corresponds to reduction of only approx. 12% in maximum displacement. This reduction of the mechanical loading has to motivated in order to comply with the failure conditions. It will - in terms of basic requirements – not be easy to defend such a value. Note that for the ventilation controlled case, varying the mechanical loading is no option at all.

Amount and direction of the reinforcement

Varying the amount of reinforcement, influences the utilization factor and has as such a similar effect on the failure conditions as varying the mechanical loading. Also in this case, the thermal response is not influenced and the input model needs only minor adaptations. From a practical point of view it is, therefore, at hand to analyse the effect of the amount of reinforcement in a systematic manner. For some calculation results, refer to Fig. 7.9. In this Figure the maximum relative deflection of the primary beam (span: 9 m) is given as function of the equivalent reinforcement thickness of the floor slab. The latter quantity is a simplified value, in which all reinforcement bars are considered as a steel plate of a certain thickness.

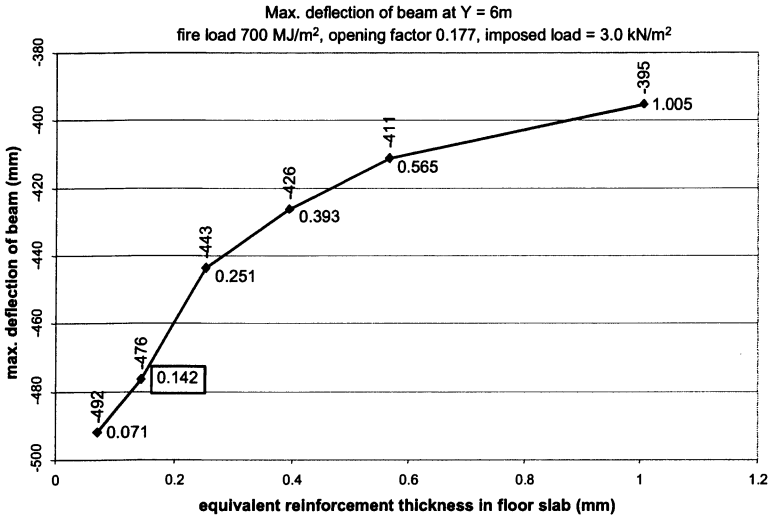

Figure 7.11 *Maximum relative deflection for various values of the equivalent reinforcement thickness*

The results show that replacing 6mm diameter bars by 16mm bars diameter (equivalent thickness 7 times higher) gives only a 17% decrease of the maximum deflection. However, the steepest part of the graph is from 0,142mm (=Ø6-200) to 0,251mm (=Ø8-200) equivalent thickness. In this range, the maximum deflection decreases 7%. If reinforcement of more than 0,251mm equivalent thickness is used, the improvement is negligible.

In the above calculations, the amount of reinforcement has been taken the same in both directions. On the basis of additional calculations it can be shown that only increasing the reinforcement in the most effective direction (i.e. the direction of the span of the slab) has an effect. The reinforcement in the other direction – although necessary for practical reasons - has only a very minor effect on the structural behaviour under fire conditions.

Structural material grades

The following structural materials are involved:

- structural steel, used for the primary and secondary beams;
- cold formed steel, used for the steel sheets;
- concrete, used for the floor slabs;
- reinforcement steel, used in the floor slabs.

None of the above design parameters will influence the temperature response of the structure. Note that the strength and stiffness properties of the various building materials at elevated temperatures appear to be proportional to the corresponding room temperature values. This means that the effect of changing these parameters will be similar to the effect of changing the mechanical loading. If, for example, the steel grade of the primary beams would be changed from S235 (yield strength: 235 N/mm^2) to S355 (yield stress: 355 N/mm^2), the effect will correspond to an decrease of the utilization factor of 235/355x100 = 66%, assuming all other design parameters remain unchanged. Further to the above discussion on the effect of the mechanical load, it will be clear that the impact of such a change will be limited. In the same way it can be shown that also a change of the quality of the concrete or the reinforcement steel will have minor influence on the structural behaviour.

Other single parameters, affecting the degree of utilization

Other design parameters which affect the degree of utilization are the dimensions of the steel beam, the depth and shape of the concrete slab and the thickness of the applied steel sheet. Note in this respect the overall depth of the floor (i.e. sum of the depths of slab, primary and secondary beams) should be considered as a "fixed" parameter, since it follows directly from the room temperature design and will be very difficult to modify under pressure of the structural fire safety design. This means that changing one of the above parameters would imply the need to change other parameters as well. Their effect can only be considered in this context. See the discussion below on "structural grid".

Normal vs. light weight concrete

One of the options to influence the mechanical performance of a composite concrete framed building in fire, without changing basically the functional concept, is to change from normal weight to light weight concrete. The differences in material properties between normal weight and light weight concrete are:

- Thermal conductivity
- Specific heat
- Unit mass
- Stiffness
- Thermal expansion

The combined effect of the above parameters has been analysed by means of a case study, which is summarized in the Final Report [21]. For some overall results, refer to Figure 7.12.

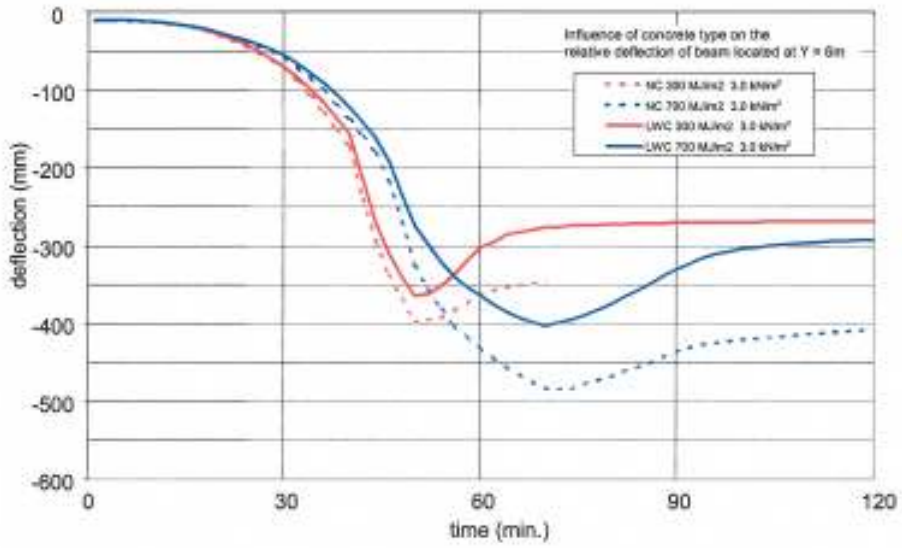

Figure 7.12 *Deflection of secondary beam with LWC and NC floor slabs*

The calculated deflections for a design in normal weight concrete has been applied, are compared to a similar situation, however applying light weight concrete. For details, refer to reference 21.

From Figure 7.12 it becomes clear that the deflections with LWC are significantly less than with NC. This holds for both imposed loads taken into account (i.e. 3 and 5 kN/m^2). On basis of a further

analysis [21], it becomes clear that the lesser deflection of light weight concrete compared to normal weight concrete is caused by

- lower unit mass
- lower Young's modulus
- lower thermal expansion

The lower unit mass decreases the total load and therefore decreases the deflection as expected. Lowering the Young's modulus and thermal expansion causes a decrease of the deflection because the compressive stresses due to thermal expansion become less.

Structural grid spacing

In the Cardington building the concrete slab is 130mm thick over secondary beams at 3m spacing. Column spacings across 21m direction are 6m-9m-6m respectively and across 45m direction are 5 x 9m bays. This grid spacing has been the basis of the calculation results presented in the previous discussions. In addition, tentative calculations have performed with an alternative (practical) grid concrete slab of 130mm thick over secondary beams at 3m spacing. Column spacings across 21m direction are 6m-9m-6m respectively and across 48m direction are 4 x 12m bays. Steel frame and floor slabs have been designed on the basis of practical, room temperature design considerations.

For some results, refer to Figure 7.13 and Figure 7.14. These show results obtained using different grid spacing but with identical thermal conditions.

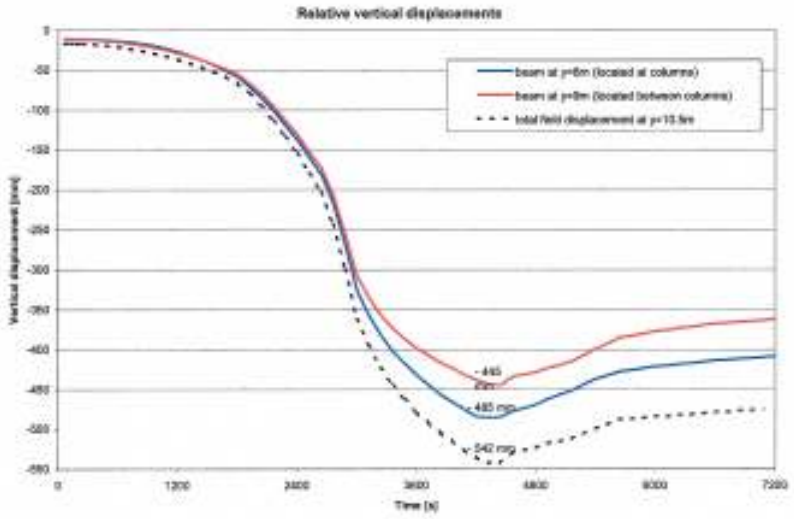

Figure 7.13 *Possible effect of changing the structural grid - structural grid spacing used in the Cardington building*

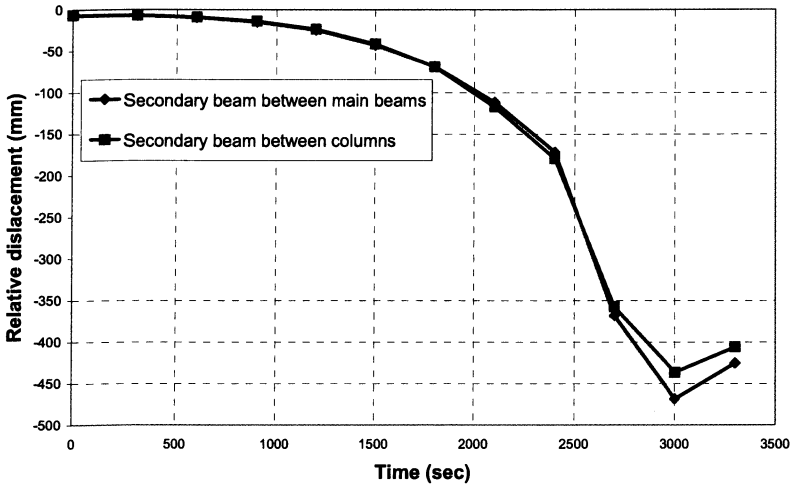

Figure 7.14 *Possible effect of changing the structural grid - alternative grid spacing compared with Cardington building*

From these Figures it may be concluded that, by choosing an alternative structural grid spacing, the deformation behaviour is significantly improved. One of the reasons is that, by choosing practical steel profiles for the alternative grid spacing, a relatively low utilisation factor for the secondary beams is achieved when compared to the original design. See for more details, refer to the discussion in the Final Report [21].

Size and location of the fire compartments:

The development of natural fires, and hence the thermal loading during such fires, depends very much on the size of the fire compartment and the window openings. It can be shown, however, that practically speaking, the effect of these parameters can taken into account by one single parameter: the so-called "opening factor". The opening factor is given by:

$$Opening\ factor\ = \frac{A_V \sqrt{h}}{A_t}$$

where,

A_v	is the area of the windows assumed to have broken
h	is the average window height
A_t	is the total area of the compartment boundaries

For some numerical proof, refer to the in the Final Report [21].

In structural fire safety engineering calculations it is therefore common to represent the effect of the size of the fire compartment and of the ventilation conditions by the opening factor.

With reference to the Cardington building and for practical design assumptions with regard to window openings and thermal insulation, the effect of the location of otherwise identical fire compartments has been studied. It is concluded that the location of the fire compartment has only of minor effect on the gas temperature development during a natural fire. See also the in the Final Report [21].

Procedural aspects

On basis of the verification procedure, if necessary complemented by fine tuning and, eventually, redesign, the actual value of the fire load density for which just no structural failure occurs, is identified. This value is denotation as: $Q_{lim,act}$.

As in the pre-design, the value of $Q_{lim,act}$ should be compared with the maximum design value, following from the room temperature design (Q_{ref}). See also Chapter 6.

If $Q_{lim,act} \geq Q_{ref}$, the design decision is that no passive protection is necessary for the floors and beams, apart from the provisions specified in Chapter 5.

If $Q_{lim,act} < Q_{ref}$, additional active fire protection measures are necessary in order to allow the floors and beams non-insulated. On the basis of the fire safety concept proposed in the NFSC project, a choice can be made out of a variety of options. For possible options, see Tables 7.1. In this table, which is directly based on the γ_n values (Table 6.2) and holds for office buildings the consequences of the detailed structural fire safety design are indicated.

Table 7.1 *Need for additional active fire safety measures*

	Design assumptions : office building (Qchar = 511 MJ/m²)				
Outcome detailed design :	$Q_{ref} = Q_{char} * 0,78 * 0,087 * \gamma_{q1} * \gamma_{q2}$				
$Q_{lim,act} / Q_{ref}$	>1	<1	<0,87	<0,7569	<0,46
$Q_{lim,act} / Q_{ref}$	--	≥0,87	≥0,7569	≥0,46	≥0,32
no additional active measures	x				
off site fire brigade		x	x	x	x
automatic fire detection (smoke)		x	x	x	x
automatic fire detection (heat)			x	x	x
automatic fire alarm (via fire brigade)		x	x	x	x
automatic fire extinguishing				x	x
2 independent water supplies					x
	⇑ ⇑ additional active measures ⇑ ⇑				

Note that the final decision on the additional fire safety measures should also take into account cost considerations should leave open the option for passive fire protection as well. Such considerations, however, are outside the scope of this study.

Off site fire brigade and automatic fire detection by smoke are generally considered and is therefore included in Q_{ref}.

8 DESIGN RECOMMENDATIONS BASED ON BRE SIMPLE METHOD

8.1 Background

Following the UK research at Cardington, a method of assessing the strength of a system of composite beams acting with a composite floor slab was developed by the UK engineering consultancy of BRE.

The model developed by BRE[22,23] combines the residual bending resistance of the composite beams with the contribution of the composite slab, calculated using a combined yield-line and membrane action.

8.1.1 Basis of model

The model of slab behaviour was developed by BRE following observations at Cardington and additional full scale testing.

The model is most easily described by considering the behaviour of an isolated floor slab supported rigidly on knife supports at its edges. As load is applied to the slab, it will initially resist the load by bending action and, as the load is further increased, yield lines will form as plastic hinges develop (Figure 8.1).

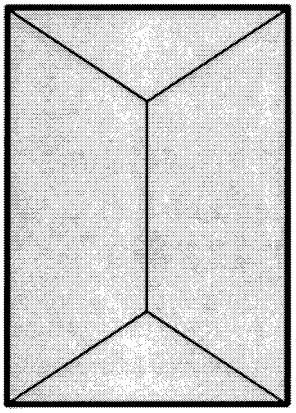

Figure 8.1 *Formation of yield lines in simply supported slab*

As the load is increased further, the structural mechanism within the slab changes from bending action to membrane action as tensions and compressions build up. A pattern of internal forces develops in which the centre of the slab is in tension and the outer parts are in compression (Figure 8.2). All applied loads are balanced by vertical reactions at the perimeter.

The slab fails when the reinforcing mesh fractures across the centre of the slab (Figure 8.3).

In the BRE model, the bending resistance (yield line) is first computed and then an enhancement factor is computed based on membrane behaviour. This factor is applied to the bending resistance to obtain the final slab resistance. For simplicity, the small residual bending resistance of the beams is added to form a total resistance of the slab and beam system.

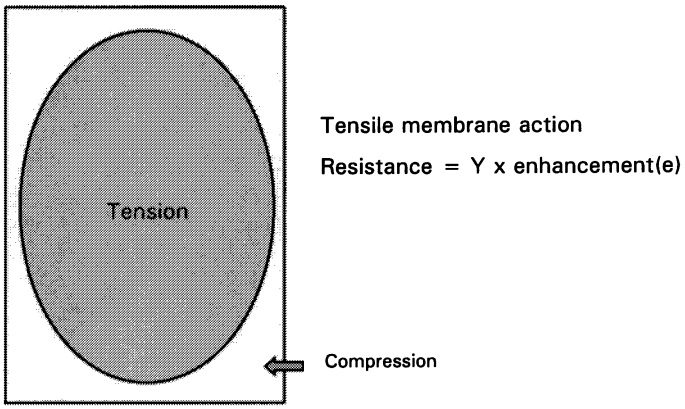

Figure 8.2 *Tensile membrane action with tensile and compressive zones*

$$\text{Total resistance} = Y \times \text{Efac} + B$$

where,

Y	is the load at which the yield line pattern develops
Efac	is the enhancement factor for membrane action
B	is the total resistance of any beams spanning across the slab (kN/m^2)

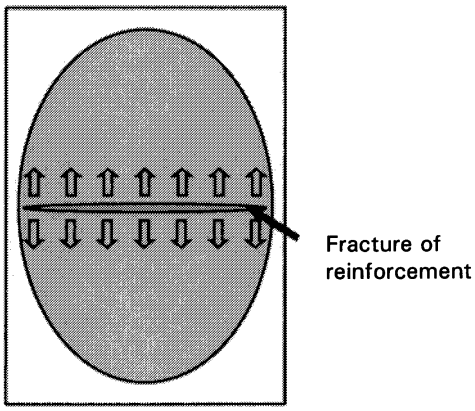

Figure 8.3 *Failure by fracture of the reinforcement.*

The model does not rely on the continuity of any mesh reinforcement around the perimeter of the slab under consideration. This is assumption is thought to be conservative because, at Cardington, it was observed that following the tests, reinforcing mesh was fractured at the edges of compartments. However, there is a strong possibility that the reinforcement actually fractured during the cooling phase of the fire.

8.1.2 Procedure

Floor design zones

Each floor in the building should be divided into a number of *floor design zones:*

- Each zone should be rectangular.
- Each zone should be bounded on all sides by beams.

- Each zone should contain within it only beams spanning in one direction.
- Each zone should contain no columns within the zone (but columns may be on the boundary.

The calculations are based on the following assumptions:

- the load supported by the flexural behaviour of the composite beams within the floor design zone is added to the lower-bound mechanism for the composite slabs (see below). The beams are assumed to be simply supported.
- the load supported by the composite slab in bending is calculated based on the lower-bound yield-line mechanism, assuming that the internal beams have zero resistance.
- an enhancement due to membrane action in the composite slab is added to the resistance of the yield-line mechanism of the slab.
- the resistances of the composite beams and slab are added to obtain the resistance of the complete system.
- thermal curvature and mechanical strain in the reinforcement limit the maximum deflection of the slab in fire conditions.

The boundary beams around the zone will normally be fire protected. They may be unprotected, provided that they are designed in fire as unprotected beams in accordance with EC3-1-2 or EC4-1-2 or, if they are at the edge of a slab, are supported by wind posts or vertical ties.

All internal beams within the zone may be left unprotected, provided that the design conditions are met. The size and spacing of these beams are not critical.

The division of a floor into zones is illustrated in Figure 8.4 and a single floor zone is illustrated in Figure 8.5. Floor zones designated 'A' may be checked in fire using the Design Tables because the beams spanning across the zone are all in the same direction. Zones designated 'B' contain internal beams spanning in two directions and are outside the scope of the recommendations but may be checked using the methods described by BRE[22]. The zone designated 'C' contains a column and is not permitted.

The recommendations are applicable to profiled steel decking up to 70 mm deep and for depths of concrete above the steel decking from 60 to 80 mm (Figure 8.6).

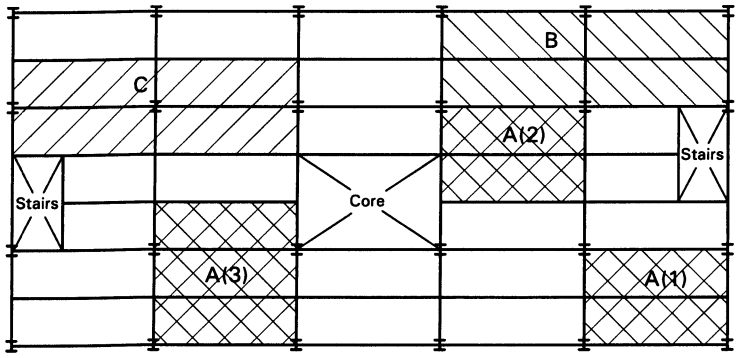

Figure 8.4 *Possible floor design zones*

Key to figure
A: Permitted area within scope of the guide
B: Permitted area outside scope of the guide
C: Not permitted – contains columns

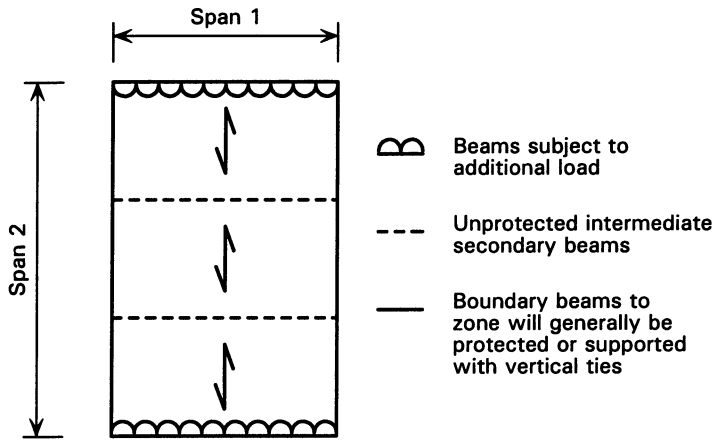

Figure 8.5 *Definition of span 1 and span 2 and beam layout*

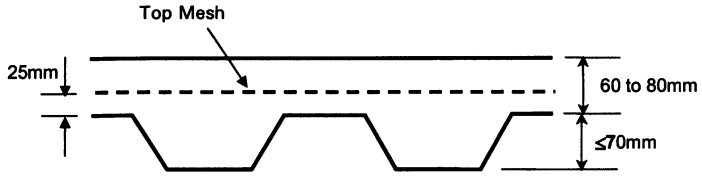

Figure 8.6 *Deck and reinforcing mesh details*

8.2 Natural Fires

In the original UK work , the design was based on standard fire resistance. Within this project, natural fires are considered with the fire model based on Ozone. (Chapter 3). The BRE method has been compared with analyses made using advanced FE models and found to be conservative. (Annex D).

In adapting the BRE method the following procedure was adopted. At one minute intervals, the slab and supporting beams are checked using the same temperature field as is used in the finite element analyses. Design information is based on the lowest value of strength calculated during the fire.

The design information has been generated for a range of fire loads and ventilation conditions. For the purpose of developing information a particular compartment size was assumed but the information generated is generally applicable.

Note:
Information has been generated using design imposed loads which have been reduced by the EC1-1 load combination factor, $\psi_{1,1}$, of 0,5. Thus, for an applied load of 3,5 kN/m^2, the load used in calculations is 1,75 kN/m^2.

Compartment details

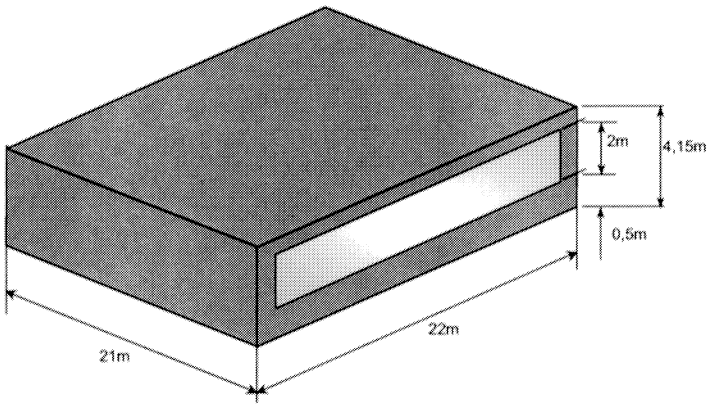

Figure 8.7 *Compartment used to develop design tables*

Concrete type	Normal weight concrete
Concrete grade	C35
Deck type	Trapezoidal
Maximum deck depth	70 mm
Minimum slab depth	Deck depth + 60 mm
Maximum slab depth	Deck depth + 80 mm
Minimum reinforcing mesh size	6mm wires @ 200mm
Reinforcing mesh position (from top of deck to mesh centre)	25 mm
Minimum span 2 beam size	A/V = 210 m^{-1}

The type of steel deck and reinforcing mesh position are illustrated in Figure 8.6. The thermal analyses were carried out using a beam with a section factor (A/V) of 210m^{-1}. This is a comparatively high value and the results are therefore applicable to a large range of beams.

Fire Load

Fire loads in the range from 200 to 700 MJ/m^2. The fire load is expressed in terms of floor area (Fire loads are sometimes expressed in terms of total area). Guidance on the calculation of the effective fire load is given in Chapter 2.

Ventilation

The thermal analyses used to develop the design tables assumed that within the 22m length, was a window opening with a length of 90% of the 22 m and with a variable height. This is illustrated in Figure 8.8. The window was assumed to exist on both sides of the compartment.

Window heights of 0,5m, 1,0m, 1,5m, 2,0m, 2,5m, 3,0m and 3,655m were analysed.

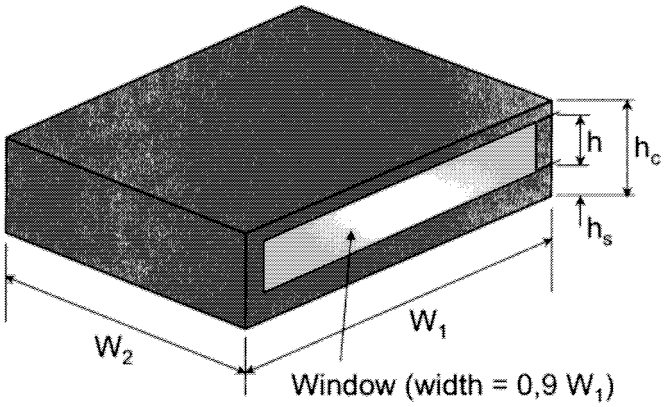

Figure 8.8 *Window openings and ventilation*

In calculating the heating rate within a fire compartment, the window area and window height are combined to form an opening factor. The opening factor characterises the heating rate in a single parameter.

$$Opening\ factor = \frac{A_V \sqrt{h}}{A_t}$$

where,

A_v	is the area of the windows assumed to have broken
h	is the average window height
A_t	is the total area of the compartment boundaries

For the cases covered in the design tables the opening factors are given in Table 8.1. The design tables are applicable to any compartment with the same opening factor.

Table 8.1 *Opening factors in design tables*

Window height, h (m)	Window area, Av (m^2)	Opening factor (m^2)
0,5	19,8	0,011
1	39,6	0,031
1,5	59,4	0,057
2	79,2	0,087
2,5	99,0	0,122
3	118,8	0,161
3,655	144,7	0,216

8.3 Design Tables

For the 6 fire loads from 200 to 700 MJ/m^2 and for 7 variations of window opening it is possible to generate 42 different design tables were generated. In many cases, the differences between tables were very small and it has therefore been possible to combine, up to a maximum 4, of these tables, resulting in 17 different design tables. These are presented in Annex C. The relationship between the 17 design tables and the range of fire loads and windows is shown in Table 8.2.

In many cases, but generally where the ventilation is either very high or very low, it was found that the unprotected beams spanning across the design zone were adequate in themselves to support the applied loads and it was not necessary to take into account any membrane action in the floor slab.

These cases are marked as "B" in Table 8.2 and the full design table is not presented. Where "B" is indicated, the beams are adequate on the basis of a simple EC4-1-2 check (Chapter 9).

Table 8.2 *Relationship between design cases and design tables*

Fire load	Window height (m), Opening factor ($m^{1/2}$)						
(MJ/m^2)	0,5	1,0	1,5	2,0	2,5	3,0	3,655
	0,011	0,031	0,057	0,087	0,122	0,161	0,216
200	B	1	2	1	B	B	B
300	B	3	4	5	6	B	B
400	9	5	7	7	8	B	B
500	9	4	10	10	3	9	B
600	9	11	12	10	13	6	B
700	9	14	15	16	17	1	B

In each table, for a range of imposed loads and span 1 and span 2 dimensions (Figure 8.5), the reinforcement requirements are given.

8.3.2 Information in Design Tables

For each combination of span 1, span 2, and applied loading, two items of design information are given in the Design Tables:

1. Reinforcing mesh size

The sizes given in the Design Tables are the minimum required reinforcing mesh size for the slab to perform adequately in fire. Reinforcing mesh sizes are assumed to be square and are given in the form of "wire diameter x spacing", e.g., 7x200, would be 7mm diameter wires at 200mm spacing in either direction. The reinforcing mesh strength is assumed to be 500 N/mm^2. The reinforcing mesh should be positioned approximately 25mm above the deck.

To ensure membrane action in the slab, care must be taken to ensure that the reinforcing mesh is properly lapped. This is especially important around columns.

2. Additional load to beams at the boundaries of the floor design zone

Normal design assumes that floor loads are supported by secondary beams which are themselves supported on primary beams. In the design model at the fire limit state, the slab transfers a proportion of the load directly to the surrounding beams by membrane action. The load supported by the boundary beams that are parallel to the internal beams (span 1) is thus increased. The total additional load (kN) for each span 1 boundary beam is tabulated. This total load is considered to be uniformly distributed along each beam. This load is added to the load that would normally be assumed to be acting on the beam at the fire limit state. In many cases this load is small and increased fire protection thicknesses will not be required.

The effect of these additional loads is to increase the utilization of these beams as follows:

$$\eta_{eff} = \eta_0 + \frac{W_a L}{8 M_c}$$

where:

η_{eff} is the effective utilization of the boundary beam
η_o is the utilization based on the normal distribution of load
W_a is the additional loading applied via the slab
M_c is the bending resistance of the boundary beam in normal conditions
L is the beam span

For boundary beams with floor design zones on both sides, the additional load from the zones on both sides must be combined. (For equal-sized zones the additional load on the boundary beams is doubled).

The effective utilization will decrease the critical temperature of the beam in fire, and hence the required thickness of fire protection may be increased.

8.4 Design Example

The compartment is illustrated in Figure 8.9. The fire load is determined using the methods given in Chapter 2. As the compartment measures 22 x 21 m and the maximum size of floor considered by the design tables is 12 x 12m, a smaller floor design zone must be considered. Assume that the largest practical zone measures 9 x 7 m and is located in the centre of the compartment (Figure 8.10).

Compartment size	22 x 21m
Compartment height	4,15m
Window height	2m
Window width	0,9 x 22 = 19,8m
Effective fire load	400 MJ/m^2
Design imposed load	3,5 kN/m^2

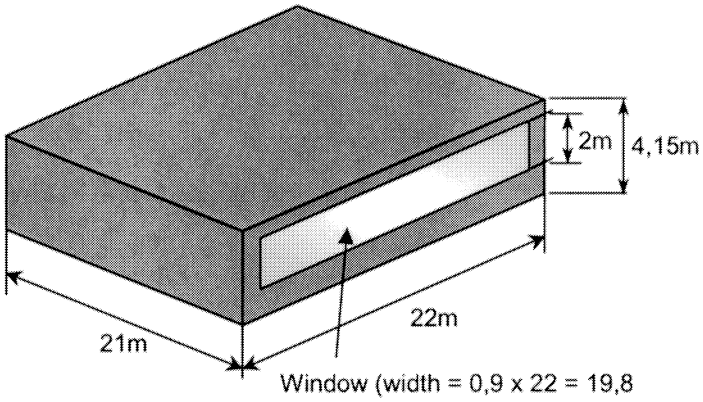

Figure 8.9 *Compartment in design example*

In the example, the window height is 2m and the fire load is 400MJ/m^2, thus, from Table 8.2 the relevant design table is number 7. An extract from design table 7 is shown in 0.

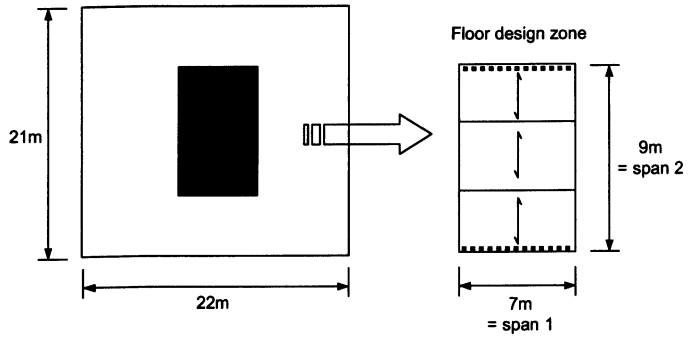

Figure 8.10 *Floor design zone within compartment*

Table 8.3 *Extract from design table 7*

Imposed load 3,5 kN/m^2					
	Span 1	Mesh/Extra Load (kN)			
Span 2	6	**>>7<<**	8	9	10
6	6x200 / 0	6x200 / 4	6x200 / 7	7x200 / 11	7x200 / 15
7	6x200 / 3	6x200 / 7	6x200 / 11	7x200 / 16	7x200 / 21
8	6x200 / 5	6x200 / 9	6x200 / 15	6x200 / 20	7x200 / 27
>>>> 9	7x200 / 6	**7x200 / 12**	6x200 / 18	6x200 / 25	7x200 / 32
10	7x200 / 8	7x200 / 14	7x200 / 21	7x200 / 28	7x200 / 36

For span 1 of 7m and span 2 of 9m the reinforcing mesh required is 7x200 and the additional loading to the edge beams parallel to span 1 is 12kN per beam.

The beams forming the boundary to the floor design zone should be fire protected. The minimum amount of fire protection should be consistent with the effective fire load and the ventilation. This can be assessed using the methods of EC1-1-2 with EC3-1-2 or EC4-1-2. However, it will normally be more convenient to apply fire protection in accordance with national practice.

9 DESIGN BASED ON EC4-1-2

9.1 General

The fire part of Eurocode 4 (EN1994-1-2) contains simple rules for the design of composite beams. Using these methods, in a limited number of circumstances, when the fire exposure is low, the use of unprotected steel may be justified.

The design can be justified using 4.3.4.2.3 (from EN1994-1-2)

4.3.4.2.3 Structural behaviour - critical temperature model

(3) The critical temperature, θ_{cr} may be determined from the load level, $\eta_{fi,t}$, applied to the composite section and from the strength of steel at elevated $f_{amax,\theta cr}$ temperatures according to the relationship:

For R30 (or less), $0{,}9\ \eta_{fi,t} = f_{amax,\theta cr} / f_{ay,20°C}$

In any other case, $1{,}00\ \eta_{fi,t} = f_{amax,\theta cr} / f_{ay,20°C}$

where,

$f_{amax,\theta cr}$ is the steel strength corresponding the maximum steel temperature
$f_{ay,20°C}$ is the strength of steel at 20 °C
$\eta_{fi,t}$ determined from the load level

For a simply supported composite beam the load level is the maximum applied moment in the fire condition divided by the moment resistance used in normal design.

An unprotected beam will normally have a fire resistance of less than R30 so for the natural fire case the R30 case can safely be assumed. Therefore,

$$0{,}9\ \eta_{fi,t} = f_{amax,\theta cr} / f_{ay,20°C}$$

The maximum temperatures calculated using the natural fire model can be converted directly into a maximum load level on any beam. The relationship between steel strength and temperature is given in Table 9.1. The load level is also shown in the table. The table is based on the material laws of EN1994-1-2.

Table 9.1 *Maximum steel temperature and load level*

Maximum steel temperature (°C)	$f_{amax,\theta cr}$ / $f_{ay,20°C}$	Load Level, $\eta_{fi,t}$
500	0,780	0,867
520	0,718	0,798
540	0,656	0,729
560	0,594	0,660
580	0,532	0,591
600	0,470	0,522
620	0,422	0,469
640	0,374	0,416
660	0,326	0,362
680	0,278	0,309
700	0,230	0,256

9.2 Design procedure

In situations where the effective fire load is low and where the ventilation is either very low or very high, it may be possible to show that, some or all of the beams may be unprotected. Generally, the temperature of the beams should be assessed using the methods described in Chapter 2 and reference should be made to EN1994-1-2 or Table 9.1. However, using the same compartment fires considered to generate the design tables described in 8.3 guidance has been developed for a number of cases.

For all the cases considered in 8.3, the maximum beam temperatures and corresponding load levels, calculated using the method described in 9.1, are presented in Table 9.2 and graphically in Figure 9.1.

Table 9.2 *Beam temperatures and load levels*

Fire load (MJ/m^2)	Window height (m) and Opening factor ($m^{1/2}$)						
	0,5 0,011	1,0 0,031	1,5 0,057	2,0 0,087	2,5 0,122	3,0 0,161	3,655 0,216
200	551/0,691	723/0,225	760/0,176	706/0,248	546/0,708	443/1,00	358/1,00
300	612/0,490	800/0,122	906/0,065	855/0,092	695/0,269	563/0,650	435/1,00
400	665/0,349	864/0,087	975/0,050	955/0,054	741/0,201	632/0,437	498/0,872
500	674/0,325	909/0,065	1022/0,040	1006/0,043	798/0,125	668/0,341	536/0,743
600	674/0,325	947/0,056	1059/0,031	1043/0,035	838/0,101	690/0,282	554/0,681
700	674/0,325	979/0,049	1089/0,025	1071/0,029	858/0,090	705/0,249	567/0,636

It can be seen in the table that, in many cases, the maximum beam temperature results in very low, impractical load levels and, in some cases, the load level is sufficient high to justify unprotected steel without further calculation. The load level may be expressed as:

$$\eta_{fi} = \frac{(\gamma_{GA} + \psi_{1,1}\zeta)}{(\gamma_G + \gamma_Q \zeta)}$$

where

γ_G is the partial safety for permanent loads
γ_{GA} is the partial safety for permanent loads in fire
γ_Q is the partial safety for variable loads
$\psi_{1,1}$ is the load combination factor
ξ is the ratio between the main variable and permanent actions

For offices:

γ_G = 1,35

γ_Q = 1,5
γ_{GA} = 1,0
$\psi_{1,1}$ = 0,5
ξ = 1,0 (typical, actual value depends on design conditions)

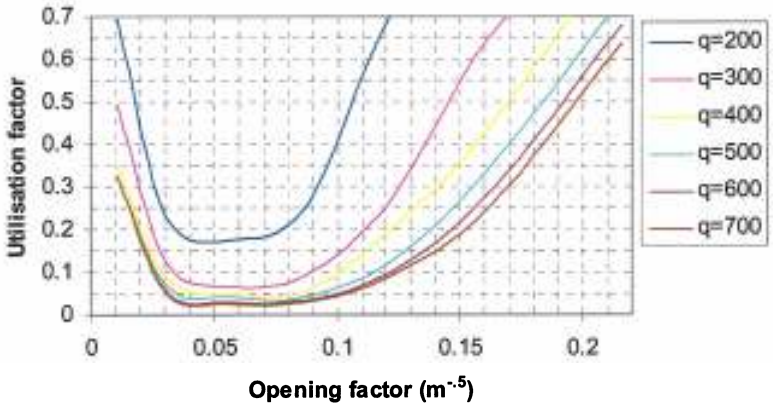

Figure 9.1 *Load level factor vs opening factor for various fire loads*

The load level will depend on the design criteria for the beam. For many beams, the design criteria may not be bending (which is normally critical in fire) so the load level will not be greater than:

$$\eta_{fi} \leq \frac{(1,0+0,5\times1,0)}{(1,35+1,5\times1,0)} = 0,53$$

From Table 9.1 it can be seen that a load level of 0,53 corresponds to a maximum steel temperature of 598°C.

If the bending strength of a beam is only 90% utilised for normal design the load level in fire will be 0,48 corresponding to a maximum steel temperature of 616°C. An additional reduction can be made if the difference in material factors, γ_M, between the normal design and the fire condition is taken into account. This can reduce the load level by a further 5%.

9.3 Effect of section size

The temperatures presented in Table 9.2 were computed using a beam with a section factor, A/V, of 210 m^{-1}. Although the heating rate of a beam depends on its section factor, in the type of fires being considered, the differences in maximum steel temperature are very small. The temperatures in the table are therefore considered to be applicable to all beam sizes.

9.4 Design Example

The compartment is assumed to be the same as was used in the previous design example (Figure 8.9). The fire load is determined using the methods given in Chapter 2 but in this example, the effective fire load is reduced to 300 MJ/m^2.

Compartment size 22 x 21m

Compartment height	4,15m
Window height	2,8m
Window width	0,9 x 22 = 19,8m
Effective fire load	300 MJ/m^2
Design imposed load	3,5 kN/m^2
Slab weight	3,1 kN/m^2
Beam section factor	$120m^{-1}$

Assume also that for normal design the bending resistance was only 90% utilised and that for normal design a material factor of 1.05 was used.

The beam load level in fire is therefore:

$$\eta_{fi} = 0{,}9 \times \frac{1}{1{,}05} \frac{(3{,}2 + 0{,}5 \times 3{,}5)}{(1{,}35 \times 3{,}2 + 1{,}5 \times 3{,}5)} = 0{,}44$$

The critical steel temperature is 631°C (EN1994-1-2 and Table 9.1). From Table 9.2, by linear interpolation, the maximum steel temperature for the assumed fire load and ventilation is 616°C so the beam may be used without applied fire protection.

Note that the calculation is based on load level. The beam span and actual form that the load may take (point load, distributed load) are not relevant.

10 REFERENCES

1 The behaviour of multi-storey steel framed buildings
A European joint research programme
British Steel Swinden Technology Centre, 1999

2 NEWMAN G.M., ROBINSON J.T., BAILEY C.G.
Fire safe design: A new approach to multi-storey steel framed buildings,
(SCI P288)
Steel Construction Institute, 2000

3 SCHLEICH J-B., CAJOT L-G., TWILT L., et al.
Final Report of the ECSC research 7210-SA/125,126,213,214,323,423, 522,623,839,937: 'Competitive Steel Buildings Through Natural Fire Safety Concept'
Part 3: WORKING GROUP 3: 'Fire Characteristics For Use In A Natural Fire Design Of Building Structures'
March 1999.

4 SCHLEICH J-B., CAJOT L-G., TWILT L., et al.
Final Report of the ECSC research 7210-SA/125,126,213,214,323,423, 522,623,839,937: 'Competitive Steel Buildings Through Natural Fire Safety Concept'
Part 2: WORKING GROUP 1: 'Natural Fire Models'
March 1999.

5 ENV 1991, Eurocode 1: Basis of design and actions on structures.
Part 1: Basis of design and Part 2.2: Actions on structures exposed to fire.
CEN 1994.

6 DIN V 18230 - Baulicher Brandschutz im Industriebau - Teil 1 - Rechnerisch Erforderliche Feuerwiderstandsdauer - September 1987

7 DD 240, Fire Safety Engineering in Buildings.
Draft for development
British Standards Institution, 1997.

8 SCHLEICH J-B., CAJOT L-G., TWILT L., et al.
Final Report of the ECSC research 7210-SA/125,126,213,214,323,423, 522,623,839,937: 'Competitive Steel Buildings Through Natural Fire Safety Concept'
Part 4: WORKING GROUP 4: 'Statistics'
March 1999.

9 SCHLEICH J-B., CAJOT L-G., TWILT L., et al.
Final Report of the ECSC research 7210-SA/125,126,213,214,323,423, 522,623,839,937: 'Competitive Steel Buildings Through Natural Fire Safety Concept'
Part 1: 'Main Text'
March 1999.

10 SCHLEICH J-B., CAJOT L-G., TWILT L., et al.
Final Report of the ECSC research 7210-SA/125,126,213,214,323,423, 522,623,839,937: 'Competitive Steel Buildings Through Natural Fire Safety Concept'
Part 2: WORKING GROUP 1: 'Natural Fire Models'
March 1999.

11 SCHLEICH J-B., CAJOT L-G., et al.
NATURAL FIRE SAFETY CONCEPT - Full Scale Tests, Implementation in the Eurocodes and Development of an User friendly Design Tool
CEC Agreement 7210-PA/PB/PC/PD/PE/PF/PR-060
Technical Report, Draft Final Report, June.2001.

12 SCHLEICH J.B., CAJOT L.G., PIERRE M., JOYEUX D., AURTENETXE G., UNANUA J., PUSTORINO S., HEISE F.J., SALOMON R., TWILT L., VAN OERLE J.
Competitive Steel Building through Natural Fire Safety Concept
C.E.C. Research 7210-SA/522; Final Report EUR 20360 EN, 2002, RPS Report N° 32/99.

13 SCHLEICH J-B., CAJOT L-G., et al.
NATURAL FIRE SAFETY CONCEPT - Full Scale Tests, Implementation in the Eurocodes and Development of an User friendly Design Tool
C.E.C. Research 7210-PR-060; Intermediate Report, RPS Report N° 29/99.

14 SCHLEICH J.B., CAJOT L.G., PIERRE M., JOYEUX D., AURTENETXE G., UNANUA J., PUSTORINO S., HEISE F.J., SALOMON R., TWILT L., VAN OERLE J.
Valorisation project - Natural Fire Safety Concept
Final Report EUR 20349 EN, 2002.

15 SCHLEICH J.B
REFAO-CAFIR, Computer assisted Analysis of the Fire Resistance of Steel and Composite Concrete-Steel Structures / C.E.C. Research 7210 SA/502
Final Report EUR 10828 EN, Luxembourg 1987, RPS Report N° 1/90

16 CAJOT L.G., MATHIEU J., SCHLEICH J.B
REFAO-II, Practical Design Tools for Composite Steel Concrete Construction Elements Submitted to ISO-FIRE, Considering the Interaction Between Axial Load N and Bending Moment M, C.E.C. Research 7210-SA/504
Final Report EUR 13309 EN, Luxembourg 1991, RPS Report N° 3/90.

17 CAJOT L.G., CHANTRAIN PH., MATHIEU J., SCHLEICH J.B
REFAO-III, Practical Design Tools for Unprotected Steel Columns Submitted to ISO-Fire, C.E.C. Research 7210-SA/505
Final Report Eur 14348 EN, Luxembourg 1992, RPS Report N° 11/91.

18 CAJOT L.G., PIERRE M., SCHLEICH J.B., WARSZTA F
Buckling Curves in Case of Fire - Part I (Main Text) and Part II (Annexes)
C.E.C. Research 7210-SA/515
Final Report EUR 18380 EN, Luxembourg 1996, RPS Report N° 25/96.

19 ENV 1993-1, Eurocode 3: Design of Steel Structures
Part 1-2, General Rules - Structural Fire Design
CEN, 1995

20 ENV 1994-1-2, Eurocode 4: Design of composite steel and concrete structures
Part 1.2, General Rules - Structural fire design
CEN, 1994

21 TWILT L et al
Design tools for the behaviour of fire exposed multi-storey steel framed buildings
ECCS project 7210 PA, PB, PC, PD112
Final report, December 2002

22. BAILEY, C.G. and MOORE, D.B.
The structural behaviour of steel frames with composite floor slabs subject to fire, Part 1: Theory
The Structural Engineer (UK), June 2000

23. BAILEY, C.G. and MOORE, D.B.
The structural behaviour of steel frames with composite floor slabs subject to fire, Part 2: Design
The Structural Engineer (UK), June 2000

ANNEX A EXAMPLE OF OZONE

Different fire scenarios have been analysed in the scope of this project. As an example, a set of data for a given fire compartment is described.

A.1 COMPARTMENT DESCRIPTION

The compartment consists in (see **Error! Reference source not found.**):

- a rectangular floor
- a flat roof
- 4 walls

The 3 dimensional parameters for the compartment are (see **Error! Reference source not found.**):

- Height : 4,155 m
- Depth : 21 m
- Length : 22 m

a) Floor and ceiling

The floor and ceiling are composed of a normal weight concrete (see Figure A.3 and **Error! Reference source not found.**):

- thickness: 11,7 cm,
- unit mass: 2300 kg/m^3
- conductivity: 2 W/mK (see § 3.3 of [1])
- specific heat: 900 J/kgK
- the relative emissivity of hot surface: 0,8
- the relative emissivity of cold surface: 0,8

b) Layers of the walls

Walls 1,2 and 4 (external wall) are made of (from inside to outside of the compartment) (see Figure A.5, Figure A.6 and Figure A.8):

For the layer 1: Mineral insulation with the following characteristics:

- thickness: 6 cm,
- unit mass : 200 kg/m^3
- conductivity: 0,0483 W/mK
- specific heat: 751 J/kgK
- the relative emissivity of hot surface: 0,8
- the relative emissivity of cold surface: 0,8

For the layer 2: Brick with the following characteristics:

- thickness: 17,5 cm,
- unit mass : 2000 kg/m^3
- conductivity: 1,04 W/mK (see § 3.3 of reference 24)
- specific heat: 1113 J/kgK
- the relative emissivity of hot surface: 0,8
- the relative emissivity of cold surface: 0,8

Wall 3 (internal wall) is made of (see **Error! Reference source not found.**): Only one layer: concrete blocks with the following characteristics:

- thickness: 20 cm,
- unit mass : 1375 kg/m^3
- conductivity: 0,42 W/mK
- specific heat: 753 J/kgK
- the relative emissivity of hot surface: 0,8
- the relative emissivity of cold surface: 0,8

c) Openings

2 identical openings have been considered on the walls 2 and 4 (façade walls) (see Figure A.6 and Figure A.8):

- Sill Height Hi = 0,5 m
- Soffit Height Hs = 2,0 m
- Width = 19,8 m

All the openings are considered completely opened from the beginning of the simulation. There is no forced ventilation.

A.2 Fire

a) Determination of the design fire load $q_{f,d}$

Usually the design fire load $q_{f,d}$ is calculated automatically by the software Ozone according the active fire fighting measures and the characteristic fire load $q_{f,k}$ depending on the occupation. That characteristic fire loads $q_{f,k}$ for the different occupancies are pre-defined.

For an office building, the pre-defined value of $q_{f,k}$ is 511 MJ/m².

However, in order to provide temperature-time curves for the range of fire loads 400, 500, 600, 700 and 800 MJ/m², fictitious characteristic fire loads and fictitious fire risk area have been introduced.

In this example, a fictitious characteristic fire load of 625 MJ/m² and fictitious fire risk area of 12,5 m² have been taken into account (see Figure A.9), so that the design fire load obtained after multiplying by the different gamma factors and the combustion efficiency factor (0,8) is equal to 500 MJ/m².

$q_{f,d} = \gamma_{q,1} \cdot \gamma_{q,2} \cdot \gamma_{ni} \cdot m \cdot q_{f,k}$ (see § 5.1 of 24)

In that case: $\gamma_{q,1} = 1$ (see table 5.10 of 24)

$\gamma_{q,2}$= 1 (see table 5.12 of 24])

γ_{ni} = 1 (see table 5.16 of 24)

m = 0,8 (see § 4.1.1 of 24)

$q_{f,d}$ = 1 . 1 . 1 . 0,8 . 625 = 500 MJ/m²

b) Combustion model (see Figure A.9):

Heat of Fuel = 17,5 MJ/kg (see § 4.1.1 of 24)

Efficiency Factor m = 0,8

Combustion Model = Extended fire duration (see § 5.1.6 of 25)

A.3 Steel profile

The unprotected section is an 305x165x40 UB exposed on three sides (see Figure A.11).

The profile is heated by Hot Zone Temperature (see Figure A.12). No localised effect has been considered.

A.4 Strategy

The Ozone simulation starts as a 2 zone model. If one of the 4 following conditions is fulfilled, the program switches to a 1 zone model (see Figure A.13):

Upper layer temperature ≥500°C

Some combustible materials are in the upper layer. The upper layer temperature is greater than the ignition temperature of these materials taken, in that case, equal to 300°C.

- Interface height ≤ 0,2 m
- Fire Area ≥ 0,25 m²

A.5 General Assumptions

(See Figure A.14)

a) Openings:

Radiation through closed openings: 0,8

Bernoulli coefficient: 0,7

b) Physical characteristics of compartment

Initial temperature: 293 °K

Initial pressure: 100000 Pa

c) Parameters of wall material

Convection coefficient at the hot surface: 25 W/m²

Convection coefficient at the cold surface: 9 W/m²

d) air entrained model

Heskestad (see § 5.1.7 of [2])

A.5.1 Results

Hot zone and steel temperature (see Figure A.15)

Rate of heat release (see Figure A.16)

Oxygen mass (see Figure A.17)

Zone interface elevation (see **Error! Reference source not found.**)

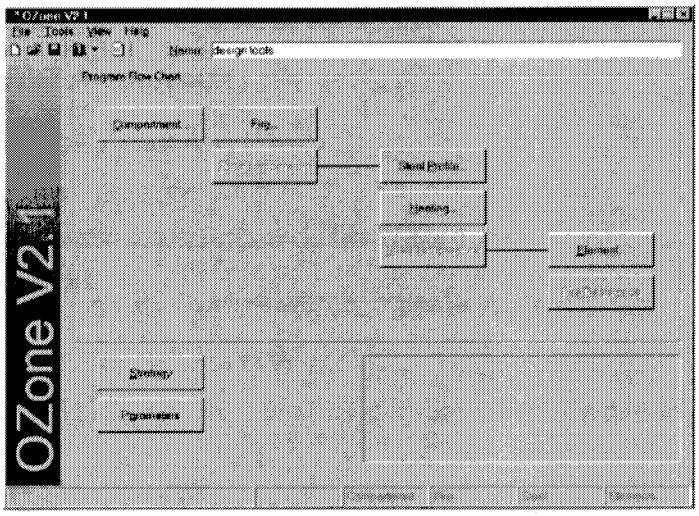

Figure A.1 *Ozone*

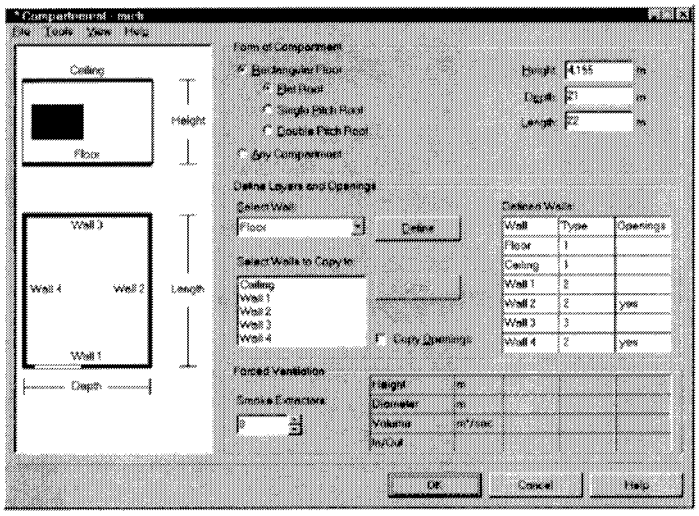

Figure A.2 *Ozone*

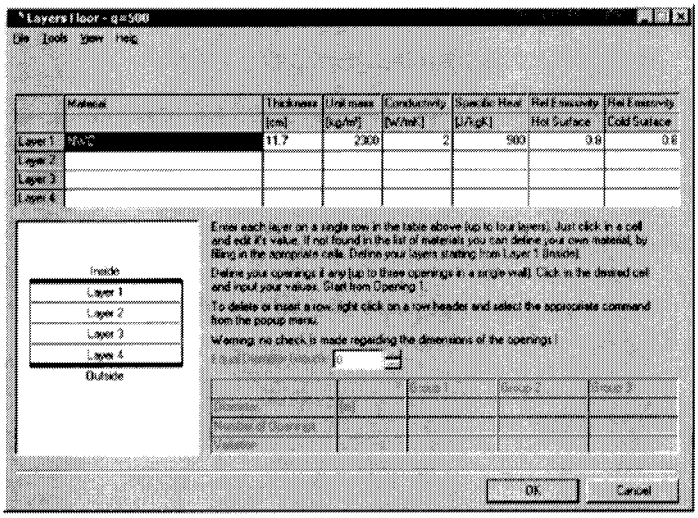

Figure A.3 *Ozone*

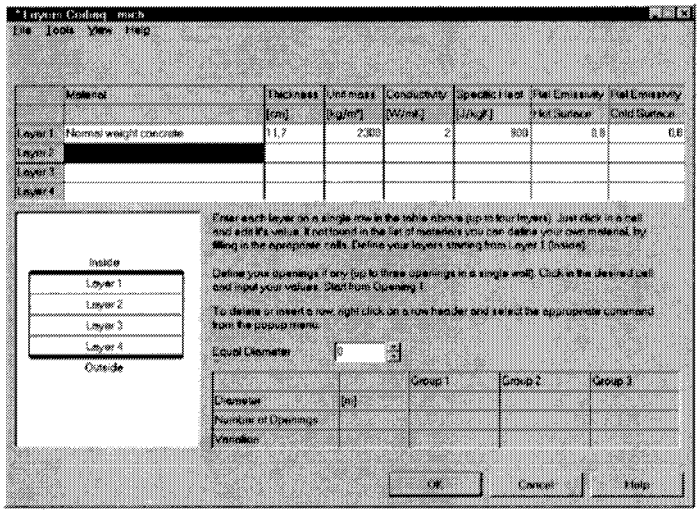

Figure A.4 *Ozone*

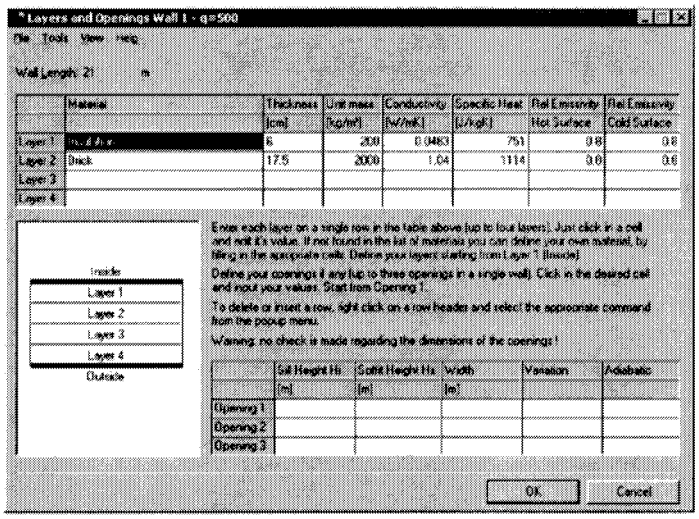

Figure A.5 *Ozone*

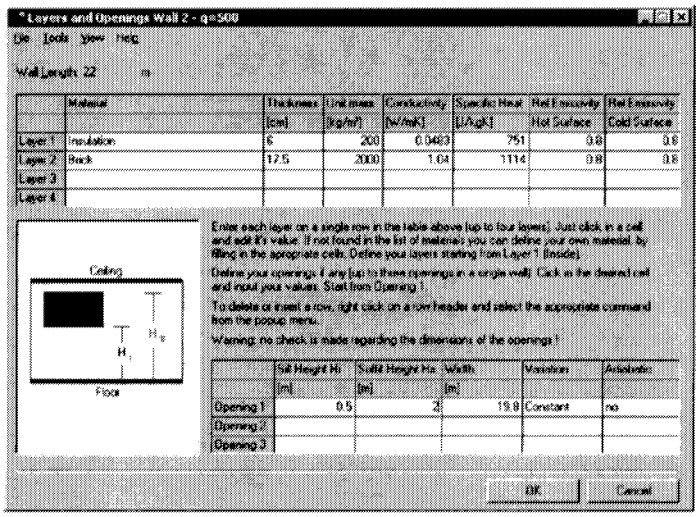

Figure A.6 *Ozone*

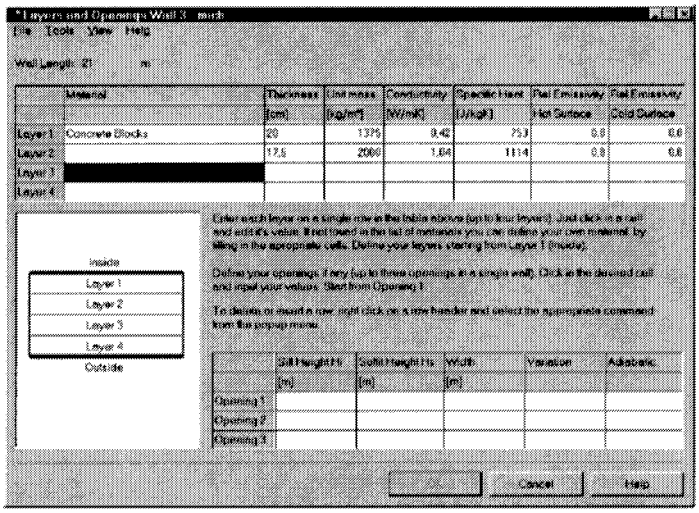

Figure A.7 *Ozone*

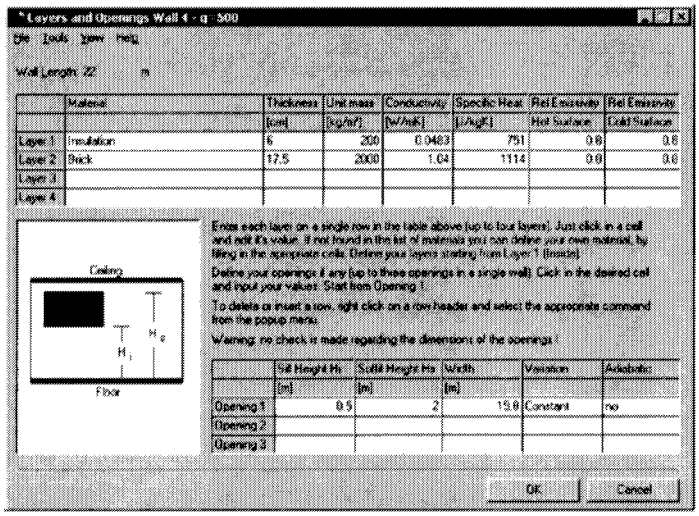

Figure A.8 *Ozone*

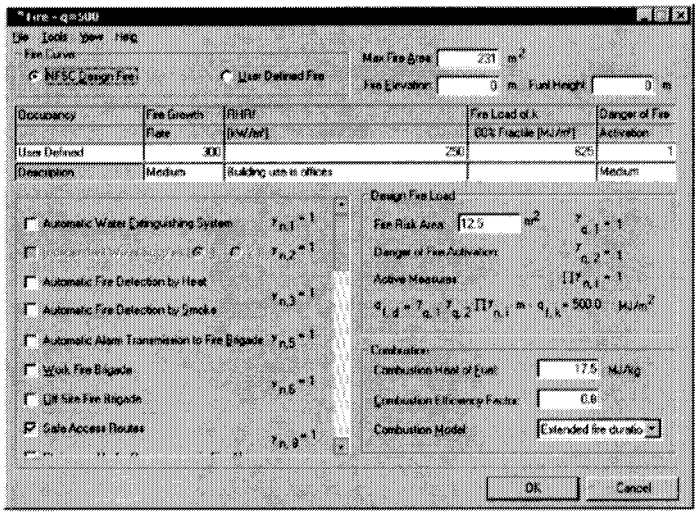

Figure A.9 *Ozone*

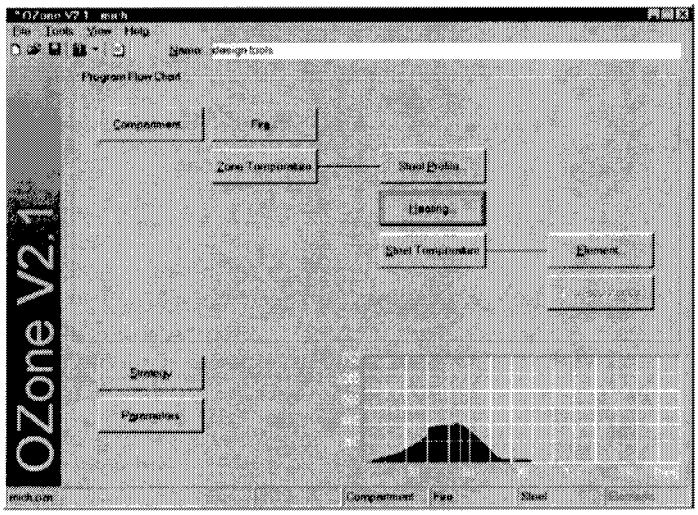

Figure A.10 *Ozone*

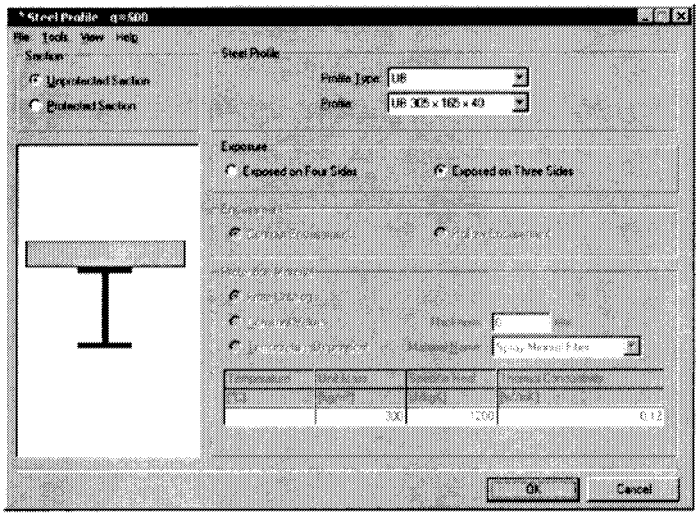

Figure A.11 *Ozone*

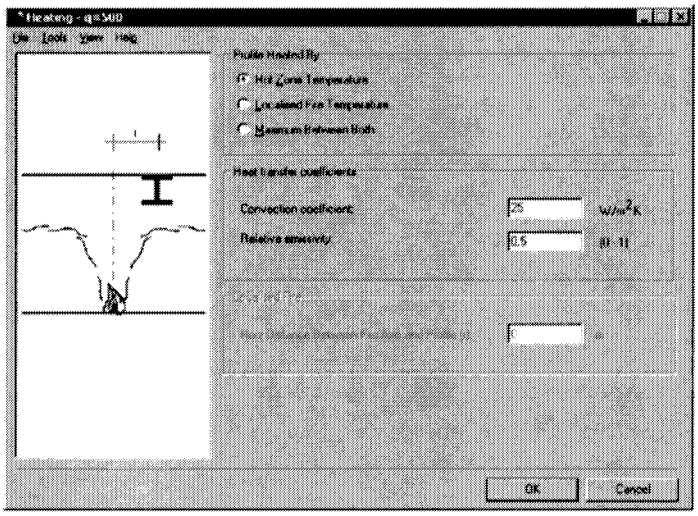

Figure A.12 *Ozone*

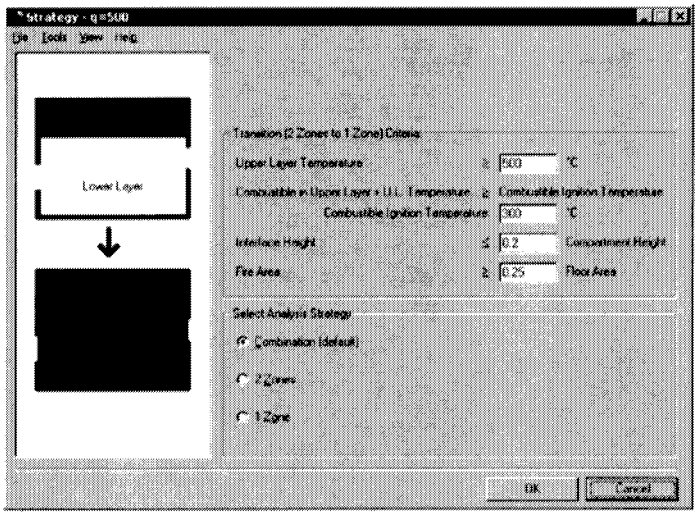

Figure A.13 *Ozone*

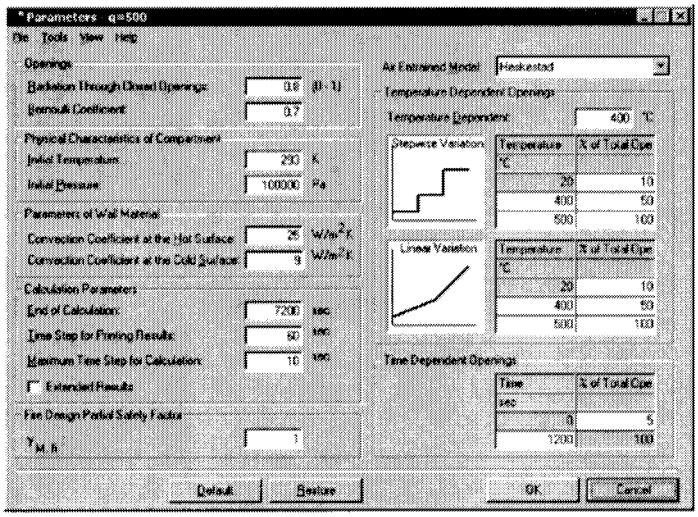

Figure A.14 *Ozone*

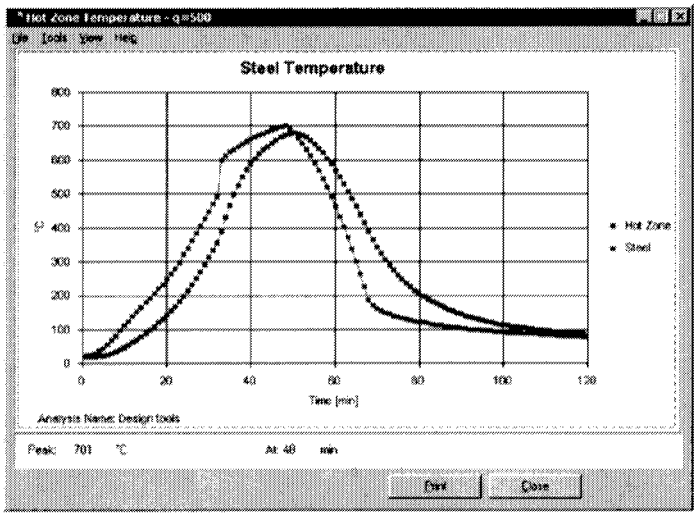

Figure A.15 *Ozone*

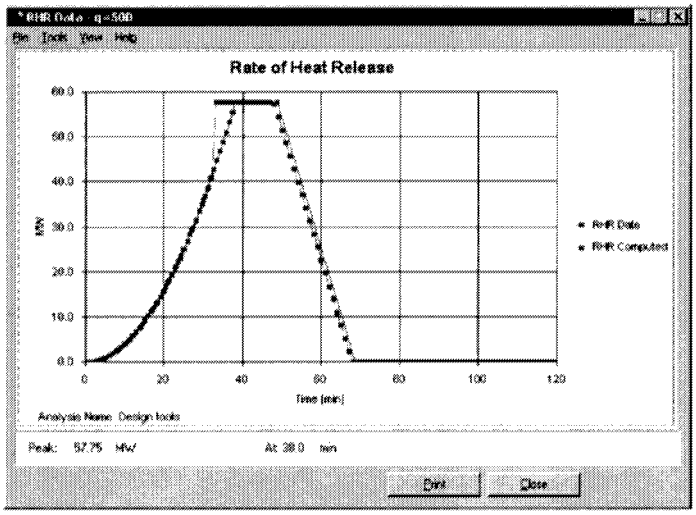

Figure A.16 *Ozone*

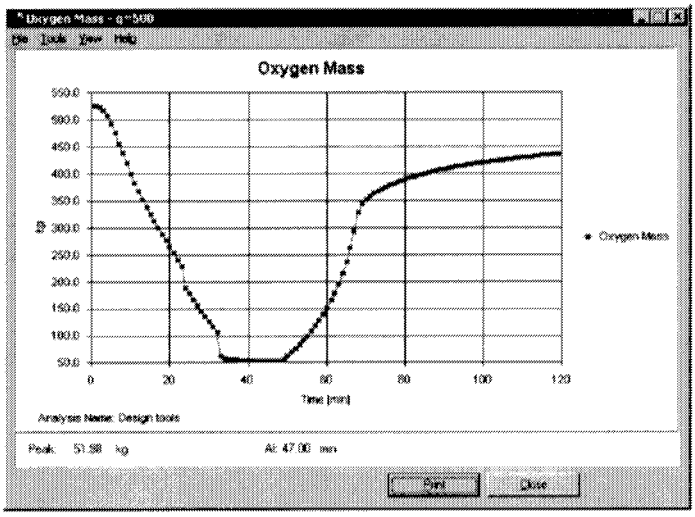

Figure A.17 *Ozone*

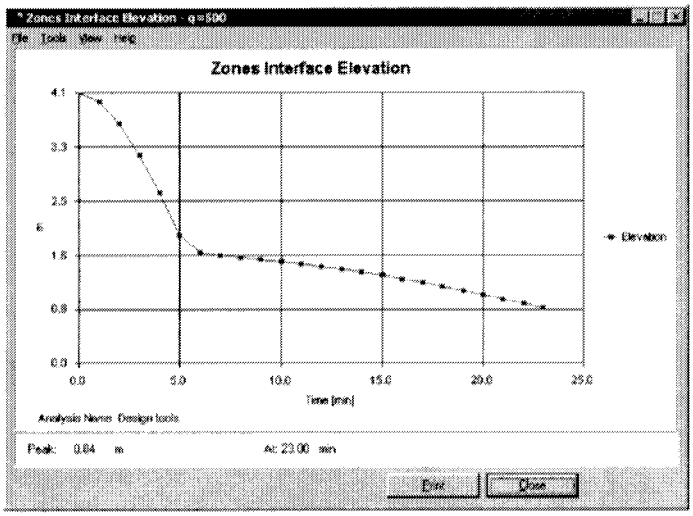

Figure A.18 *Ozone*

References in Annex A

24 SCHLEICH J-B., CAJOT L-G., et al
"Valorisation Project: Natural Fire Safety Concept"
CEC Agreement 7215-PA/PB/PC – 042
August 2001.

25 SCHLEICH J-B., CAJOT L-G., et al
"Natural Fire Safety Concept". Full Scale Tests, Implementation in the Eurocodes and Development of an User-friendly Design Tool
CEC Agreement 7210-PA/PB/PC/PD/PE/PF/PR – 060
June 2001.

ANNEX B DEFORMATION CRITERIA

The aim of any structural fire safety analysis is to determine whether, for a specified period of time, the fire exposed structure will fail or not. In a design based on classification, the required fire resistance time refers to the standard fire curve. In the natural fire safety concept, often a complete burnout is considered (i.e. the effect of active fire safety measures is implicitly taken into account via the design fire load density, see Chapter 2). If it is not necessary for the building to survive a complete burnout, the required time is related to the time necessary for inspection by the fire services and evacuation of the occupants.

In either case it is necessary to specify objective and functional performance criteria for failure.

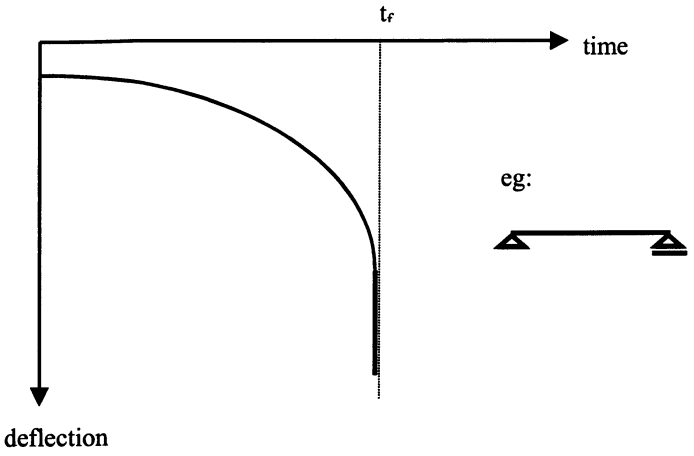

Figure B.1 *A typical run-away situation*

Under standard fire conditions (i.e. monotonically rising gas temperature) and for structural components for which there are no geometrical non-linearities, a typical "run-a-way" situation will occur, provided unlimited deformation capacity is available (see Figure B.1). The failure conditions follow from:

$$Limit\ t \Rightarrow t_f \ \frac{d\delta}{dt} = \infty$$

where:

t	is	time
tf	is	fire resistance time
δ	is	deflection

In standard fire tests it is not possible to measure an infinitive high rate of deflection. Therefore, a arbitrary (but relatively high) limit is set to the rate of deflection:

$$\frac{d\delta}{dt} = \frac{L^2}{9000h}$$

where

L	is	span
h	is	depth of the member

If the (measured) maximum value of dδ/dt is beyond the limiting value, the load bearing capacity of the structural element under consideration is assumed to be exhausted. In order to avoid that any "dip" in an early stage of the deflection history is be considered as "failure", the high limiting rate of deflection is not applied until the relative deformation δ/L exceeds L/30.

In calculations, the temperature field for which the above condition is fulfilled follows from an analysis of the structural element at elevated temperatures. Such analyses do not necessarily give information on the state of deformation of the structure. The so-called "simple" calculation methods in EC3-1-2 and EC4-1-2[19, 20]("structural fire design") for steel and steel concrete structures are based on plasticity theory and follow this approach.

When the above conditions hold, both the interpretation of standard fire tests and the outcomes of theoretical analyses confirm that "run-away" occurs very suddenly. Setting an additional limit to the deformation - which may be necessary for practical reasons – has, under such conditions, only a marginal effect on the fire resistance and may be ignored.

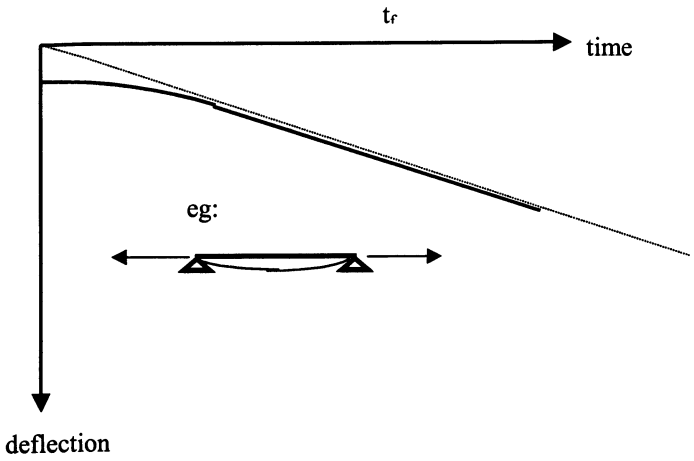

Figure B.2 *Effect of membrane action*

However, there are situations in which "run-away" will be suppressed or will not occur at all. A well known example is a beam or slab, with fixed supports, under standard fire test conditions. When deflection increases, membrane forces will develop and the load bearing capacity will gradually transform from bending into membrane action. See Fig. n+1. Such a beam/slab may reach extreme large deflections, without ever approaching a run-away condition. This may lead to unacceptable situations in practice, such as malfunctioning of fire partitions, occurrence of gaps in joints between floor slabs, damage to structural fire protection etc. Hence, for interpreting the results of standard fire tests, in addition to a maximum rate of deformation, a limit to deformations is set (symbols as defined above):

$$\delta = \frac{L^2}{400\,h}$$

When analysing a structural system under natural fire conditions, similar complications occur. First of all, the analysis is not limited to one single member exposed to fire – as in the case of standard fire tests – but applies to a structural system, parts of which are exposed to fire, other parts are not. This means that membrane action may – depending on the design features – play an important role and

reduce any run-away effects. Also, since natural fire exposure is considered, the gas temperature is not continuously increasing – as in the case of standard fire conditions - but will, during the decay period of the fire, decrease. Consequently, the temperatures in the structure will, with some delay, also reduce. This effect is of special importance when the structural behaviour during the complete burnout is relevant. When the construction cools down, the deformations will (partially) recover.

For some typical time-temperature and time-deflection curves resulting from an analysis of a structural system under natural fire conditions, see Figure B.3 and Figure B.4.

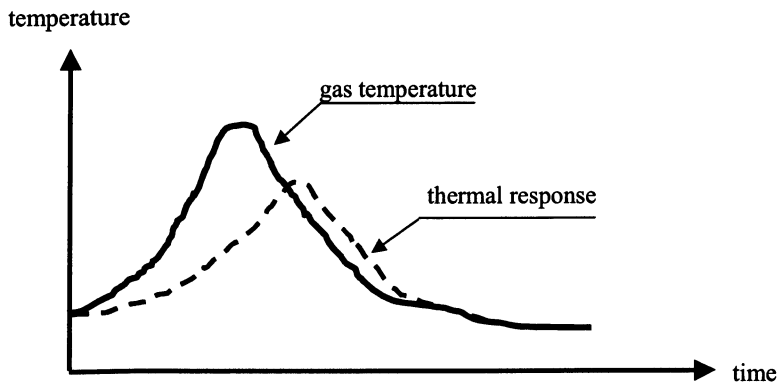

Figure B.3 *Gas temperature and thermal response in a natural fire analysis*

Figure B.4 *Mechanical response in a natural fire analysis*

In a similar manner to that of a simple beam under membrane action, the structural system may undergo extreme deformation without breaching the rate of deflection failure condition, since no run-away occurs. As indicated before, this is not acceptable and the introduction of a deformation criterion is necessary. For practical reasons, in this Design Guide, the same limiting value will be used as has been agreed upon for the interpretation of standard fire testing, however with the following modification: δ is the relative deflection of the structural member under consideration (with reference to its supports) and not the absolute value, as when interpreting standard fire test results. The reason is that the curvature of the member is the significant aspect and not so much its maximum displacement. For the interpretation of the result of a standard fire test this is not of importance, since during a test

the member is rigidly supported on the furnace wall. Hence, the following deformation criteria is adopted:

$$\delta_{rel} = \frac{L^2}{400\,h}$$

with

δrel	is	the maximum relative deflection of the member with reference to the supports
L	is	span of the member
h	is	depth of the member

With L/h ≈ 20 for hot rolled steel beams, this condition can be simplified to:

$$\delta_{rel} = \frac{L}{20}$$

However, it must be emphasised that the above limiting value has an arbitrary character only. It has been introduced because of the need to avoid, for practical reasons, extreme deformations in fire exposed structural systems. By choosing a value identical to the one on which international agreement has been reached in the adjacent field of fire testing, hopefully the probability of acceptance will increase.

ANNEX C DESIGN TABLES

C.1 General

In this Annex Design Tables are presented for use with the BRE simple method, described in Section 8. The use of the Tables, together with a design example, is described in Section 8.2

For convenience, the relationship between the 42 cases examined and the 17 Design Tables is repeated here (Table 8.2).

Table 8.2 *Relationship between design cases and design tables*

Fire load (MJ/m^2)	Window height (m), Opening factor ($m^{1/2}$)						
	0,5	1,0	1,5	2,0	2,5	3,0	3,655
	0,011	0,031	0,057	0,087	0,122	0,161	0,216
200	B	1	2	1	B	B	B
300	B	3	4	5	6	B	B
400	9	5	7	7	8	B	B
500	9	4	10	10	3	9	B
600	9	11	12	10	13	6	B
700	9	14	15	16	17	1	B

Note:

The imposed load specified in each tables the load used for normal design. For the fire condition, the load has been reduced in accordance with EC1-1-2 to 50%. For each span 1 and span 2 combination, a minimum reinforcing mesh is given together with the additional, total load to be applied to the edge beams parallel to span 1. Refer to Section 8.2 for more details.

Design Table 1

Fire load (MJ/m^2)/ Opening factor (m$^{1/2}$) 200 / 0,031, 200 / 0,087 700 / 0,016

200.2

Imposed load 2,5 kN/m2

	Span 1	Mesh/Extra Load (kN)					
Span 2	6	7	8	9	10	11	12
6	6x200 / 0	6x200 / 0	6x200 / 0	6x200 / 0	6x200 / 2	6x200 / 5	6x200 / 8
7	6x200 / 0	6x200 / 0	6x200 / 0	6x200 / 3	6x200 / 5	6x200 / 9	6x200 / 12
8	6x200 / 0	6x200 / 0	6x200 / 2	6x200 / 5	6x200 / 8	6x200 / 12	6x200 / 16
9	6x200 / 0	6x200 / 0	6x200 / 3	6x200 / 7	6x200 / 11	6x200 / 15	6x200 / 20
10	6x200 / 0	6x200 / 1	6x200 / 4	6x200 / 8	6x200 / 13	6x200 / 18	6x200 / 23
11	6x200 / 0	6x200 / 1	6x200 / 5	6x200 / 10	6x200 / 15	6x200 / 20	6x200 / 26
12	6x200 / 0	6x200 / 2	6x200 / 6	6x200 / 11	6x200 / 17	6x200 / 23	6x200 / 29

Imposed load 3,5 kN/m2

	Span 1	Mesh/Extra Load (kN)					
Span 2	6	7	8	9	10	11	12
6	6x200 / 0	6x200 / 0	6x200 / 0	6x200 / 0	6x200 / 1	6x200 / 4	7x200 / 7
7	6x200 / 0	6x200 / 0	6x200 / 0	6x200 / 2	6x200 / 5	6x200 / 8	7x200 / 11
8	6x200 / 0	6x200 / 0	6x200 / 0	6x200 / 4	6x200 / 7	6x200 / 11	6x200 / 16
9	6x200 / 0	6x200 / 0	6x200 / 2	6x200 / 6	6x200 / 10	6x200 / 15	6x200 / 19
10	6x200 / 0	6x200 / 0	6x200 / 3	6x200 / 7	6x200 / 12	6x200 / 17	6x200 / 23
11	6x200 / 0	6x200 / 0	6x200 / 4	6x200 / 9	6x200 / 14	6x200 / 20	6x200 / 26
12	7x200 / 0	7x200 / 1	6x200 / 5	6x200 / 10	6x200 / 16	6x200 / 22	6x200 / 29

Imposed load 4,5 kN/m2

	Span 1	Mesh/Extra Load (kN)					
Span 2	6	7	8	9	10	11	12
6	6x200 / 0	6x200 / 0	6x200 / 0	6x200 / 0	6x200 / 1	6x200 / 3	7x200 / 6
7	6x200 / 0	6x200 / 0	6x200 / 0	6x200 / 1	6x200 / 4	6x200 / 7	7x200 / 11
8	6x200 / 0	6x200 / 0	6x200 / 0	6x200 / 3	6x200 / 7	6x200 / 11	7x200 / 15
9	6x200 / 0	6x200 / 0	6x200 / 1	6x200 / 5	6x200 / 9	6x200 / 14	7x200 / 19
10	6x200 / 0	6x200 / 0	6x200 / 2	6x200 / 7	6x200 / 12	6x200 / 17	6x200 / 23
11	6x200 / 0	6x200 / 0	6x200 / 3	6x200 / 8	6x200 / 14	6x200 / 20	6x200 / 26
12	7x200 / 0	7x200 / 0	7x200 / 4	7x200 / 10	6x200 / 16	6x200 / 22	6x200 / 29

Imposed load 5,5 kN/m2

	Span 1	Mesh/Extra Load (kN)					
Span 2	6	7	8	9	10	11	12
6	6x200 / 0	6x200 / 0	6x200 / 0	6x200 / 0	6x200 / 0	7x200 / 2	7x200 / 6
7	6x200 / 0	6x200 / 0	6x200 / 0	6x200 / 0	6x200 / 3	6x200 / 7	7x200 / 10
8	6x200 / 0	6x200 / 0	6x200 / 0	6x200 / 2	6x200 / 6	6x200 / 10	7x200 / 15
9	6x200 / 0	6x200 / 0	6x200 / 0	6x200 / 4	6x200 / 8	6x200 / 14	7x200 / 19
10	6x200 / 0	6x200 / 0	6x200 / 1	6x200 / 6	6x200 / 11	6x200 / 16	7x200 / 23
11	7x200 / 0	6x200 / 0	6x200 / 2	6x200 / 7	6x200 / 13	6x200 / 19	7x200 / 26
12	7x200 / 0	7x200 / 0	7x200 / 3	7x200 / 9	7x200 / 15	7x200 / 22	6x200 / 29

Note: The imposed load is the load used for normal design. For the fire condition, the load has been reduced in accordance with EC1-1-2 to 50%.
For each span 1 and span 2 combination, a minimum reinforcing mesh is given together with the additional, total load to be applied to the edge beams parallel to span 1.

Design Table 2

Fire load (MJ/m^2)/ Opening factor (m$^{1/2}$) 200 / 0,057

200.3

Imposed load 2,5 kN/m2

Span 2	Span 1 Mesh/Extra Load (kN)						
	6	7	8	9	10	11	12
6	6x200 / 0	6x200 / 0	6x200 / 1	6x200 / 3	6x200 / 6	7x200 / 9	7x200 / 12
7	6x200 / 0	6x200 / 0	6x200 / 3	6x200 / 6	6x200 / 10	6x200 / 14	7x200 / 18
8	6x200 / 0	6x200 / 2	6x200 / 5	6x200 / 9	6x200 / 14	6x200 / 18	7x200 / 23
9	6x200 / 0	6x200 / 3	6x200 / 7	6x200 / 12	6x200 / 17	6x200 / 22	7x200 / 27
10	6x200 / 1	6x200 / 4	6x200 / 9	6x200 / 14	6x200 / 20	6x200 / 25	7x200 / 32
11	7x200 / 1	6x200 / 6	6x200 / 11	6x200 / 16	6x200 / 22	6x200 / 29	6x200 / 36
12	7x200 / 2	7x200 / 7	7x200 / 12	7x200 / 18	7x200 / 25	6x200 / 32	6x200 / 39

Imposed load 3,5 kN/m2

Span 2	Span 1 Mesh/Extra Load (kN)						
	6	7	8	9	10	11	12
6	6x200 / 0	6x200 / 0	6x200 / 0	6x200 / 3	6x200 / 6	7x200 / 9	7x200 / 12
7	6x200 / 0	6x200 / 0	6x200 / 3	6x200 / 6	6x200 / 10	7x200 / 14	7x200 / 18
8	6x200 / 0	6x200 / 1	6x200 / 5	6x200 / 9	6x200 / 14	7x200 / 19	7x200 / 24
9	6x200 / 0	6x200 / 3	6x200 / 7	6x200 / 12	6x200 / 17	7x200 / 23	7x200 / 29
10	6x200 / 0	6x200 / 4	6x200 / 9	6x200 / 14	6x200 / 20	7x200 / 27	7x200 / 33
11	7x200 / 1	7x200 / 5	7x200 / 11	7x200 / 16	7x200 / 23	6x200 / 30	7x200 / 37
12	7x200 / 1	7x200 / 6	7x200 / 12	7x200 / 18	7x200 / 26	7x200 / 33	7x200 / 41

Imposed load 4,5 kN/m2

Span 2	Span 1 Mesh/Extra Load (kN)						
	6	7	8	9	10	11	12
6	6x200 / 0	6x200 / 0	6x200 / 0	6x200 / 2	7x200 / 6	7x200 / 9	8x200 / 13
7	6x200 / 0	6x200 / 0	6x200 / 2	6x200 / 6	7x200 / 10	7x200 / 14	7x200 / 19
8	6x200 / 0	6x200 / 1	6x200 / 5	6x200 / 9	7x200 / 14	7x200 / 19	7x200 / 25
9	6x200 / 0	6x200 / 2	6x200 / 7	6x200 / 12	7x200 / 18	7x200 / 24	7x200 / 30
10	7x200 / 0	7x200 / 3	7x200 / 9	7x200 / 15	6x200 / 21	7x200 / 28	7x200 / 35
11	7x200 / 0	7x200 / 5	7x200 / 10	7x200 / 17	7x200 / 24	7x200 / 31	7x200 / 39
12	8x200 / 1	7x200 / 6	7x200 / 12	7x200 / 19	7x200 / 26	7x200 / 35	7x200 / 43

Imposed load 5,5 kN/m2

Span 2	Span 1 Mesh/Extra Load (kN)						
	6	7	8	9	10	11	12
6	6x200 / 0	6x200 / 0	6x200 / 0	6x200 / 2	7x200 / 5	7x200 / 9	8x200 / 13
7	6x200 / 0	6x200 / 0	6x200 / 2	6x200 / 6	7x200 / 10	7x200 / 15	8x200 / 20
8	6x200 / 0	6x200 / 0	6x200 / 4	6x200 / 9	7x200 / 14	7x200 / 20	7x200 / 26
9	6x200 / 0	6x200 / 2	6x200 / 7	6x200 / 12	7x200 / 18	7x200 / 25	7x200 / 31
10	7x200 / 0	7x200 / 3	7x200 / 9	7x200 / 15	7x200 / 22	7x200 / 29	7x200 / 37
11	7x200 / 0	7x200 / 4	7x200 / 10	7x200 / 17	7x200 / 25	7x200 / 33	7x200 / 41
12	8x200 / 0	8x200 / 5	7x200 / 12	7x200 / 19	7x200 / 27	7x200 / 36	7x200 / 45

Note: The imposed load is the load used for normal design. For the fire condition, the load has been reduced in accordance with EC1-1-2 to 50%.
For each span 1 and span 2 combination, a minimum reinforcing mesh is given together with the additional, total load to be applied to the edge beams parallel to span 1

Design Table 3

Fire load (MJ/m^2)/ Opening factor (m$^{1/2}$) 300 / 0,031, 500 / 0,122

300.2

Imposed load 2,5 kN/m2

	Span 1	Mesh/Extra Load (kN)					
Span 2	6	7	8.00	9	10	11	12
6	6x200 / 0	6x200 / 1	6x200 / 3	6x200 / 7	7x200 / 10	7x200 / 13	7x200 / 17
7	6x200 / 0	6x200 / 3	6x200 / 7	6x200 / 11	6x200 / 15	7x200 / 19	7x200 / 24
8	6x200 / 1	6x200 / 5	6x200 / 9	6x200 / 14	6x200 / 19	7x200 / 25	7x200 / 30
9	6x200 / 3	6x200 / 7	6x200 / 12	6x200 / 17	6x200 / 23	7x200 / 29	7x200 / 36
10	7x200 / 4	6x200 / 9	6x200 / 14	6x200 / 20	6x200 / 27	7x200 / 34	7x200 / 41
11	7x200 / 5	7x200 / 10	7x200 / 16	7x200 / 23	7x200 / 30	6x200 / 38	7x200 / 46
12	7x200 / 6	7x200 / 11	7x200 / 18	7x200 / 25	7x200 / 33	7x200 / 41	7x200 / 50

Imposed load 3,5 kN/m2

	Span 1	Mesh/Extra Load (kN)					
Span 2	6	7	8.00	9	10	11	12
6	6x200 / 0	6x200 / 0	6x200 / 3	6x200 / 7	7x200 / 10	7x200 / 14	8x200 / 18
7	6x200 / 0	6x200 / 3	6x200 / 7	6x200 / 11	7x200 / 16	7x200 / 21	8x200 / 26
8	6x200 / 1	6x200 / 5	6x200 / 10	6x200 / 15	7x200 / 21	7x200 / 27	7x200 / 33
9	6x200 / 2	6x200 / 7	6x200 / 13	6x200 / 19	7x200 / 25	7x200 / 32	7x200 / 39
10	7x200 / 4	7x200 / 9	7x200 / 15	7x200 / 22	7x200 / 29	7x200 / 37	7x200 / 45
11	7x200 / 5	7x200 / 11	7x200 / 17	7x200 / 25	7x200 / 33	7x200 / 41	7x200 / 50
12	8x200 / 6	8x200 / 12	7x200 / 19	7x200 / 27	7x200 / 36	7x200 / 45	7x200 / 55

Imposed load 4,5 kN/m2

	Span 1	Mesh/Extra Load (kN)					
Span 2	6	7	8	9	10	11	12
6	6x200 / 0	6x200 / 0	6x200 / 3	7x200 / 7	7x200 / 11	8x200 / 15	8x200 / 20
7	6x200 / 0	6x200 / 3	6x200 / 7	7x200 / 12	7x200 / 17	7x200 / 22	8x200 / 28
8	6x200 / 1	6x200 / 5	6x200 / 10	7x200 / 16	7x200 / 22	7x200 / 29	8x200 / 35
9	7x200 / 2	7x200 / 7	7x200 / 13	7x200 / 20	7x200 / 27	7x200 / 34	8x200 / 42
10	7x200 / 4	7x200 / 9	7x200 / 16	7x200 / 23	7x200 / 31	7x200 / 39	7x200 / 48
11	8x200 / 5	7x200 / 11	7x200 / 18	7x200 / 26	7x200 / 35	7x200 / 44	7x200 / 54
12	8x200 / 6	8x200 / 13	8x200 / 20	8x200 / 29	7x200 / 38	7x200 / 48	7x200 / 59

Imposed load 5,5 kN/m2

	Span 1	Mesh/Extra Load (kN)					
Span 2	6	7	8	9	10	11	12
6	6x200 / 0	6x200 / 0	7x200 / 3	7x200 / 7	7x200 / 12	8x200 / 16	8x200 / 21
7	6x200 / 0	6x200 / 3	7x200 / 7	7x200 / 12	7x200 / 18	8x200 / 24	8x200 / 30
8	7x200 / 0	7x200 / 5	7x200 / 11	7x200 / 17	7x200 / 24	8x200 / 31	8x200 / 38
9	7x200 / 2	7x200 / 8	7x200 / 14	7x200 / 21	7x200 / 29	8x200 / 37	8x200 / 45
10	7x200 / 4	7x200 / 10	7x200 / 17	7x200 / 25	7x200 / 33	7x200 / 42	8x200 / 52
11	8x200 / 5	8x200 / 12	8x200 / 19	8x200 / 28	7x200 / 37	7x200 / 47	8x200 / 58
12	8x200 / 6	8x200 / 13	8x200 / 22	8x200 / 31	8x200 / 41	8x200 / 52	7x200 / 63

Note: The imposed load is the load used for normal design. For the fire condition, the load has been reduced in accordance with EC1-1-2 to 50%.
For each span 1 and span 2 combination, a minimum reinforcing mesh is given together with the additional, total load to be applied to the edge beams parallel to span 1

Design Table 4

Fire load (MJ/m^2)/ Opening factor (m$^{1/2}$) 300 / 0,057, 500 / 0,031

500.2

Imposed load 2,5 kN/m2

Span 2 \ Span 1	6	7	8	9	10	11	12
	Mesh/Extra Load (kN)						
6	6x200 / 0	6x200 / 3	6x200 / 6	7x200 / 10	7x200 / 14	8x200 / 18	8x200 / 22
7	6x200 / 2	6x200 / 6	6x200 / 10	7x200 / 15	7x200 / 20	7x200 / 25	8x200 / 31
8	6x200 / 4	6x200 / 9	6x200 / 14	7x200 / 17	7x200 / 26	7x200 / 32	8x200 / 36
9	7x200 / 6	7x200 / 11	7x200 / 15	6x200 / 23	7x200 / 30	7x200 / 38	7x200 / 45
10	7x200 / 7	7x200 / 13	7x200 / 20	7x200 / 27	7x200 / 35	7x200 / 43	7x200 / 51
11	8x200 / 8	7x200 / 15	7x200 / 22	7x200 / 30	7x200 / 39	7x200 / 48	7x200 / 57
12	8x200 / 10	8x200 / 17	8x200 / 23	7x200 / 33	7x200 / 42	7x200 / 52	7x200 / 62

Imposed load 3,5 kN/m2

Span 2 \ Span 1	6	7	8	9	10	11	12
	Mesh/Extra Load (kN)						
6	6x200 / 0	6x200 / 3	7x200 / 7	7x200 / 11	7x200 / 15	8x200 / 20	8x200 / 25
7	6x200 / 2	6x200 / 7	7x200 / 10	7x200 / 17	7x200 / 22	8x200 / 28	8x200 / 34
8	7x200 / 4	7x200 / 9	6x200 / 15	7x200 / 22	7x200 / 28	8x200 / 35	8x200 / 43
9	7x200 / 6	7x200 / 12	7x200 / 19	7x200 / 26	7x200 / 34	7x200 / 42	8x200 / 50
10	7x200 / 8	7x200 / 14	7x200 / 22	7x200 / 30	7x200 / 38	7x200 / 47	8x200 / 57
11	8x200 / 9	8x200 / 16	8x200 / 24	7x200 / 33	7x200 / 43	7x200 / 53	8x200 / 57
12	8x200 / 11	8x200 / 18	8x200 / 27	8x200 / 36	8x200 / 47	8x200 / 51	7x200 / 69

Imposed load 4,5 kN/m2

Span 2 \ Span 1	6	7	8.00	9	10	11	12
	Mesh/Extra Load (kN)						
6	6x200 / 0	6x200 / 3	7x200 / 8	7x200 / 12	8x200 / 17	8x200 / 22	10x200 / 27
7	6x200 / 2	6x200 / 7	7x200 / 12	7x200 / 18	8x200 / 24	8x200 / 31	10x200 / 37
8	7x200 / 5	7x200 / 10	7x200 / 17	7x200 / 24	8x200 / 31	8x200 / 39	8x200 / 47
9	7x200 / 7	7x200 / 13	7x200 / 20	7x200 / 28	7x200 / 37	8x200 / 46	8x200 / 55
10	8x200 / 9	8x200 / 16	8x200 / 24	7x200 / 33	7x200 / 42	8x200 / 52	8x200 / 63
11	8x200 / 10	8x200 / 18	8x200 / 27	8x200 / 36	8x200 / 47	8x200 / 54	8x200 / 70
12	10x200 / 11	10x200 / 20	8x200 / 29	8x200 / 40	8x200 / 51	8x200 / 63	8x200 / 76

Imposed load 5,5 kN/m2

Span 2 \ Span 1	6	7	8	9	10	11	12
	Mesh/Extra Load (kN)						
6	6x200 / 0	7x200 / 4	7x200 / 8	8x200 / 13	8x200 / 18	10x200 / 24	10x200 / 30
7	7x200 / 3	7x200 / 8	7x200 / 13	8x200 / 20	8x200 / 26	8x200 / 33	10x200 / 41
8	7x200 / 5	7x200 / 11	7x200 / 18	7x200 / 26	8x200 / 34	8x200 / 42	10x200 / 51
9	8x200 / 7	8x200 / 14	7x200 / 22	7x200 / 31	8x200 / 40	8x200 / 50	10x200 / 55
10	8x200 / 9	8x200 / 17	8x200 / 26	8x200 / 35	8x200 / 46	8x200 / 57	8x200 / 68
11	10x200 / 11	8x200 / 19	8x200 / 29	8x200 / 40	8x200 / 51	8x200 / 63	8x200 / 76
12	10x200 / 12	10x200 / 22	10x200 / 32	10x200 / 39	8x200 / 56	8x200 / 69	8x200 / 83

Note: The imposed load is the load used for normal design. For the fire condition, the load has been reduced in accordance with EC1-1-2 to 50%.
For each span 1 and span 2 combination, a minimum reinforcing mesh is given together with the additional, total load to be applied to the edge beams parallel to span 1

Design Table 5

Fire load (MJ/m^2)/ Opening factor (m$^{1/2}$) 300 / 0,087, 400 / 0,031

300.4

Imposed load 2,5 kN/m2

Span 2 \ Span 1	6	7	8	9	10	11	12
6	6x200 / 0	6x200 / 2	6x200 / 5	6x200 / 8	7x200 / 12	7x200 / 16	8x200 / 20
7	6x200 / 1	6x200 / 5	6x200 / 9	6x200 / 13	7x200 / 18	7x200 / 23	8x200 / 28
8	6x200 / 3	6x200 / 7	6x200 / 12	6x200 / 17	7x200 / 23	7x200 / 28	7x200 / 35
9	6x200 / 4	6x200 / 9	6x200 / 15	6x200 / 21	7x200 / 27	7x200 / 34	7x200 / 41
10	7x200 / 6	7x200 / 11	7x200 / 17	7x200 / 24	7x200 / 31	7x200 / 39	7x200 / 47
11	7x200 / 7	7x200 / 13	7x200 / 19	7x200 / 27	7x200 / 35	7x200 / 43	7x200 / 52
12	8x200 / 8	8x200 / 14	7x200 / 21	7x200 / 29	7x200 / 38	7x200 / 47	7x200 / 57

Imposed load 3,5 kN/m2

Span 2 \ Span 1	6	7	8	9	10	11	12
6	6x200 / 0	6x200 / 2	6x200 / 5	7x200 / 9	7x200 / 13	8x200 / 17	8x200 / 22
7	6x200 / 1	6x200 / 5	6x200 / 9	7x200 / 14	7x200 / 19	7x200 / 25	8x200 / 30
8	6x200 / 3	6x200 / 8	6x200 / 13	7x200 / 19	7x200 / 25	7x200 / 31	8x200 / 38
9	7x200 / 5	7x200 / 10	7x200 / 16	7x200 / 22	7x200 / 30	7x200 / 37	8x200 / 45
10	7x200 / 6	7x200 / 12	7x200 / 19	7x200 / 26	7x200 / 34	7x200 / 42	8x200 / 51
11	8x200 / 7	7x200 / 14	7x200 / 21	7x200 / 29	7x200 / 38	7x200 / 47	7x200 / 57
12	8x200 / 8	8x200 / 15	8x200 / 23	8x200 / 32	8x200 / 42	7x200 / 52	7x200 / 62

Imposed load 4,5 kN/m2

Span 2 \ Span 1	6	7	8	9	10	11	12
6	6x200 / 0	6x200 / 2	7x200 / 6	7x200 / 10	7x200 / 14	8x200 / 19	10x200 / 24
7	6x200 / 1	6x200 / 5	7x200 / 10	7x200 / 15	7x200 / 21	8x200 / 27	8x200 / 33
8	7x200 / 3	7x200 / 8	7x200 / 14	7x200 / 20	7x200 / 27	8x200 / 34	8x200 / 41
9	7x200 / 5	7x200 / 11	7x200 / 17	7x200 / 24	7x200 / 32	8x200 / 40	8x200 / 49
10	7x200 / 6	7x200 / 13	7x200 / 20	7x200 / 28	7x200 / 37	8x200 / 46	8x200 / 56
11	8x200 / 8	8x200 / 15	8x200 / 23	8x200 / 32	8x200 / 41	7x200 / 51	8x200 / 62
12	10x200 / 9	8x200 / 16	8x200 / 25	8x200 / 35	8x200 / 45	8x200 / 56	8x200 / 68

Imposed load 5,5 kN/m2

Span 2 \ Span 1	6	7	8	9	10	11	12
6	6x200 / 0	6x200 / 2	7x200 / 6	7x200 / 10	8x200 / 15	8x200 / 20	10x200 / 26
7	6x200 / 1	7x200 / 5	7x200 / 11	7x200 / 16	8x200 / 22	8x200 / 29	10x200 / 36
8	7x200 / 3	7x200 / 8	7x200 / 15	7x200 / 22	8x200 / 29	8x200 / 37	8x200 / 45
9	7x200 / 5	7x200 / 11	7x200 / 18	7x200 / 26	8x200 / 35	8x200 / 44	8x200 / 53
10	8x200 / 7	8x200 / 14	8x200 / 22	8x200 / 30	8x200 / 40	8x200 / 50	8x200 / 61
11	8x200 / 8	8x200 / 16	8x200 / 25	8x200 / 34	8x200 / 45	8x200 / 56	8x200 / 67
12	10x200 / 9	10x200 / 18	8x200 / 27	8x200 / 38	8x200 / 49	8x200 / 61	8x200 / 74

Note: The imposed load is the load used for normal design. For the fire condition, the load has been reduced in accordance with EC1-1-2 to 50%.
For each span 1 and span 2 combination, a minimum reinforcing mesh is given together with the additional, total load to be applied to the edge beams parallel to span 1

Design Table 6

Fire load (MJ/m^2)/ Opening factor (m$^{1/2}$) 300 / 0,122, 700 / 0,161

300,5

Imposed load 2,5 kN/m2

	Span 1	Mesh/Extra Load (kN)					
Span 2	6	7	8	9	10	11	12
6	6x200 / 0	6x200 / 0	6x200 / 0	6x200 / 0	6x200 / 0	6x200 / 1	6x200 / 3
7	6x200 / 0	6x200 / 0	6x200 / 0	6x200 / 0	6x200 / 2	6x200 / 4	6x200 / 7
8	6x200 / 0	6x200 / 0	6x200 / 0	6x200 / 1	6x200 / 4	6x200 / 7	6x200 / 10
9	6x200 / 0	6x200 / 0	6x200 / 0	6x200 / 2	6x200 / 5	6x200 / 9	6x200 / 13
10	6x200 / 0	6x200 / 0	6x200 / 0	6x200 / 3	6x200 / 7	6x200 / 11	6x200 / 15
11	6x200 / 0	6x200 / 0	6x200 / 1	6x200 / 5	6x200 / 9	6x200 / 13	6x200 / 18
12	6x200 / 0	6x200 / 0	6x200 / 2	6x200 / 6	6x200 / 10	6x200 / 15	6x200 / 20

Imposed load 3,5 kN/m2

	Span 1	Mesh/Extra Load (kN)					
Span 2	6	7	8	9	10	11	12
6	6x200 / 0	6x200 / 0	6x200 / 0	6x200 / 0	6x200 / 0	6x200 / 0	6x200 / 2
7	6x200 / 0	6x200 / 0	6x200 / 0	6x200 / 0	6x200 / 0	6x200 / 3	6x200 / 5
8	6x200 / 0	6x200 / 0	6x200 / 0	6x200 / 0	6x200 / 2	6x200 / 5	6x200 / 8
9	6x200 / 0	6x200 / 0	6x200 / 0	6x200 / 0	6x200 / 4	6x200 / 7	6x200 / 11
10	6x200 / 0	6x200 / 0	6x200 / 0	6x200 / 1	6x200 / 5	6x200 / 9	6x200 / 14
11	6x200 / 0	6x200 / 0	6x200 / 0	6x200 / 3	6x200 / 7	6x200 / 11	6x200 / 16
12	6x200 / 0	6x200 / 0	6x200 / 0	6x200 / 3	6x200 / 8	6x200 / 13	6x200 / 18

Imposed load 4,5 kN/m2

	Span 1	Mesh/Extra Load (kN)					
Span 2	6	7	8	9	10	11	12
6	6x200 / 0	6x200 / 0	6x200 / 0	6x200 / 0	6x200 / 0	6x200 / 0	6x200 / 1
7	6x200 / 0	6x200 / 0	6x200 / 0	6x200 / 0	6x200 / 0	6x200 / 1	6x200 / 4
8	6x200 / 0	6x200 / 0	6x200 / 0	6x200 / 0	6x200 / 0	6x200 / 3	6x200 / 7
9	6x200 / 0	6x200 / 0	6x200 / 0	6x200 / 0	6x200 / 2	6x200 / 5	6x200 / 9
10	6x200 / 0	6x200 / 0	6x200 / 0	6x200 / 0	6x200 / 3	6x200 / 7	6x200 / 12
11	6x200 / 0	6x200 / 0	6x200 / 0	6x200 / 1	6x200 / 5	6x200 / 9	6x200 / 14
12	6x200 / 0	6x200 / 0	6x200 / 0	6x200 / 1	6x200 / 6	6x200 / 11	6x200 / 16

Imposed load 5,5 kN/m2

	Span 1	Mesh/Extra Load (kN)					
Span 2	6	7	8	9	10	11	12
6	6x200 / 0	6x200 / 0	6x200 / 0	6x200 / 0	6x200 / 0	6x200 / 0	6x200 / 0
7	6x200 / 0	6x200 / 0	6x200 / 0	6x200 / 0	6x200 / 0	6x200 / 0	6x200 / 2
8	6x200 / 0	6x200 / 0	6x200 / 0	6x200 / 0	6x200 / 0	6x200 / 2	6x200 / 5
9	6x200 / 0	6x200 / 0	6x200 / 0	6x200 / 0	6x200 / 0	6x200 / 4	6x200 / 8
10	6x200 / 0	6x200 / 0	6x200 / 0	6x200 / 0	6x200 / 1	6x200 / 6	6x200 / 10
11	6x200 / 0	6x200 / 0	6x200 / 0	6x200 / 0	6x200 / 3	6x200 / 7	6x200 / 12
12	6x200 / 0	6x200 / 0	6x200 / 0	6x200 / 0	6x200 / 4	6x200 / 9	6x200 / 14

Note: The imposed load is the load used for normal design. For the fire condition, the load has been reduced in accordance with EC1-1-2 to 50%.
For each span 1 and span 2 combination, a minimum reinforcing mesh is given together with the additional, total load to be applied to the edge beams parallel to span 1

Design Table 7

Fire load (MJ/m^2)/ Opening factor (m$^{1/2}$) 400 / 0,057, 400 / 0,087

400.4

Imposed load 2,5 kN/m2

	Span 1	Mesh/Extra Load (kN)					
Span 2	6	7	8	9	10	11	12
6	6x200 / 0	6x200 / 4	6x200 / 7	7x200 / 11	7x200 / 15	7x200 / 19	8x200 / 23
7	6x200 / 3	6x200 / 7	6x200 / 11	7x200 / 16	7x200 / 21	7x200 / 26	8x200 / 32
8	6x200 / 5	6x200 / 9	6x200 / 15	6x200 / 20	7x200 / 27	7x200 / 33	7x200 / 40
9	7x200 / 6	7x200 / 12	6x200 / 18	6x200 / 25	7x200 / 32	7x200 / 39	7x200 / 47
10	7x200 / 8	7x200 / 14	7x200 / 21	7x200 / 28	7x200 / 36	7x200 / 44	7x200 / 53
11	7x200 / 9	7x200 / 16	7x200 / 23	7x200 / 31	7x200 / 40	7x200 / 49	7x200 / 59
12	8x200 / 10	8x200 / 18	7x200 / 26	7x200 / 34	7x200 / 44	7x200 / 54	7x200 / 64

Imposed load 3,5 kN/m2

	Span 1	Mesh/Extra Load (kN)					
Span 2	6	7	8	9	10	11	12
6	6x200 / 0	6x200 / 4	7x200 / 8	7x200 / 12	7x200 / 16	8x200 / 21	8x200 / 26
7	6x200 / 3	6x200 / 7	7x200 / 12	7x200 / 18	7x200 / 23	8x200 / 29	8x200 / 36
8	7x200 / 5	7x200 / 10	6x200 / 16	7x200 / 23	7x200 / 30	8x200 / 37	8x200 / 44
9	7x200 / 7	7x200 / 13	7x200 / 20	7x200 / 27	7x200 / 35	7x200 / 43	8x200 / 52
10	7x200 / 9	7x200 / 15	7x200 / 23	7x200 / 31	7x200 / 40	7x200 / 49	8x200 / 59
11	8x200 / 10	8x200 / 17	8x200 / 26	7x200 / 35	7x200 / 45	7x200 / 55	8x200 / 66
12	8x200 / 11	8x200 / 19	8x200 / 28	8x200 / 38	8x200 / 49	8x200 / 60	7x200 / 72

Imposed load 4,5 kN/m2

	Span 1	Mesh/Extra Load (kN)					
Span 2	6	7	8	9	10	11	12
6	6x200 / 0	6x200 / 4	7x200 / 8	7x200 / 13	8x200 / 18	8x200 / 23	10x200 / 29
7	6x200 / 3	6x200 / 8	7x200 / 13	7x200 / 19	8x200 / 26	8x200 / 32	10x200 / 39
8	7x200 / 6	7x200 / 11	7x200 / 18	7x200 / 25	8x200 / 32	8x200 / 40	8x200 / 49
9	7x200 / 8	7x200 / 14	7x200 / 22	7x200 / 30	7x200 / 39	8x200 / 48	8x200 / 57
10	8x200 / 9	8x200 / 17	8x200 / 25	7x200 / 34	7x200 / 44	8x200 / 54	8x200 / 65
11	8x200 / 11	8x200 / 19	8x200 / 28	8x200 / 38	8x200 / 49	8x200 / 60	8x200 / 72
12	10x200 / 12	10x200 / 21	8x200 / 31	8x200 / 42	8x200 / 54	8x200 / 66	8x200 / 79

Imposed load 5,5 kN/m2

	Span 1	Mesh/Extra Load (kN)					
Span 2	6	7	8	9	10	11	12
6	6x200 / 0	7x200 / 4	7x200 / 9	8x200 / 14	8x200 / 20	10x200 / 25	10x200 / 31
7	7x200 / 3	7x200 / 9	7x200 / 15	8x200 / 21	8x200 / 28	8x200 / 35	10x200 / 43
8	7x200 / 6	7x200 / 12	7x200 / 19	7x200 / 27	8x200 / 35	8x200 / 44	10x200 / 53
9	8x200 / 8	8x200 / 15	7x200 / 24	7x200 / 33	8x200 / 42	8x200 / 52	10x200 / 63
10	8x200 / 10	8x200 / 18	8x200 / 27	8x200 / 37	8x200 / 48	8x200 / 59	8x200 / 71
11	10x200 / 12	8x200 / 21	8x200 / 31	8x200 / 42	8x200 / 53	8x200 / 66	8x200 / 79
12	10x200 / 13	10x200 / 23	10x200 / 34	10x200 / 46	8x200 / 58	8x200 / 72	8x200 / 86

Note: The imposed load is the load used for normal design. For the fire condition, the load has been reduced in accordance with EC1-1-2 to 50%.
For each span 1 and span 2 combination, a minimum reinforcing mesh is given together with the additional, total load to be applied to the edge beams parallel to span 1

Design Table 8

Fire load (MJ/m^2)/ Opening factor (m$^{1/2}$) 400 / 0,122

400.5

Imposed load 2,5 kN/m2

	Span 1	Mesh/Extra Load (kN)					
Span 2	6	7	8	9	10	11	12
6	6x200 / 0	6x200 / 0	6x200 / 0	6x200 / 2	6x200 / 4	6x200 / 7	7x200 / 10
7	6x200 / 0	6x200 / 0	6x200 / 1	6x200 / 4	6x200 / 8	6x200 / 11	7x200 / 15
8	6x200 / 0	6x200 / 0	6x200 / 3	6x200 / 7	6x200 / 11	6x200 / 15	6x200 / 19
9	6x200 / 0	6x200 / 1	6x200 / 5	6x200 / 9	6x200 / 14	6x200 / 18	6x200 / 23
10	6x200 / 0	6x200 / 2	6x200 / 7	6x200 / 11	6x200 / 16	6x200 / 22	6x200 / 27
11	6x200 / 0	6x200 / 3	6x200 / 8	6x200 / 13	6x200 / 18	6x200 / 24	6x200 / 31
12	7x200 / 0	7x200 / 4	6x200 / 9	6x200 / 15	6x200 / 21	6x200 / 27	6x200 / 34

Imposed load 3,5 kN/m2

	Span 1	Mesh/Extra Load (kN)					
Span 2	6	7	8	9	10	11	12
6	6x200 / 0	6x200 / 0	6x200 / 0	6x200 / 1	6x200 / 4	7x200 / 6	7x200 / 10
7	6x200 / 0	6x200 / 0	6x200 / 1	6x200 / 4	6x200 / 7	6x200 / 11	7x200 / 15
8	6x200 / 0	6x200 / 0	6x200 / 3	6x200 / 6	6x200 / 11	6x200 / 15	7x200 / 20
9	6x200 / 0	6x200 / 0	6x200 / 4	6x200 / 9	6x200 / 13	6x200 / 19	7x200 / 24
10	6x200 / 0	6x200 / 2	6x200 / 6	6x200 / 11	6x200 / 16	6x200 / 22	7x200 / 28
11	7x200 / 0	6x200 / 3	6x200 / 7	6x200 / 13	6x200 / 18	6x200 / 25	6x200 / 31
12	7x200 / 0	7x200 / 3	7x200 / 9	7x200 / 14	7x200 / 21	6x200 / 28	6x200 / 35

Imposed load 4,5 kN/m2

	Span 1	Mesh/Extra Load (kN)					
Span 2	6	7	8	9	10	11	12
6	6x200 / 0	6x200 / 0	6x200 / 0	6x200 / 0	6x200 / 3	7x200 / 6	7x200 / 9
7	6x200 / 0	6x200 / 0	6x200 / 0	6x200 / 3	6x200 / 7	7x200 / 11	7x200 / 15
8	6x200 / 0	6x200 / 0	6x200 / 2	6x200 / 6	6x200 / 10	7x200 / 15	7x200 / 20
9	6x200 / 0	6x200 / 0	6x200 / 4	6x200 / 8	6x200 / 13	7x200 / 19	7x200 / 24
10	6x200 / 0	6x200 / 1	6x200 / 5	6x200 / 10	6x200 / 16	6x200 / 22	7x200 / 29
11	7x200 / 0	7x200 / 2	7x200 / 7	7x200 / 12	6x200 / 19	6x200 / 25	7x200 / 32
12	7x200 / 0	7x200 / 3	7x200 / 8	7x200 / 14	7x200 / 21	7x200 / 28	7x200 / 36

Imposed load 5,5 kN/m2

	Span 1	Mesh/Extra Load (kN)					
Span 2	6	7	8	9	10	11	12
6	6x200 / 0	6x200 / 0	6x200 / 0	6x200 / 0	7x200 / 2	7x200 / 6	7x200 / 9
7	6x200 / 0	6x200 / 0	6x200 / 0	6x200 / 2	6x200 / 6	7x200 / 11	7x200 / 15
8	6x200 / 0	6x200 / 0	6x200 / 1	6x200 / 5	6x200 / 10	7x200 / 15	7x200 / 20
9	6x200 / 0	6x200 / 0	6x200 / 3	6x200 / 8	6x200 / 13	7x200 / 19	7x200 / 25
10	7x200 / 0	6x200 / 0	6x200 / 5	6x200 / 10	6x200 / 16	7x200 / 22	7x200 / 29
11	7x200 / 0	7x200 / 1	7x200 / 6	7x200 / 12	7x200 / 19	7x200 / 26	7x200 / 33
12	7x200 / 0	7x200 / 2	7x200 / 7	7x200 / 14	7x200 / 21	7x200 / 29	7x200 / 37

Note: The imposed load is the load used for normal design. For the fire condition, the load has been reduced in accordance with EC1-1-2 to 50%.
For each span 1 and span 2 combination, a minimum reinforcing mesh is given together with the additional, total load to be applied to the edge beams parallel to span 1

Design Table 9

Fire load (MJ/m^2)/ Opening factor (m$^{1/2}$) 400 / 0,011, 500 / 0,011
500 / 0,161, 600 / 0,011
700 / 0,011

500.1

Imposed load 2,50 kN/m2

Span 2 \ Span 1	6	7	8	9	10	11	12
6	6x200 / 0	6x200 / 0	6x200 / 0	6x200 / 0	6x200 / 0	6x200 / 0	6x200 / 0
7	6x200 / 0	6x200 / 0	6x200 / 0	6x200 / 0	6x200 / 0	6x200 / 0	6x200 / 0
8	6x200 / 0	6x200 / 0	6x200 / 0	6x200 / 0	6x200 / 0	6x200 / 0	6x200 / 2
9	6x200 / 0	6x200 / 0	6x200 / 0	6x200 / 0	6x200 / 0	6x200 / 1	6x200 / 4
10	6x200 / 0	6x200 / 0	6x200 / 0	6x200 / 0	6x200 / 0	6x200 / 2	6x200 / 5
11	6x200 / 0	6x200 / 0	6x200 / 0	6x200 / 0	6x200 / 0	6x200 / 3	6x200 / 6
12	6x200 / 0	6x200 / 0	6x200 / 0	6x200 / 0	6x200 / 1	6x200 / 4	6x200 / 8

Imposed load 3,50 kN/m2

Span 2 \ Span 1	6	7	8	9	10	11	12
6	6x200 / 0	6x200 / 0	6x200 / 0	6x200 / 0	6x200 / 0	6x200 / 0	6x200 / 0
7	6x200 / 0	6x200 / 0	6x200 / 0	6x200 / 0	6x200 / 0	6x200 / 0	6x200 / 0
8	6x200 / 0	6x200 / 0	6x200 / 0	6x200 / 0	6x200 / 0	6x200 / 0	6x200 / 0
9	6x200 / 0	6x200 / 0	6x200 / 0	6x200 / 0	6x200 / 0	6x200 / 0	6x200 / 0
10	6x200 / 0	6x200 / 0	6x200 / 0	6x200 / 0	6x200 / 0	6x200 / 0	6x200 / 1
11	6x200 / 0	6x200 / 0	6x200 / 0	6x200 / 0	6x200 / 0	6x200 / 0	6x200 / 2
12	6x200 / 0	6x200 / 0	6x200 / 0	6x200 / 0	6x200 / 0	6x200 / 0	6x200 / 3

Imposed load 4,50 kN/m2

Span 2 \ Span 1	6	7	8	9	10	11	12
6	6x200 / 0	6x200 / 0	6x200 / 0	6x200 / 0	6x200 / 0	6x200 / 0	6x200 / 0
7	6x200 / 0	6x200 / 0	6x200 / 0	6x200 / 0	6x200 / 0	6x200 / 0	6x200 / 0
8	6x200 / 0	6x200 / 0	6x200 / 0	6x200 / 0	6x200 / 0	6x200 / 0	6x200 / 0
9	6x200 / 0	6x200 / 0	6x200 / 0	6x200 / 0	6x200 / 0	6x200 / 0	6x200 / 0
10	6x200 / 0	6x200 / 0	6x200 / 0	6x200 / 0	6x200 / 0	6x200 / 0	6x200 / 0
11	6x200 / 0	6x200 / 0	6x200 / 0	6x200 / 0	6x200 / 0	6x200 / 0	6x200 / 0
12	6x200 / 0	6x200 / 0	6x200 / 0	6x200 / 0	6x200 / 0	6x200 / 0	6x200 / 0

Imposed load 5,50 kN/m2

Span 2 \ Span 1	6	7	8	9	10	11	12
6	6x200 / 0	6x200 / 0	6x200 / 0	6x200 / 0	6x200 / 0	6x200 / 0	6x200 / 0
7	6x200 / 0	6x200 / 0	6x200 / 0	6x200 / 0	6x200 / 0	6x200 / 0	6x200 / 0
8	6x200 / 0	6x200 / 0	6x200 / 0	6x200 / 0	6x200 / 0	6x200 / 0	6x200 / 0
9	6x200 / 0	6x200 / 0	6x200 / 0	6x200 / 0	6x200 / 0	6x200 / 0	6x200 / 0
10	6x200 / 0	6x200 / 0	6x200 / 0	6x200 / 0	6x200 / 0	6x200 / 0	6x200 / 0
11	6x200 / 0	6x200 / 0	6x200 / 0	6x200 / 0	6x200 / 0	6x200 / 0	6x200 / 0
12	6x200 / 0	6x200 / 0	6x200 / 0	6x200 / 0	6x200 / 0	6x200 / 0	6x200 / 0

Note: The imposed load is the load used for normal design. For the fire condition, the load has been reduced in accordance with EC1-1-2 to 50%.
For each span 1 and span 2 combination, a minimum reinforcing mesh is given together with the additional, total load to be applied to the edge beams parallel to span 1

Design Table 10

Fire load (MJ/m^2)/ Opening factor (m$^{1/2}$) 500 / 0,057, 500 / 0,087 600 / 0,087

500.4

Imposed load 2,5 kN/m2

Span 2 \ Span 1	6	7	8	9	10	11	12
6	6x200 / 1	6x200 / 4	6x200 / 8	6x200 / 12	7x200 / 16	7x200 / 20	8x200 / 24
7	6x200 / 3	6x200 / 7	6x200 / 12	6x200 / 17	7x200 / 22	7x200 / 28	8x200 / 33
8	6x200 / 5	6x200 / 10	6x200 / 16	6x200 / 22	7x200 / 28	7x200 / 34	7x200 / 41
9	6x200 / 7	6x200 / 13	6x200 / 19	6x200 / 26	7x200 / 33	7x200 / 41	7x200 / 49
10	7x200 / 9	7x200 / 15	7x200 / 22	7x200 / 29	6x200 / 38	7x200 / 46	7x200 / 55
11	7x200 / 10	7x200 / 17	7x200 / 24	7x200 / 33	7x200 / 42	7x200 / 51	7x200 / 61
12	8x200 / 11	8x200 / 19	7x200 / 27	7x200 / 36	7x200 / 46	7x200 / 56	7x200 / 67

Imposed load 3,5 kN/m2

Span 2 \ Span 1	6	7	8	9	10	11	12
6	6x200 / 1	6x200 / 4	6x200 / 8	7x200 / 13	7x200 / 17	8x200 / 22	8x200 / 27
7	6x200 / 4	6x200 / 8	6x200 / 13	7x200 / 19	7x200 / 25	8x200 / 31	8x200 / 37
8	6x200 / 6	6x200 / 11	6x200 / 17	7x200 / 24	7x200 / 31	7x200 / 38	8x200 / 46
9	7x200 / 8	7x200 / 14	7x200 / 21	7x200 / 29	7x200 / 37	7x200 / 45	8x200 / 54
10	7x200 / 10	7x200 / 16	7x200 / 24	7x200 / 33	7x200 / 42	7x200 / 52	7x200 / 62
11	8x200 / 11	8x200 / 19	7x200 / 27	7x200 / 37	7x200 / 47	7x200 / 57	7x200 / 68
12	8x200 / 12	8x200 / 21	8x200 / 30	8x200 / 40	7x200 / 51	7x200 / 62	7x200 / 75

Imposed load 4,5 kN/m2

Span 2 \ Span 1	6	7	8	9	10	11	12
6	6x200 / 1	6x200 / 5	7x200 / 9	7x200 / 14	8x200 / 19	8x200 / 24	10x200 / 30
7	6x200 / 4	6x200 / 9	7x200 / 14	7x200 / 21	8x200 / 27	8x200 / 34	8x200 / 41
8	7x200 / 6	7x200 / 12	7x200 / 19	7x200 / 26	7x200 / 34	8x200 / 42	8x200 / 51
9	7x200 / 8	7x200 / 15	7x200 / 23	7x200 / 32	7x200 / 40	8x200 / 50	8x200 / 60
10	8x200 / 10	8x200 / 18	7x200 / 27	7x200 / 36	7x200 / 46	7x200 / 57	8x200 / 68
11	8x200 / 12	8x200 / 20	8x200 / 30	8x200 / 40	7x200 / 51	7x200 / 63	8x200 / 75
12	10x200 / 14	8x200 / 23	8x200 / 33	8x200 / 44	8x200 / 56	8x200 / 69	8x200 / 82

Imposed load 5,5 kN/m2

Span 2 \ Span 1	6	7	8	9	10	11	12
6	6x200 / 1	7x200 / 5	7x200 / 10	8x200 / 15	8x200 / 21	10x200 / 27	10x200 / 33
7	7x200 / 4	7x200 / 10	7x200 / 16	7x200 / 22	8x200 / 30	8x200 / 37	10x200 / 45
8	7x200 / 7	7x200 / 13	7x200 / 21	7x200 / 29	8x200 / 37	8x200 / 46	10x200 / 56
9	8x200 / 9	7x200 / 17	7x200 / 25	7x200 / 34	8x200 / 44	8x200 / 55	8x200 / 66
10	8x200 / 11	8x200 / 20	8x200 / 29	8x200 / 39	7x200 / 51	8x200 / 62	8x200 / 74
11	10x200 / 13	8x200 / 22	8x200 / 33	8x200 / 44	8x200 / 56	8x200 / 69	8x200 / 83
12	10x200 / 15	10x200 / 25	10x200 / 36	8x200 / 48	8x200 / 61	8x200 / 75	8x200 / 90

Note: The imposed load is the load used for normal design. For the fire condition, the load has been reduced in accordance with EC1-1-2 to 50%.
For each span 1 and span 2 combination, a minimum reinforcing mesh is given together with the additional, total load to be applied to the edge beams parallel to span 1

Design Table 11

Fire load (MJ/m^2)/ Opening factor (m$^{1/2}$) 600 / 0,031

600.2

Imposed load 2,5 kN/m2

Span 2	Span 1 6	7	8	9	10	11	12
	Mesh/Extra Load (kN)						
6	6x200 / 0	6x200 / 3	7x200 / 7	7x200 / 11	8x200 / 15	8x200 / 19	10x200 / 23
7	6x200 / 3	6x200 / 7	7x200 / 11	7x200 / 16	8x200 / 20	8x200 / 26	10x200 / 31
8	7x200 / 5	7x200 / 9	7x200 / 14	7x200 / 20	8x200 / 26	8x200 / 33	8x200 / 40
9	7x200 / 6	7x200 / 12	7x200 / 18	7x200 / 24	8x200 / 28	8x200 / 38	8x200 / 47
10	8x200 / 8	8x200 / 13	8x200 / 20	8x200 / 24	7x200 / 36	8x200 / 43	8x200 / 53
11	8x200 / 9	8x200 / 16	8x200 / 23	8x200 / 31	8x200 / 39	8x200 / 47	8x200 / 58
12	10x200 / 10	10x200 / 17	8x200 / 25	8x200 / 34	8x200 / 43	8x200 / 53	8x200 / 63

Imposed load 3,5 kN/m2

Span 2	Span 1 6	7	8	9	10	11	12
	Mesh/Extra Load (kN)						
6	6x200 / 0	7x200 / 4	7x200 / 8	8x200 / 11	8x200 / 16	10x200 / 21	10x200 / 26
7	7x200 / 3	7x200 / 7	7x200 / 12	8x200 / 17	8x200 / 23	10x200 / 28	10x200 / 35
8	7x200 / 5	7x200 / 10	7x200 / 16	8x200 / 22	8x200 / 29	8x200 / 36	10x200 / 43
9	8x200 / 7	8x200 / 12	8x200 / 19	8x200 / 24	8x200 / 35	8x200 / 43	10x200 / 50
10	8x200 / 9	8x200 / 15	8x200 / 23	8x200 / 31	8x200 / 39	8x200 / 49	10x200 / 53
11	10x200 / 10	10x200 / 16	8x200 / 26	8x200 / 35	8x200 / 44	8x200 / 54	8x200 / 65
12	10x200 / 11	10x200 / 19	10x200 / 28	10x200 / 37	10x200 / 43	8x200 / 60	8x200 / 71

Imposed load 4,5 kN/m2

Span 2	Span 1 6	7	8	9	10	11	12
	Mesh/Extra Load (kN)						
6	7x200 / 0	7x200 / 4	8x200 / 8	8x200 / 13	10x200 / 17	10x200 / 23	10x200 / 28
7	7x200 / 3	7x200 / 8	8x200 / 12	8x200 / 19	8x200 / 25	10x200 / 32	10x200 / 39
8	8x200 / 5	8x200 / 10	8x200 / 16	8x200 / 25	8x200 / 32	10x200 / 40	10x200 / 48
9	8x200 / 7	8x200 / 14	8x200 / 21	8x200 / 29	8x200 / 38	10x200 / 46	10x200 / 57
10	10x200 / 9	8x200 / 17	8x200 / 25	8x200 / 34	8x200 / 44	10x200 / 51	10x200 / 64
11	10x200 / 11	10x200 / 19	10x200 / 28	10x200 / 37	10x200 / 46	8x200 / 60	10x200 / 70
12	10x200 / 12	10x200 / 21	10x200 / 31	10x200 / 42	10x200 / 53	10x200 / 64	10x200 / 75

Imposed load 5,5 kN/m2

Span 2	Span 1 6	7	8	9	10	11	12
	Mesh/Extra Load (kN)						
6	7x200 / 0	7x200 / 4	8x200 / 9	8x200 / 14	10x200 / 19	10x200 / 25	10x200 / 31
7	7x200 / 3	7x200 / 8	8x200 / 14	8x200 / 21	10x200 / 27	10x200 / 35	10x200 / 42
8	8x200 / 6	8x200 / 12	8x200 / 19	8x200 / 27	10x200 / 34	10x200 / 44	10x200 / 53
9	8x200 / 8	8x200 / 15	8x200 / 23	8x200 / 32	10x200 / 40	10x200 / 52	10x200 / 62
10	10x200 / 10	10x200 / 18	10x200 / 27	10x200 / 36	8x200 / 48	10x200 / 58	10x200 / 71
11	10x200 / 12	10x200 / 21	10x200 / 30	10x200 / 41	10x200 / 53	10x200 / 64	10x200 / 79
12	10x200 / 13	10x200 / 23	10x200 / 33	10x200 / 45	10x200 / 58	10x200 / 71	10x200 / 85

Note: The imposed load is the load used for normal design. For the fire condition, the load has been reduced in accordance with EC1-1-2 to 50%.
For each span 1 and span 2 combination, a minimum reinforcing mesh is given together with the additional, total load to be applied to the edge beams parallel to span 1

Design Table 12

Fire load (MJ/m^2)/ Opening factor (m$^{1/2}$) 600 / 0,057

600.3

Imposed load 2,5 kN/m2

Span 2	Span 1 6	7	8	9	10	11	12
	Mesh/Extra Load (kN)						
6	6x200 / 1	6x200 / 5	6x200 / 8	7x200 / 12	7x200 / 16	8x200 / 21	8x200 / 26
7	6x200 / 4	6x200 / 8	6x200 / 13	7x200 / 17	7x200 / 23	7x200 / 29	8x200 / 35
8	6x200 / 6	6x200 / 11	6x200 / 17	7x200 / 20	7x200 / 29	7x200 / 36	8x200 / 40
9	7x200 / 8	7x200 / 12	7x200 / 17	6x200 / 27	7x200 / 34	7x200 / 42	7x200 / 51
10	7x200 / 9	7x200 / 16	7x200 / 23	7x200 / 31	7x200 / 37	7x200 / 48	7x200 / 57
11	8x200 / 11	7x200 / 18	7x200 / 26	7x200 / 34	7x200 / 44	7x200 / 53	7x200 / 64
12	8x200 / 12	8x200 / 20	8x200 / 26	7x200 / 37	7x200 / 47	7x200 / 58	7x200 / 69

Imposed load 3,5 kN/m2

Span 2	Span 1 6	7	8	9	10	11	12
	Mesh/Extra Load (kN)						
6	6x200 / 1	6x200 / 5	7x200 / 9	7x200 / 14	8x200 / 16	8x200 / 23	10x200 / 29
7	6x200 / 4	6x200 / 9	7x200 / 12	7x200 / 20	7x200 / 26	8x200 / 32	8x200 / 39
8	7x200 / 7	7x200 / 10	7x200 / 15	7x200 / 25	7x200 / 33	8x200 / 37	8x200 / 48
9	7x200 / 9	7x200 / 15	7x200 / 22	7x200 / 30	7x200 / 38	7x200 / 47	8x200 / 57
10	8x200 / 8	7x200 / 18	7x200 / 26	7x200 / 34	7x200 / 44	7x200 / 54	8x200 / 60
11	8x200 / 12	8x200 / 20	8x200 / 26	7x200 / 38	7x200 / 49	7x200 / 60	7x200 / 71
12	10x200 / 13	8x200 / 22	8x200 / 31	8x200 / 42	8x200 / 50	7x200 / 65	7x200 / 78

Imposed load 4,5 kN/m2

Span 2	Span 1 6	7	8	9	10	11	12
	Mesh/Extra Load (kN)						
6	6x200 / 1	7x200 / 4	7x200 / 10	7x200 / 15	8x200 / 20	8x200 / 26	10x200 / 32
7	7x200 / 3	6x200 / 10	7x200 / 16	7x200 / 22	8x200 / 29	8x200 / 36	10x200 / 43
8	7x200 / 7	7x200 / 13	7x200 / 20	7x200 / 28	8x200 / 33	8x200 / 44	8x200 / 53
9	7x200 / 9	7x200 / 17	7x200 / 25	7x200 / 33	7x200 / 43	8x200 / 52	8x200 / 63
10	8x200 / 11	8x200 / 19	8x200 / 26	7x200 / 38	7x200 / 48	8x200 / 56	8x200 / 71
11	8x200 / 13	8x200 / 22	8x200 / 32	8x200 / 42	8x200 / 51	8x200 / 58	8x200 / 79
12	10x200 / 15	10x200 / 24	8x200 / 35	8x200 / 46	8x200 / 59	8x200 / 72	8x200 / 80

Imposed load 5,5 kN/m2

Span 2	Span 1 6	7	8	9	10	11	12
	Mesh/Extra Load (kN)						
6	6x200 / 2	7x200 / 6	7x200 / 11	8x200 / 16	8x200 / 22	10x200 / 28	10x200 / 35
7	7x200 / 5	7x200 / 11	7x200 / 17	8x200 / 24	8x200 / 31	10x200 / 34	10x200 / 47
8	7x200 / 8	7x200 / 15	7x200 / 22	8x200 / 26	8x200 / 39	8x200 / 49	10x200 / 58
9	8x200 / 10	8x200 / 18	8x200 / 23	7x200 / 36	8x200 / 47	8x200 / 57	10x200 / 62
10	8x200 / 12	8x200 / 21	8x200 / 31	8x200 / 42	8x200 / 49	8x200 / 65	8x200 / 78
11	10x200 / 14	10x200 / 20	8x200 / 35	8x200 / 46	8x200 / 59	8x200 / 72	8x200 / 86
12	10x200 / 16	10x200 / 26	10x200 / 38	10x200 / 45	8x200 / 64	8x200 / 79	8x200 / 94

Note: The imposed load is the load used for normal design. For the fire condition, the load has been reduced in accordance with EC1-1-2 to 50%.
For each span 1 and span 2 combination, a minimum reinforcing mesh is given together with the additional, total load to be applied to the edge beams parallel to span 1

Design Table 13

Fire load (MJ/m^2)/ Opening factor (m$^{1/2}$) 600 / 0,122

600.5

Imposed load 2,5 kN/m2

Span 2 \ Span 1	6	7	8	9	10	11	12
	Mesh/Extra Load (kN)						
6	6x200 / 0	6x200 / 2	6x200 / 5	6x200 / 8	7x200 / 11	7x200 / 15	8x200 / 19
7	6x200 / 1	6x200 / 4	6x200 / 8	6x200 / 12	7x200 / 17	7x200 / 22	7x200 / 27
8	6x200 / 2	6x200 / 7	6x200 / 11	6x200 / 16	7x200 / 22	7x200 / 27	7x200 / 33
9	6x200 / 4	6x200 / 9	6x200 / 14	6x200 / 20	6x200 / 26	7x200 / 32	7x200 / 39
10	7x200 / 5	7x200 / 10	7x200 / 16	6x200 / 23	6x200 / 30	7x200 / 37	7x200 / 45
11	7x200 / 6	7x200 / 12	7x200 / 18	7x200 / 26	7x200 / 33	7x200 / 41	7x200 / 50
12	8x200 / 7	7x200 / 13	7x200 / 20	7x200 / 28	7x200 / 36	7x200 / 45	7x200 / 55

Imposed load 3,5 kN/m2

Span 2 \ Span 1	6	7	8	9	10	11	12
	Mesh/Extra Load (kN)						
6	6x200 / 0	6x200 / 1	6x200 / 5	7x200 / 8	7x200 / 12	8x200 / 16	8x200 / 21
7	6x200 / 1	6x200 / 4	6x200 / 9	7x200 / 13	7x200 / 18	7x200 / 23	8x200 / 29
8	6x200 / 2	6x200 / 7	6x200 / 12	7x200 / 18	7x200 / 23	7x200 / 30	8x200 / 36
9	7x200 / 4	7x200 / 9	7x200 / 15	6x200 / 21	7x200 / 28	7x200 / 36	7x200 / 43
10	7x200 / 5	7x200 / 11	7x200 / 18	7x200 / 25	7x200 / 32	7x200 / 41	7x200 / 49
11	8x200 / 6	7x200 / 13	7x200 / 20	7x200 / 28	7x200 / 36	7x200 / 45	7x200 / 55
12	8x200 / 8	8x200 / 14	8x200 / 22	7x200 / 31	7x200 / 40	7x200 / 50	7x200 / 60

Imposed load 4,5 kN/m2

Span 2 \ Span 1	6	7	8	9	10	11	12
	Mesh/Extra Load (kN)						
6	6x200 / 0	6x200 / 1	6x200 / 5	7x200 / 9	7x200 / 13	8x200 / 18	8x200 / 22
7	6x200 / 0	6x200 / 4	6x200 / 9	7x200 / 14	7x200 / 20	8x200 / 25	8x200 / 31
8	6x200 / 2	6x200 / 7	6x200 / 13	7x200 / 19	7x200 / 25	8x200 / 32	8x200 / 40
9	7x200 / 4	7x200 / 10	7x200 / 16	7x200 / 23	7x200 / 31	7x200 / 39	8x200 / 47
10	7x200 / 5	7x200 / 12	7x200 / 19	7x200 / 27	7x200 / 35	7x200 / 44	8x200 / 54
11	8x200 / 7	8x200 / 14	8x200 / 21	7x200 / 30	7x200 / 39	7x200 / 49	8x200 / 60
12	8x200 / 8	8x200 / 15	8x200 / 24	8x200 / 33	8x200 / 43	8x200 / 54	7x200 / 65

Imposed load 5,5 kN/m2

Span 2 \ Span 1	6	7	8	9	10	11	12
	Mesh/Extra Load (kN)						
6	6x200 / 0	6x200 / 1	7x200 / 5	7x200 / 9	8x200 / 14	8x200 / 19	10x200 / 24
7	6x200 / 0	6x200 / 5	7x200 / 10	7x200 / 15	8x200 / 21	8x200 / 27	8x200 / 34
8	7x200 / 2	7x200 / 8	7x200 / 14	7x200 / 20	7x200 / 27	8x200 / 35	8x200 / 43
9	7x200 / 4	7x200 / 10	7x200 / 17	7x200 / 25	7x200 / 33	8x200 / 42	8x200 / 51
10	8x200 / 6	8x200 / 12	7x200 / 20	7x200 / 29	7x200 / 38	8x200 / 48	8x200 / 58
11	8x200 / 7	8x200 / 14	8x200 / 23	8x200 / 32	8x200 / 42	8x200 / 53	8x200 / 65
12	10x200 / 8	8x200 / 16	8x200 / 25	8x200 / 36	8x200 / 47	8x200 / 58	8x200 / 71

Note: The imposed load is the load used for normal design. For the fire condition, the load has been reduced in accordance with EC1-1-2 to 50%.
For each span 1 and span 2 combination, a minimum reinforcing mesh is given together with the additional, total load to be applied to the edge beams parallel to span 1

Design Table 14

Fire load (MJ/m^2)/ Opening factor (m$^{1/2}$) 700 / 0,031

700.2

Imposed load 2,5 kN/m2

	Span 1	Mesh/Extra Load (kN)					
Span 2	6	7	8	9	10	11	12
6	7x200 / 0	7x200 / 4	8x200 / 7	8x200 / 11	10x200 / 14	10x200 / 19	10x200 / 24
7	7x200 / 3	7x200 / 7	8x200 / 11	8x200 / 16	10x200 / 20	10x200 / 27	10x200 / 33
8	8x200 / 5	8x200 / 9	8x200 / 14	8x200 / 21	8x200 / 27	10x200 / 33	10x200 / 41
9	8x200 / 7	8x200 / 12	8x200 / 18	8x200 / 25	8x200 / 32	10x200 / 38	10x200 / 47
10	10x200 / 8	10x200 / 13	8x200 / 21	8x200 / 29	8x200 / 37	10x200 / 43	10x200 / 53
11	10x200 / 10	10x200 / 16	10x200 / 23	10x200 / 31	10x200 / 39	8x200 / 50	10x200 / 58
12	10x200 / 11	10x200 / 18	10x200 / 26	10x200 / 35	10x200 / 44	10x200 / 53	10x200 / 63

Imposed load 3,5 kN/m2

	Span 1	Mesh/Extra Load (kN)					
Span 2	6	7	8	9	10	11	12
6	7x200 / 1	8x200 / 3	8x200 / 8	10x200 / 11	10x200 / 17	10x200 / 22	10x200 / 0
7	8x200 / 3	8x200 / 7	8x200 / 13	10x200 / 17	10x200 / 24	10x200 / 30	10x200 / 36
8	8x200 / 5	8x200 / 11	8x200 / 17	8x200 / 23	10x200 / 30	10x200 / 38	10x200 / 45
9	10x200 / 6	10x200 / 12	8x200 / 20	8x200 / 28	10x200 / 35	10x200 / 44	10x200 / 53
10	10x200 / 9	10x200 / 16	10x200 / 23	10x200 / 31	10x200 / 39	10x200 / 50	10x200 / 60
11	10x200 / 11	10x200 / 18	10x200 / 26	10x200 / 35	10x200 / 45	10x200 / 55	10x200 / 67
12	10x200 / 0	10x200 / 20	10x200 / 29	10x200 / 39	10x200 / 50	10x200 / 61	10x200 / 72

Imposed load 4,5 kN/m2

	Span 1	Mesh/Extra Load (kN)					
Span 2	6	7	8	9	10	11	12
6	7x200 / 1	8x200 / 4	8x200 / 9	10x200 / 13	10x200 / 18	10x200 / 24	10x200 / 0
7	8x200 / 3	8x200 / 8	8x200 / 14	10x200 / 20	10x200 / 26	10x200 / 33	10x200 / 0
8	8x200 / 6	8x200 / 12	8x200 / 18	10x200 / 25	10x200 / 33	10x200 / 41	10x200 / 50
9	10x200 / 8	10x200 / 14	10x200 / 22	10x200 / 29	10x200 / 39	10x200 / 49	10x200 / 59
10	10x200 / 10	10x200 / 17	10x200 / 26	10x200 / 35	10x200 / 45	10x200 / 56	10x200 / 67
11	10x200 / 12	10x200 / 20	10x200 / 29	10x200 / 39	10x200 / 50	10x200 / 62	10x200 / 74
12	10x200 / 0	10x200 / 0	10x200 / 32	10x200 / 43	10x200 / 55	10x200 / 67	10x200 / 81

Imposed load 5,5 kN/m2

	Span 1	Mesh/Extra Load (kN)					
Span 2	6	7	8	9	10	11	12
6	8x200 / 0	8x200 / 5	10x200 / 9	10x200 / 15	10x200 / 20	10x200 / 0	10x200 / 0
7	8x200 / 4	8x200 / 9	10x200 / 14	10x200 / 22	10x200 / 29	10x200 / 36	10x200 / 0
8	10x200 / 6	10x200 / 12	10x200 / 19	10x200 / 28	10x200 / 36	10x200 / 45	10x200 / 0
9	10x200 / 9	10x200 / 16	10x200 / 24	10x200 / 33	10x200 / 43	10x200 / 53	10x200 / 0
10	10x200 / 11	10x200 / 19	10x200 / 28	10x200 / 38	10x200 / 49	10x200 / 61	10x200 / 73
11	10x200 / 0	10x200 / 22	10x200 / 32	10x200 / 43	10x200 / 55	10x200 / 67	10x200 / 81
12	10x200 / 0	10x200 / 0	10x200 / 0	10x200 / 0	10x200 / 60	10x200 / 74	10x200 / 88

Note: The imposed load is the load used for normal design. For the fire condition, the load has been reduced in accordance with EC1-1-2 to 50%.
For each span 1 and span 2 combination, a minimum reinforcing mesh is given together with the additional, total load to be applied to the edge beams parallel to span 1

Design Table 15

Fire load (MJ/m^2)/ Opening factor (m$^{1/2}$) 700 / 0,057

700.3

Imposed load 2,5 kN/m2

Span 2 \ Span 1	6	7	8	9	10	11	12
	Mesh/Extra Load (kN)						
6	6x200 / 2	6x200 / 5	7x200 / 8	7x200 / 13	8x200 / 16	8x200 / 21	10x200 / 25
7	6x200 / 4	6x200 / 8	7x200 / 12	7x200 / 18	8x200 / 20	8x200 / 29	8x200 / 36
8	7x200 / 6	7x200 / 10	7x200 / 15	7x200 / 23	7x200 / 30	8x200 / 35	8x200 / 44
9	7x200 / 8	7x200 / 14	7x200 / 20	7x200 / 27	7x200 / 35	8x200 / 40	8x200 / 51
10	8x200 / 9	8x200 / 13	7x200 / 24	7x200 / 32	7x200 / 40	7x200 / 49	8x200 / 56
11	8x200 / 11	8x200 / 18	8x200 / 25	8x200 / 32	7x200 / 45	7x200 / 54	8x200 / 60
12	10x200 / 12	8x200 / 20	8x200 / 29	8x200 / 38	8x200 / 47	8x200 / 54	8x200 / 62

Imposed load 3,5 kN/m2

Span 2 \ Span 1	6	7	8	9	10	11	12
	Mesh/Extra Load (kN)						
6	6x200 / 2	7x200 / 5	7x200 / 10	8x200 / 12	8x200 / 19	10x200 / 23	10x200 / 29
7	7x200 / 4	7x200 / 8	7x200 / 15	8x200 / 16	8x200 / 26	8x200 / 33	10x200 / 39
8	7x200 / 7	7x200 / 13	7x200 / 19	7x200 / 26	8x200 / 32	8x200 / 41	10x200 / 45
9	8x200 / 7	8x200 / 12	7x200 / 23	7x200 / 31	8x200 / 36	8x200 / 48	8x200 / 58
10	8x200 / 11	8x200 / 18	8x200 / 25	8x200 / 32	8x200 / 39	8x200 / 53	8x200 / 66
11	10x200 / 11	8x200 / 21	8x200 / 30	8x200 / 39	8x200 / 48	8x200 / 57	8x200 / 72
12	10x200 / 14	10x200 / 22	10x200 / 29	8x200 / 43	8x200 / 54	8x200 / 66	8x200 / 76

Imposed load 4,5 kN/m2

Span 2 \ Span 1	6	7	8	9	10	11	12
	Mesh/Extra Load (kN)						
6	7x200 / 0	7x200 / 6	7x200 / 11	8x200 / 16	10x200 / 17	10x200 / 27	10x200 / 32
7	7x200 / 5	7x200 / 10	7x200 / 16	8x200 / 22	8x200 / 29	10x200 / 35	10x200 / 44
8	7x200 / 8	7x200 / 14	7x200 / 21	8x200 / 27	8x200 / 37	10x200 / 41	10x200 / 54
9	8x200 / 10	8x200 / 17	8x200 / 24	8x200 / 31	8x200 / 43	8x200 / 54	10x200 / 61
10	10x200 / 9	8x200 / 20	8x200 / 29	8x200 / 39	8x200 / 48	8x200 / 61	10x200 / 67
11	10x200 / 14	10x200 / 21	10x200 / 29	8x200 / 44	8x200 / 55	8x200 / 67	8x200 / 81
12	10x200 / 15	10x200 / 25	10x200 / 35	10x200 / 45	10x200 / 55	8x200 / 74	8x200 / 88

Imposed load 5,5 kN/m2

Span 2 \ Span 1	6	7	8	9	10	11	12
	Mesh/Extra Load (kN)						
6	7x200 / 2	7x200 / 6	8x200 / 11	8x200 / 17	10x200 / 22	10x200 / 29	10x200 / 36
7	7x200 / 5	7x200 / 11	8x200 / 16	8x200 / 25	10x200 / 30	10x200 / 40	10x200 / 48
8	8x200 / 8	8x200 / 14	8x200 / 20	8x200 / 31	10x200 / 35	10x200 / 49	10x200 / 60
9	8x200 / 11	8x200 / 19	8x200 / 28	8x200 / 37	8x200 / 48	10x200 / 56	10x200 / 70
10	10x200 / 13	10x200 / 20	10x200 / 27	8x200 / 43	8x200 / 55	10x200 / 60	10x200 / 78
11	10x200 / 15	10x200 / 25	10x200 / 35	10x200 / 45	10x200 / 54	8x200 / 74	10x200 / 84
12	10x200 / 17	10x200 / 27	10x200 / 39	10x200 / 52	10x200 / 65	10x200 / 76	10x200 / 87

Note: The imposed load is the load used for normal design. For the fire condition, the load has been reduced in accordance with EC1-1-2 to 50%.
For each span 1 and span 2 combination, a minimum reinforcing mesh is given together with the additional, total load to be applied to the edge beams parallel to span 1

Design Table 16

Fire load (MJ/m^2)/ Opening factor (m$^{1/2}$) 700 / 0,087

700.4

Imposed load 2,5 kN/m2

Span 2	Span 1 6	7	8	9	10	11	12
	Mesh/Extra Load (kN)						
6	6x200 / 1	6x200 / 5	6x200 / 8	7x200 / 12	7x200 / 17	7x200 / 21	8x200 / 26
7	6x200 / 4	6x200 / 8	6x200 / 13	6x200 / 18	7x200 / 23	7x200 / 29	8x200 / 35
8	6x200 / 6	6x200 / 11	6x200 / 17	6x200 / 23	7x200 / 29	7x200 / 36	7x200 / 43
9	7x200 / 8	6x200 / 14	6x200 / 20	6x200 / 27	7x200 / 35	7x200 / 43	7x200 / 51
10	7x200 / 9	7x200 / 16	7x200 / 23	7x200 / 31	6x200 / 40	7x200 / 48	7x200 / 58
11	7x200 / 11	7x200 / 18	7x200 / 26	7x200 / 35	7x200 / 44	7x200 / 54	7x200 / 64
12	8x200 / 12	8x200 / 20	7x200 / 28	7x200 / 38	7x200 / 48	7x200 / 59	7x200 / 70

Imposed load 3,5 kN/m2

Span 2	Span 1 6	7	8	9	10	11	12
	Mesh/Extra Load (kN)						
6	6x200 / 1	6x200 / 5	6x200 / 9	7x200 / 14	7x200 / 19	8x200 / 24	8x200 / 29
7	6x200 / 4	6x200 / 9	6x200 / 14	7x200 / 20	7x200 / 26	8x200 / 33	8x200 / 39
8	6x200 / 7	6x200 / 12	6x200 / 19	7x200 / 26	7x200 / 33	7x200 / 41	8x200 / 49
9	7x200 / 9	7x200 / 15	7x200 / 23	7x200 / 30	7x200 / 39	7x200 / 48	8x200 / 57
10	7x200 / 11	7x200 / 18	7x200 / 26	7x200 / 35	7x200 / 44	7x200 / 54	7x200 / 65
11	8x200 / 12	8x200 / 20	7x200 / 29	7x200 / 39	7x200 / 49	7x200 / 60	7x200 / 72
12	8x200 / 14	8x200 / 22	8x200 / 32	8x200 / 42	7x200 / 54	7x200 / 66	7x200 / 78

Imposed load 4,5 kN/m2

Span 2	Span 1 6	7	8	9	10	11	12
	Mesh/Extra Load (kN)						
6	6x200 / 2	6x200 / 6	7x200 / 10	7x200 / 15	8x200 / 21	8x200 / 26	10x200 / 32
7	6x200 / 5	6x200 / 10	7x200 / 16	7x200 / 22	8x200 / 29	8x200 / 36	8x200 / 43
8	7x200 / 7	7x200 / 14	7x200 / 21	7x200 / 28	7x200 / 36	8x200 / 45	8x200 / 54
9	7x200 / 10	7x200 / 17	7x200 / 25	7x200 / 34	7x200 / 43	8x200 / 53	8x200 / 63
10	8x200 / 12	8x200 / 20	7x200 / 29	7x200 / 38	7x200 / 49	7x200 / 60	8x200 / 72
11	8x200 / 13	8x200 / 22	8x200 / 32	8x200 / 43	7x200 / 54	7x200 / 67	8x200 / 79
12	10x200 / 15	8x200 / 24	8x200 / 35	8x200 / 47	8x200 / 59	8x200 / 73	7x200 / 87

Imposed load 5,5 kN/m2

Span 2	Span 1 6	7	8	9	10	11	12
	Mesh/Extra Load (kN)						
6	6x200 / 2	7x200 / 6	7x200 / 11	8x200 / 17	8x200 / 23	10x200 / 29	10x200 / 35
7	7x200 / 5	7x200 / 11	7x200 / 17	7x200 / 24	8x200 / 32	8x200 / 39	10x200 / 48
8	7x200 / 8	7x200 / 15	7x200 / 23	7x200 / 31	8x200 / 40	8x200 / 49	10x200 / 59
9	8x200 / 10	7x200 / 18	7x200 / 27	7x200 / 37	8x200 / 47	8x200 / 58	8x200 / 69
10	8x200 / 13	8x200 / 22	8x200 / 31	8x200 / 42	7x200 / 54	8x200 / 66	8x200 / 79
11	10x200 / 15	8x200 / 24	8x200 / 35	8x200 / 47	8x200 / 60	8x200 / 73	8x200 / 87
12	10x200 / 16	10x200 / 27	10x200 / 38	8x200 / 51	8x200 / 65	8x200 / 80	8x200 / 95

ote: The imposed load is the load used for normal design. For the fire condition, the load has been reduced in accordance with EC1-1-2 to 50%.
For each span 1 and span 2 combination, a minimum reinforcing mesh is given together with the additional, total load to be applied to the edge beams parallel to span 1

Design Table 17

Fire load (MJ/m^2)/ Opening factor (m$^{1/2}$) 700 / 0,122

700.5

Imposed load 2,5 kN/m2

Span 2	Span 1 Mesh/Extra Load (kN) 6	7	8	9	10	11	12
6	6x200 / 0	6x200 / 2	6x200 / 5	6x200 / 9	7x200 / 12	7x200 / 16	8x200 / 20
7	6x200 / 1	6x200 / 5	6x200 / 9	6x200 / 13	7x200 / 18	7x200 / 23	7x200 / 28
8	6x200 / 3	6x200 / 7	6x200 / 12	6x200 / 17	7x200 / 23	7x200 / 29	7x200 / 35
9	6x200 / 4	6x200 / 9	6x200 / 15	6x200 / 21	6x200 / 27	7x200 / 34	7x200 / 41
10	7x200 / 6	7x200 / 11	7x200 / 17	6x200 / 24	6x200 / 31	7x200 / 39	7x200 / 47
11	7x200 / 7	7x200 / 13	7x200 / 20	7x200 / 27	7x200 / 35	7x200 / 43	7x200 / 52
12	8x200 / 8	7x200 / 14	7x200 / 22	7x200 / 29	7x200 / 38	7x200 / 47	7x200 / 57

Imposed load 3,5 kN/m2

Span 2	Span 1 Mesh/Extra Load (kN) 6	7	8	9	10	11	12
6	6x200 / 0	6x200 / 2	6x200 / 5	7x200 / 9	7x200 / 13	8x200 / 18	8x200 / 22
7	6x200 / 1	6x200 / 5	6x200 / 9	7x200 / 14	7x200 / 19	7x200 / 25	8x200 / 31
8	6x200 / 3	6x200 / 8	6x200 / 13	7x200 / 19	7x200 / 25	7x200 / 31	8x200 / 38
9	7x200 / 5	7x200 / 10	7x200 / 16	7x200 / 23	7x200 / 30	7x200 / 37	7x200 / 45
10	7x200 / 6	7x200 / 12	7x200 / 19	7x200 / 26	7x200 / 34	7x200 / 43	7x200 / 52
11	8x200 / 7	7x200 / 14	7x200 / 21	7x200 / 29	7x200 / 38	7x200 / 48	7x200 / 57
12	8x200 / 8	8x200 / 15	8x200 / 23	7x200 / 32	7x200 / 42	7x200 / 52	7x200 / 63

Imposed load 4,5 kN/m2

Span 2	Span 1 Mesh/Extra Load (kN) 6	7	8	9	10	11	12
6	6x200 / 0	6x200 / 2	7x200 / 6	7x200 / 10	7x200 / 14	8x200 / 19	8x200 / 24
7	6x200 / 1	6x200 / 5	7x200 / 10	7x200 / 15	7x200 / 21	8x200 / 27	8x200 / 33
8	7x200 / 3	7x200 / 8	7x200 / 14	7x200 / 20	7x200 / 27	8x200 / 34	8x200 / 42
9	7x200 / 5	7x200 / 11	7x200 / 17	7x200 / 25	7x200 / 32	7x200 / 41	8x200 / 49
10	7x200 / 6	7x200 / 13	7x200 / 20	7x200 / 28	7x200 / 37	7x200 / 47	8x200 / 56
11	8x200 / 8	8x200 / 15	8x200 / 23	7x200 / 32	7x200 / 42	7x200 / 52	8x200 / 63
12	8x200 / 9	8x200 / 17	8x200 / 25	8x200 / 35	8x200 / 46	8x200 / 57	7x200 / 68

Imposed load 5,5 kN/m2

Span 2	Span 1 Mesh/Extra Load (kN) 6	7	8	9	10	11	12
6	6x200 / 0	6x200 / 2	7x200 / 6	7x200 / 11	8x200 / 15	8x200 / 20	10x200 / 26
7	6x200 / 1	6x200 / 5	7x200 / 11	7x200 / 16	8x200 / 23	8x200 / 29	10x200 / 36
8	7x200 / 3	7x200 / 9	7x200 / 15	7x200 / 22	8x200 / 29	8x200 / 37	8x200 / 45
9	7x200 / 5	7x200 / 11	7x200 / 19	7x200 / 26	7x200 / 35	8x200 / 44	8x200 / 53
10	8x200 / 7	8x200 / 14	8x200 / 22	7x200 / 31	7x200 / 40	8x200 / 50	8x200 / 61
11	8x200 / 8	8x200 / 16	8x200 / 25	8x200 / 34	8x200 / 45	8x200 / 56	8x200 / 68
12	10x200 / 9	10x200 / 18	8x200 / 27	8x200 / 38	8x200 / 49	8x200 / 61	8x200 / 74

Note: The imposed load is the load used for normal design. For the fire condition, the load has been reduced in accordance with EC1-1-2 to 50%.
For each span 1 and span 2 combination, a minimum reinforcing mesh is given together with the additional, total load to be applied to the edge beams parallel to span 1

ANNEX D COMPARISON WITH THE BRE SIMPLE METHOD

D.1 General

The main quantitative design guidance in this design guide is in Chapter 8. The guidance is based on a method developed by BRE in the UK. The original guidance was developed for standard fires and fire resistance periods of 30 and 60 minutes. In this publication the method has been adapted for use with natural fires. In order to verify the method several comparisons have been made between the BRE method and finite element calculations. Two of these comparisons are presented in this Annex.

D.2 Comparison 1

An analysis was performed using DIANA on the compartment shown in Figure D.1. The fire was fuel bed controlled with a fire load of 300 MJ/m^2 and the opening factor was 0,12 m^{-2}. The slab depth was 130 mm and the reinforcing mesh was 6x200.

For applied loadings of 3 kN/m^2 and 5 kN/m^2 the maximum displacement at the centre of the slab is shown in Figure D.2. The self weight of the floor slab and beams was assumed to be 3,115 kN/m^2.

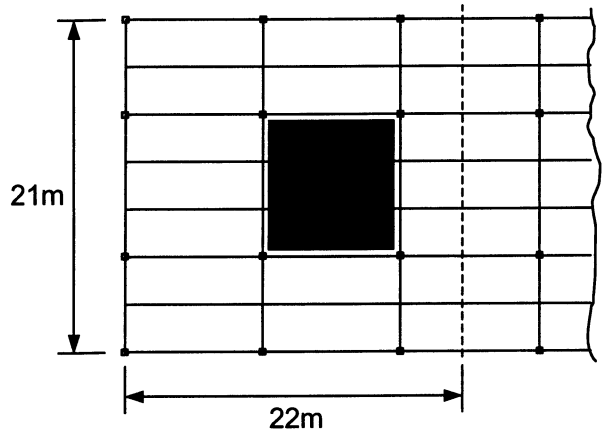

Figure D.1 *22 x 21 m compartment and smaller 9x9m zone used in BRE method*

The total loads in the two cases was 6,115 kN/m^2 and 8,115.

It can be seen from Figure D.2 that for both levels of load the deformation reach a maximum and then start to reduce. This indicates, together with other checks not described here, that the structure is stable in fire. However, if the deflection limit of span/20 is applied, the 5 kN/m^2 case fails – 9000/521 ~ span/17.3. The deflection of the 3 kN/m^2 case was 442 mm – span/20,4.

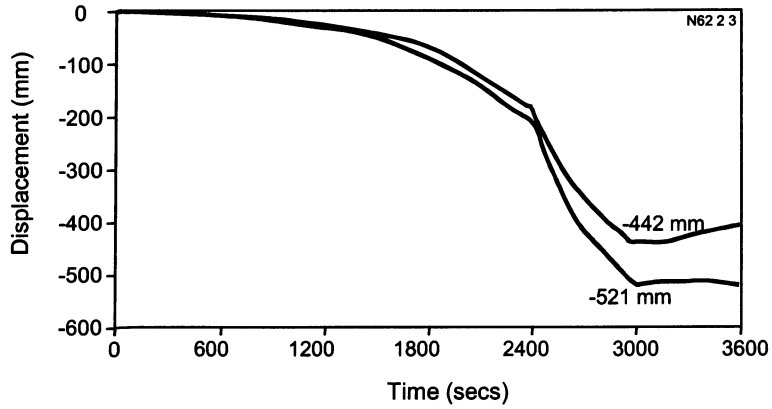

Figure D.2 *Maximum displacements for ventilation controlled fire*

Using the same thermal data, and slab depth, the structural resistance has been computed for different reinforcing mesh sizes using the BRE method. These are presented in Table D.1.

In using the BRE method a floor design zone of 9 m x 9 m has been assumed. The perimeter beams around this zone would, using this method, usually be fire protected. In the DIANA analyses the area of unprotected beams was much greater and measured 22 m x 18 m.

In the table it can be seen that as time increases, the structural resistance reduces and then starts to increase. The minimum value for 6x200 reinforcing mesh is 6.31 kN/m^2 and for 7x200 reinforcing mesh is 7,36 kN/m^2. The associated displacement, was 394 mm for both cases.

Table D.1 *Variation of slab resistance with time (q=300)*

Mesh size		6x200	7x200
Time	Disp (mm)	Resistance (kN/m^2)	Resistance (kN/m^2)
46	360	7,92	8,90
47	374	7,06	8,06
48	385	6,53	7,56
49	394	>>6,31<<	>>7,36<<
50	401	6,35	7,41
51	405	6,60	7,67
52	406	7,05	8,12
53	405	7,68	8,75
54	402	8,46	9,53

For the same reinforcing mesh size as was used in the DIANA (6x200), the total resistance using the BRE method was 6,31 kN/m^2 compared with the total applied load for the DIANA analysis of 6,115 kN/m^2. However, the DIANA analysis did not fail and the structure analysed was much larger. The BRE method can therefore be assumed to be conservative in this case.

Although the DIANA analysis was deemed to have failed for the higher imposed load of 5 kN/m^2 because of excessive deflection, the total applied of 8,115 kN/m^2 was larger than the total resistance calculated (7,36 kN/m^2) using the BRE method with a larger reinforcing mesh (7x200). This again indicates that the BRE method is conservative.

D.3 Comparison 2

In this comparison, an identical structural layout was uses (to comparison 1) but the fire was ventilation controlled with a fire load of 700 MJ/m^2 and the opening factor was 0,16 m^{-2}.

For an applied an loading of 5,5 kN/m^2 the maximum displacement at the centre of the slab is shown in Figure D.2. The total load was 8,615 kN/m^2.

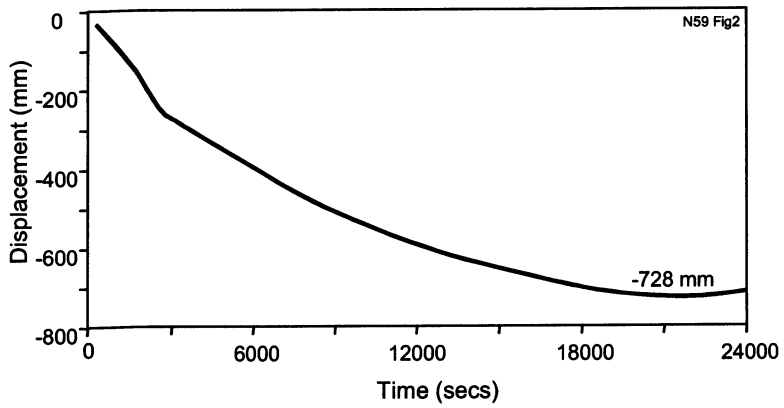

Figure D.3 *Maximum displacements for ventilation controlled fire*

It can be seen from Figure D.3 that the deformation reach a maximum and then start to reduce. This indicates, together with other checks not described here, that the structure is stable in fire. However the deflection limit of span/20 is exceeded - 9000/728 ~ span/12,4.

Using the same thermal data, and slab depth, the structural resistance has been computed for different reinforcing mesh sizes using the BRE method. These are presented in Table D.2.

In using the BRE method a floor design zone of 9 m x 9 m has been assumed. The perimeter beams around this zone would, using this method, usually be fire protected. In the DIANA analyses the area of unprotected beams was much greater and measured 22 m x 18 m.

In the table it can be seen that as time increases, the structural resistance reduces and then starts to increase. The minimum value for 6x200 reinforcing mesh is 6,24 kN/m^2 and for 7x200 reinforcing mesh is 7,38 kN/m^2. The associated displacement, was 435 mm for both cases.

For the same reinforcing mesh size as was used in the DIANA (6x200), the total resistance using the BRE method was 6,24 kN/m^2 compared with the total applied load for the DIANA analysis of 8,615 kN/m^2. However, the DIANA analysis did not fail and the structure analysed was much larger. The BRE method can therefore be assumed to be conservative in this case.

Table D.2 *Variation of slab resistance with time (q=700)*

Mesh size		6x200	7x200
Time	Disp (mm)	Resistance (kN/m^2)	Resistance (kN/m^2)
64	424	6,43	7,54
65	427	6,35	7,47
66	430	6,28	7,40
67	432	6,25	7,38
68	435	6,24	7,38
69	436	6,27	7,40
70	437	6,33	7,46

Although the DIANA analysis was deemed to have failed because of excessive deflection, the total applied of 8.615 kN/m^2 was larger than the total resistance calculated (7.38 kN/m^2) using the BRE method with a larger reinforcing mesh (7x200). This again indicates that the BRE method is conservative.

List of Figures

List of Tables

European Commission

EUR 20953 — Steel structures
Design tools for the behaviour of multi-storey steel-framed buildings exposed to natural fires

L. Twilt, C. Both, A. J. Breunese, D. O'Callaghan, M. O'Connor, M. Rotter, A. Usmani, L. G. Cajot, B. Zhao, G. M. Newman

Luxembourg: Office for Official Publications of the European Communities

2004 — 240 pp. — 21 x 29.7 cm

Technical steel research series

ISBN 92-894-0749-2

Price (excluding VAT) in Luxembourg: EUR 35